THE ROLE OF CYR61 AND LASP1 IN GROWTH AND METASTASIS OF HUMAN HEPATOCELLULAR CARCINOMA

WANG BEI

(B.Sc, Wuhan University)

A THESIS SUBMITTED

FOR THE DEGREE OF DOCTOR OF PHILOSOPHY

DEPARTMENT OF MICROBIOLOGY

NATIONAL UNIVERSITY OF SINGAPORE

2007

ACKNOWLEDGEMENT

Four years ago, when I stepped into this tiny but tidy city – Singapore, everything is NEW to me, the fresh environment, the unfamiliar people around, and the totally different life leading to the road of science – Ph.D.…… Now, when I am sitting down to start writing my thesis, I feel myself completely accustomed to my life in Singapore, as almost everybody I encountered here is warmhearted, courteous and always well prepared for his/her generous help so that I could finish my work that efficiently and smoothly.

Firstly, I would like to express my deepest respect and appreciation to my supervisor, Associate Professor REN Ee Chee, for his guidance, support, and persistent encouragement throughout the course of this project. I am eternally grateful for many opportunities and unlimited room provided by him for me to learn and to grow. I express my gratitude to my Thesis Advisory Committee member Professor CHAN Soh Ha as well, for his invaluable advice on my thesis.

I sincerely thank Dr FENG Ping for her valuable advice, guidance and generous help in the whole project. In addition, I wish to extend my regards to all others who have assisted me in this study: XIAO Ziwei did the follow-up study, JIANG Jianming instructed me in my ChIP experiments, XIAO Yong and Candy ZHUANG from BSF (Biopolis Shared Facilities) helped in setting up the machine for scanning the confocal images.

Special acknowledgements are also addressed to:

All the lab members at GIS, Dr. Lisa Ng, Dr. Neo Soek Ying, Dyan Kwek, Diane Simarmata, Agathe Lora Virgine and Gayathri Mohanakrishnan.

All staff at the WHO Immunology Centre of NUS, Meera, Lini, Jerming, Soo, Mei Fong, etc.

All my friends, Lian Qun, Hai Xia, Hong Xiang, Yi Chuan, Pan Hong, Ru Bing, Lin Sen for their encouragement and companionship.

National University of Singapore for providing me with research scholarship, and Genome Institute of Singapore for supporting me to complete this project.

Last but not least, to my family members, especially my beloved parents and my husband for their understanding, support and endless love to me.

TABLE OF CONTENTS

SUMMARY

Hepatocellular carcinoma (HCC) is the fifth most common cancer in the world with poor prognosis associated with tumor invasion and metastasis. Our previous microarray analysis had revealed two metastasis related genes – Cyr61 and Lasp1, which have aberrant expression of being down-regulated and up-regulated, respectively in HCC by comparing matched HCC tumor and non-tumor liver samples (Neo *et al*. 2004). Here we report the functional characterization of Cyr61 and Lasp1, and the results indicate that these genes may play important roles in the growth and metastasis of human HCC.

The effect on cell growth was investigated using Gateway constructs of these two genes for over-expression and specific siRNA for gene knockdown. After transfection with either expression construct or siRNA, the WST-1 cell proliferation assay and soft agar assay were performed to examine the anchorage dependent and independent growth, respectively. As a potential tumor suppressor in HCC, over-expression of Cyr61 inhibited HCC cell growth both in monolayer and in soft agar, whereas knockdown of endogenous Cyr61 by siRNA promoted cell proliferation rate. In contrast, knockdown of Lasp1 by siRNA significantly inhibited HCC cell growth, while further over-expression of Lasp1 enhanced cell proliferation, supporting the potential role of Lasp1 as an oncogene in HCC. These results suggest that aberrant expression of Cyr61 and Lasp1 might contribute to the growth advantage of HCC tumors.

Next, the cell adhesion ability to ECM proteins plus the cell migratory and invasive activities were explored. Over-expression of Cyr61 exerted an inhibitory effect on HCC cell migration and invasion, most probably by interfering with ECM-

integrin signaling pathways, as suggested by the enhanced cell adhesion to ECM proteins. Interestingly, both siRNA knockdown and over-expression of Lasp1 in HCC cells suppressed cell migration and invasion ability, suggesting that Lasp1 functions within a certain optimal concentration. Confocal microscopy studies indicated that Lasp1 may inhibit HCC invasion and metastasis through recruiting and/or sequestering focal adhesion associated proteins, such as zyxin, VASP, and paxillin, and thus influencing F-actin dynamics.

A surprising finding was that both Cyr61 and Lasp1 were found to be linked to the central master regulator p53. Cell cycle analysis showed that over-expression of Cyr61 induced G2/M arrest with concomitant up-regulation of p53 protein in HepG2 cells carrying wild-type p53, suggesting that Cyr61 may act as an upstream molecule of p53 and suppress HCC cell growth through both p53 dependent and alternative pathways. Lasp1, on the other hand, was identified as a p53 downstream target. We have provided a series of biochemical and biological evidences showing that Lasp1 is a *bona fide* p53 target gene, which is transcriptionally suppressed by p53.

In conclusion, this study provides insights into the roles of two interesting genes which are involved in tumor metastasis and growth. The data also strengthens the understanding of the effect of p53 on cellular processes in the molecular pathogenesis of HCC and may present additional targets as diagnostic markers and therapeutics to control the progression and metastasis of human HCC.

LIST of FIGURES

1. Figure of Chapter 1

2. Figure of Chapter 2

3. Figure of Chapter 3

4. Figure of Chapter 4

LIST of TABLES

Table of Chapter 2

ABBREVIATIONS

AFB1	aflatoxin B1
AFP	alpha-fetoprotein
APS	ammonium persulfate
Arg	Arginine
BM	basement membrane
bp	base pair
BSA	bovine serum albumin
C	Cysteine
CCN	Cyr61/CTGF/Nov
cDNA	complementary DNA
ChIP	chromatin immuno-precipitation
Ct	threshold cycle(s)
Cyr61	cysteine-rich 61
D	Aspartate
DMEM	Dulbecco's Modified Eagle's Medium
DMSO	dimethysulfoxide
DNA	deoxyribonucleic acid
DNase	deoxyribonuclease
dNTP	2'-deoxyrobonucleoside-5'-triphosphate
E	Glutamate
E.coli	*Escherichia coli*
ECM	extracellular matrix
EDTA	ethylenediamine tetra-acetic acid
FAK	focal adhesion kinase
FBS	fetal bovine serum
5-FU	5'-Fluorouracil
g	gram
× g	times gravity
G	Glycine
G418	geneticin
GFP	green fluorescence protein
H	Histidine
HBV	hepatitis B virus

HBxAg	hepatitis B virus X antigen
HCC	hepatocellular carcinoma
HCV	hepatitis C virus
HNF-3	Hepatic nuclear factor 3
hr/hrs	hour/hours
IGF-1R	insulin-like growth factor receptor 1
IGF-2	insulin-like growth factor 2
K	Lysine
kb	kilo base pair
kDa	kilo Dalton (the unit of molecular mass)
Lasp1	LIM and SH3 protein 1
LB	Luria bertani
LIM	Lin11/Isl1/MEC-3
LOH	loss of heterozygosity
LPP	lipoma preferred partner
mA	milliampere
MAPK	Mitogen-activated protein kinase
M:F	Male:Female
mg	milligram
min/mins	minute/minutes
ml	mililiter
mM	milimolar
mRNA	messenger RNA
NF-κB	Nuclear factor kappa B
ng	nanogram
nm	nanometer
nmol	nanomolar
NSCLC	non-small-cell lung cancer
OD	optical density
ORF	open reading frame
P	Proline
P	P-value
PAGE	polyacrylamide gel electrophoresis
PBS	phosphate buffered saline

PCR	polymerase chain reaction
PEG	polyethylene glycol
PET	paired-end ditag
PKA/PKG	cAMP/cGMP-dependent protein kinase
PMSF	phenylmethysulfonyl fluoride
RE	response element
RNA	ribonucleic acid
RNase	ribonuclease
rpm	revolutions per minute
RT-PCR	Reverse-transcription polymerase chain reaction
qPCR	quantitative polymerase chain reaction
SDS	Sodium dodecyl sulphate
sec	Second
Ser/S	Serine
STAT	signal transducer and activators of transcription
T	Threonine
TEMED	N,N,N',N'-tetramethylethylenediamine
TFBS	transcription factor binding site(s)
TGF-α/β	transforming growth factor alpha/beta
Tm	Melting temperature
tRNA	total RNA
TSP1	Thrombospondin type 1
U	unit of enzyme
UV	ultraviolet
µg	microgram
µl	microliter
µM	micromolar
V	Voltage
VASP	vasodilator stimulated phosphoprotein
VWC	Von Willebrand type C
W	Tryptophan
Y	Tyrosine

CHAPTER 1

INTRODUCTION

1.1. Hepatocellular carcinoma (HCC)

1.1.1. Epidemiology of HCC

Liver cancer comprises histologically distinct primary hepatic neoplasms, including hepatocellular carcinoma, intrahepatic bile duct carcinoma (cholangiocarcinoma), hepatoblastoma, bile duct cystadenocarcinoma, hemangiosarcoma and epitheliod hemangioendothelioma (Anthony 2002). American Cancer Society estimated that over 667,000 new cases of liver cancer occurred worldwide in 2005. Among these, HCC, which represents 83% of all cases, is the most frequent type of liver cancer (Farazi and DePinho 2006).

HCC is the fifth most common neoplasm in the world, with more than 500,000 new cases emerging annually, and an age-adjusted incidence of 5.5-14.0 per 100,000 populations (Parkin *et al*. 2001; Llovet *et al*. 2003). The incidence of HCC is geographically variable, with the highest frequency observed in Southeast Asia and sub-Saharan Africa (Thomas and Zhu 2005). HCC is also predominantly male associated, with an overall M:F ratio of about 3:1. The male predominance is more obvious in relatively young age ranges in high risk regions but in older age ranges in low incidence countries (Kew 2002).

HCC is rapidly fatal, with an average life expectancy of 6 months from time of diagnosis, and a less than 3% survival rate for untreated cancer over 5 years. Death is often due to severe liver failure associated with cirrhosis and/or rapid outgrowth of multilobular HCC (Feitelson *et al*. 2002). Although early HCC is cured by surgical resection, most HCC patients are diagnosed at advanced stages that preclude the optimum surgical treatment, and for those 20-30% resectable tumors, 5-year recurrence rates approach as high as 75% to 100%, mainly due to invasion and metastasis (Tung-Ping Poon *et al*. 2000; Llovet *et al*. 2003).

1.1.2. Etiology of HCC

The various causes of HCC are perhaps better understood than those of any other cancers in human. The major etiological factors of HCC, including the chronic infections with hepatitis B virus (HBV) or hepatitis C virus (HCV) and prolonged dietary exposure to aflatoxin B1, are responsible for about 80% of human HCCs (Bosch *et al*. 1999; Thorgeirsson and Grisham 2002).

HCC is frequently the long-term result of chronic viral infections. In developing countries, it affects young patients with chronic hepatitis B virus infection. Approximately 2 billion individuals worldwide have HBV infection, and in endemic areas, the carrier rate is up to 10-20% of the population. The chronic HBV carriers have a 100-fold relative risk of developing HCC compared with non-carriers. HBV causes an estimated 320,000 deaths annually, in which approximately 30-50% is attributable to HCC (Llovet *et al*. 2003; Farazi and DePinho 2006). Numerous evidences support the direct involvement of HBV in the transformation process through HBV genome integration (Wang *et al*. 1990; Tokino *et al*. 1991; Gozuacik *et al*. 2001; Murakami *et al*. 2005), HBxAg transactivation activity (Nijhara *et al*. 2001; Tarn *et al*. 2001) or direct binding of HBxAg to inactivate the tumor suppressor p53 (Ueda *et al*. 1995). Despite the high incidence of HBV infection, the development of an effective vaccine for HBV, combined with its universal administration in endemic regions, will significantly reduce the incidence of HCC within the next generation (Feitelson *et al*. 2002) .

While HCC is highly prevalent in developing regions where HBV infections are prevalent, the incidence has been continuously rising in economically developed countries, including Japan, Western Europe, and the United States for the last two decades, mostly due to an increasing rate of HCV infection (El-Serag and Mason 1999; Thomas and Zhu 2005). In these countries, HCC appears in relatively older patients

with cirrhosis related to hepatitis C virus infection. About 20% of chronic HCV cases develop liver cirrhosis, and 2.5% develop HCC (Bowen and Walker 2005). According to a report by WHO (1997), around 170 million people in the world are infected with hepatitis C virus, but unfortunately, specific vaccination is not yet available (Forns *et al*. 2002; Farazi and DePinho 2006) .

Besides virus infections, prolonged exposure to the fungal toxin, aflatoxin B1, also poses an elevated risk for the development of HCC. Aflatoxin B1 is produced as a secondary metabolite by the fungus Aspergillus flavus, which is found on many food products such as nuts, spices and oilseeds. This toxin seems to function as a mutagen, and is associated with a specific p53 mutation at codon Ser249 (Bressac *et al*. 1991; Hussain and Harris 1998), and with cooperating mutational activation of oncogenes such as HRAS (Riley *et al*. 1997). In addition, it is noteworthy that aflatoxin B1 intake, often co-exists with HBV infection, will cause a 5~10 fold increased risk of developing HCC in such individuals compared with exposure to only one of these factors (Kew 2003) .

Alcohol abuse is another important HCC risk factor. Alcohol can damage the liver through oxidative-stress mechanisms, which might contribute to hepatocarcinogenesis in several aspects, such as promoting the development of fibrosis and cirrhosis (Campbell *et al*. 2005), affecting HCC-relevant signaling pathways (Osna *et al*. 2005) and causing the accumulation of oncogenic mutations (Marrogi *et al*. 2001).

Furthermore, other etiological factors associated with HCC include long-term oral contraceptive use in women, certain metabolic disorders, diabetes, non-alcoholic fatty liver disorders and non-alcoholic steatohepatitis. All these factors are believed to lead to the development of fibrosis or cirrhosis, which therefore might further contribute to HCC development (Farazi and DePinho 2006).

1.1.3. Molecular pathogenesis of HCC

HCC commonly develops in an order of liver cell injury, which leads to inflammation, hepatocyte regeneration, liver matrix remodeling, fibrosis, cirrhosis, and ultimately HCC (Thomas and Zhu 2005). In the slow process of hepatocarcinogenesis, genomic changes progressively alter the hepatocellular phenotype to produce cellular intermediates that evolve into HCC (Thorgeirsson and Grisham 2002). Nearly every carcinogenic pathway is altered to some degree in HCC. In hepatic inflammation and chronic hepatitis, alterations in hepatocyte growth factor expression, somatic mutations, protease and matrix metalloproteinase over-expression and oncogene expression are frequently seen, and as the liver injury progresses through fibrosis, cirrhosis, dysplastic foci to HCC, these changes become more extensive (Thomas and Zhu 2005).

As reviewed by Thorgeirsson and Grisham (2002), during the long pre-neoplastic stage, at which the liver is often the sites of chronic hepatitis virus infection and/or cirrhosis, hepatocyte proliferation is enhanced by up-regulated mitogenic pathways. Increased expression of transforming growth factor-α (TGF-α) and insulin-like growth factor-2 (IGF-2), mostly through epigenetic mechanisms, is believed to account for accelerated hepatocyte cycling. Aberrant methylation also modifies CpG groups of genes and chromosomal segments, with DNA methyltransferases being greatly up-regulated in HCC (Lin *et al*. 2001; Saito *et al*. 2001). With altered gene expressions and signal pathways, hepatocytes proliferate repeatedly, which initiates the development of monoclonal populations of aberrant and dysplastic hepatocytes.

A number of molecular changes that likely represent early changes in the development of HCC tumor occur in high frequency within cirrhotic tissue and small tumor nodules. During chronic HBV infection, HBxAg has been shown to bind to and functionally inactivate the tumor suppressor p53 and the negative growth regulator p55

by cytoplasmic sequestration (Wang *et al*. 1994; Ueda *et al*. 1995; Huo *et al*. 2001; Feitelson *et al*. 2002). HBxAg relieves the p53 suppression of the alpha-fetoprotein (AFP) gene, which may provide a reasonable explanation for the up-regulation of AFP in up to 80% of HCCs (Ogden *et al*. 2000). HBxAg has also been shown to transcriptionally suppress the expression of the translation initiation factor, sui1, as well as the cyclin dependent kinase inhibitor, p21, both of which function to inhibit hepatocellular growth (Feitelson 1999). In addition, the activation of expression of insulin-like growth factor 2 (IGF2) (d'Arville *et al*. 1991) and insulin-like growth factor receptor 1 (IGFR1) by HBxAg supports the growth of cells independent of other serum growth factors (Kim *et al*. 1996). HBxAg stimulated cell growth also appears to be associated with constitutive activation of the Ras–Raf–MAPK and NFκB signal transduction pathways (Lucito and Schneider 1992; Benn and Schneider 1994).

Another important early event in hepatocarcinogenesis involves the mutation of β-catenin. β-catenin is a component of the Wnt signal pathway, which targets a number of genes such as c-*myc*, cyclin D1, fibronectin, the connective tissue growth factor WISP, and matrix metalloproteinases (MMPs). The findings of mutated β-catenin in early stages of HCC and the stimulated expression of extracellular matrix (ECM) protein genes by constitutively active β-catenin in the nuclei suggests that β-catenin mutations may result in alterations in normal cell-cell interactions and play a significant role in the development of fibrosis and cirrhosis (Calvisi *et al*. 2001).

Genome-wide structural alterations, such as amplifications, mutations, deletions and transpositions, which develop slowly in a few genes and chromosomal loci during the pre-neoplastic stage, increase markedly in dyplastic hepatocytes and HCCs (Thorgeirsson and Grisham 2002). Loss of heterozygocity (LOH) at chromosome 1p, 4q, 6q and 8q (Konishi *et al*. 1993; De Souza *et al*. 1995; Kuroki *et al*. 1995; Kishimoto

et al. 1996; Niketeghad *et al*. 2001; Yeh *et al*. 2001) occur sporadically in pre-neoplastic liver or in small differentiated tumors (Huang *et al*. 1999). Majority of these losses have been mapped to tumor suppressor genes that normally limit hepatocellular growth and survival, and genes involved in other functions like DNA repair, carcinogen metabolism or protection against oxidative damage (Feitelson *et al*. 2002).

The increasing number of chromosomal aberrations underlines the genetic instability in HCC with tumor progression (Kimura *et al*. 1996). The frequency of aneuploidy becomes more prominent as the lesions show an increasing resemblance to tumors (Attallah *et al*. 1999). LOH at 1p, 4q, 5q, 6q, 8p, 9p, 13q, 16p, 16q, and 17p were reported to occur at late stage or in large undifferentiated tumors, and in turn inactivate some well-known tumor suppressors including RB1 (13q14.3), LEU1 (13q14), BRCA2 (13q12.3), RB2/p130 (16q12.2), p53 (17p13) and one or more JAK binding proteins (16p13) that negatively regulate the JAK/STAT pathway (Konishi *et al*. 1993; De Souza *et al*. 1995; Kuroki *et al*. 1995; Kishimoto *et al*. 1996; Boige *et al*. 1997; Marchio *et al*. 1997; Knuutila *et al*. 1999; Kusano *et al*. 1999; Wong *et al*. 1999; Laurent-Puig *et al*. 2001; Niketeghad *et al*. 2001; Wang *et al*. 2001; Yeh *et al*. 2001). Allelic gains or amplifications have also been reported on 1q, 6p, 8q and 17q (Wang *et al*. 2001), which presumably encode one or more oncogenes, for example, erbB2/NEU at 17q12-q21 (Knuutila *et al*. 1999).

In some instances, epigenetic changes precede structural alterations in the same genes. For example, over-expression of the gene c-*myc* in HCCs is initially correlated with promoter hypo-methylation and later with gene amplification at 8q24.12-13 (Kusano *et al*. 1999; Wong *et al*. 1999; Niketeghad *et al*. 2001). Reduced expression of $p16^{INK4}$ is associated predominantly with promoter hyper-methylation, but loss of

heterozygosity at 9p21 (Wang *et al*. 2001), bi-allelic loss and mutation also contribute to the loss of expression of this gene in HCC (Biden *et al*. 1997; Huang *et al*. 2000).

In summary, all genetic and epigenetic changes during the progression of HCC suggest that the molecular pathogenesis of HCC is accompanied by a sequential loss of differentiation, loss of normal cell adhesion, loss of the extracellular matrix, and constitutive activation of selected signal pathways that lead to accelerated cell growth and prolonged cell survival (Feitelson *et al*. 2002).

1.1.4. Metastasis of HCC

Biology of tumor metastasis

Tumor metastasis is an extremely complex process, which occurs through a series of stepwise processes including the invasion of adjacent tissues, intravasation, transport through the circulatory system, arrest at a secondary site, extravasation and growth in a secondary organ (Mehlen and Puisieux 2006). In order for tumors to initiate metastasis and grow, neoplastic and endothelial cells must invade and migrate into surrounding tissues. The phenotypic change is mediated by alterations in the expression of cell-surface molecule integrins, release of proteases to remodel the extracellular matrix (ECM) and the deposition of new ECM proteins. These processes then activate a cascade of signaling pathways that regulate gene expression, cytoskeletal organization, cell adhesion and survival. Consequently, cancer cells acquire the abilities to be more invasive, migratory and able to survive in different microenvironments (Hood and Cherish 2002).

During migration, cells project lamellipodia which attach to the ECM, and simultaneously break existing ECM contacts at their trailing edge. This allows the cell to pull itself forward (Sheetz *et al*. 1999). Extension of the lamellipodia is induced by

actin polymerization and facilitated by a localized decrease in membrane tension (Raucher and Sheetz 2000). Retraction of the cell edge is dependent on the adhesive extent of the environment. Usually, in highly adhesive environments, slow migration happens by fracturing the cell–ECM linkage, while in less adhesive environment, the retraction is achieved by simple dissociation of integrins and fast migration often occurs (Palecek *et al*. 1998; Palecek *et al*. 1999). Whereas, during invasion, cells release proteases that degrade and remodel the ECM, promoting cell passage through to the stroma and entrance into new tissues. This proteolytic process must be precisely controlled so that the ECM is sufficiently degraded to facilitate cell passage, but not so extensively degraded to make sure that the cellular traction is not lost (Hood and Cheresh 2002).

ECM components

The cellular migration and invasion are governed by several factors at both the extracellular and intracellular levels, and depend on the cell's carefully balanced dynamic interaction with the ECM, which have to be tightly controlled (Hood and Cheresh 2002). As an essential component involved in cell migration and invasion, the extracellular matrix supports adhesion of cells and transmits signals through cell-surface adhesion receptors. The ECM contains collagens, non-collageneous glycoproteins and proteoglycans. Alternative ECM constituents, such as tenascin, fibronectin and variant isoforms of laminin, are found in tumors and might stimulate cancer progression (Bissell and Radisky 2001). Vitronectin, on the other hand, is a multifunctional non-collageneous glycoprotein present in the ECM and in blood (Schvartz *et al*. 1999). The basement membrane (BM), a specialized ECM that separates the epithelial cells from the underlying stroma, provides the initial barrier

against invasion of carcinomas. It has a complex molecular architecture that mainly consists of laminins, type IV collagen, osteonectin, entactin and heparin sulphate proteoglycans. Fibrillar collagens (type I, II, III, V and XI) form fibrils and influence cellular functions through interactions with integrins, while the most prevalent basement membrane (BM) proteins – type IV collagens – are network-forming collagens of the BM. This covalent binding of collagens provides the mechanical stability of the basement membrane (Egeblad and Werb 2002; Hood and Cheresh 2002).

Alterations in cell adhesion to these ECM/BM components are associated with various tumors. As an initial step towards metastasis, many epithelial tumors alter expression or localization of laminin-binding integrins, such as α6β4, which seems to promote both invasion through the BM and increased motility in the stroma, where tumor cells frequently remodel the matrix by depositing laminin. In addition, the expression of fibronectin-binding integrin α5β1 often disappears in tumor and its re-expression in cell lines markedly reduces tumorigenesis (Varner *et al*. 1995). Previous studies also reported that many proteases that are up-regulated in metastatic tumors show high enzymatic activity against type IV collagen, and inhibition of these enzymes inhibits tumor invasion. Besides collagens, the non-collageneous glycoprotein vitronectin may play an important role in wound healing and in tumor progression as well, in view of the involvement of its receptor – integrin αvβ3 in angiogenesis (Varner and Cheresh 1996; Mousa 2002).

Focal adhesion components

The sites where the extracellular matrix (ECM), integrins and the cytoskeleton interact are called focal contacts or focal adhesion sites (Burridge and Fath 1989). These focal contacts are specialized regions where actin filaments are anchored, and

where integrins cluster and interact with ECM proteins and dynamic groups of structural and regulatory proteins that relay information bi-directionally across the plasma membrane to regulate cell proliferation, survival, adhesion and motility. To date, more than 50 different adhesion proteins have been identified as focal adhesion components that physically link the integrin receptor to actin, building the connection to the cytoskeleton (Partridge and Marcantonio 2006). For instance, the integrin-binding proteins paxillin and talin recruit focal adhesion kinase (FAK) and vinculin to focal contacts (Sastry and Burridge 2000; Calderwood and Ginsberg 2003). The α-actinin, a cytoskeletal protein that is phosphorylated by FAK, binds to vinculin and crosslinks actin stress fibers and tethers them to focal adhesion sites. Zyxin is an α-actinin- and stress-fibre-binding protein that is usually present in mature contacts, which are necessary for cell adhesion and spreading (Beckerle 1997; Mitra *et al*. 2005).

In response to integrin engagement, tyrosine kinases FAK and Src are activated and recruited to the developing focal adhesions. Subsequent tyrosine phosphorylation of focal adhesion components promotes further recruitment of signaling and structural molecules and development of fully mature focal adhesions. These processes are mediated by multiple signaling pathways triggered by the tyrosine kinase activity at the focal contacts. For example, FAK signaling activates Rho-family of GTPases (RhoA/Rac/Cdc42) directing local actin assembly into stress fibers, lamellipodia or filopodia and thus control cytoskeletal dynamics and cell migration (Mitra *et al*. 2005). Upon activation, the Rho GTPases also activate a wide range of effector proteins that regulate cell adhesion as well as gene transcription (Bishop and Hall 2000). When bound to Grb2-Sos complex, tyrosine-phosphorylated FAK also activates Ras-Raf-MEK-MAPK and PI3K-Akt pathway involved in gene expression and cell proliferation (Mitra and Schlaepfer 2006). As dynamic regulation of focal

adhesions and reorganization of the actin cytoskeleton are crucial determinants for cell migration, dysregulation of these focal adhesion components and signaling is highly associated with tumor invasion and metastases (Carragher and Frame 2004).

Clinical importance of HCC metastasis

Tumor metastases are the primary cause of death in cancer patients, which are responsible for almost 90% of human cancer deaths (Nguyen and Massague 2007). Metastasis remains as one of the major challenges before HCC can be finally conquered. Though early HCC can be cured by surgical resection, the 5-year survival rate remains rather low as most patients encounter the recurrence of cancer, mostly due to metastasis (Llovet *et al*. 2003; Thomas and Zhu 2005). Case studies have showed that the human primary hepatocellular carcinoma can be metastasized to a wide range of organs, including skin (Yamanishi *et al*. 1989), mandible (Lalikos *et al*. 1992), spleen (Nakamuta *et al*. 1992), brain (Tanabe *et al*. 1994), lymph node (Ueno *et al*. 2001), renal (Aron *et al*. 2004), adrenal (Hanada *et al*. 2004), heart (Masci *et al*. 2004), bone (Fontana *et al*. 2004), pharynx (Oida *et al*. 2005), etc.

Genetic determinants and bio-markers for HCC metastasis

Despite its clinical importance, little is known about the underlying mechanisms or the genetic and biochemical determinants of HCC metastasis. Endeavors in the past decade have focused on identifying the molecular and genetic determinants for HCC metastasis and have claimed biomarkers as having the potential to predict metastatic recurrence and prognosis of HCC patients. These include genes covering a broad range of functional categories, such as tumor suppressor genes (e.g. p53, PTEN), oncogenes (e.g. c-*myc*, c-*met*), cell cycle regulators (e.g. cyclin D1, INK4 family), apoptosis-

associated genes (e.g. Bcl-xL, *survivin*), angiogenic factors (e.g. VEGF, HIF-1α, angiopoietins), growth factor receptors (e.g. EGFR, leptin receptor), as well as those genes directly involved in invasion and metastasis process (e.g. MMP-2, E-cadherin) (Ueki *et al*. 1997; Yamamoto *et al*. 1997; Ito *et al*. 1999; Kawate *et al*. 1999; Niu *et al*. 2000; Ito *et al*. 2001; Hu *et al*. 2003a; Matsuda *et al*. 2003; Fields *et al*. 2004; Watanabe *et al*. 2004; Huang *et al*. 2005; Iso *et al*. 2005; Wada *et al*. 2006; Wang *et al*. 2006). This wide coverage of gene functional groups, to some degree, reflects the fact that HCC metastasis is a complicated, multi-step and changing process. Nevertheless, it is recognizable that the knowledge on the roles of metastasis-associated genes in HCC is still rather limited. In a previous report from our lab, two metastasis related genes, Cyr61 and Lasp1 were identified to have aberrant expression of being down-regulated and up-regulated, respectively in HCC by comparing 37 pairs of matched HCC tumor and non-tumor liver samples using cDNA microarray analysis (Neo *et al*. 2004). Characterizing the functions of metastasis-associated genes, such as Cyr61 and Lasp1, will no doubt provide a more solid basis for the prediction and prevention of the metastasis and metastatic recurrence of HCC.

1.2. The human Cyr61 (Cysteine-rich 61) gene

1.2.1. The human CCN (Cyr61/CTGF/Nov) gene family

Members of the human CCN gene family

Cysteine-rich 61 (Cyr61) is the first cloned member of the CCN family, which includes Cyr61/CCN1, connective tissue growth factor (CTGF/CCN2), nephroblastoma overexpressed (Nov/CCN3), Wnt-1 induced secreted protein 1 (Wisp-1/CCN4), Wisp-2/CCN5, and Wisp-3/CCN6 (Perbal 2004). Although originally regarded as a simple group of related proteins, the CCN family is now known to be more complex, with biologically active CCN isoforms generated either by post-translational processing or alternative splicing. According to the recommendations by the international CCN society, these isoforms are designated as CCN1-V1, CCN2-V1, CCN2-V2, CCN2-V3, CCN3-V1, CCN3-V2, CCN4-V1, and CCN6-V1, which are either expressed in normal conditions or in pathological conditions (Perbal 2004).

Modular structures and functions

Members of the CCN family are 30~40 kDa proteins that are extremely cysteine-rich (10% by mass). One of the most important features of CCN proteins is that they are multi-modular mosaic proteins containing a signal peptide and four conserved modules that resemble functional domains previously identified in major extracellular regulatory proteins (Figure 1.1). Module 1 is an insulin-like growth factor (IGF)-binding domain, module 2 is a von Willebrand type C domain, module 3 is a thrombospondin-1 domain, and module 4 is a C-terminal domain containing a putative cystine knot (Bork 1993; Brigstock 1999; Lau and Lam 1999; Perbal 2001).

Although the biological roles for all these conserved modules are not fully identified, progress has been made to address the relationship between the structure and

function of the CCN protein family. The signal peptide encoded by all CCN proteins is generally believed to be responsible for secretion just as other proteins carrying signal peptide. Module I was named as IGFBP module, but it shares only 32% identity with the N-terminal part of the Insulin-like Growth Factor Binding Proteins (IGFBPs) (Bork 1993). As such, the proposition that CCN proteins bind to IGF remains controversial and the biological significance of the structural relationship between IGFBPs and CCN proteins is still very much debated (Planque and Perbal 2003). Module II comprises a Von Willebrand type C repeat (VWC) that occurs in Von Villebrand factor as well as various secretory proteins such as mucins, thrombospondins, and collagens (Bork 1993). This module contains sequences that are proposed to drive protein oligomerization. Module III contains sequences sharing identity with the Thrombospondin type 1 repeat (TSP1) (WSXCSXXCG), and appears to be a cell attachment motif that is implicated in the binding of sulfated glycoconjugates (Holt *et al*. 1990). The presence of a TSP1 module in the CCN proteins suggests that they might be implicated in functional interactions with multiple components of the ECM or play an active role in cell adhesion. Module IV, also designated as CT domain, exists in the C-termini of a wide range of unrelated extracellular proteins as well, including Von Willebrand factor and mucins, and appears to be critical for several of the biological functions attributed to the CCN proteins. Sequences similarities to Heparin-binding motifs are also found within this domain (Brigstock *et al*. 1997). The structure found in CT domain, known as "cystine knot" formed by six cysteines, is implicated in the dimerization of growth factors such as TGF-β, PDGF, and Nerve Growth Factor (NGF) (Schlunegger and Grutter 1993). The cystine knot in the CCN proteins might allow both homotypic and heterotypic interactions with proteins containing a similar structure, such as Fibulin 1C,

Notch1, and even CCN protein itself, which were thought to be critical for controlling the cell adhesion (Perbal *et al*. 1999; Perbal 2001; Sakamoto *et al*. 2002).

Gene expression and biological functions of human CCN family

Early studies showed human CCN gene expression in a great variety of tissues during normal development (Brigstock 1999). The amount of RNA species appears to be controlled by tight spatiotemporal regulation, thus in most tissues that stained positive, high concentrations of CCN1 and CCN2 RNA are also detected. Low to high levels of CCN3 RNA are generally present in most positive tissues (Perbal 2001), whereas CCN5 and CCN6 have a more restricted expression pattern compared to CCN1-3 (Perbal *et al*. 2003). As the CCN proteins contain a signal peptide driving their secretion, whether they act at their site of production or can be transported away to execute their functions elsewhere remains as a central question (Perbal 2004).

The CCN genes encode secreted proteins associated with the extracellular matrix (ECM) and cell membrane. The CCN family proteins were once thought as a new family of growth factor as they acted in a similar fashion to classical growth factors, but the attempts to identify unique signal transducing receptors with high affinity and specificity have been unproductive (Brigstock 2003). Based on results obtained over the past decades, CCN family proteins were believed to act as matricellular regulatory factors that bridge the functional and physical gap between ECM-associated proteins and cell surface molecules (Lau and Lam 1999; Perbal 2004).

A number of studies showed that Cyr61/CCN1, CTGF/CCN2, and Nov/CCN3 can bind to cell surface integrins and thereby induce intracellular signaling events that include kinase activation and gene transcription (Lau and Lam 1999; Chen *et al*. 2000; Chen *et al*. 2001a; Grzeszkiewicz *et al*. 2001; Grzeszkiewicz *et al*. 2002; Leu *et al*.

2002; Schober *et al*. 2002). The fact that CCN proteins and their corresponding RNA are widely expressed in tissues originating from the three germ layers with major sites of expression suggests that CCN family members have roles in the differentiation and functioning of nervous system, vasculature, muscle, bone etc. (Brigstock 1999; Planque and Perbal 2003). Collectively, CCN proteins exhibit multiple functions including proliferation, differentiation, survival, adhesion, migration, apoptosis, extracellular matrix (ECM) production, placentation, implantation, angiogenesis, embryogenesis, chondrogenesis and endochondral ossification (Brigstock 2003; Planque and Perbal 2003; Perbal 2004).

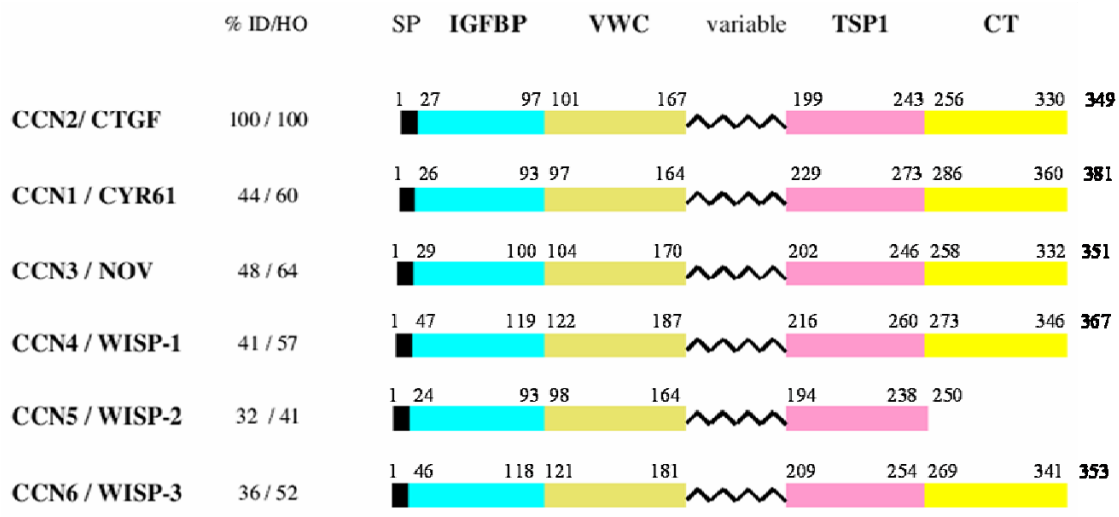

Figure 1.1 Modular structure of the CCN protein family. (Modified from Brigstock 2003; Planque and Perbal 2003) Residues are numbered according to the human orthologs of each protein. SP, Signal Peptide; IGFBP, Insulin-like Growth Factor Binding Protein-like module; VWC, Von Willebrand Factor-like module; TSP1, Thrombospondin-like module; CT, cystine knot containing family of growth regulator-like module. ID: identity; HO: homology.

1.2.2. Expression and biological functions of Cyr61

Cyr61, originally designated 3CH61, was first identified in 1985 as a growth factor inducible immediate-early gene in serum-stimulated mouse BALB/c 3T3 fibroblasts (Lau and Nathans 1985). Its chicken ortholog (Cef-10) was cloned as a gene induced following the transformation of chick embryo fibroblasts by the v-src oncogene of the Rous Sarcoma Virus (RSV) (Simmons *et al*. 1989). In 1997, the complete cDNA of the human Cyr61 gene isolated from an embryonic source was mapped to chromosome 1p22-31 and shown to encode a protein with 381 amino acids carrying a signal peptide of 26 residues (Jay *et al*. 1997; Brigstock 2003).

Encoded by a growth factor inducible immediate-early gene, Cyr61 can be transcriptionally activated by a variety of growth factors and other stimuli, such as fresh medium, platelet-derived growth factor (PDGF), fibroblast growth factor (FGF) and TPA (12-*O*-tetradecanoylphorbol-13-acetate) (O'Brien *et al*. 1990). Human Cyr61 is widely expressed in multiple adult tissues such as heart, uterus, pancreas, brain, lung and skeletal muscle (O'Brien *et al*. 1990; Jay *et al*. 1997; Kolesnikova and Lau 1998). In mouse embryos, Cyr61 mRNA is present at high levels on days 9.5-14.5, whereas placental expression of Cyr61 is highest on days 17.5-18.5 (O'Brien and Lau 1992).

Cyr61 is a secreted protein and is associated with the extracellular matrix (ECM) and cell surfaces. Similar to other CCN family members, the multi-modular structure of Cyr61 provides the basis for its interactions with multiple ECM proteins and cell membrane receptors and hence the combinatorial cellular functions. As a heparin-binding protein and a ligand to various integrins, including αIIbβ3, αvβ5, αvβ3, α6β1 and αMβ1 (Jedsadayanmata *et al*. 1999; Grzeszkiewicz *et al*. 2001; Grzeszkiewicz *et al*. 2002; Schober *et al*. 2002; Menendez *et al*. 2005), Cyr61 has been shown to participate in a great variety of cellular events including chondrongenesis, osteogenesis,

angiogenesis, cell proliferation and survival, adhesion and migration (Kireeva *et al*. 1996; Wong *et al*. 1997; Babic *et al*. 1998; Chen *et al*. 2001b). The diverse activities of Cyr61 are often thought to be mediated in part through interaction with multiple integrin receptors and cell surface heparin sulfate proteoglycans in a cell type specific and cellular context dependent manner.

1.2.3. Association of Cyr61 with cancer

Associations of human CCN proteins with cancer

The structural similarity observed between CCN and a number of ECM proteins, their localization in the ECM, and their ability to interact with several types of cell membrane receptors and regulatory proteins suggest that CCN proteins represent a new class of signaling matricellular molecules playing a critical role in the regulation of cell growth. Therefore, the production of abnormal levels of normal or altered CCN proteins might be associated with or involved in the initiation and progression of tumor growth (Planque and Perbal 2003).

Increasing lines of evidence now draw relationships between aberrant expression of CCN proteins in a number of tumors and tumorigenesis. Including CCN1, all CCN family proteins have been shown to be highly related to the tumorigenesis of various types of tumors. CCN2 was found up-regulated in dermatofibromas, pyogenic granuloma, pancreatic tumors, endothelial cells of angiolipomas and angioleiomyomas, glioblastoma tumor cells, and mononuclear cells of the patients with acute lymphoblastic leukemia (Igarashi *et al*. 1998; Wenger *et al*. 1999; Pan *et al*. 2002; Vorwerk *et al*. 2002). The expression of CCN3 was reported to be correlated to increased proliferative index in the case of the prostate and renal cell carcinoma (Glukhova *et al*. 2001; Maillard *et al*. 2001). CCN4 and CCN6 expression was

significantly increased in most colon adenocarcinomas (Pennica *et al*. 1998). All these observations are in favor of the point that CCN proteins play a positive role in tumorigenesis by providing the stimulatory effects on cell growth that are required for the increased lifespan of tumor cells. The relationship that was built between increased expression of CCN proteins and tumorigenicity might involve a partial or complete abrogation of apoptotic pathway and affect the communication of tumor cells with the surrounding environment.

By decreasing the adhesive activity of the cells and by providing an increased ability to migrate and invade surrounding tissues, the CCN proteins might also be key factors participating in the angiogenesis and metastasis of tumor cells. For example, elevated level of CCN2 was observed in breast carcinoma with more advanced features, invasive mammary ductal carcinoma, and high grade of astrocytomas (Frazier and Grotendorst 1997). The expression of CCN3 was also reported to be correlated to the higher metastatic potential of the Ewing's carcinoma cells (Manara *et al*. 2002)

Interestingly, anti-proliferative effects of CCN family proteins were also observed in a number of tumors. Both CCN2 and CCN3 were reported to be down-regulated in Wilm's tumors and the expression of CCN3 was shown to match striated muscular differentiation. A strong association between CCN3 expression and tumor differentiation was also observed in neuroblastomas, chondrosarcomas, rhabdomyosarcomas and other musculoskeletal tumors, suggesting that the level of CCN3 expression may be used as a marker for heterotypic differentiation of these tumors (Maillard *et al*. 2001; Perbal 2001; Yu *et al*. 2003).

Associations of Cyr61 with cancer

An increasing body of studies reveals sophisticated roles of Cyr61 in tumorigenesis like other members of CCN protein family, by interfering with complex signaling pathways. Up-regulation of Cyr61 expression is associated with advanced breast cancer, pancreatic cancer, gastric cancer, and gliomas (Tsai *et al*. 2002; Xie *et al*. 2004; Holloway *et al*. 2005; Lin *et al*. 2005). Multiple critical signal pathways were reported being manipulated by Cyr61 to promote tumor development, either by promoting cell proliferation and survival, cell motility and invasion, or inducing resistance to apoptosis (Xie *et al*. 2004; Lin *et al*. 2005; Menendez *et al*. 2005). For example, increased Cyr61 protein expression was observed in a large number of primary breast tumors that were progesterone receptor positive but estrogen receptor negative – suggesting that it might be a novel mediator of progesterone activity in breast cancer (Sampath *et al*. 2002). Invasive breast cancer cell lines expressed high level of Cyr61 whereas less tumorigenic breast cancer cells, such as MCF-7, expressed lower; normal breast cells showed almost none. Forced expression of Cyr61 in MCF-7 cells was sufficient to induce anchorage-independent cell growth in the absence of estrogen and to form colonies in matrigel in a αvβ3 integrin-dependent way. The tumors induced by these cells in ovariectomised athymic nude mice resembled human invasive carcinomas and were highly vascularised (Tsai *et al*. 2000; Xie *et al*. 2001; Tsai *et al*. 2002). These observations suggested that Cyr61 was involved in the progression to more advanced stages of breast cancer.

On the other hand, decreased Cyr61 expression is also frequently noted in prostate cancer, endometrial cancer, uterine leiomyoma, papillary thyroid carcinoma, and non-small cell lung carcinoma (Pilarsky *et al*. 1998; Sampath *et al*. 2001; Tong *et al*. 2001; Wasenius *et al*. 2003; Chien *et al*. 2004). Tong *et al* reported that Cyr61 is a

tumor suppressor in non-small cell lung carcinoma (Tong *et al*. 2001). It was also demonstrated that Cyr61 suppressed the growth of non-small-cell lung cancer cells by triggering the β-catenin─c-*myc*─p53 signal pathway (Tong *et al*. 2004).

The paradoxical expression of Cyr61 in different types of tumors suggests that Cyr61 may exert important and disparate functions in carcinogenesis depending on the tissue of origin and cellular context. Therefore, the identification of Cyr61 interacting partners in a particular cell type would be very helpful in establishing whether abnormal expression or associations of Cyr61 with physiological targets are involved in these processes.

Associations of Cyr61 with HCC

At least 5 previous studies reported the expression of Cyr61 in HCC. Three of them showed that Cyr61 was down-regulated in HCC (Xu *et al*. 2001; Chen *et al*. 2002a; Wang *et al*. 2005), but two other studies failed to detect any difference of Cyr61 expression (Hirasaki *et al*. 2001) or observed up-regulated Cyr61 (Zeng *et al*. 2004) in HCC. It was also demonstrated that increased d(CA) microsatellite repeat instability in the Cyr61 promoter may account in part for the down-regulation of Cyr61 in HCC (Wang *et al*. 2005). However, the potential roles of Cyr61 in the development of HCC have not yet been explored.

1.3. The human Lasp1 (LIM and SH3 protein 1) gene

1.3.1. The human LIM (LIN-11/Isl1/MEC-3) protein family

Members of the human LIM protein family

The Human LIM proteins represent a group of proteins containing the LIM domain, a tandem zinc-finger structure that thought to function as a modular protein-binding interface. The term "LIM" was derived from the names of the first three discovered members – LIN-11, Isl1 and MEC-3. The LIM domain is found in proteins from a wide variety of eukaryotic organisms. In the human genome, there are at least 135 identifiable LIM-encoding sequences located within 58 genes, as shown in Figure 1.2b. Figure 1.2a shows the human LIM proteins and LIM-protein families that have been molecularly characterized so far (Kadrmas and Beckerle 2004).

Individual LIM domains comprise of approximately 55 amino acids with 8 highly conserved residues that are located at defined intervals. Normally, the 8 conserved residues are either Cysteine or Histidine. The classical LIM consensus sequence was defined as $CX_2CX_{16-23}HX_2CX_2CX_2CX_{16-21}CX_2$(C/H/D) (X denotes any amino acid) (Schmeichel and Beckerle 1994). The number and spacing of the highly conserved cysteine and histidine residues indicated that the LIM domain might be a metal-binding structure. In 1993, Michelsen *et al*. reported that the LIM motif defined a specific zinc-binding protein domain. There are eight most highly conserved residues functioning in binding to zinc, establishing a tandem zinc-finger topology (Michelsen *et al*. 1993).

Human LIM proteins can contain as many as 1-5 LIM domains found either internally or near the N or C terminus. LIM proteins can be comprised of LIM domains only, or LIM domains can be linked to other domains including homeodomains, catalytic domains, cytoskeletal-binding domains or other protein-binding modules such

as src homology 3 (SH3) domain, LD or PDZ domains. These features highlight the modular nature of the LIM domain and the functional diversity of LIM proteins (Kadrmas and Beckerle 2004).

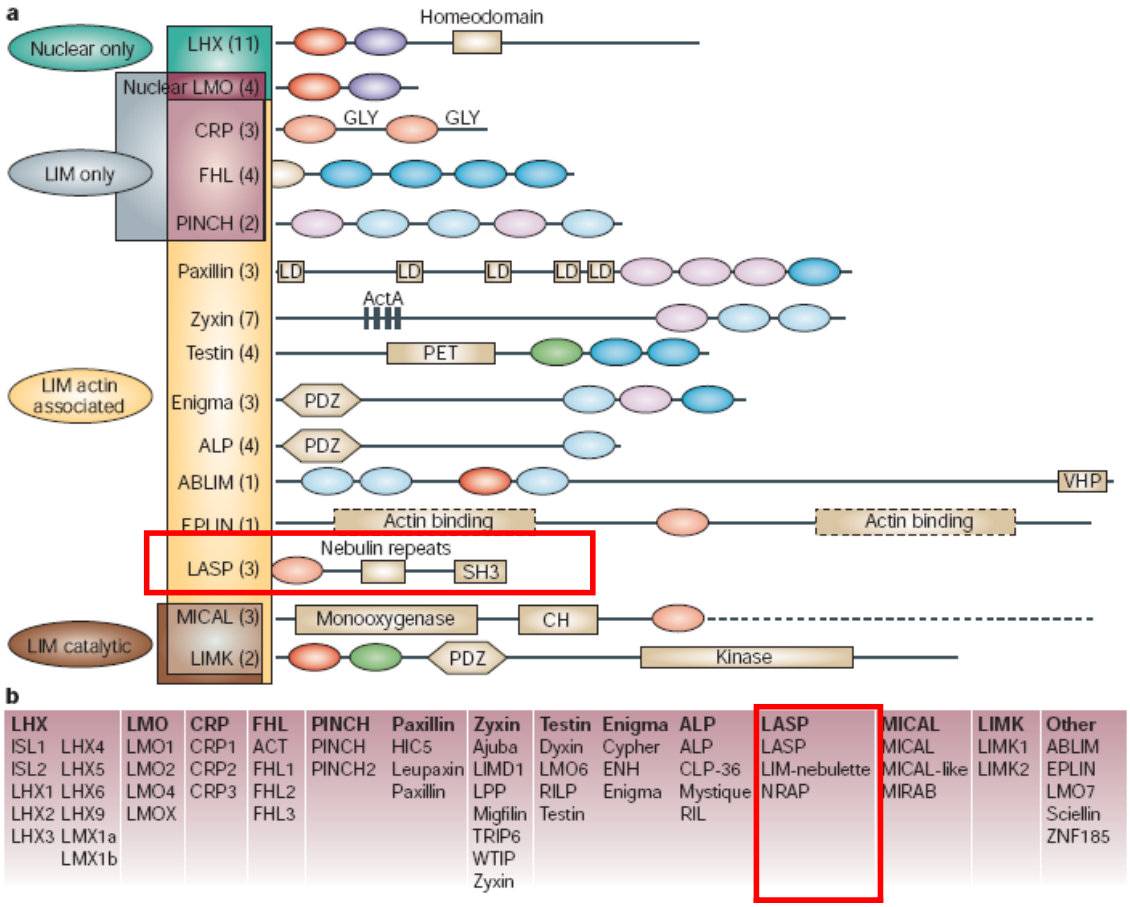

Figure 1.2 Human LIM proteins. (Adapted from Kadrmas and Beckerle 2004) (a) Domain structures of the founding member and/or the best characterized example of the main LIM-protein families are shown. The number of known members of each family is indicated in parentheses. The colored boxes represent several commonly used categorization schemes. Individual LIM domains are shown as colored ovals that have been grouped according to the similarity within the LIM sequence. Heterologous domains include the LD motif, the mono-oxygenase domain, actin-binding domain and nebulin repeats. Domains with boundaries that are not precisely defined are shown as dashed boxes. Dashed lines indicate that scale is not preserved. (b) List of the identified members of each LIM family. ABLIM, actin-binding LIM protein; ACT, activator of cyclic AMP response element modulator (CREM) in the testis; ALP, α-actinin-associated LIM protein; CH, calponin homology; CRP, cysteine-rich protein; EPLIN, epithelial protein lost in neoplasm; FHL, four-and-a-half LIM; GLY, glycine-rich region; LASP, LIM and SH3 protein (red box); LHX, LIM-homeodomain protein; LIMK, LIM kinase; LMO, LIM only; MICAL, molecule interacting with CASL protein-1; PDZ, postsynaptic density-95, Discs large, zona occludens-1; PET, prickle, espinas and testin; PINCH, particularly interesting new cysteine and histidine-rich protein; SH3, Src-homology-3; VHP, villin head piece.

Biological functions of the human LIM protein family

A large body of literature supports the point that the LIM domain functions as a modular protein-binding interface to mediate protein-protein interactions (Feuerstein *et al*. 1994; Arber and Caroni 1996; Kadrmas and Beckerle 2004). However, no specific consensus binding sequence or structural element has been defined as the general features of the LIM domain binding partners, as the LIM motif seems to recognize different protein targets in a variable manner that is dependent on the specific targeted proteins (Velyvis *et al*. 2003). By analyzing a huge number of LIM partners, LIM domains are now thought to contribute as either one or combination of the following four functions: adaptors, competitors, conformers and localizers (Kadrmas and Beckerle 2004).

LIM proteins have been identified in both the nucleus and the cytoplasm. Some LIM proteins, such as the LIM homeodomain proteins, are expressed exclusively in nucleus and have clear transcriptional roles during development (Hobert and Westphal 2000). Nevertheless, most characterized LIM proteins are known to interact with the actin cytoskeleton in a direct or indirect way. Interestingly, many LIM proteins such as members of the zyxin, four-and-a-half LIM (FHL) and cysteine-rich protein (CRP) families, which were initially identified as cytoskeleton associated proteins, are now believed to be able to shuttle between the cytoplasm and nucleus of the cells to regulate gene expression (Muller *et al*. 2002; Chang *et al*. 2003; Cattaruzza *et al*. 2004). The ability of the dual localization of these LIM proteins is the most striking theme on global examination of LIM functions in encompassing aspects of cytoskeletal function and the control of gene expression.

By binding to their partners, the LIM proteins participate in a wide variety of biological processes, including regulation of actin structure and dynamics, neuronal

pathfinding, integrin-dependent adhesion and signaling, cell-fate determination and tissue-specific gene expression. In the cytoplasm, several LIM proteins, for example, EPLIN (epithelial protein lost in neoplasm) and ALP (α-actinin-associated LIM protein) have been shown to directly regulate actin polymerization and de-polymerization (Xia *et al*. 1997; Pomies *et al*. 1999). In D. melanogaster, MICAL has been shown to be expressed in axons and paly a role in repulsive axon guidance (Terman *et al*. 2002). Like MICAL, an actin-binding domain containing protein, ABLIM, is essential for high-fidelity axon pathfinding. A high percentage of LIM protein is found localized at focal adhesions, such as migfilin (a distant zyxin-family member) (Takafuta *et al*. 2003; Tu *et al*. 2003) and NRAP (a muscle-specific protein of the LASP family) (Luo *et al*. 1999; Tadokoro *et al*. 2003). These focal-adhesion LIM proteins can mediate integrin signaling. Moreover, LIM proteins from the LHX and LMO protein families have established their roles in tissue-specific gene expression and cell-fate determination.

1.3.2. The human LASP gene family

LASP (LIM and SH3 Protein) gene family, one sub-family of the LIM protein family, now includes Lasp1 (Tomasetto *et al*. 1995), Lasp2 (LIM-nebulette) (Li *et al*. 2004), and NRAP (Luo *et al*. 1997). Besides the N-terminal LIM domain, they also contain a C-terminal SH3 (src-homology-3) domain, which is involved in the protein-protein interactions through binding to proline-rich sequences. All of the three proteins can also be classified as members of the nubulin family, which are modular proteins with key structural feature of the 35-residue nebulin modules (Panaviene and Moncman 2007). This nebulin module, defined by an N-terminal sequence motif of "SDXXYK" and a central sequence motif of "TPD/E" (Jin and Wang 1991), functions to bind to different actin isoforms.

Although all of the family members contain the actin-binding domain (nebulin module), each protein interacts with distinct cellular structures and has different expression profiles. Lasp1 and LIM-nebulette (Lasp2) are found in non-muscle cells and are components of the focal adhesions, membrane skeleton, and stress fibers (Chew *et al*. 1998; Li *et al*. 2004). Unlike Lasp1, the LIM-nebulette (Lasp2), which is the most recently identified member of the nebulin family of actin-binding proteins, is actually a splice variant of nebulette and contains much of the nebulette C-terminal sequences (Moncman and Wang 2000). The expression of LIM-nebulette has been analyzed, which has demonstrated high levels of expression in lung, brain, and kidney. Low levels of the mRNA have also been found in human and mouse adult heart (Li *et al*. 2004; Terasaki *et al*. 2004). NRAP, on the other hand, mainly found in both skeletal and cardiac muscle, localizes to cellular junctions, such as the myotendinous junction and intercalated disks (Luo *et al*. 1997) and has been shown to be up-regulated in animal model systems of dilated cardiomyopathies (Ehler *et al*. 2001).

1.3.3. Expression and biological functions of Lasp1

Modular structure and expression of Lasp1

Lasp1 (LIM and SH3 protein) was initially identified from a cDNA library of human breast cancer metastases (Tomasetto *et al*. 1995). Human Lasp1 gene is mapped to chromosome 17q21 and encodes a protein of 261 amino acids containing an N-terminal LIM domain followed by two actin binding sites and a C-terminal src homology SH3 domain (Figure 1.3). The actin binding domain is believed to be functioning as a mediator for protein-protein interactions between Lasp1 and the actin cytoskeleton, while the SH3 domain at the C-terminus is involved in binding to proline-

rich sequences (Schreiber *et al*. 1998b; Chew *et al*. 2002; Butt *et al*. 2003; Keicher *et al*. 2004).

Lasp1 was shown to be widely expressed in normal epithelial tissues, muscles and brain (Chew *et al*. 1998). The murine Lasp1 expression was ubiquitous in almost all adult tissues and was detected from 7.5 to 17.5 days post-coitum of mouse embryonic stem cells, indicating its essential roles (Schreiber *et al*. 1998a). Lasp1 was previously reported to be localized within multiple sites of dynamic actin assembly such as focal contacts, focal adhesions, lamellipodia, membrane ruffles, and pseudopodia. At peripheral cell extentions in individual epithelial cells and in transformed fibroblastic cells, Lasp1 was revealed to co-localize with actin (Schreiber *et al*. 1998b). In 2002, Chew *et al* reported that Lasp1 was expressed not only in gastric parietal cells but also in focal adhesions and focal complexes as well as in the extreme tips of lamellipodia and filopodia in gastric mucosal fibroblasts (Chew *et al*. 2002). In a more recent study, Lasp1 was reported to be highly expressed by CNS (Central Nervous System) neurons and is concentrated at synaptic sites, suggesting that it may also regulate cytoskeletal reorganization in dendritic spines, which is a known factor in synaptogenesis and plasticity (Phillips *et al*. 2004).

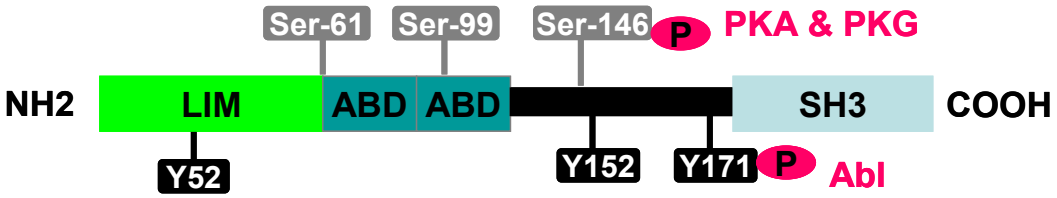

Figure 1.3 Modular structure of Lasp1. The modular domains and the protein kinase phosphorylation sites of Lasp1 are shown. LIM domain (light green); ABD: actin binding domain (dark green); SH3 domain: src homology 3 domain (light blue). The PKA/PKG phosphorylation sites are on Serine-61,-99, and -146. The Abl tyrosine kinase phosphorylation sites are on Tyrosine-52, -152, and -171.

Binding partners and biological functions of Lasp1

Although a number of studies have been performed in order to identify the binding partners of Lasp1, the specific cellular functions of this LIM and SH3 domain containing protein have not yet to be fully characterized. Current knowledge only defines Lasp1 as a focal adhesion adaptor protein involved in cell migration based on its ability to interact and/or co-localize with a series of focal adhesion proteins, such as F-actin, zyxin, lipoma preferred partner (LPP, member of the zyxin subfamily of LIM domain proteins), Krp1, vasodilator stimulated phosphoprotein (VASP) and dynamin, and the binding occurs between the C-terminal SH3 domain of Lasp-1 and the N-terminal proline-rich domains of LPP, zyxin or VASP (Chew *et al*. 1998; Okamoto *et al*. 2002; Keicher *et al*. 2004; Li *et al*. 2004; Spence *et al*. 2006).

Regulations of Lasp1

As a novel gene with its specific biological function largely unexplored, the knowledge on the regulation of Lasp1 gene expression and activity is also rather limited. Several reports have revealed Lasp1 as a phosphoprotein that can be phosphorylated by cAMP- or cGMP-dependent protein kinase, and c-Abl kinase (The phosphorylation sites are indicated in Figure 1.3) (Chew *et al*. 1998; Butt *et al*. 2003; Lin *et al*. 2004). These phosphorylation and de-phosphorylation processes tightly control the localization and function of Lasp1. For example, Lasp1 binds to non-muscle filamentous actin (F-actin) *in vitro* in a phosphorylation-dependent manner (Chew *et al*. 2002). It was also reported that Abl kinase specifically phosphorylates Lasp1 in apoptotic cells, preventing Lasp1 translocation to focal complexes (Lin *et al*. 2004).

On the other hand, Lasp1 was shown to be transcriptionally up-regulated in response to the morphogen Sonic Hedgehog in pluripotent mesenchymal cells (Ingram

et al. 2002) and induced in cells transformed by over-expression of IGF-1 receptor dependent on PI3-Kinase activities (Loughran *et al*. 2005). As both altered Sonic Hedgehog and IGF-1 signaling have been reported to be associated with cancer progression (Hellawell *et al*. 2002; Lopez and Hanahan 2002; Nishimaki *et al*. 2004), it would be interesting to examine the expression and functional roles of Lasp1 in human cancer as well.

1.3.4. Association of Lasp1 with cancer

Since Lasp1 was initially identified from human breast cancer metastases by Tomasetto *et al* in 1995, both the expression level and functional roles of Lasp1 in breast cancer progression and metastases were reported (Tomasetto *et al*. 1995; Grunewald *et al*. 2006). Lasp1 was shown to be highly expressed in breast cancer tissue and metastatic breast cancer cells. Silencing of Lasp1 by siRNA retarded the cell proliferation and cell migration of breast cancer cells *in vitro* without influencing the expression of other proteins related to Lasp1 signaling pathway. In addition, knockdown of Lasp1 severely affected zyxin localization (Grunewald *et al*. 2006). More recently, Lasp1 has been shown to be involved in ovarian cancer. Knockdown of Lasp1 in ovarian cancer cells had the same effect as in breast cancer cells in arresting cells at G2/M phase, reducing cell proliferation and affecting zyxin localization (Grunewald *et al*. 2007). Apart from these previous studies, it is recognized that the potential roles of Lasp1 in the carcinogenesis of other types of tumors have not been noticed so far and deserve to be characterized.

1.4. The tumor suppressor p53

1.4.1. The TP53 gene

The tumor suppressor p53 was first reported as a 53kDa cellular protein associated with large T antigen in SV40 transformed cells by several independent studies in 1979 (Kress *et al*. 1979; Lane and Crawford 1979; Linzer and Levine 1979). It was initially described as an oncogene, since the sequences originally isolated from tumor cells which were later confirmed as missense mutants, induced neoplastic transformation (Oren and Levine 1983; Eliyahu *et al*. 1984; Harlow *et al*. 1985). As mutations in p53 and loss of heterozygosity at chromosome 17q (where the p53 resides) were later frequently noted in primary human tumors (Mackay *et al*. 1988; Baker *et al*. 1989; Hollstein *et al*. 1991; Greenblatt *et al*. 1994), researchers started to re-define the role of p53. Further studies re-classify p53 as a tumor suppressor in view of the fact that the wild-type P53 protein derived from normal cells was found to inhibit tumor growth instead of triggering cellular transformation (Finlay *et al*. 1989; Baker *et al*. 1990; Mercer *et al*. 1990).

The TP53 gene encodes a multi-modular protein containing 393 amino acids which is commonly divided into three major functional domains. The transcriptional activation activity of p53 requires its acidic amino-terminal domain, where its negative regulator MDM2 can bind (Chen *et al*. 1995). Most of the interactions between p53 and its abundant downstream target genes take place in the central core DNA-binding domain (Ho *et al*. 2006; Veprintsev *et al*. 2006). The carboxyl-terminal end containing a nuclear export signal, 3 nuclear localization sequences and the C-terminal regulatory domain, is also responsible for the oligomerization and functioning of p53 protein as it binds to the DNA targets as a tetramer (McLure and Lee 1998; Shu *et al*. 2007).

When two genes — p63 and p73 exhibiting remarkable sequence homology with p53 were found, the TP53 gene was further characterized as a member of a small family of related proteins (Caput 1997; Jost *et al*. 1997; Yang *et al*. 1998; Melino *et al*. 2002). Although structurally and functionally related, p63 and p73 have clear roles in normal development (Irwin and Kaelin 2001), whereas p53 seems to have evolved in higher organisms as a key tumor suppressor protein at the crossroads of cellular stress response pathways to prevent tumor development (Hussain and Harris 2006). It mainly functions as a transcription factor which is activated in response to several malignancy-associated stress signals. These signals including loss of survival signals, ribonucleotide depletion, DNA damage, oncogenes, telomere erosion, and hypoxia/anoxia, often induce p53 by stabilizing the p53 protein, which leads to an accumulation in cellular p53 levels (Vousden and Lu 2002). Upon activation, p53 protein binds to specific DNA sequence located on the promoter or intron of a large number of its downstream target genes, activates or represses the expression of these genes and results in cell growth inhibition or cell death. The specific p53 binding motif is termed as the p53 response element (RE) with consensus sequences of "PuPuPu**C**(A/T)(A/T)**G**PyPyPy † PuPuPu **C**(A/T)(A/T)**G**PyPyPy" (Pu: purine, Py: pyrimidine, †: spacer of 0-13 nucleotides) (el-Deiry *et al*. 1992).

Characterizing the molecular targets of p53 provides critical information in uncovering its physiological and pathological functions. More than 150 identified p53-regulated genes characterized so far have already well defined its role in cell cycle control, DNA damage repair, apoptosis, hypoxia, and angiogenesis (Dameron *et al*. 1994; Polyak *et al*. 1997; Bouvet *et al*. 1998). A simple illustration of the p53 pathway involving its activation regulation and the main categories of its downstream target genes is shown in Figure 1.4. However, though the number of identified p53 targets

keeps growing, it is conceivable that a large number of p53 downstream genes have not been identified yet.

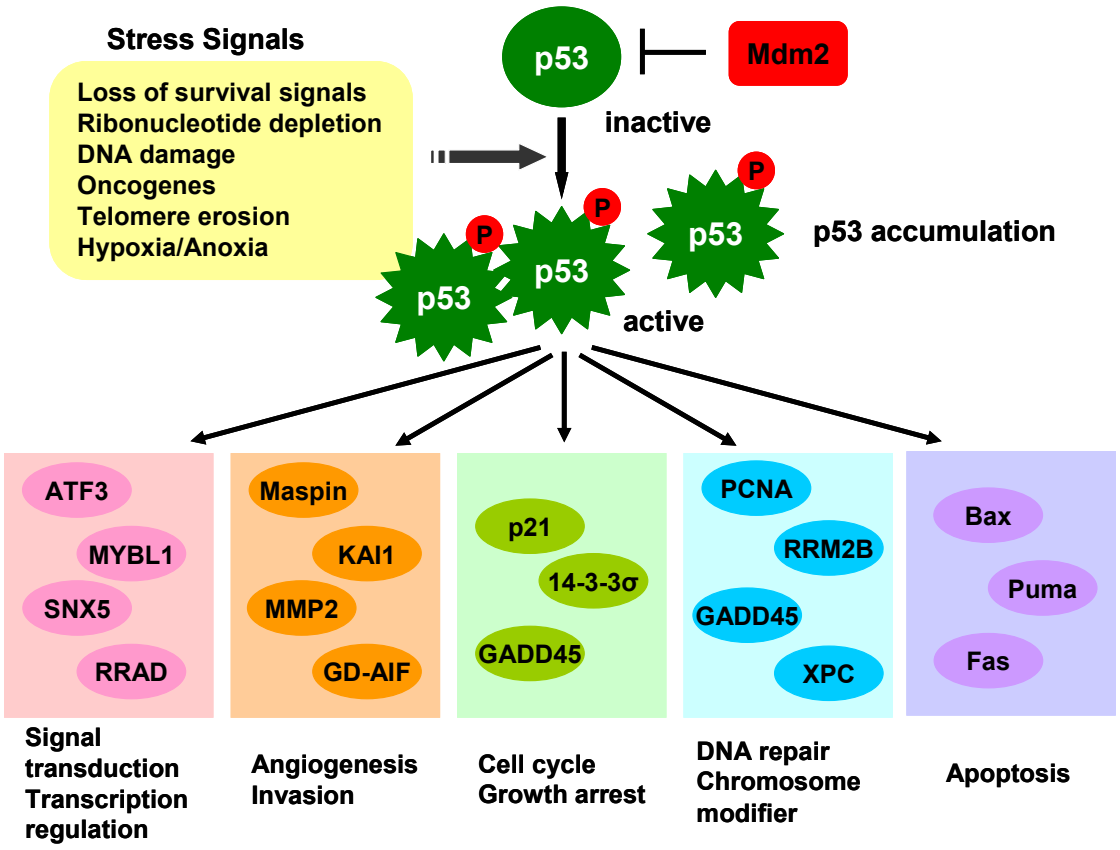

Figure 1.4 Main categories of p53 target genes. In normal unstressed cells, the level of p53 protein is downregulated by binding of proteins such as MDM2, which promote p53 degradation via the ubiquitin/proteasome pathway. Stress signals (listed in yellow box) leads to activation of p53 in a two-step process. Firstly, p53 protein level is rapidly increased via the inhibition of its interaction with MDM2 and the other negative regulators. Secondly, a series of modulators (e.g. kinases) will activate p53 transcriptional activity by phosphorylation. Upon p53 activation, a number of genes are activated by the transactivating properties of p53. This occurs via specific DNA binding of the p53 protein to a p53 response element that is found either in the promoter or in the intron of target genes (Tokino and Nakamura 2000; Vousden and Lu 2002).

1.4.2. Association of p53 with cancer

The malignant progression is largely dependent on loss of p53 function, either through mutation in the TP53 gene itself that is frequently observed in the majority of human cancers or by defects in the signaling pathways that are upstream or downstream of p53. Unlike the mutational spectrum that is usually seen in most of other tumor suppressor genes, in which large deletions, frameshift or nonsense mutations often cause disappearance or aberrant synthesis of the proteins, tumor-associated mutations in TP53 are predominantly point mutations that result in single amino acid substitutions. Interestingly, six residues — 175, 245, 248, 249, 273 and 282 — of p53 show an unexpectedly high frequency of mutations, altogether accounting for 28% of p53 mutations. These missense mutations lead to the synthesis of a relatively stable mutant protein losing the specific DNA-binding activity and accumulating in the nucleus of tumor cells (Vousden and Lu 2002; Soussi *et al*. 2005). In addition, many tumors that harbor point mutations in p53 also show loss of heterozygosity, which further eliminates the wild-type allele of TP53 (Greenblatt *et al*. 1994).

Association of p53 with HCC

Specifically in HCC, the defect in p53 pathway is frequently observed though the mutation spectra vary in different geographic areas. Somatic mutations in p53 detected in HCC are often associated with AFB1 (aflatoxin B1) or viral infections as reviewed by Hussain *et al* (2007). AFB1 exposure frequently induces a point mutation of p53 at codon 249 leading to Arg → Ser (AGG → AGT) substitute and the resulting 249^{Ser} mutant effectively inhibits wild-type p53-mediated apoptosis, making tumor cells gain growth advantages (Bressac *et al*. 1991; Aguilar *et al*. 1993; Wang *et al*. 1995). The p53 mutation is also attributed to viral infections as it was suggested that the

combination of AFB1 intake and HBV infection may be critical to the high frequency of 249^{Ser} mutation of p53 in HCC (Ming *et al*. 2002). As this 249^{Ser} mutation of p53 is uncommon in other cancer types and it could be detected in serum and plasma of HCC patients, it may be used as a specific biomarker for AFB1 exposure and possibly early HCC (Kirk *et al*. 2000; Kirk *et al*. 2005). As introduced in section 1.1.2, HBxAg transactivation activity (Nijhara *et al*. 2001; Tarn *et al*. 2001) or its direct binding to p53 may inactivate the p53-dependent activities, including p53 sequence-specific DNA-binding activity *in vitro* and p53-mediated transcriptional activity *in vivo*, and even repress the transcription of TP53 gene (Feitelson *et al*. 1993; Wang *et al*. 1994; Ueda *et al*. 1995; Lee and Rho 2000). In order to further examine the role of p53 in HCC, Okada *et al* (2003) analysed a number of TP53 mutant and TP53 wild-type HCC cases by microarray, showing that HCV-infected HCCs with wild-type p53 and those with mutant p53 differ significantly in their gene expression profiles. Some cell cycle and cell proliferation related genes were over-expressed in mutant p53 tumors compared to wild-type p53 tumors, suggesting that HCV infection also contributes to hepatocarcinogenesis involving p53 pathways, and the mutant p53 HCC tumors have a high malignant potential than those carrying wild-type p53 (Okada *et al*. 2003).

Association of p53 with cancer metastasis

Recently, increasing lines of evidences indicate that p53 also functions in regulating cell migration, invasion, and cancer metastasis through targeting genes functionally linked to cytoskeletons. Several tumor metastasis suppressor genes, such as Maspin, KAI1/CD82 have been demonstrated to be *bona fide* p53 targets which can be transcriptionally activated by p53 (Mashimo *et al*. 1998; Zou *et al*. 2000; Liu and Zhang 2006). Maspin was discovered as a human mammary tumor suppressor in 1994 (Zou *et*

al. 1994) and has been shown to inhibit tumor cell invasion and metastasis in breast tumor cells (Zou *et al*. 2000; Hojo *et al*. 2001; Maass *et al*. 2001). Its anti-tumor effects are also linked to prostate cancer (Sheng *et al*. 1996) and pancreatic cancer (Maass *et al*. 2001). KAI1 was initially identified as a metastasis suppressor of prostate cancer (Dong *et al*. 1995), but it is now thought as a wide-spectrum tumor metastasis suppressor by primarily inhibiting cancer motility and invasiveness (Liu and Zhang 2006). Its expression was reported to be down-regulated during prostate tumor progression and low expression of KAI1 correlates well with the loss of p53 function. Despite the variable frequency of p53 mutations reported in primary prostate tumors, metastatic tumors exhibit a higher incidence of p53 mutations (Effert *et al*. 1992; Heidenberg *et al*. 1996). These findings provide a mechanistic explanation for the increased metastatic susceptibility of tumors carrying p53 mutants, and suggest that elucidating the roles of p53 downstream target genes may contribute to the emerging p53 functions.

1.5. Objectives of the study

As the fifth most common cancer in the world, the prognosis in HCC is dismal, with high morbidity and mortality rates associated with tumor invasion and metastasis (Llovet *et al*. 2003). Metastasis is the major barrier to curative cancer treatments and the primary cause of death in cancer patients (Hunter 2006). However, the mechanisms underlying metastasis of HCC have not been completely elucidated (Tang *et al*. 2004). Thus characterizing roles of metastasis-associated genes will strengthen our understanding in the molecular pathogenesis of HCC metastasis as well as hepatocarcinogenesis for developing early diagnostic markers and effective therapeutic interventions.

A number of gene expression profiling studies have been performed to reveal multiple genetic aberrations and heterogeneous dysregulation of oncogenic pathways in HCC development (Okabe *et al*. 2001; Shirota *et al*. 2001; Chen *et al*. 2002a). Our previous cDNA microarray study identified two metastasis related genes Cyr61 and Lasp1, which have aberrant expression of being down-regulated and up-regulated, respectively in HCC (Neo *et al*. 2004). As described in previous sections, both Cyr61 and Lasp1 are located at the focal adhesion signaling network and functionally related to the dynamics of cytoskeleton and cell migration. In addition, Cyr61 is a well-studied gene associated with progression and angiogenesis of a variety of tumors, while Lasp1 is thought to be highly related to breast cancer metastasis. However, their roles in the development and metastasis of HCC have yet to be explored. Therefore, the present study is mainly focused on investigating the potential roles of Cyr61 and Lasp1 in growth and metastasis of human HCC by *in vitro* study using HCC cell lines.

The transcription factor p53 may also function in regulating tumor metastasis. However, though several tumor metastasis suppressor genes have been demonstrated to

be p53 targets that can be transcriptionally activated by p53, the understanding to the downstream targets of p53 involved in invasion/metastasis remains rather limited. In a recent study from Genome Institute of Singapore, 20 previously unidentified p53 targets involved in cell motility, adhesion, and migration were reported, suggesting that a number of novel p53 targets could be involved in p53-mediated suppression of tumor metastasis. Functional analysis of these genes could help to reveal a broader spectrum of p53 functions. Interestingly, Lasp1 was identified as one of the potential p53 target genes through this study by coupled ChIP with the paired-end ditag technologies (ChIP-PET) (Wei *et al*. 2006) (Supplemental Data). These findings provide us with a clue that p53 may play a more diversified role in regulating cell migration by transcriptionally suppressing mRNA expression of genes involved in the dynamics of cytoskeletons as well. As such, the aims of the current study also include the validation of Lasp1 as a novel *bona fide* p53 target by showing the role of p53 in transcriptionally suppressing Lasp1 expression, which suggests a novel mechanism of p53 in inhibiting tumor metastasis.

From the literature review, we noticed that Cyr61 inhibits the growth of the non-small-cell lung cancer by up-regulating p53 through the Cyr61–integrin–β-catenin–c-*myc*–p53 pathway (Tong *et al*. 2004). Since our microarray data showed that Cyr61 is also down-regulated in HCC, identification of the potential role of Cyr61 in up-regulating p53 in HCC cells as well would be an appealing idea as it links Cyr61 and Lasp1 to the central master regulator of p53 in HCC. Hence, this study also aims to construct a pathway involving Cyr61 and Lasp1 by showing Cyr61 as an upstream regulator of p53 in HCC cells and in turn contribute to the existing knowledge and the comprehensive view of mechanisms of HCC progression and metastasis.

The scope of this study thus includes the following aspects:

1. To validate the microarray data of aberrant expression of Cyr61 and Lasp1 using HCC clinical tumor samples and HCC cell lines.
2. To identify the roles of Cyr61 and Lasp1 in regulating cell growth, adhesion, migration and invasion ability in HCC cell lines.
3. To investigate possible mechanisms of Lasp1 in influencing cell migration and invasion in HCC cell lines.
4. To explore possible mechanisms of Cyr61 in regulating HCC cell growth involving p53.
5. To verify the role and mechanism of p53 in transcriptionally suppress Lasp1 expression.

CHAPTER 2

MATERIALS AND METHODS

Media, Buffers and Solutions, and Chemicals

The media, buffer and solutions, and chemicals used in this study are listed in Appendix I.

2.1. Patient samples

Total RNA from 8 pairs of matched tumor and non-tumor liver tissues were randomly selected from a collection of 37 HCC patients used in a previous microarray study (Neo *et al*., 2004).

2.2. Cell culture techniques

The human hepatocellular cancer cell lines HepG2 (ATCC HB-8065), Hep3B (ATCC HB-8064), Huh-7 and PLC/PRF/5 (ATCC CRL-8024) were originally obtained from the American Type Culture Collection (Manassas, VA) and stored frozen in liquid nitrogen at WHO Immunology Centre, National University of Singapore. The human colon cancer cell line HCT116 and its derived isogenic p53-/- cells were kindly provided by Dr. Bert Vogelstein (Johns Hopkins University, Baltimore, MD).

2.2.1. Growth of HCC cell lines and colon cancer cell lines

HCC cell lines stored frozen in liquid nitrogen were thawed quickly at 37°C water bath and re-suspended in 10ml of DMEM/10%FBS (Appendix I) under sterile conditions. Cells pelleted by centrifuging at 900rpm for 5 minutes were gently re-suspended in 7ml of DMEM/10% FBS and transferred to 25ml culture flasks (Falcon, BD Biosciences, Franklin Lakes, NJ). The cell culture was incubated at 37°C in a 5% CO_2 humidified incubator. The density of the cells was monitored and culture medium was changed as necessary. When cell density reached 90-100% confluence,

the cells were trypsinized in 0.25% trypsin/EDTA (Invitrogen, Carlsbad, CA) for 5min at 37°C and stopped by adding fresh DMEM/10%FBS. Then all cells were transferred to a new 75ml culture flask. Cells were then maintained in 75ml culture flask or expanded into 150ml culture flasks depending on the number of cells needed for experiments.

2.2.2. Freezing HCC cell lines and colon cancer cell lines

Upon achieving 80-90% confluent growth, the cells cultured in 75ml or 150ml flask were trypsinized and collected by centrifuging at 1000rpm for 5 minutes and the supernatant discarded. The pellet was re-suspended in 3ml (75ml flask) or 5ml (150ml flask) ice-cold freezing medium (Appendix I) and transferred into labeled NUNC CyroTube vials (1ml per vial) (Thermo Fisher Scientific, Rochester, NY). The vials were kept at -80°C overnight before stored at liquid nitrogen.

2.2.3. Harvesting HCC cell lines and colon cancer cell lines

Upon achieving confluent growth, the cell cultures in the culture flask or culture plate were trypsinized and collected by centrifuging at 1000rpm for 5 minutes and the supernatant discarded. The pellet was washed in 1ml phosphate buffered saline (PBS) (Appendix I) after transferred to 1.7ml eppendorf tubes and centrifuged at 500 × g for 5 minutes, with the supernatant once again discarded. Cell pellets were then subjected to total RNA or lysate collection or kept at -80°C for short term storage.

2.3. Polymerase chain reaction (PCR)

2.3.1. Total RNA extraction

As mentioned above, total RNA from 8 pairs of matched tumor and non-tumor liver tissues were randomly selected from a collection of 37 HCC patients used in a previous microarray study. Total RNA samples from 15 types of normal human tissues were purchased from Stratagene (La Jolla, CA). Total RNA from the experimental cells was extracted using the RNeasy Mini Kit (Qiagen, Valencia, CA) according to the manufacturer's instructions. After quantified by Nanodrop (ND-1000) (Nanodrop Technologies, Delaware, USA), these RNA samples were either directly used for subsequent one-step real-time quantitative RT-PCR or subjected to cDNA (complementary DNA) synthesis followed by two-step real-time quantitative or semi-quantitative RT-PCR.

2.3.2. cDNA synthesis

The cDNA was synthesized using Omniscript® RT kit (Qiagen) according to the manufacturer's instructions. Briefly, total RNA was pretreated at 65°C for 10min and immediately transferred onto ice for 5min to denature the secondary structure of RNA. The 1st strand cDNA was synthesized in a total volume of 20μl reaction mixture, containing 2μl of 10 × buffer RT, 2μl of 5mM dNTP mix, 2μl of oligo-$(dT)_{15\text{-}18}$ primer (1μM final concentration), 1μl of RNase inhibitor (RNaseOut, Invitrogen), 1μl of omniscript reverse transcriptase, and 1μg of total RNA as template. The reaction was performed by incubating at 37°C waterbath for 1 hour and chilled on ice for 5min to stop the reaction. The first strand cDNA was then 10 times diluted by DNase/RNase free H_2O (Invitrogen), aliquoted and stored at -20°C until use.

2.3.3. Real-time quantitative RT-PCR

One-step real-time RT-PCR

To validate the microarray data, the expression of Cyr61 or Lasp1 mRNA in eight pairs of liver tissues was analyzed by one-step real-time quantitative RT-PCR using RNA Master SYBR Green I kit in a LightCycler (Roche Applied Science, Mannheim, Germany) with previously collected total RNA samples (Neo *et al.*, 2004). All primers were synthesized by Sigma-Proligo (Singapore) and dissolved in DNase/RNase free H_2O to give a final working concentration of 10μM (sequence listed in Table 2.1). In brief, 10ng of total RNA for each sample was loaded (in duplicate) in a 10μl reaction volume containing 3.7μl of 2.7 × RNA Master Mix SYBR, 0.65μl of $Mn(OAc)_2$ stock solution (3.25mM final concentration), 0.5μM of each forward and reverse primer. After normalized to a housekeeping gene HPRT, data were presented as the fold change of the gene expression in each non-tumor tissue against its corresponding tumor sample for down-regulated gene (Cyr61) or that in each tumor against its matched non-tumor sample for up-regulated gene (Lasp1).

Two-step real-time RT-PCR

To measure the knockdown effect of siRNA and to examine the role of p53 in transcriptionally suppressing Lasp1 gene expression, two-step real-time quantitative RT-PCR was performed. After total RNA extraction, the first stand cDNA was synthesized using the Omniscript® RT kit. The real-time RT-PCR was then performed with 2μl of cDNA (10 times diluted) as the template in a 10μl reaction in triplicates using 2 × SYBR Green 1 PCR Master Mix (Applied Biosystems, Foster City, CA) according to the manufacturer's instructions in the ABI PRISM 7500

system. The primer sequences were listed in Table 2.1, with HPRT used as the housekeeping gene.

2.3.4. Gel-based semi-quantitative RT-PCR

RT-PCR was carried out in an ABI GeneAmp PCR 9700 system in a final volume of 20μl reaction containing 0.5μl of synthesized cDNA (5μl of 10 × diluted cDNA) as template, 0.5μM of each forward or reverse primer (Table 2.2), and 10μl of 2 × High Fidelity PCR Master Mix (Roche). After initial denaturing at 94°C for 2 min, the amplification was carried out for 25-35 cycles each consisting of denaturing for 30sec at 94°C, annealing for 30-60sec at 52-60°C (depending on primers' Tm), and extension for 30-120sec (depending on the product size) at 68 or 72°C, followed by a final extension for 6-20 min at 68 or 72°C before cooling down to 4°C. Total PCR products were separated on 1-1.5% agarose gel electrophoresis in TBE buffer (Appendix I) and stained with ethidium bromide (Bio-Rad, Hercules, CA). Gel photos were taken under UV transilluminator and the band intensities of gel-based RT-PCR product were measured by densitometry.

Table 2.1 Oligonucleotide primers used in real-time quantitative RT-PCR

GENE	Primer Name	Oligonucleotide Sequence	Length	Position	Product Size
Cyr61	Cyr61-F1	5' AAGGGGCTGGAATGCAA 3'	17bp	220-236	193bp
	Cyr61-R1	5' GTTCTTGGGGACACAGAGGA 3'	20bp	412-393	
Lasp1	Lasp1-F	5' GTATCCCACGGAGAAGGTGA 3'	20bp	111-130	275bp
	Lasp1-R	5' TGTCTGCCACTACGCTGAAA 3'	20bp	385-366	
p53	p53-F	5' CCAGGGCAGCTACGGTTTC 3'	19bp	429-447	205bp
	p53-R	5' CTCCGTCATGTGCTGTGACTG 3'	21bp	633-613	
p21	p21-F	5' GACACCACTGGAGGGTGACT 3'	20bp	403-422	331bp
	p21-R	5' GGATTAGGGCTTCCTCTTGG 3'	20bp	733-714	
HPRT	HPRT-F	5' GTAATGACCAGTCAACAGGGGAC 3'	23bp	402-424	177bp
	HPRT-R	5' CCAGCAAGCTTGCGACCTTGACCA 3'	24bp	578-555	

Table 2.2 Oligonucleotide primers used in gel-based semi-quantitative RT-PCR

GENE	Primer Name	Primer Sequence	Length	Position	Product Size
Cyr61	Cyr61-F2	5' TCCCTGTTTTTGGAATGGAG 3'	20bp	657-676	240bp
	Cyr61-R2	5' TGGTCTTGCTGCATTTCTTG 3'	20bp	896-877	
Lasp1	Lasp1-F	5' GTATCCCACGGAGAAGGTGA 3'	20bp	111-130	275bp
	Lasp1-R	5' TGTCTGCCACTACGCTGAAA 3'	20bp	385-366	
14-3-3σ	14-3-3σ-F	5' ACCACAGTCCATGCCATCA 3'	19bp	56-74	279bp
	14-3-3σ-R	5' TCCACCACCCTGTTGCTGTA 3'	20bp	334-315	
GADD45	GADD45-F	5' ACGAGGACGACGACAGAGAT 3'	20bp	468-487	262bp
	GADD45-R	5' TCCCGGCAAAAACAAATAAG 3'	20bp	729-710	
GAPDH	GAPDH-F	5' ACCACAGTCCATGCCATCA 3'	19bp	601-619	452bp
	GAPDH-R	5' TCCACCACCCTGTTGCTGTA 3'	20bp	1052-1033	

2.4. Molecular cloning techniques

2.4.1. General cloning protocol

Insert preparation

The Insert DNA was prepared by PCR using High Fidelity PCR Master Kit (Roche) in ABI GeneAmp PCR 9700 system following the manufacturer's instructions. The template used was cDNA (for gene open reading frame, ORF) or genomic DNA (for gene promoter region) from certain tissue samples or cell lines. The primer sequences were listed in Table 2.3 and Table 2.6. The PCR products were monitored for quantity and quality by 1% agarose gel electrophoresis and were used directly or purified (PEG purification, gel purification, or by PCR purification kit) before any cloning reactions will be performed.

Enzyme digestion

The purified PCR products, the parental vectors or the intermediate vectors were digested at 37°C waterbath for 2 hours or overnight in a 30-100µl total reaction volume containing PCR products or 1-6µg of plasmids, 1/10 total volume of 10 × appropriate NEB buffer, 1µl 100 × BSA (10mg/ml), and 5-20U of specific restriction enzyme(s) (New England Biolabs, Ipswich, MA) (Table 2.4 and Table 2.7). The DNA fragments with expected sizes or linearized vectors were gel purified or phenol/chloroform purified.

Ligation

The ligation reaction was normally performed at 16°C waterbath with overnight incubation (for blunt ends) or at room temperature for 30 minutes (quick ligation for sticky ends) in a 20µl reaction containing 4µl of ligation buffer (5 ×), 1µl

of linearized vector DNA, 1~14µl of insert DNA, and 1µl of T4 DNA ligase (Invitrogen).

Transformation

The library efficiency® DH5α™ chemically competent *E.coli* (Invitrogen) was chosen for all transformations in this study. For each transformation, 50µ1 of competent cells were aliquoted into a sterile 5ml polypropylene falcon tube. 1~2µ1 of the cloning reaction product was added into the tube containing the competent cells and mixed gently by tapping followed by incubation on ice for 30 minutes. Heat-shock the cells for 45-60 seconds at 42ºC waterbath without shaking before immediately transferred onto the ice. Add 250~450µ1 of room-temperature S.O.C. medium (Invitrogen) and shake the tube horizontally at 200rpm in a 37ºC incubator shaker for 30-60min to recover the cells. Spread 20~100µ1 from each transformation on a pre-warmed LB plate containing appropriate antibiotics (50µg/ml Kanamycin or 100µg/ml Ampicillin) and incubate at 37ºC overnight.

Screening for positive clones

6~12 clones were initially screened by colony PCR using cloning primers or internal primers for specific genes. Then those clones showing positive PCR results with correct sizes were inoculated and propagated by culturing in LB medium containing appropriate antibiotics with overnight shaking incubation at 37°C. The bacteria cultures were then subjected to plasmid extraction using Wizard® Plus SV Minipreps DNA Purification System (Promega). The isolated plasmids were used for enzyme digestion and further confirmation by sequencing analysis.

Sequencing

All sequencing analysis was performed by the Scientific Community Sequencing Facility (SCSF) at Genome Institute of Singapore. The primers used in sequencing the vectors constructed in this study were summarized below in Table 2.5 and 2.8.

2.4.2. Gateway cloning for gene ORF

The Gateway™ Technology with lambda-based recombination system from Invitrogen was used in this study to clone Cyr61 and Lasp1 gene ORF into two pcDNA3.1 derived expression vectors, pcDNA-DEST40 with V5-epitope tag and pcDNA-DEST47 with fused green fluorescent protein (GFP). The pDONR™221 (Figure 2.1), pcDNA-DEST40 (Figure 2.2) and pcDNA-DEST47 vectors (Figure 2.3) were kindly provided by Dr. Chia-Lin Wei (Genome Institute of Singapore, Singapore). Briefly, the full ORF of Cyr61 or Lasp1 was amplified from normal liver cDNA and normal colon cDNA respectively by two rounds of PCR. A BP recombination reaction was then performed by using the *att*B-flanking Cyr61 or Lasp1 PCR product and the *att*P-containing pDONR™221 vector to create a Cyr61-221 and Lasp1-221 entry clone. Further LR recombination reactions between the *att*L-containing entry clone and the *att*R-containing destination vectors (pcDNA-DEST40 or pcDNA-DEST47) produced the final Cyr61 and Lasp1 expression constructs pDEST40-Cyr61/V5, pDEST47-Cyr61/GFP, pDEST40-Lasp1/V5 and pDEST47-Lasp1/GFP.

Propagating Gateway vectors

Due to the lethal effects of the *Ccd*B protein, all Gateway vectors containing the *ccd*B gene must be propagated in an *E.coli* strain that is resistant to *Ccd*B effects. Hence, the DB3.1 *E.coli* strain (Invitrogen) which contains a gyrase mutation (*gyr*A462) rendering it resistant to *Ccd*B effects was used in propagating the Gateway vectors pDONR221, pcDNA-DEST40 and pcDNA-DEST47.

Insert preparation

Two rounds of PCR reactions were performed to amplify the Cyr61 or Lasp1 ORF from normal liver total RNA and normal colon cDNA respectively. Primers were dissolved in DNase/RNase free H_2O to give a final concentration of 10μM. The first set of primers were for gene-specific amplification and included 12 bases of the *att*B1 or *att*B2 site on the 5' end of forward or reverse primer respectively (GW-Cyr61-F, GW-Cyr61-R; GW-Lasp1-F, GW-Lasp1-R). The second set of adaptor-primers to install the complete *att*B sequences were *att*B1 (forward) and *att*B2 (reverse) (sequence listed in Table 2.3, with the *att*B-flanking sequences highlighted in blue).

Table 2.3 Oligonucleotide primers used in Gateway cloning

GENE	Primer Name	Primer Sequence	Length
Cyr61	GW-Cyr61-F	5' AAAAAGCAGGCTCCACAATGAGCTCCCGCATC 3'	32bp
	GW-Cyr61-R	5' AGAAAGCTGGGTAGTCCCTAAATTTGTGAATGTC 3'	34bp
Lasp1	GW-Lasp1-F	5' AAAAAGCAGGCTCAACCATGAACCCCAACTGC 3'	32bp
	GW-Lasp1-R	5' AGAAAGCTGGGTAGATGGCCTCCACGTAGTTG 3'	32bp
	att B1	5' GGGGACAAGTTTGTACAAAAAAGCAGGCT 3'	29bp
	att B2	5' GGGGACCACTTTGTACAAGAAAGCTGGGT 3'	29bp

The compositions of the RT-PCR reaction mixtures were as the following:

For 1st PCR:

2 × PCR Master Mix (Tube 1)	12.5 µl
Forward Primer (10µM)	0.5 µ1
Reverse Primer (10µM)	0.5 µ1
Template cDNA	1 µ1
H_2O (PCR grade) (Tube 2)	10.5 µl
Total Volume	25 µl

The PCR profile was as follows:

1 cycle	94ºC	2min
15~18 cycles	94ºC	15sec
	53~58ºC	30sec
	68ºC	1min per 1kb
1 cycle	4ºC	forever

For 2nd PCR:

2 × PCR Master Mix (Tube 1)	25 µl
*att*B1 (10µM)	2.5 µ1
*att*B2 (10µM)	2.5 µ1
1st PCR product	10 µ1
H_2O (PCR grade) (Tube 2)	10 µl
Total Volume	50 µl

The PCR profile was as follows:

1 cycle	94ºC	2min
5 cycles	94ºC	15sec
	45ºC	30sec
	68ºC	1min per 1kb
20 cycles	94ºC	15sec
	53~58ºC	30sec
	68ºC	1min per 1kb
1 cycle	68ºC	7min
	4ºC	forever

The 2nd PCR reaction product (2-3µl) was analyzed using agarose gel electrophoresis in order to verify the quality and yield. Then purification of the PCR product by PEG/$MgCl_2$ solution was performed in order to remove *att*B primers and any primer-dimers. Firstly, add 150µl of TE buffer (pH 8.0) and 100µl of 30% PEG 8000/30mM $MgCl_2$ (Invitrogen) to a 50µl amplification reaction containing the *att*B-PCR product. After thoroughly mixed by vortexing, the mixture was centrifuged immediately at 10,000 × g for 15 minutes at room temperature. Carefully remove the supernatant, dissolve the pellet in 50µl TE buffer (to concentration > 10ng/µl), and check the quality and quantity of the recovered *att*B-PCR product on an agarose gel again.

BP recombination cloning

BP recombination reaction was performed between PEG purified *att*B-PCR product and the Gateway donor vector pDONR™221. The following components were added in order into a 0.2ml PCR tube at room temperature and mix.

*att*B-PCR product	1-10 µl
pDONR™221 (150ng/µl)	2 µ1
5 × BP Clonase™ Reaction Buffer	4 µ1
TE Buffer (pH 8.0)	to 16 µ1

Remove BP Clonase enzyme mix from -80ºC and thaw on ice (~2min). After vortexing twice briefly (~2 sec each time), add 4µl to each reaction and vortex briefly to mix well. Incubate the reaction at 25ºC in a PCR machine for 1 hour. Add 2µ1 of Proteinase K into each reaction and incubate at 37ºC waterbath for 10 minutes. Then 1µl of the BP recombination reaction product was transformed into the library efficiency® DH5α™ chemically competent *E.coli* according to standard protocol as described in section 2.4.1. Spread 50~100µ1 from each transformation on a pre-

warmed LB plate containing 50μg/ml of Kanamycin and incubate at 37ºC overnight. 10~12 clones were initially screened by colony PCR using internal primers of Cyr61 or Lasp1 gene. Then positive clones were inoculating and propagating by culturing in LB medium containing 50μg/ml of Kanamycin overnight for plasmid extraction. The isolated plasmids were used for enzyme digestion (Table 2.4) and further confirmation by sequencing (Table 2.5).

LR recombination cloning

LR recombination reaction was performed between *att*L-containing entry clone Cyr61-DONOR221 or Lasp1-DONOR221 and the *att*R-containing destination vector pcDNA-DEST40 or pcDNA-DEST47. The following components were added in order into a 0.2ml PCR tube at room temperature and mix.

Cyr61-DONOR221/Lasp1-DONOR221 (50ng/μl)	6 μl
pcDNA-DEST40/pcDNA-DEST47 (150ng/μl)	2 μ1
5 × BP Clonase™ Reaction Buffer	4 μ1
TE Buffer (pH 8.0)	4 μ1

Similarly as in BP reaction, add 4μl of LR Clonase enzyme mix to each LR reaction and vortex briefly to mix well. Incubate the reaction at 25ºC in a PCR machine for 1 hour. Add 2μ1 of Proteinase K into each reaction and incubate at 37ºC waterbath for 10 minutes. Then 1μ1 of the LR recombination reaction product was transformed into the library efficiency® DH5α™ chemically competent *E.coli* according to standard protocol as described before. Spread 30~50μ1 from each transformation on a pre-warmed LB plate containing 100μg/ml of Ampicillin and incubate at 37ºC overnight. 4-6 colonies were picked for each transformation and inoculated into 3ml LB medium containing 100μg/ml of Ampicillin and cultured

overnight for plasmid extraction. The isolated plasmids were used for enzyme digestion (Table 2.4) and further confirmation by sequencing (Table 2.5).

Propagating expression vectors

The final constructed expression vectors (Cyr61-DEST40, Cyr61-DEST47, Lasp1-DEST40, and Lasp1-DEST47) were propagated in LB medium and extracted by using QIAfilter™ Plasmid Maxi kit (Qiagen) according to the manufacturer's instructions.

Table 2.4 Restriction enzymes used in Gateway cloning

Construct	Restriction Enzyme	Buffer	Expected Fragment Size
Cyr61-DONOR221	Nco I + EcoR V	NEB3	749bp, 2943bp
Cyr61-DEST40	Pvu II	NEB2	538bp, 1071bp, 1096bp, 3879bp
Cyr61-DEST47	Hind III	NEB2	1291bp, 5931bp
	Nco I	NEB1~4	735bp, 814bp, 814bp, 1512bp, 3347bp
Lasp1-DONOR221	EcoR V + Sph I	NEB2	815bp, 2517bp
Lasp1-DEST40	Nco I	NEB1~4	487bp, 735bp, 1655bp, 3347bp
Lasp1-DEST47	Hind III	NEB2	931bp, 5931bp
	Nco I	NEB1~4	490bp, 735bp, 778bp, 1512bp, 3347bp

Table 2.5 Oligonucleotide primers used in sequencing Gateway vectors

Primer Name	Primer Sequence	Length	Vector Origin
M13-forward	5' GTAAAACGACGGCCAG 3'	16bp	pDONR221
M13-reverse	5' CAGGAAACAGCTATGAC 3'	17bp	pDONR221
T7-promoter	5' TAATACGACTCACTATAGGG 3'	20bp	pcDNA-DEST40, pcDNA-DEST47
att B2	5' GGGGACCACTTTGTACAAGAAAGCTGGGT 3'	29bp	pcDNA-DEST40, pcDNA-DEST47

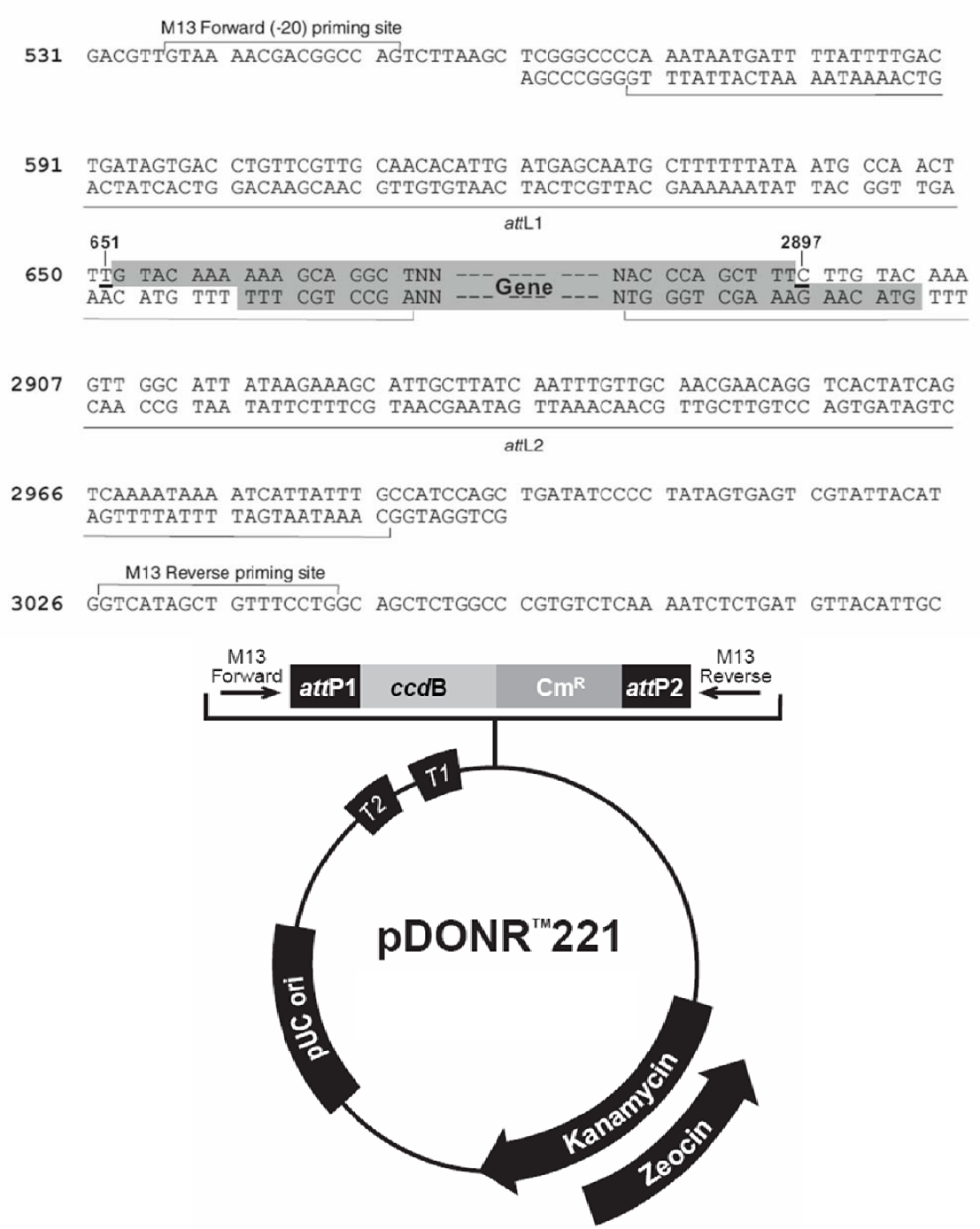

Figure 2.1 Map of the pDONR™221 vector. The map shows the cloning frames and main features of the vector. The *att* sites and M13 forward and reverse priming sites are indicated.

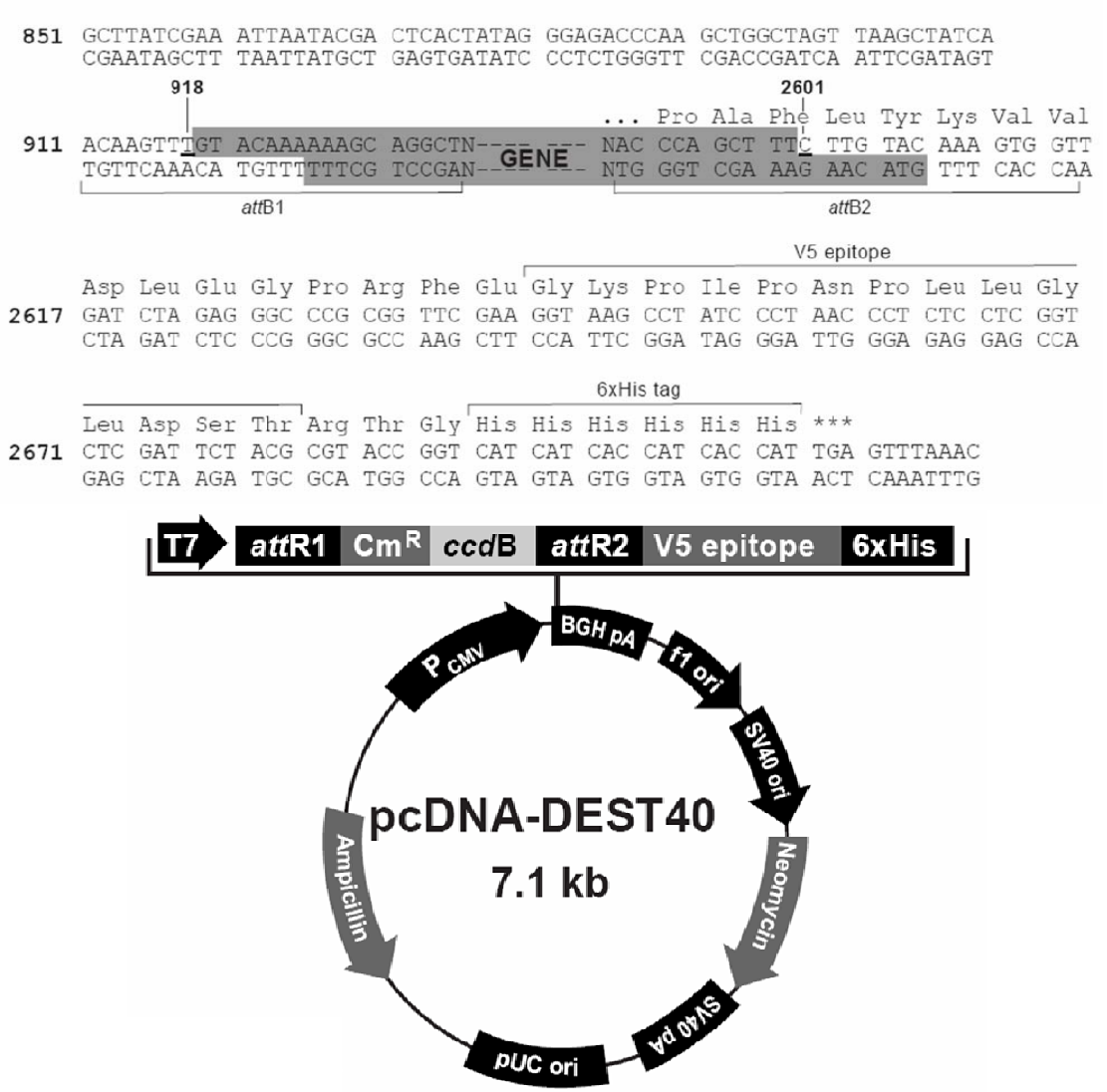

Figure 2.2 Map of the pcDNA-DEST40 vector. The map shows the features of the recombination region and all basic elements of the vector. The V5 epitope and 6 × His tag are indicated.

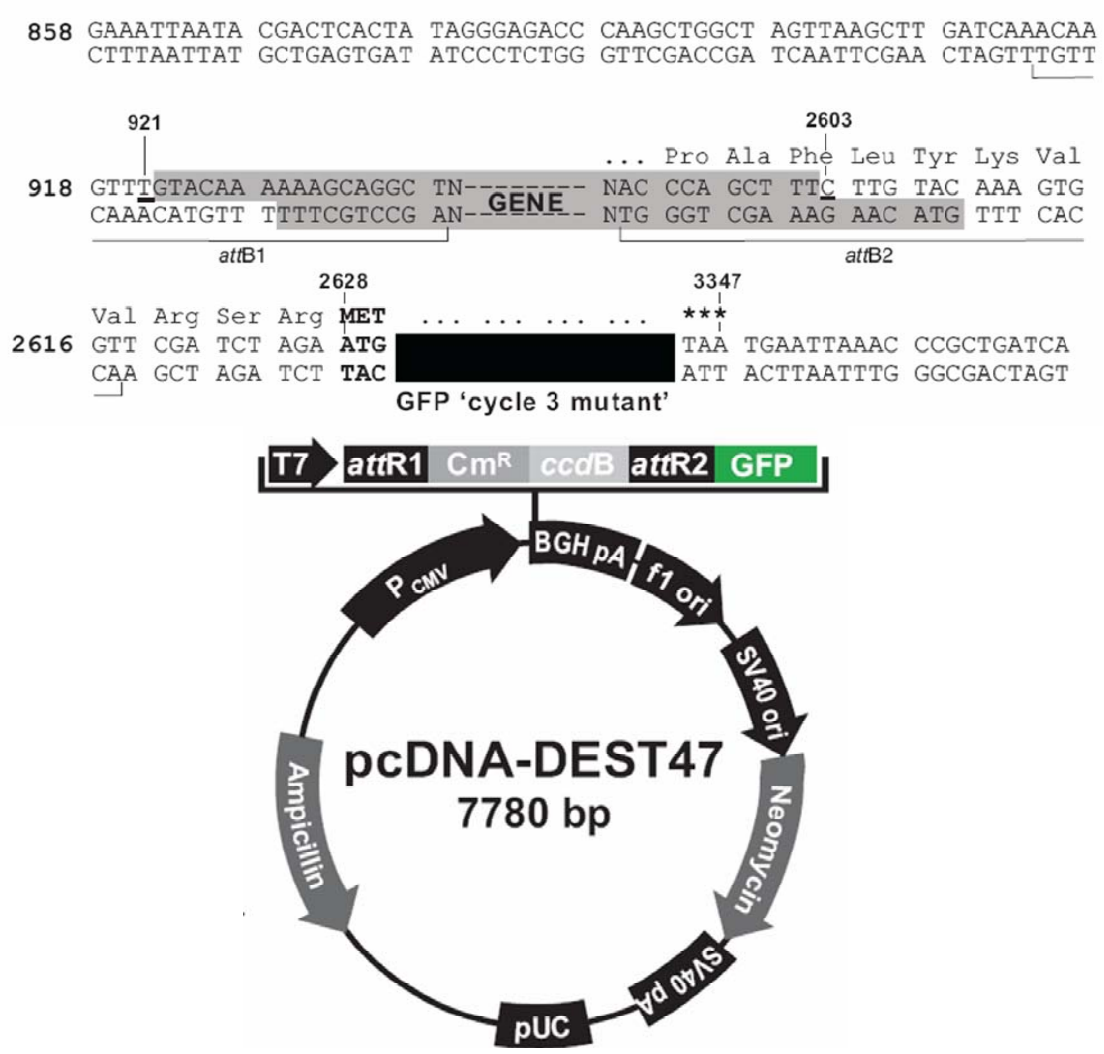

Figure 2.3 Map of the pcDNA-DEST47 vector. The map shows the features of the recombination region and all basic elements of the vector. The GFP tag is indicated.

2.4.3. pGL3- cloning for gene promoter region

The pGL3 luciferase reporter vector system (Promega) provides a basis for the quantitative analysis of factors that potentially regulate mammalian gene expression. In this study, pGL3-Basic vector was chosen to clone the DNA of Lasp1 promoter region for luciferase assay in order to investigate the role of p53 in regulating Lasp1 promoter activity. Briefly, part of the Lasp1 promoter DNA was amplified from genomic DNA extracted from HepG2 cells and cloned into pCR®-TOPO-BluntII (Invitrogen) (Figure 2.4) as an intermediate vector. Then the Lasp1-PR was sub-cloned into the pGL3-Basic vector (Figure 2.5).

Genomic DNA extraction

Genomic DNA was extracted from HepG2 cells using DNeasy Mini Kit (Qiagen) according to manufacturer's instructions and quantified by Nanodrop.

Insert preparation

To prepare the insert, PCR reaction was performed by using HepG2 genomic DNA as template. In order to efficiently amplify the GC-rich Lasp1 promoter region, the PCR grade DMSO (5%) was included in the PCR reaction. The primer sequences were listed in Table 2.6.

The compositions of the PCR reaction mixtures were as the following:

2 × PCR Master Mix (Tube 1)	12.5 µl	
Lasp1-PR-F (10µM)	1 µ1	
Lasp1-PR-R (10µM)	1 µ1	
Total DNA template (50ng/µl)	2 µ1	
H_2O (PCR grade) (Tube 2)	7.25 µl	
DMSO (PCR grade)	1.25 µl	(5%)
Total Volume	25 µl	

The PCR profile was as follows:

1 cycle	94ºC	2min
40 cycles	94ºC	15sec
	53ºC	45sec
	72ºC	2.5min
1 cycle	72ºC	20min
	4ºC	forever

The PCR products (5µl) were separated in a 1.0% agarose gel and visualized under UV transilluminator for quality and quantity control. The PCR product with expected size (~1.9kb) was purified by QIAquick PCR purification kit (Qiagen) according to the manufacturer's instruction before used for the following TOPO-Blunt cloning.

TOPO-Blunt cloning

According to the guide of pCR®-Blunt II-TOPO cloning kit (Invitrogen), 1µl salt solution, 4µl purified PCR product and 1µl linearized pCR®-Blunt II-TOPO vector (Figure 2.4) were mixed up gently in a total 6µl reaction volume in a 0.2ml PCR tube and incubate at room temperature for at least 5 minutes. Then the reaction product was transformed into the library efficiency® DH5α^{TM} chemically competent *E.coli* according to standard protocol. Spread 50~100µ1 from the transformation on a pre-warmed LB plate containing 50µg/ml of Kanamycin and incubate at 37ºC overnight. To analyze positive clones, around 10 colonies were initially screened by colony PCR using the original primer set for PCR. Then positive clones were inoculated and propagated by culturing in LB medium containing 50µg/ml of Kanamycin overnight for plasmid extraction. The isolated plasmids were used for enzyme digestion (Table 2.7) and further confirmation by sequencing (Table 2.8). The

constructed plasmid was defined as TOPO-Lasp1-PR, which was then propagated in LB medium and extracted using QIAfilter™ Plasmid Maxi kit.

Sub-clone from TOPO-Lasp1-PR to pGL3-Basic vector

15μg of TOPO-Lasp1-PR vector (1μg/μl) was digested by Kpn I and EcoR V in a total 100μl reaction volume at 37°C overnight and the DNA fragment with expected size (~2kb) was cut out and purified using a QIAquick Gel Extraction Kit (Qiagen) according to the manufacturer's instruction. 20μl of DNase/RNase free H_2O was used to re-dissolve the Lasp1-PR DNA fragment carrying the Kpn I and EcoR V overhang. 6μg of pGL3-Basic vector (Figure 2.5) was first digested by Kpn I to generate a Kpn I sticky end, and the digested vector was purified by phenol/chloroform followed by ethanol purification. Then the linearized vector was digested by Smal I to generate a blunt end which can be ligated to the EcoR V end. The digested vector was treated with 2μl of CIP (Calf Intestine Phosphatase) for 1 hour before purified by phenol/chloroform. The ethanol precipitated DNA was re-dissolved in 25μl DNase/RNase free H_2O. The ligation reaction was then performed at 16°C waterbath with overnight incubation in a 20μl reaction containing 4μl of ligation buffer (5 ×), 1μl of linearized vector DNA, 14μl of insert DNA, and 1μl of T4 DNA ligase. Then 2μl of the ligation reaction product was transformed into the library efficiency® DH5α™ chemically competent *E.coli* according to standard protocol. Spread 100μ1 recovered culture on a pre-warmed LB plate containing 100μg/ml of Ampicillin and incubate at 37ºC overnight. 10-12 colonies were inoculated and propagated by culturing in LB medium containing 100μg/ml of Ampicillin overnight for plasmid extraction. The isolated plasmids were used for enzyme digestion (Table 2.7) and further confirmation by sequencing using primers

listed in Table 2.8. The constructed positive clone was defined as pGL3-Lasp1-PR, which was then propagated and prepared by QIAfilter™ Plasmid Maxi kit.

pGL3-Lasp1-PR deletion construct cloning

11 forward primers plus 1 common reverse primer (sequence listed in Table 2.6, with Kpn I or Hind III restriction sites highlighted as bold) were designed to produce a series of deletion constructs carrying different sizes of Lasp1 promoter region. PCR amplification using pGL3-Lasp1-PR as template DNA was performed to generate DNA fragment of Lasp1 promoter region with different sizes carrying Kpn I and Hind III restriction sites. After purified by QIAquick PCR purification kit (Qiagen), the PCR product was cloned into pCR®4-TOPO® vector (Figure 2.6) and transformed into the library efficiency® DH5α™ chemically competent *E.coli* according to standard protocol. Spread 100µ1 recovered culture on a pre-warmed LB plate containing 50µg/ml of Kanamycin and incubate at 37ºC overnight. Positive clones were confirmed by double enzymatic digestion (Kpn I + Hind III) and sequencing.

Both pGL3-Basic vector and those positive clones were digested by Kpn I and Hind III. The linearized vector was purified by phenol/chloroform and precipitated in ethanol, while the DNA fragments with expected sizes (listed in Table 2.6) were cut out and purified by QIAquick gel purification kit. The ligation reaction was performed at 16°C waterbath with overnight incubation in a 20µl reaction containing 4µl of ligation buffer (5 ×), 1µl of linearized vector DNA, 14µl of insert DNA, and 1µl of T4 DNA ligase. Then 2µl of the ligation reaction product was transformed into the library efficiency® DH5α™ chemically competent *E.coli* according to standard protocol. Spread 100µ1 recovered culture on a pre-warmed LB plate containing

100μg/ml of Ampicillin and incubate at 37ºC overnight. To select positive clones, 6 colonies for each deletion construct were picked for plasmid extraction, and the isolated plasmids were used for enzyme digestion (Table 2.7) and further confirmation by sequencing analysis (Table 2.8). The positive clones with correct sequences were designated as pGL3-Lasp1-PR-DelA~K as listed in Table 2.7.

Table 2.6 Oligonucleotide primers used in pGL3- cloning

Primer Name	Primer Sequence	Length	Product Size
Lasp1-PR-F	5' TAAAACTGGTTCCTCCTGGGTTTTGC 3'	26bp	1946bp
Lasp1-PR-R	5'GTTCCGAGAAAAGCTGGGGCGGGGAC 3'	26bp	
Lasp1-PR-1561F (DelA)	5' **GGTACC**ACGCAGCCAGCAGATACTTG 3'	26bp	1690bp
Lasp1-PR-1273F (DelB)	5' **GGTACC**GGATGAACACAGCACGTCCA 3'	26bp	1402bp
Lasp1-PR-1087F (DelC)	5' **GGTACC**TCTGACCCATCTGAGGCT 3'	24bp	1216bp
Lasp1-PR-952F (DelD)	5' **GGTACC**GGTTGAAAAATGAGGAAGATA 3'	27bp	1081bp
Lasp1-PR-790F (DelE)	5' **GGTACC**GATCTGCAGTCAAATGCTC 3'	25bp	919bp
Lasp1-PR-544F (DelF)	5' **GGTACC**GCAGGGTCCAAGAGGGAGG 3'	25bp	673bp
Lasp1-PR-446F (DelG)	5' **GGTACC**CGGTCCGCAGATTCATGCC 3'	25bp	575bp
Lasp1-PR-255F (DelH)	5' **GGTACC**CAGTCAGCCTGAGAGCGCT 3'	25bp	384bp
Lasp1-PR-97F (DelI)	5' **GGTACC**CCCCGCTGTGTTTATTAGG 3'	25bp	226bp
Lasp1-PR-27F (DelJ)	5' **GGTACC**GCTGCCTGTGTAGTTGCAGC 3'	26bp	156bp
Lasp1-PR+10F (DelK)	5' **GGTACC**CAGCTCGCCTCGGGGAA 3'	23bp	120bp
Lasp1-PR-del-R	5' **AAGCTT**ACTTAGATCGCAGATCTCGAGCC 3'	29bp	

Table 2.7 Restriction enzymes used in pGL3- cloning

Construct	Restriction Enzyme	Buffer	Expected Fragment Size
TOPO-Lasp1-PR	Kpn I + EcoR V	NEB2	3488bp, 1977bp
pGL3-Basic	Kpn I	NEB1	linearized vector, 4818bp
pGL3-Basic-Kpn I	Sma I	NEB4	4795bp, 23bp
pGL3-Lasp1-PR	Kpn I + Hind III	NEB2	4770bp, 2002bp
pGL3-Lasp1-PR-Del A	Kpn I + Hind III	NEB2	4770bp, 1690bp
pGL3-Lasp1-PR-Del B	Kpn I + Hind III	NEB2	4770bp, 1402bp
pGL3-Lasp1-PR-Del C	Kpn I + Hind III	NEB2	4770bp, 1216bp
pGL3-Lasp1-PR-Del D	Kpn I + Hind III	NEB2	4770bp, 1081bp
pGL3-Lasp1-PR-Del E	Kpn I + Hind III	NEB2	4770bp, 919bp
pGL3-Lasp1-PR-Del F	Kpn I + Hind III	NEB2	4770bp, 673bp
pGL3-Lasp1-PR-Del G	Kpn I + Hind III	NEB2	4770bp, 575bp
pGL3-Lasp1-PR-Del H	Kpn I + Hind III	NEB2	4770bp, 384bp
pGL3-Lasp1-PR-Del I	Kpn I + Hind III	NEB2	4770bp, 226bp
pGL3-Lasp1-PR-Del J	Kpn I + Hind III	NEB2	4770bp, 156bp
pGL3-Lasp1-PR-Del K	Kpn I + Hind III	NEB2	4770bp, 120bp

Table 2.8 Oligonucleotide primers used in sequencing TOPO- and pGL3-Vectors

Primer Name	Primer Sequence	Length	Vector Origin
M13-forward	5' GTAAAACGACGGCCAG 3'	16bp	pCR-BluntII-TOPO, pCR4-TOPO
M13-reverse	5' CAGGAAACAGCTATGAC 3'	17bp	pCR-BluntII-TOPO, pCR4-TOPO
RVprimer3	5’ CTAGCAAAATAGGCTGTCCC 3’	20bp	pGL3-Basic
GLprimer2	5’ CTTTATGTTTTTGGCGTCTTCCA 3’	23bp	pGL3-Basic
Lasp1-PR-Int	5’ TTTATACCCACCCCCTCCTC 3’	20bp	pCR-BluntII-TOPO, pGL3-Basic

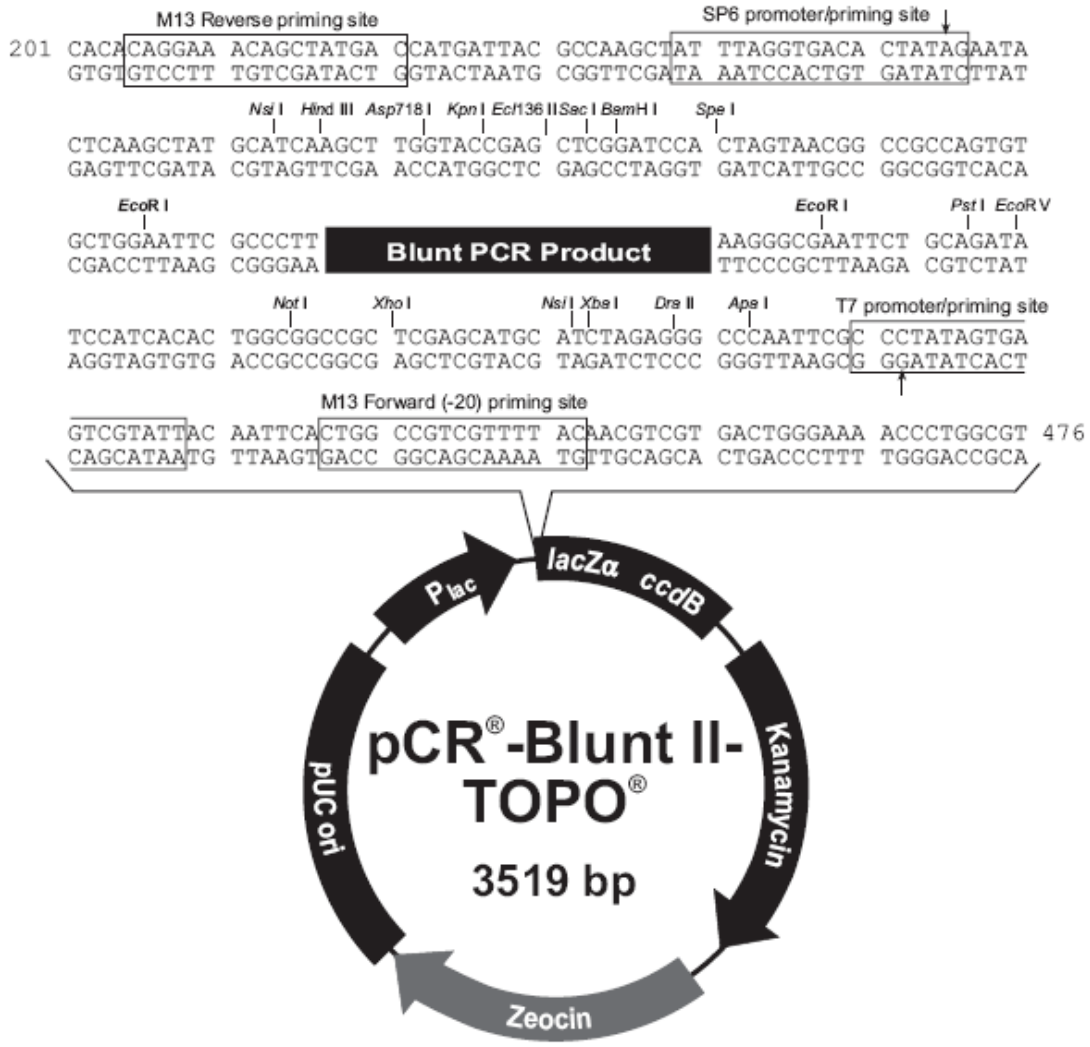

Figure 2.4 Map of the pCR®-Blunt II-TOPO® vector. The map shows the features of pCR®-Blunt II-TOPO® and the sequence surrounding the TOPO® cloning site. Restriction sites are labeled to indicate the actual cleavage site. The arrows indicate the start of transcription for the T7 and SP6 polymerases.

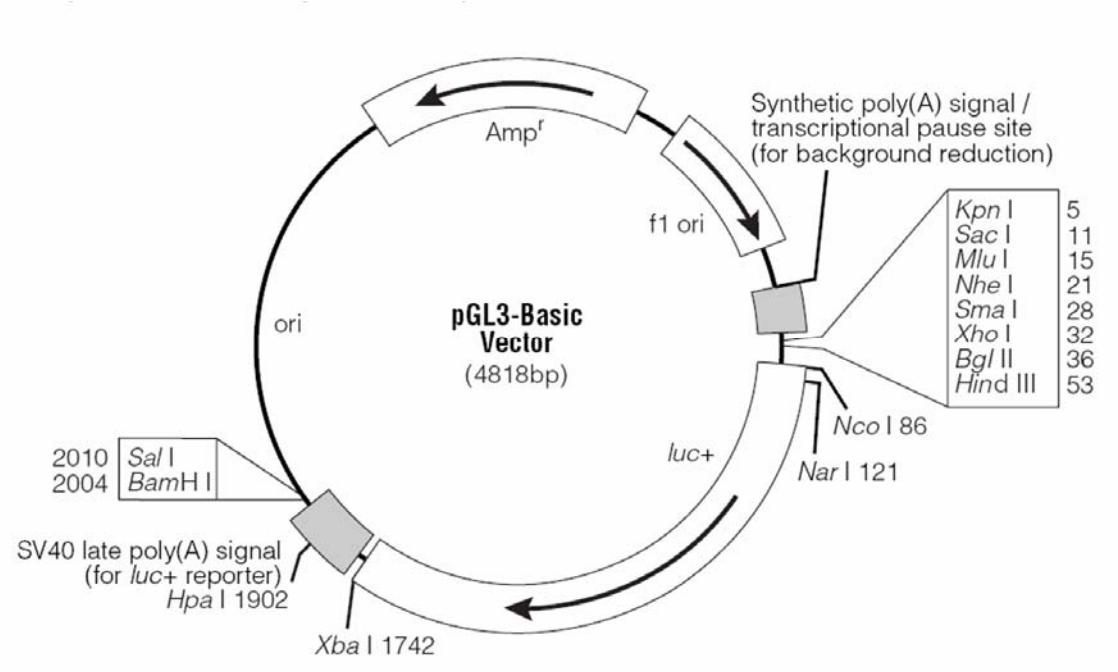

Figure 2.5 Map of the pGL3-Basic vector. The map shows the main features of this vector and the restriction enzyme sites surrounding the multiple cloning sites. The luciferase gene is also indicated.

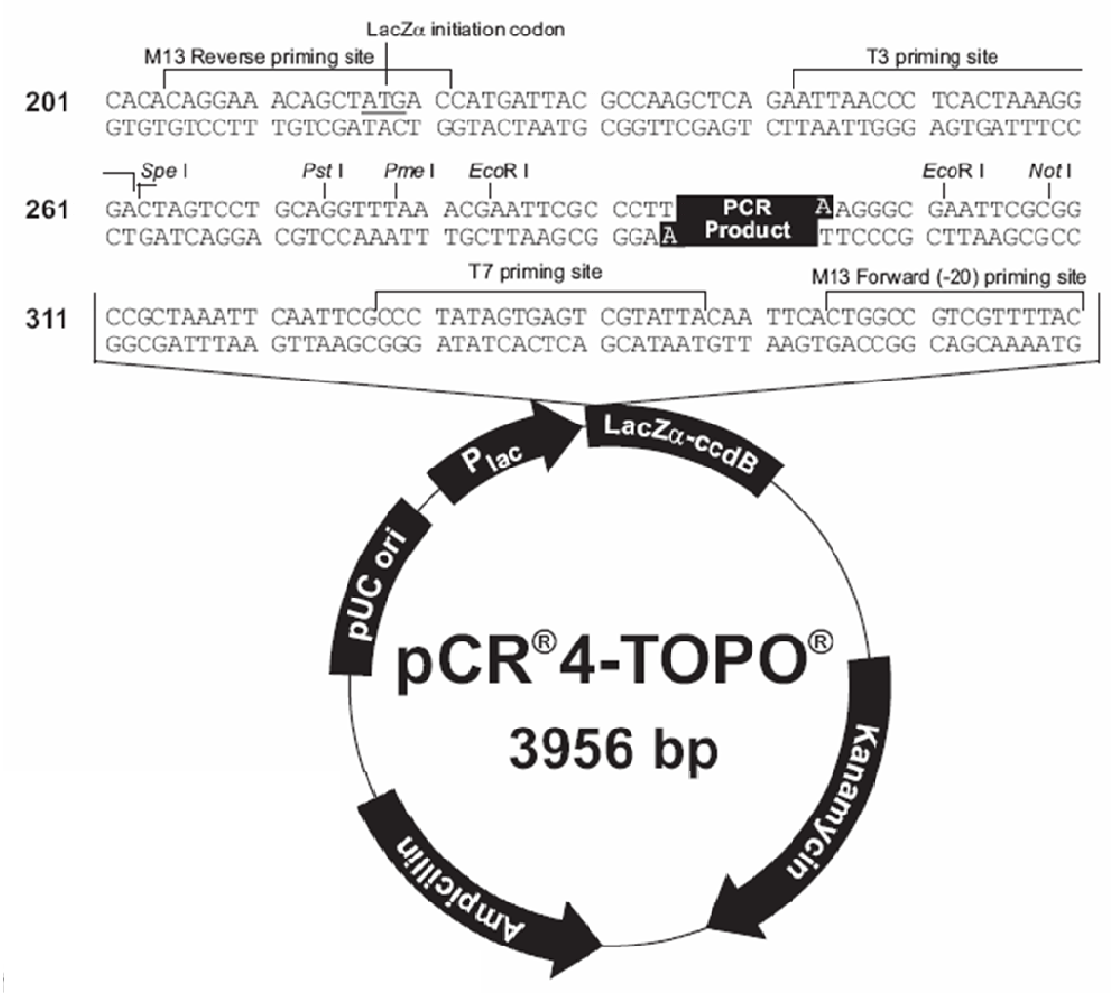

Figure 2.6 Map of the pCR®4-TOPO® vector. The map shows the features of pCR®4-TOPO® and the sequence surrounding the TOPO® cloning sites. Restriction sites are labeled to indicate the actual cleavage site.

2.5. Transfection

Transfection of either plasmids or siRNAs into human HCC cell lines or human colon cancer cell lines was mediated by Lipofectamine2000 reagent (Invitrogen). The optimal cell seeding amount for transfection of different types of DNA (plasmid/siRNA) or different cell lines or for different experimental purpose was optimized by checking the overnight confluence and listed below in Table 2.9.

Table 2.9 Cell seeding amount for transfection

Plate Format	**6-well plate**		**96-well plate**
O/N Confluence (%)	**30-40%**	**80-90%**	**50-60%**
Purpose / Cell Lines	**siRNA (Ambion)**	**1. Over-expression 2. siRNA (Dharmacon)**	**Luciferase Assay**
HepG2	1.25×10^6	2.5×10^6	
Hep3B	0.45×10^6	0.9×10^6	0.9×10^4
Huh-7	0.5×10^6	1.0×10^6	
PLC/PRF/5	0.5×10^6	1.0×10^6	
HCT116 (p53+/+)	1.5×10^6	3.0×10^6	
HCT116 (p53-/-)	1.5×10^6	3.0×10^6	3.0×10^4

2.5.1. Plasmid transfection

Transient transfection of the expression plasmids (4-6μg/well) into HCC or colon cancer cells plated in 6-well plates with 80-90% confluence was mediated by Lipofectamine 2000 reagents according to the manufacturer's instructions.

As the transient transfection efficiency of HepG2 cells is usually low, stable-transfected cells were established from HepG2 cells 48 hours after transfection with Cyr61-DEST40/V5 or Lasp1-DEST40/V5. The cells were trypsinized and replated in DMEM/10% FBS supplemented with 800μg/ml geneticin (G418) (Invitrogen). Two to three weeks later, around 20 well-isolated cell colonies were picked and re-seeded

in 96-well plates. The clones were expanded to 24-well plates and the stable expression of the V5 fusion proteins were screened by Western blot. Two G418-resistant stable clones for each gene (HepG2-Cyr61-1, HepG2-Cyr61-2; HepG2-Lasp1-1, HepG2-Lasp1-2) were selected. One G418-resistant clone isolated from empty vector pcDNA3.1 transfected cells was designated as HepG2-Neo control. These stable clones were expanded, freezed and stored in liquid nitrogen until use.

For luciferase assay, Hep3B or HCT116 (p53-/-) cells were seeded in 96-well Flat Bottom Black Polystyrene Plates (Corning Inc. Lindfield, Australia) with 50-60% overnight confluence. The pGL3- constructs were co-transfected with PRL-null and p53, p53-R175H or pcDNA3.1 control plasmid by using Lipofectamine 2000 reagents. The detailed protocol will be described in 2.13.

2.5.2. siRNA transfection

The siRNA oligos targeting Cyr61 (#1, ID 10104; #2, ID 10192) and Lasp1 (#1, ID 17398; #2, ID 17494) and Negative Control siRNA (Catalog No: 4611) that does not target any human gene product were synthesized by Ambion, Inc. (Austin, TX). The siRNA targeting TP53 (sip53, Catalog No: M-003329-01) and its corresponding control siRNA (siControl) were purchased from Dharmacon (Lafayette, CO). The oligos were re-constituted in RNase free H_2O (supplied by Ambion) or buffer (supplied by Dharmacon) to make a 100μM stock.

Transient transfection of siRNA (40-100nM) into HepG2, Hep3B or HCT116 (p53+/+) cells seeded in 6-well plates with 30-40% (Cyr61 and Lasp1 siRNA) or 80-90% (p53 siRNA) overnight confluence was mediated by Lipofectamine 2000 reagents according to the manufacturer's instructions.

2.6. Western blot

2.6.1. SDS-polyacrylamide gel electrophoresis (SDS-PAGE)

Extraction of protein lysate

Cell pellets of HCC cell lines including HA22T, Huh-1, Huh-4, Tong, SNU182, SNU449, SNU475, Huh-6, Mahlavu, and SK-Hep1 were kindly provided by the WHO Immunology Center, (Singapore). The experimental cells or cell pellets were washed twice with PBS and then lysed in NP-40 lysis buffer (Appendix I) containing 1 × complete mini protease inhibitor mixture (Roche Applied Science) and 1mM phenylmethylsulfonyl fluoride (PMSF) (Sigma-Aldrich, St. Louis, MO) on ice for 30min. The lysates were centrifuged at 13,200 rpm for 15 min at 4°C, and the protein concentration was measured using a Bradford Protein Assay Kit (Bio-Rad). Briefly, standard bovine serum albumin (BSA) was diluted to give 4 different concentrations ranging from 500μg/ml to 4000μg/ml. 1μl of each of standards or samples was mixed with 1ml of diluted dye reagent (1 ×) in separate cuvette. The mixture was incubated at room temperature for at least 5min (less than 30min) prior to measuring the absorbance at 595nm. A standard calibration curve was constructed by plotting absorbance versus concentration of the BSA standards and the concentration of samples was then calculated according to the calibration curve.

Preparation of SDS-polyacrylamide gels

Separating gels with acrylamide concentrations of 7.5%, 10%, 12.5% were used in this study, while 5% of stacking gels was consistently applied. Gels were cast using the Mini-PROTEAN electrophoresis cell apparatus (Bio-Rad). Gel Formulas were listed in Table 2.10. The recipes were sufficient for the preparation of 2 slab mini-gels (1.5mm thick and 100 × 70mm^2) and the components were mixed in the order shown. Polymerization began as soon as 10% APS and TEMED added.

Sample preparation and electrophoresis

While the stacking gel was polymerizing, the protein samples were mixed with equal amount of 2 × SDS-PAGE sample buffer (Appendix I) and heated at 100°C for 6 minutes. The ECL DualVue Western Blotting Marker (Amersham Pharmacia Biotech, Piscataway, NJ) was used as a marker for the transfer efficiency and an indication of the protein molecular weight when exposed to film in the following Western blot. Up to 30µl (20-30µg) of each sample and sample buffer mixture was loaded into the bottom of the wells. Electrophoresis was carried out in the presence of 1 × Tris-Glycine SDS-PAGE running buffer (Appendix I) under the constant current of 20mA per gel. The running was stopped when the dye front reached the bottom of the separating gel. After removed quickly from the electrophoresis apparatus, the gel could be used to establish a Western blot.

Table 2.10 SDS-PAGE gel recipes

Separating gels	**7.5%**	**10%**	**12.5%**
H_2O	9.7ml	8.0ml	6.4ml
30% acrylamide mix (Bio-Rad)	5.0ml	6.6ml	8.3ml
1.5M Tris (pH8.8) (Bio-Rad)	5.0ml	5.0ml	5.0ml
10% SDS	200µl	200µl	200µl
10% APS (Bio-Rad)	100µl	100µl	100µl
TEMED (Bio-Rad)	20µl	20µl	20µl
Total (for 2 gels)	20ml	20ml	20ml
Stacking gels	**5%**	**5%**	**5%**
H_2O	2.84ml	2.84ml	2.84ml
30% acrylamide mix (Bio-Rad)	0.83ml	0.83ml	0.83ml
0.5M Tris (pH6.8) (Bio-Rad)	1.25ml	1.25ml	1.25ml
10% SDS	50µl	50µl	50µl
10% APS (Bio-Rad)	25µl	25µl	25µl
TEMED (Bio-Rad)	5µl	5µl	5µl
Total (for 2 gels)	5ml	5ml	5ml

2.6.2. Western blot

About 20~30μg of protein was separated on 7.5%-12.5% SDS-polyacrylamide gel electrophoresis, and transferred to Hybond PVDF membranes (Amersham Pharmacia) by using a semi-dry Transblot apparatus (Bio-Rad). Briefly, the gel was equilibrated in 1 × Transfer buffer (Appendix I) and meanwhile the PVDF membrane cut to gel size was re-activated in methanol before transferred into the 1 × Transfer buffer in a separate container. A sandwich was assembled by putting a sheet of extra thick filter paper (100 × 70mm, Bio-Rad) pre-soaked in 1 × Transfer buffer onto the platinum anode, followed by the pre-wetted PVDF membrane, the equilibrated gel, and another sheet of soaked filter paper. Air bubbles should be carefully removed from between each layer. After the cathode and the safety cover were placed onto the stack, the electrophoretic transfer was performed at a constant voltage of 20V for 30-60 minutes at room temperature.

Antibodies against V5-tag (mouse monoclonal) (Invitrogen), Cyr61 (42kDa) (rabbit polyclonal), p53 (53kDa) (mouse monoclonal, DO-1), p21 (21kDa) (rabbit polyclonal) (Santa Cruz Biotechnology, Santa Cruz, CA), Lasp1 (30kDa) (rabbit polyclonal) (Chemicon International, Temecula, CA), zyxin (82kDa) (mouse monoclonal) (Invitrogen), VASP (50kDa) (mouse monoclonal) (BD Biosciences), paxillin (68kDa) (mouse monoclonal) (Millipore-Upstate) were used as primary antibodies in this study for protein detection, followed by reacting to appropriate HRP-conjugated Goat-anti-Mouse or Donkey-anti-Rabbit secondary antibodies (Dako, Denmark). Equal loading of protein samples was verified with antibodies to α-tubulin (50kDa) (mouse monoclonal) (Sigma-Aldrich) or β-actin (42kDa) (mouse monoclonal) (Chemicon International). The membranes were extensively washed with TBST buffer (Appendix I), and the immunoreactive signals were visualized by reacting with

enhanced chemiluminescence (ECL Plus™) reagents followed by exposure to the Hyperfilm (Amersham Pharmacia).

2.7. WST-1 cell proliferation assay

Cell proliferation rate in monolayer was analyzed by a modified MTT assay (WST-1 reagent, Roche Applied Science) according to the manufacturer's protocol. Briefly, HepG2, Hep3B, Huh-7 or PLC/PRF/5 cells seeded in 6-well plates were transiently transfected with either plasmid or siRNA. 24 hours after transfection, the cells were trypsinized in 0.05% trypsin/EDTA (Invitrogen) and replated into 96-well plates at the concentration of 1-5 × 10^4 cells/well in 100µl DMEM/10%FBS in triplicates and cultured for additional 3-5 days. 10µl of WST-1 reagent was then added into each well at different time points followed by incubation at 37°C for 40 min. The absorbance was measured by a multiscan plate reader at 450nm with 690nm reference (Thermo Labsystems, Cambridge, UK). For each different cell line, a standard curve was constructed by plotting absorbance versus the number of cells plating in single well (range from 1 × 10^4 to 100 × 10^4 per well) and the number of the experimental cells cultured in the plate was then calculated according to the standard curve. The growth rate of stably transfected HepG2 cells cultured up to 6 days in 96-well plates was analyzed in a similar manner.

2.8. Soft agar assay

For the anchorage-independent colony formation assay, HepG2, Huh-7 or PLC/PRF/5 cells were trypsinized 24 hours after transfection with either expression plasmid or siRNA, and 0.5 - 1 × 10^4 cells re-suspended in 0.25ml of 0.35% agar dissolved in DMEM/10%FBS were plated in 24-well plate in triplicates overlying a 0.7% agar bottom layer and cultured at 37°C with 5% CO_2. Fresh medium was added

every 4 to 5 days. Three weeks later, the medium was gently removed and the top layer of the culture was stained with 1mg/ml *p*-iodonitrotetrazolium (Sigma-Aldrich). The colonies were visualized and photographed under an MZFL3 stereomicroscope (Leica Microsystems, Heidelberg, Germany), and the colonies > 100μm in diameter were then counted and analyzed using the Leica QWin imaging software.

2.9. Cell adhesion, migration and invasion assay

2.9.1. Cell adhesion assay

Cell adhesion activity was determined by using the CytoMatrix^{TM} screening kit (Chemicon International) according to the manufacturer's instruction with modifications. Briefly, HepG2 or Hep3B cells transfected with equal amount of expression plasmids (4μg/well for 6-well plates) or siRNA oligos (40nM) were harvested with 0.05% trypsin/EDTA 48 hours after transfection. Cells were washed once with PBS and resuspended in serum-free medium (DMEM/0.5%FBS) at 2×10^6 cells/ml. 100μl of the cell suspension was added into 96-well plates individually pre-coated with fibronectin, vitronectin, laminin, collagen I, and collagen IV, each in triplicates. After 1 hour incubation at 37°C in a CO_2 incubator, the wells were gently washed 3 times with PBS containing Ca^{++}/Mg^{++} (Appendix I), and 110μl of DMEM medium containing 10μl of WST-1 reagent was added, followed by additional 40min incubation at 37°C. The number of adhesive cells in the wells was determined by measuring the absorbance at 450nm with 690nm reference.

2.9.2. Cell migration and invasion assay

Cell migration and invasion activities were analyzed using 24-well fluorimetric migration kit (ECM509) and invasion kit (ECM554) respectively based on the Boyden chamber principle according to the manufacturer's protocols

(Chemicon International). The migration assay was performed in microporous membrane inserts with an 8μm pore size, while the invasion assay utilized same inserts coated with an extra layer of ECMatrix™, a reconstituted basement membrane matrix of proteins derived from the Engelbreth Holm-Swarm (EHS) mouse tumor. Briefly, 24 hours after transfection (transient transfection) or seeding (stable transfection), cells were starved in serum-free medium (DMEM/0.5%FBS) for another 24 hours. Both migration and invasion inserts need to be pre-warmed to room temperature and the invasion inserts were re-hydrated with 300μl serum-free medium. Then 0.5 - 6.0 × 10^5 of cells resuspended in 250μl DMEM/0.5%FBS were added into the migration or invasion inserts which were loaded in wells of 24-well plate containing 500μl of DMEM/10%FBS. After cultured in 37°C with 5% CO_2 for 16-18 hours, the migrated or invaded cells towards the DMEM/10%FBS to the bottom of the insert membrane were dissociated from the membrane by incubating with Cell Detachment Buffer and subsequently lysed and detected by CyQuant GR® dye staining. The fluorescent intensity was measured in a fluorescent microplate reader (Tecan, Mannedorf, Switzerland) using 480/520nm filter set.

2.10. 5-Fluorouracil (5-FU) and UV treatment

2.10.1. 5-FU and UV treatment for cell cycle analysis

In order to study the role of Cyr61 in cell cycle regulation, stable cell lines HepG2-Cyr61-1, HepG2-Cyr61-2 and HepG2-Neo controls were plated in 6-well plates in DMEM/10%FBS/G418 (800μg/ml). Upon reaching 50-60% confluences, the cells were treated with 5-FU (50μg/ml, Sigma-Aldrich) or UV irradiation (20J/m^2) and cultured for additional 24 hours. Then cells were ready for harvest and the following PI staining for flow cytometry analysis.

2.10.2. 5-FU and UV treatment for Cyr61 expression study

To investigate the endogenous expression of Cyr61 upon genotoxic stress induction, the HCC cell lines HepG2 and Hep3B were plated in 6-well plates for overnight incubation. At 50-60% confluences, the cells were treated with 5-FU (50μg/ml) or UV irradiation (20J/m^2). At different time points up to 48 hours, cells were harvested for total RNA and lysate collection separately. These total RNA and lysates were used for following RT-PCR or Western blot analysis. To further confirm the observation, the colon cancer cell lines HCT116 and HCT116 (p53-/-) were also treated with 5-FU (50μg/ml) and the cell lysates were collected for Western blot analysis.

2.10.3. 5-FU treatment for Lasp1 expression regulation study

To examine the role of p53 in transcriptionally suppress Lasp1, the HCC cell lines HepG2, Hep3B and the colon cancer cell lines HCT116 and HCT116 (p53-/-) were treated with 5-FU (50μg/ml) to induce the activation and accumulation of endogenous p53. Total RNA and cell lysates were collected for time course analysis of Lasp1 mRNA and protein expression by real-time quantitative RT-PCR and Western blot, respectively.

2.11. Flow cytometry

Cell cycle progression was analyzed in stable cell lines HepG2-Cyr61-1, HepG2-Cyr61-2 and HepG2-Neo controls at 60-70% confluences either untreated or treated with 5-FU or UV irradiation. The cells were harvested by trypsinization using 0.05% trypsin/EDTA to obtain single-cell suspension and the cells were fixed in ice-cold 70% ethanol overnight. After wash with ice-cold PBS for twice, the cells were treated with RNase A (100μg/ml) for 5min and then stained with propidium iodide (50μg/ml) (Sigma-Aldrich) for 60min in dark at room temperature. The DNA content of the stained cells was analyzed using FACSCalibur and CellQuest software (BD Biosciences).

2.12. Chromatin immunoprecipitation (ChIP)

ChIP assays using HCT116 or HepG2 cells were carried out as described by Weinmann *et al.* (Weinmann *et al*. 2001; Wells and Farnham 2002). Briefly, at 50-60% confluence, cells seeded in 500cm^2 cell culture dishes (Corning Inc.) were treated with 5-FU (375μM). Six hours later, cells were cross-linked with 1% formaldehyde (final concentration) (Sigma-Aldrich) for 10min at room temperature. Formaldehyde was inactivated by addition of 125mM glycine. After wash with ice-cold PBS, cells were harvested and lysed in FA cell lysis buffer (Appendix I) followed by sonication to shear the chromatin-DNA. Then chromatin extracts containing DNA fragments of average size of 500bp were immuno-precipitated using anti-p53 DO1 monoclonal antibody (Santa Cruz Biotechnology) and Dynabead® Protein G (Invitrogen). After extensive wash of the immuno-precipitated complex in a series of washing buffers (0.1% SDS FA lysis buffer, NP-40/LiCl buffer), the DNA-protein complex was eluted in ChIP elution buffer (Appendix I). Finally, 2.5M

glycine was added to de-crosslink the protein from DNA. After purification by Phenol/Chlorofom and ethanol precipitation, the purified ChIP-DNA dissolved in TE buffer was ready as the template for ChIP-qPCR. All ChIP-qPCR primers were designed by Oligo 6 software and the sequences were listed in Table 2.11. The analyses for the ChIP-qPCR were performed using ABI PRISM 7900 Sequence Detection System and SYBR Green Master Mix. Threshold cycles (Ct) were determined for both immuno-precipitated DNA and a known amount of DNA from the input sample for different primer pairs. Relative occupancy values (also known as fold enrichments) were calculated by determining the immuno-precipitation efficiency (ratios of the amount of immuno-precipitated DNA to that of the input sample) and normalized to the level observed at a control region, which was defined as 1.0.

Table 2.11 Oligonucleotide primers used in ChIP-qPCR

Primer Set	Primer Name	Primer Sequence	Length	Position	Product Size
P1	ChIP-L-F1	ATTAATAGTCAAGGATGAACACAGCACGTC	30bp	-1285~-1256	213bp
	ChIP-L-R1	CTCAGATGGGTCAGACAGTTCGAGGTG	27bp	-1073~-1099	
P2	ChIP-L-F2	CCTCCACCCCCAAAAGGAACGCCAAGTTGA	30bp	-1179~-1150	156bp
	ChIP-L-R2	CATTACTCGCGCCAGAGGTGTAGGGATTTC	30bp	-1024~-1053	
P3	ChIP-L-F3	GAAGGTGCACTGCAGGGGCTCGAGAG	26bp	-598~-573	216bp
	ChIP-L-R3	CCTGAACGCTGGAACTGATTCACCGCATTC	30bp	-383~-412	
P4	ChIP-L-F4	GGAAAGGGTGTGGGCCGGAAGAGAGCTAAG	30bp	-501~-472	169bp
	ChIP-L-R4	GCGGGAGGCGGGCTAACCCCTCAAG	25bp	-333~-357	
P5	ChIP-L-F5	CTGTGTTTATTAGGGGAAGGAGGGCGGAGG	30bp	-92~-63	189bp
	ChIP-L-R5	CCGGGCGCAGTTGGGGTTCATGGTTCCGAG	30bp	+96~+67	
P6	ChIP-L-F6	TGTTTATTAGGGGAAGGAGGGCGGAGG	27bp	-89~-63	158bp
	ChIP-L-R6	CGGGCGCAGTTGGGGTTCATGGTTCCGA	27bp	+68~+42	
P7	ChIP-L-F7	AGGAGATCTGGGGCGAGGCGGGAAGTCCAC	30bp	+315~+344	98bp
	ChIP-L-R7	TCCCCCAACACACCCCGGCGCCTGAC	26bp	+412~+387	
P8	ChIP-L-F8	GGCTGGGGGGCCCTGCAAAACCGTC	25bp	+581~+605	153bp
	ChIP-L-R8	CGACTGAATCCAAGGGGGTGCAGGTCGTTC	30bp	+733~+704	

2.13. Luciferase assay

2.13.1. Study of the role of p53 in regulating Lasp1 promoter

HCT116 (p53-/-) or Hep3B cells were transfected by Lipofectamine2000 reagent (Invitrogen) according to the manufacturer's instructions. Transfections were done in triplicates. Briefly, exponentially growing cells were plated at a density of 30000/well for HCT116 (p53-/-) or 9000/well for Hep3B in 150µl DMEM/10%FBS in 96-well Flat Bottom Black Polystyrene Plates (Corning Inc.). Cells were cultured overnight before transfection. For each well, 100ng of luciferase reporter construct pGL3-Lasp1-PR or positive control vector pGL3-PTPRM2-PR were co-transfected with increasing doses (2, 10, 25 and 50ng) of wild-type (pCMV-p53) or mutant p53 (pCMV-p53-R175H) expression vectors (kindly provided by Dr. Bert Vogelstein), together with 1ng of Renilla luciferase control vector PRL-null (Promega). The total amount of transfected DNA in each well was kept constant by adding empty vector pcDNA3.1 plasmid. 36 hours after transfection, the culture medium was discarded and the cells were washed with PBS twice. Then the reporter Firefly luciferase activity was measured using the Dual-Luciferase® Reporter Assay System kit (Promega). Firstly, cells were lysed in passive lysis buffer provided by the kit at room temperature for 30min with gentle shaking at 400rpm. Next, the luciferase activity was measured in Dual-Injector Luminometer System (Centro LB 960, Berthold Technologies, Germany) with pre-defined program. To correct for variations in transfection efficiency, the reporter Firefly luciferase activity was normalized to Renilla luciferase activity (F/R ratio).

2.13.2. Localization study of the important regulators in Lasp1 promoter

The deletion constructs were constructed as described in section 2.4.3. As in section 2.13.1, exponentially growing HCT116 (p53-/-) or Hep3B cells plated in 96-well Flat Bottom Black Polystyrene Plates were cultured overnight before transfection. For each well, 100ng of luciferase reporter constructs (pGL3-Lasp1-PR; pGL3-Lasp1-PR-DelA, B, C, D, E, F, G, H, I, J, K) were co-transfected with 1ng of Renilla luciferase control vector PRL-null. 36 hours post transfection, the reporter Firefly luciferase activity was measured by the Dual-luciferase Reporter Assay System kit with normalization to the Renilla luciferase activity (F/R ratio) to correct for variation in transfection efficiency.

2.13.3. Localization study of the p53 response element in Lasp1 promoter

In order to define the genuine p53 response element in Lasp1 promoter, all pGL3- constructs containing fragments of different sizes of Lasp1 promoter region plus the pGL3-Basic vector (100ng/well) were co-transfected with p53 wild-type expression vector (pCMV-p53) or control vector (pcDNA3.1) (10ng/well) into HCT116 (p53-/-) or Hep3B cells plated in 96-well plate. 36 hours post transfection, the reporter Firefly luciferase activity was measured by the Dual-luciferase Reporter Assay System kit as described above. The response to p53 for each deletion construct was presented as the F/R ratio observed in pCMV-p53 co-transfected cells standardized to the ratio in control vector pcDNA3.1 co-transfected cells, which was arbitrarily set at 100%.

2.14. Confocal microscopy

2.14.1. Cellular localization analysis of Cyr61

For cellular localization analysis for Cyr61, HepG2, Hep3B and Huh-7 cells were seeded on coverslips in 6-well plates for overnight culture and transfected with pDEST47-Cyr61/GFP plasmids at 70% confluences. 48 hours after transfection, the coverslips were washed twice with PBS and then fixed with 4% paraformaldehyde for 30min at room temperature. After briefly rinsed with PBS, the coverslips were placed upside down to clean slides applied with Vectashield® mounting medium (Vector Laboratories, Burlingame, CA) and sealed with nail polish. Fluorescent images were observed and photographed under a confocal microscope (LSM510 Meta, Carl Zeiss, UK) using Plan-Neofluar 100×/1.3 oil immersion objective with 488nm wavelength.

2.14.2. Mechanism analysis of Lasp1 over-expression in regulating HCC cell migration and invasion

To investigate the mechanism of Lasp1 further over-expression in regulating cell migration and invasion ability in HCC cells, the co-localization of Lasp1 with a series of focal adhesion and/or F-actin binding proteins were examined. Hep3B and Huh-7 cells were seeded in 6-well plates for overnight culturing and transfected with pDEST47-Lasp1/GFP plasmids at 70-80% confluences. Twenty-four hours after transfection, the cells were trypsinized by 0.05% trypsin/EDTA and re-plated onto the 35mm glass bottom microwell dishes (MatTek Corporation, Ashland, MA) at a concentration to reach 50-60% confluence after overnight incubation. Cells were washed three times with PBS and fixed with 4% paraformaldehyde for 10min at room temperature. Fixed cells were permeabilized in 0.1% Triton-X100 (Bio-Rad) for 3 minutes. Before antibody incubation, cells were blocked in 5% BSA in PBS at room

temperature for 2 hours. Then mouse monoclonal antibodies specific to zyxin (Invitrogen), VASP (BD Biosciences), and paxillin (Upstate) were used as primary antibodies to stain the respective cellular proteins at 4°C overnight. On the next day, goat-anti-mouse secondary antibodies conjugated with Alexa Fluor® 647 (Molecular Probes, Invitrogen) were applied and incubated at room temperature for 30min. F-actin was stained by Alexa Fluor® 635 phalloidin (Molecular Probes) at room temperature for 20min according to the manufacturer's instructions. Finally, the cells were mounted with the Prolong Gold Antifade Reagent (Molecular Probes) after the excessive moisture had been removed and the culture dishes stored at 4°C overnight were ready for con-focal microscopy analysis. Note that the extensive wash by PBS for 3 times was applied between each step. Fluorescent images were observed and photographed under a confocal microscope (LSM510 DUO system, Carl Zeiss) using Plan-Neofluar 63×/1.40 oil DIC immersion objective with 488nm (Argon laser) and 633nm (Hene laser) wavelength.

2.15. Statistical analysis

All functional tests were carried out in triplicates and repeated three times with similar results. Representative data were shown as mean ± SD from triplicate wells. Differences of averages and percentages between controls and Cyr61 or Lasp1 plasmid/siRNA transfectants were statistically analyzed using Student's *t*-test. The correlation between the fold change of Cyr61 or Lasp1 mRNA expression in matched HCC tissues measured by real-time quantitative PCR and cDNA microarray study was established by calculating the Pearson's correlation coefficient (r). *P*-value less than 0.05 was considered statistically significant. (* $P < 0.05$; ** $P < 0.01$).

CHAPTER 3

RESULTS

3.1. Part I: Cyr61 exerted inhibitory roles in HCC growth and metastasis

3.1.1. Expression study of Cyr61 in HCC

Expression of Cyr61 in HCC clinical samples

The current study started from the validation of our previous microarray data. An experimental procedure was established in this study to validate the microarray data (section 2.3.3, modified from Neo *et al.*, 2004). To confirm our early observation from cDNA microarray analysis that Cyr61 was down-regulated in HCC tumors, mRNA expression of Cyr61 in clinical specimens was assessed by quantitative real-time PCR. Eight pairs of HCC tumor and adjacent non-tumor samples were randomly chosen from a set of 37 HCC patients (Neo *et al.*, 2004). Total RNA was subjected to one-step real-time quantitative RT-PCR using Cyr61 specific primers (Cyr61-F1, Cyr61-R1, sequence listed in Table 2.1). The run has been repeated for three times and representative result was shown in Figure 3.1A. Data were presented as the fold change of Cyr61 expression in each non-tumor tissue relative to its corresponding tumor sample after normalized to a housekeeping gene HPRT. In almost all eight pairs of samples, Cyr61 expression was down-regulated in tumor tissues compared to the corresponding non-tumor liver specimens. Moreover, the fold change of Cyr61 expression for each pair of samples was well correlated to the value obtained in our earlier cDNA microarray study by calculating the Pearson's correlation coefficient ($r = 0.878$, $P < 0.05$, Figure 3.1B), further confirming the down-regulated expression of Cyr61 observed in HCC tumors (Neo *et al.*, 2004).

Expression of Cyr61 in normal tissues

Next, the expression level of Cyr61 in normal human tissues was checked by semi-quantitative RT-PCR. Complementary DNA (cDNA) was synthesized as

described in section 2.3.2 from a collection of total RNA of 15 different normal human tissues. Then the cDNA was subjected to semi-quantitative gel-based RT-PCR using internal primer set specific to Cyr61 (Cyr61-F2, Cyr61-R2) with housekeeping gene GAPDH as a quality and quantity control (sequence listed in Table 2.2). The results showed that Cyr61 was ubiquitously expressed in 13 normal adult human tissues of a variety of organs, including male and female adult liver tissues, while its expression was barely detectable in fetal liver tissues (Figure 3.2). This finding suggests that Cyr61 expression may be under certain extent of suppression in newly regenerating hepatocytes, which had been known to resemble hepatic neoplasm in many aspects.

Expression of Cyr61 in HCC cell lines

The expression profile of Cyr61 protein was further analyzed in 14 HCC cell lines by Western blot. Cell lysates from 14 HCC cell lines were extracted and the protein concentrations were measured by Bradford protein assay as described in section 2.6.1. Then the proteins were separated by 10% SDS-PAGE followed by Western blot using a specific rabbit-anti-Cyr61 antibody with α-tubulin as a protein loading control. As shown in Figure 3.3, Cyr61 protein level was fairly low or undetectable in 10 out of 14 cell lines tested, e.g. Hep3B, Huh-7 and HepG2 cells, though it had moderate to high expression in HA22T, SNU449, Mahlavu and Sk-Hep1 cells.

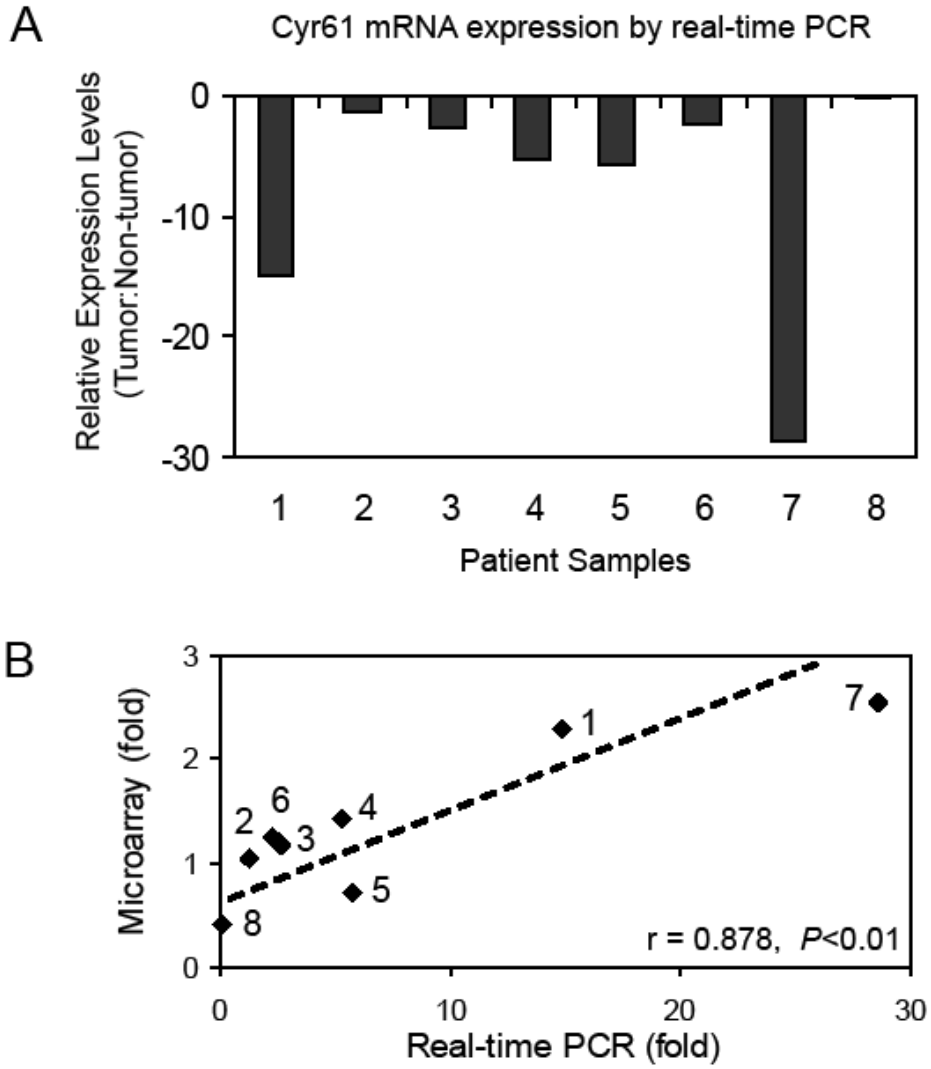

Figure 3.1 Cyr61 mRNA expression in HCC clinical samples. (A) Cyr61 mRNA expression was down-regulated in eight randomly chosen HCC tumors detected by one-step real-time quantitative RT-PCR. Data were presented as the fold change of the gene expression in each non-tumor tissue sample against its corresponding tumor sample after normalized to a housekeeping gene HPRT. Negative number reflects decreased fold change. (B) Correlation of the fold changes in each paired tumor and non-tumor samples between the results of real-time quantitative RT-PCR and the original cDNA microarray. r: correlation coefficient.

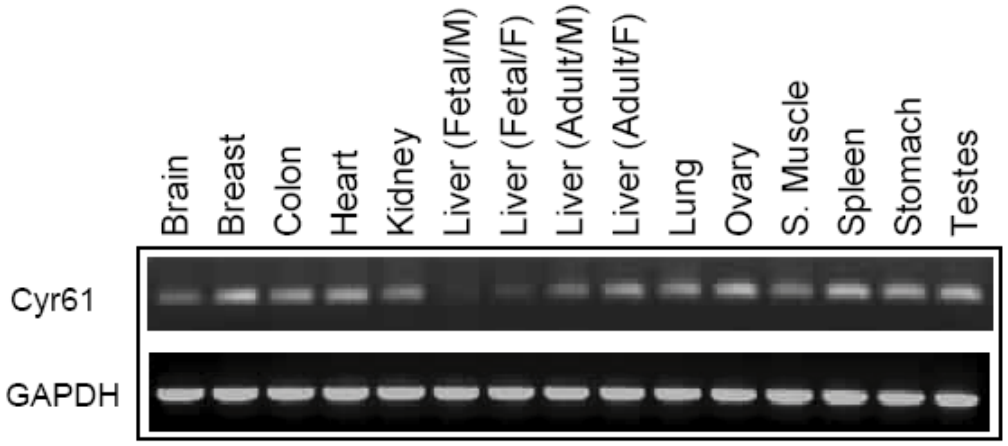

Figure 3.2 Cyr61 mRNA expression in human normal tissues. Cyr61 mRNA expression in 15 normal human tissues was measured by semi-quantitative RT-PCR analysis. GAPDH was used as an internal control for the quality and quantity of RNA samples.

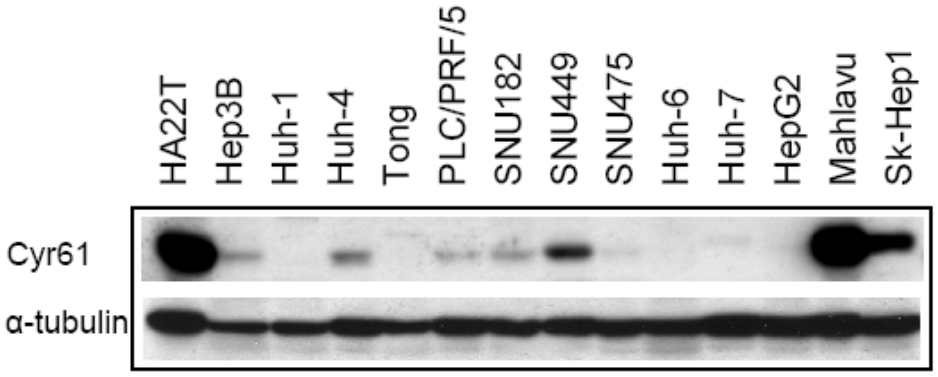

Figure 3.3 Cyr61 protein expression in HCC cell lines. 20μg of cell lysates from 14 HCC cell lines were separated on 10% SDS-PAGE gel and analyzed by Western blot with specific antibody against Cyr61. α-tubulin was used as a control for protein loading and transfer.

3.1.2. Gateway cloning of Cyr61 expression constructs

To examine the potential biological roles of Cyr61 in HCC cell growth and metastasis, two recombinant expression vectors pDEST40-Cyr61/V5 and pDEST47-Cyr61/GFP were constructed by using Gateway cloning system. The detailed protocol of the Gateway cloning strategy was described in Chapter 2.4.2. The constructed Cyr61 Gateway plasmids were illustrated in Figure 3.4A. Briefly, the full Cyr61 ORF (1143bp) was first amplified from normal adult liver cDNA by two rounds of PCR by using gene-specific primers including part of *att*B1 or *att*B2 site sequence (GW-Cyr61-F, GW-Cyr61-R) and a set of adaptor-primers (*att*B1, *att*B2) (sequence listed in Table 2.3) (Figure 3.4B). A BP recombination reaction was then performed by using the *att*B-flanking Cyr61 PCR product (~1200bp) and the *att*P-containing pDONR^{TM}221 vector (Figure 2.1 in section 2.4.2) to create a Cyr61-221 entry clone (also named as Cyr61-DONOR221). Further LR recombination reactions between the *att*L-containing entry clone Cyr61-221 and the *att*R-containing destination vectors pcDNA-DEST40 (Figure 2.2) or pcDNA-DEST47 (Figure 2.3) produced the final Cyr61 expression constructs pDEST40-Cyr61/V5 (also named as Cyr61-DEST40 or Cyr61-40) and pDEST47-Cyr61/GFP (also named as Cyr61-DEST47 or Cyr61-47). Enzymatic digestion (Figure 3.4C) and sequencing validated the sequence of the desired donor and expression vectors, with reference to the Cyr61 ORF sequence (NM_001554).

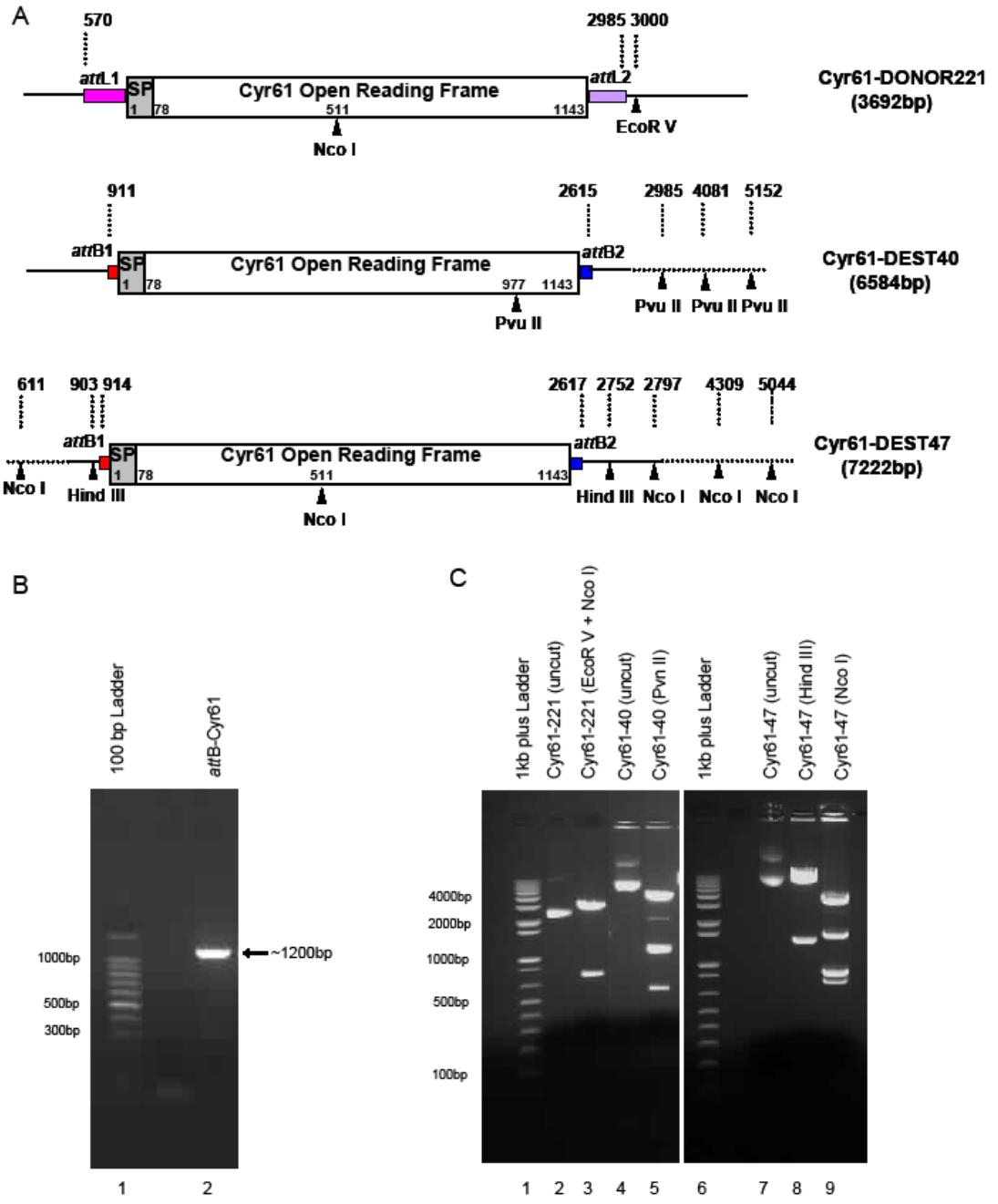

Figure 3.4 Gateway cloning for Cyr61 ORF. (A) Illustrations of the constructed plasmids. SP: Signal Peptide. *att*L1 (pink), *att*L2 (purple), *att*B1 (red), *att*B2 (blue) sites and the restriction enzyme sites (▲) are indicated. (B) PCR amplification of Cyr61 ORF carrying part of *att*B recombination sites. Lane1: 100bp DNA Ladder; Lane2: *att*B-Cyr61 PCR product of about 1200bp. (C) Enzyme digestion of the constructed donor and expression vectors. Lane1 and Lane6: 1kb plus DNA ladder; Lane2: Cyr61-DONOR221 uncut; Lane3: Cyr61-DONOR221 EcoR V + Nco I digested, 2 fragments (749bp, 2943bp); Lane4: Cyr61-DEST40 uncut; Lane5: Cyr61-DEST40 Pvu II digested, 4 fragments (538bp, 1071bp, 1096bp, 3879bp); Lane7: Cyr61-DEST47 uncut; Lane8: Cyr61-DEST47 Hind III digested, 2 fragments (1291bp, 5913bp); Lane9: Cyr61-DEST47 Nco I digested, 5 fragments (735bp, 814bp, 814bp, 1512bp, 3347bp).

The constructed Cyr61 expression vectors were transfected into HCC cell lines with low abundant endogenous Cyr61. Also, two HepG2 stable cell lines with Cyr61 over-expression (HepG2-Cyr61-1 and HepG2-Cyr61-2) and one control clone with Neo-resistant gene (HepG2-Neo) were established by selecting in DMEM/G418, which usually generate more consistent results by removing the variability of different transient transfection efficiency frequently observed in HepG2 cells. Next, a series of functional assays, such as WST-1 cell proliferation assay, soft agar assay, cell adhesion assay, cell migration and invasion assay, cell cycle analysis by flow cytometry, and cellular localization study by confocal microscopy, were performed based on Cyr61 transient or stable over-expression.

In addition, in order to expand our understanding in the roles of Cyr61 in hepatocarcinogenesis, we obtained commercially available Cyr61 specific siRNA to further knockdown Cyr61 level in HCC cell lines and examined the function of Cyr61 in HCC cell growth.

3.1.3. Function study of Cyr61 on HCC cell growth

Effect of Cyr61 transient over-expression in monolayer

The recombinant plasmid pDEST40-Cyr61/V5 and pcDNA3.1 control plasmid were transfected into HepG2, Hep3B and Huh-7 HCC cell lines, all of which had minimal levels of Cyr61 protein (Figure 3.3). Over-expression of Cyr61-V5 fusion protein in these cell lines was confirmed by Western blot by using specific mouse anti-V5 antibody with α-tubulin blotting as a protein loading control (Figure 3.5). 24 hours after transfection, the cells were trypsinized, counted and replated proportionally into 96-well plates (1-4 × 10^4 per well) in triplicates. Then the effect of Cyr61 expression on cell growth in monolayer was measured by WST-1 cell

proliferation assay daily as described in section 2.7. As shown in Figure 3.6, all three HCC cell lines with over-expressed Cyr61-V5 exhibited suppressed proliferation rate over a 3-day culturing period as compared to corresponding control cells transfected with pcDNA3.1 empty vector. At Day 3 post transfection, the cell number of Cyr61 over-expressed HepG2 cells reached 119.7×10^3 per well, which is only 55.6% of that of the pcDNA3.1 control transfected cells (215.2×10^3 per well). While in Hep3B and Huh-7 cells, the cell number of pDEST40-Cyr61/V5 transfected cells were about 42.6% (Hep3B) and 68.4% (Huh-7) respectively of that of the corresponding control cells ($P < 0.01$).

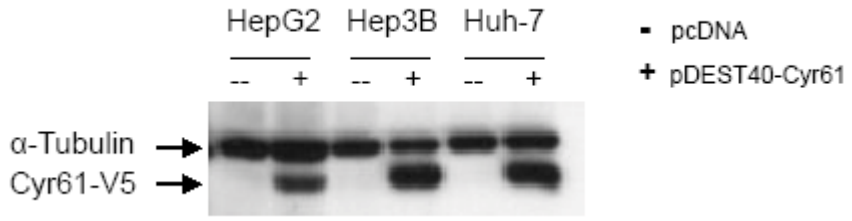

Figure 3.5 Cyr61-V5 fusion protein expression in transient Cyr61 over-expressed HCC cells. 48 hours after transfection of pDEST40-Cyr61/V5 (+: pDEST40-Cyr61) or pcDNA3.1 (–: pcDNA) into HepG2, Hep3B or Huh-7 cells, the cell lysates were collected and the proteins were separated by 10% SDS-PAGE followed by Western blot using a specific anti-V5 antibody. The V5-tagged over-expressed protein is shown as indicated by the arrow. α-tubulin blotting was used as a protein loading control.

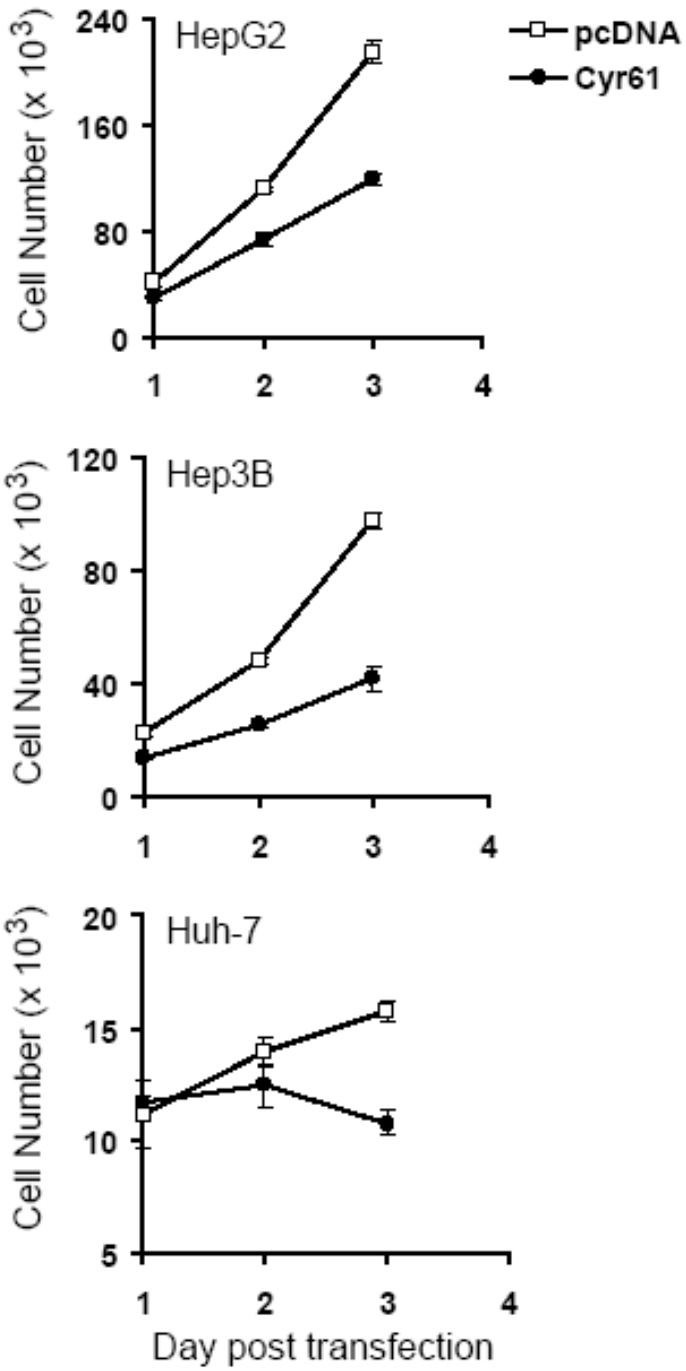

Figure 3.6 Cyr61 transient over-expression inhibited HCC cell proliferation in monolayer. pcDNA3.1 (pcDNA, open square) or pDEST40-Cyr61/V5 (Cyr61, filled circle) transfected HepG2, Hep3B or Huh-7 cells were replated into 96-well plates in triplicates 24 hours after transfection. The growth rates at indicated time points were measured by WST-1 reagent. The mean ± SD of triplicates are also shown for each point. In all three cell lines, pDEST40-Cyr61/V5 transfected cells showed a reduced cell proliferation rate compared to pcDNA3.1 transfected cells.

Effect of Cyr61 stable over-expression in monolayer

Two HepG2 stable cell lines with Cyr61 over-expression (HepG2-Cyr61-1 and HepG2-Cyr61-2) and one control cell line with Neo-resistant gene (HepG2-Neo) were established for this study. Firstly, HepG2 stable transfectants were selected after cultured in DMEM/10%FBS supplemented with 800μg/ml geneticin (G418) for 2 weeks. The stable over-expression of Cyr61 was confirmed by Western blot. As shown in Figure 3.7, over-expression of Cyr61-V5 fusion protein was maintained in HepG2-Cyr61-1 and HepG2-Cyr61-2 stable cell lines up to 4 passages. The HepG2-Cyr61-2 had an even higher Cyr61-V5 expression level than HepG2-Cyr61-1 at the same passage, while in HepG2-Neo control cells, Cyr61 level remained to be undetectable as shown by blotting with rabbit anti-Cyr61 specific antibody.

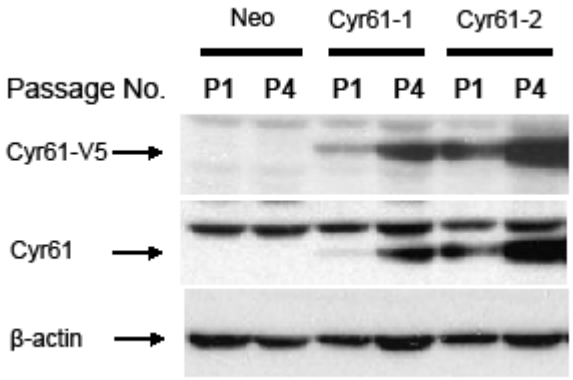

Figure 3.7 Cyr61-V5 fusion protein expression in HepG2-Cyr61 stable cell lines. HepG2 stable transfectants were selected in DMEM/10% FBS supplemented with 800μg/ml G418. Cell lysates from different passages were collected and the over-expression of Cyr61 in two HepG2-Cyr61 stable clones (Cyr61-1, Cyr61-2) compared to the HepG2-Neo control clone (Neo) was confirmed by Western blot with both specific anti-V5 and anti-Cyr61 antibody. β-actin blotting was used as a protein loading control.

At the passage of three to four, these two HepG2-Cyr61 stable cell lines and HepG2-Neo control cells cultured in tissue culture flask were trypsinized, counted, seeded at the same concentration (~2 × 10^4 /well) into 96-well plates in triplicates. The WST-1 cell proliferation assay was performed daily to monitor the growth rate of each cell line. In order to remove the variations generated by manual cell counting, the data were presented at each time point as the percentage relative to the cell number seeded at Day 0 for each line, which was arbitrarily set at 100% as Day 0 control. Figure 3.8 clearly demonstrated that HepG2-Cyr61 stable expression also exhibited inhibitory effect on cell growth in monolayer. At Day 4 post seeding, the cell number of Cyr61 stable clones was only 71.8% (HepG2-Cyr61-1) (749.4% of Day 0 control) and 38.7% (HepG2-Cyr61-2) (404.2% of Day 0 control) respectively of that of HepG2-Neo control cells (1043.8% of Day 0 control) ($P < 0.05$). The fact that HepG2-Cyr61-2 had a higher Cyr61-V5 expression level than HepG2-Cyr61-1 (Figure 3.7) may explain the observation that HepG2-Cyr61-2 had a stronger effect in inhibiting cell growth.

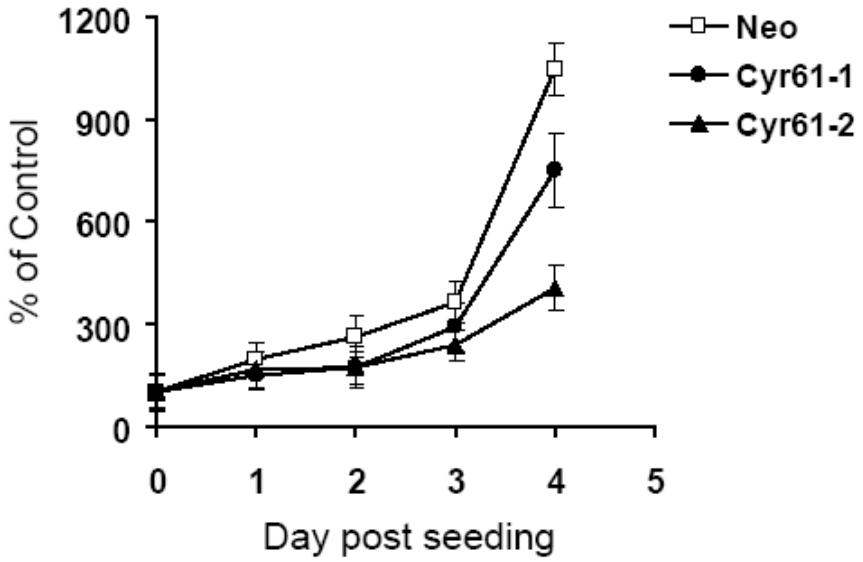

Figure 3.8 Cyr61 stable over-expression inhibited cell proliferation in HepG2 cells. Two HepG2-Cyr61 stable transfectants (HepG2-Cyr61-1, HepG2-Cyr61-2) and one HepG2-Neo control cell line were seeded in 96-well plate in triplicates and the cell growth rates were monitored daily by WST-1 assay. Data were presented as the percentage at each time point relative to the cell number seeded at Day 0 for each line, which was arbitrarily set at 100% as Day 0 control. The mean ± SD of triplicates are shown for each point. Both HepG2-Cyr61-1 (filled circle) and HepG2-Cyr61-2 (filled triangle) stable cell lines showed reduced cell proliferation rate compared to HepG2-Neo (open square) control cells over a 4-day continuous culture.

Effect of Cyr61 siRNA knockdown in monolayer

To examine the role of endogenous Cyr61, siRNA was introduced into HepG2 and Hep3B cells. 48 hours after transfection, total RNA and cell lysates were separately collected and the knockdown effect was measured by both two-step real-time quantitative RT-PCR and Western blot. After normalized to a housekeeping gene HPRT, the Cyr61 mRNA expression in Negative Control siRNA transfected cells was arbitrarily set as 1.0. As shown in Figure 3.9A, both Cyr61 siRNA oligos down-regulated Cyr61 mRNA to the level lower than 40% of that of the control. The protein level was further reduced based on the trace amount of Cyr61 protein left in the parental HepG2 and Hep3B cells, as indicated by showing the Cyr61 protein in Negative Control siRNA transfected cells (Figure 3.9B). A relatively long exposure time was utilized here so that the extremely low level of endogenous Cyr61 protein can be detected, through which the knockdown effect could be observed easily.

The WST-1 assay of both cell lines transfected with Cyr61 siRNA oligos (Cyr61#1, Cyr61#2) showed an increase in cell proliferation rate compared to Negative Control siRNA transfected cells. At Day 4 post transfection in Hep3B, the cell number of Cyr61#1 and Cyr61#2 oligo transfected cells was 143.4% (93.1×10^3 per well) and 131.8% (85.5×10^3 per well) of that of Negative Control siRNA transfected cells (64.9×10^3 per well), respectively ($P < 0.01$). Whereas in HepG2 cells, the effect of Cyr61 siRNA knockdown was more prominent, as the cell number of the siRNA treated cells reached 220.8% (321.9×10^3 per well) (Cyr61#1) and 232.4% (338.9×10^3 per well) (Cyr61#2) of control (145.8×10^3 per well) ($P < 0.01$) (Figure 3.10). In conclusion, these results demonstrated that Cyr61 exerted growth inhibitory effects on HCC cells in monolayer.

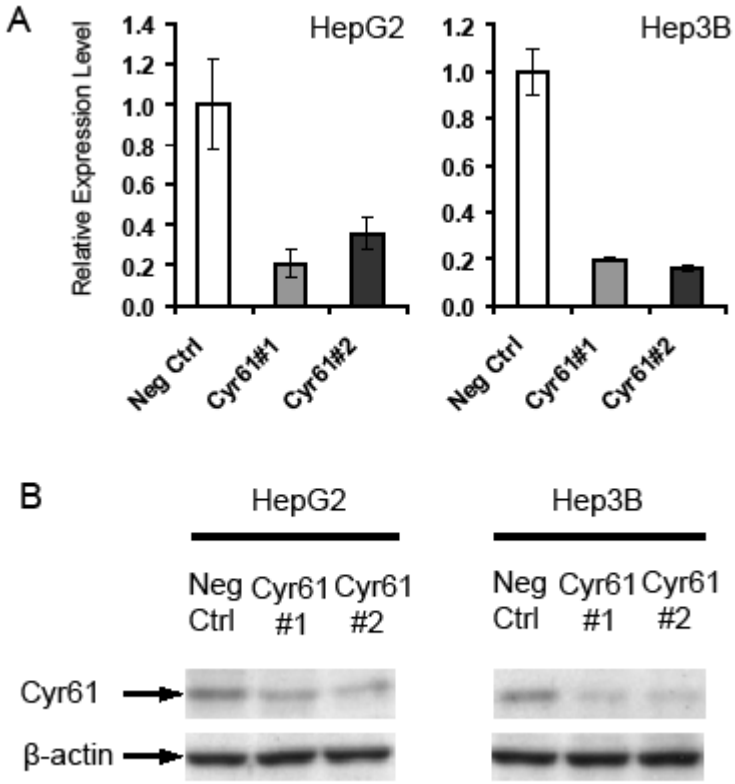

Figure 3.9 Cyr61 siRNA oligos further down-regulated the mRNA and protein expression in HCC cells. Both Cyr61 mRNA and protein level was down-regulated by Cyr61 siRNA oligos (Cyr61#1, Cyr61#2) compared to Negative Control siRNA (Neg Ctrl) transfected HepG2 or Hep3B cells. 48 hours after transfection, the total RNA and cell lysates were separately collected. (A) Total RNA was subjected to cDNA synthesis and subsequent real-time quantitative RT-PCR analysis. In each cell line, after normalized to a housekeeping gene HPRT, the Cyr61 mRNA expression in Negative Control siRNA (Neg Ctrl) transfected cells was arbitrarily set as 1.0. The mean ± SD of triplicates are shown. (B) Protein lysates were separated on 10% SDS-PAGE followed by Western blot using a rabbit anti-Cyr61 specific antibody with β-actin included as a protein loading control.

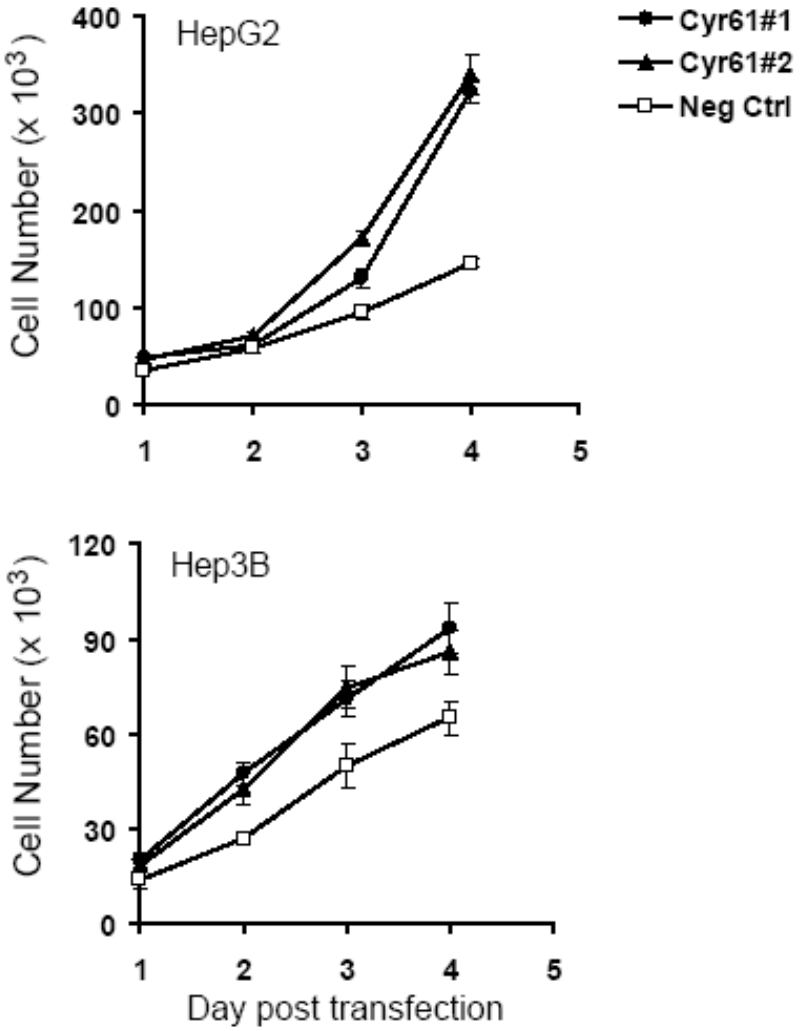

Figure 3.10 Cyr61 siRNA knockdown enhanced HCC cell proliferation in monolayer. Negative Control siRNA (open square), Cyr61#1 (filled circle), or Cyr61#2 (filled triangle) transfected HepG2 or Hep3B cells were replated into 96-well plates in triplicates 24 hours after transfection and the growth rates at indicated time points were measured by WST-1 reagent. The mean ± SD of triplicates are shown for each point. Both siRNA oligos (Cyr61#1, Cyr61#2) transfected HepG2 or Hep3B cells showed an increased cell proliferation rate than Negative Control siRNA transfected cells.

Effect of Cyr61 transient over-expression in soft agar assay

To further explore the inhibitory effects of Cyr61 on HCC cell growth under more stringent conditions, an anchorage-independent assay was performed to examine the colony formation ability in soft agar culture. Anchorage-independent growth is a hallmark of cellular transformation, and colony formation in semi-solid medium such as soft agar is a key assay for measuring this growth (Shin *et al*. 1975). The colony number and colony size formed in soft agar usually reflect the cloning efficiency and cell proliferation rate, respectively (Claassen *et al.* 2004). As described in section 2.8, HepG2 cells transfected with either pDEST40-Cyr61/V5 or pcDNA3.1 control plasmid were replated for soft agar assay. After culture at 37°C for additional three weeks, the colonies were stained, photographed and the colonies > 100μm in diameter were counted. The images clearly showed that, in sharp contrast to the controls transfected with pcDNA3.1, HepG2 cells transfected with pDEST40-Cyr61/V5 formed much fewer and smaller colonies in semi-soft agar (Figure 3.11A), the colony forming efficiency of which was only about 40% of control as reflected by colony count ($P < 0.05$) (Figure 3.11B). These results indicated that over-expression of Cyr61 significantly reduced the anchorage-independent growth of HepG2 cells, suggesting that Cyr61 can inhibit both HCC cell proliferation rate and cloning efficiency.

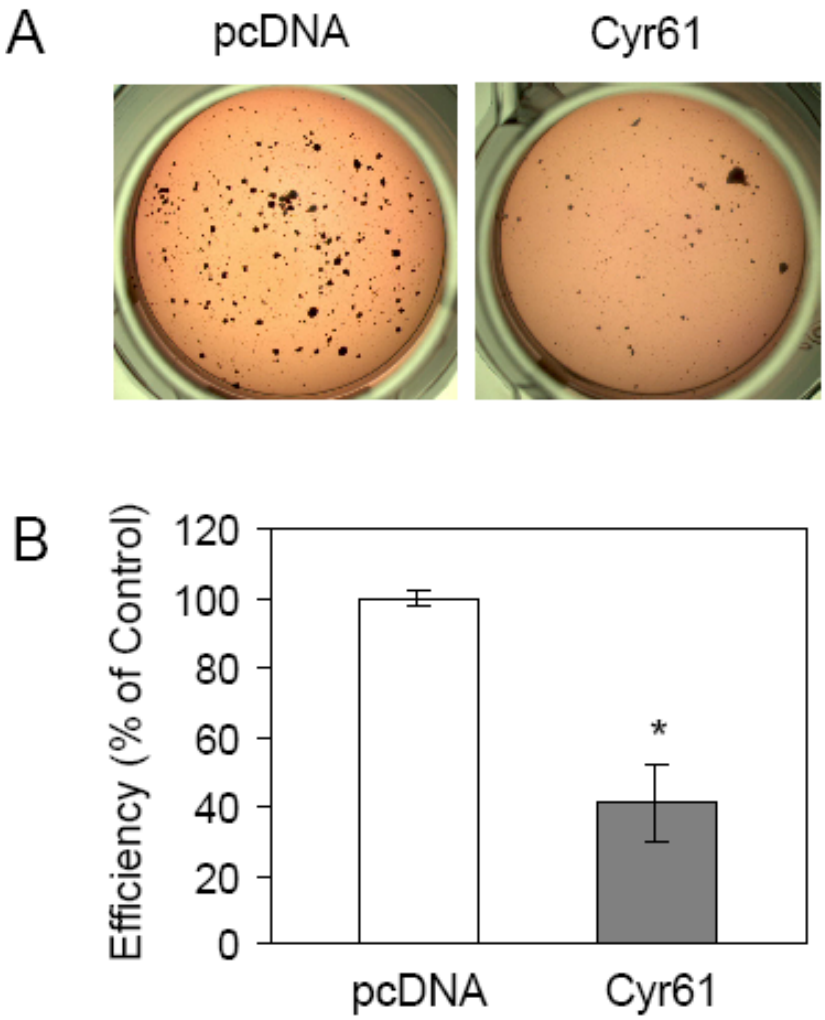

Figure 3.11 Cyr61 over-expression inhibited anchorage-independent growth of HepG2 cells in soft agar. HepG2 cells transfected with pDEST40-Cyr61/V5 or pcDNA3.1 control were trypsinized 24 hours after transfection. 1×10^4 cells were re-suspended in 0.25ml of 0.35% agar dissolved in DMEM/10%FBS and plated in 24-well plate in triplicates overlying a 0.7% agar bottom layer and cultured at 37°C with 5% CO_2 for 3 weeks. Then the cells were stained and the colonies were visualized and photographed under microscope. (A) Representative images showed that HepG2 cells transfected with pDEST40-Cyr61/V5 (Cyr61) formed much smaller and fewer colonies in soft agar than those transfected with pcDNA3.1 control (pcDNA). (B) The colonies > 100μm in diameter were counted by Leica QWin imaging software. The colony forming efficiency was calculated as the percentage of the colony number formed by pDEST40-Cyr61/V5 transfected cells (grey bar) relative to that formed by pcDNA3.1 transfected cells (white bar), which was arbitrarily set at 100% (mean± SD of triplicates). *$P < 0.05$.

3.1.4. Function study of Cyr61 on HCC cell adhesion, migration and invasion

Effect of Cyr61 on cell adhesion to ECM proteins

As a secreted heparin-binding protein, Cyr61 has been shown to be associated with altered ECM-cell interactions to regulate the adhesion activities of a variety of cells, such as fibroblasts, endothelial cells, and smooth muscle cells (Chen *et al*. 2000; Grzeszkiewicz *et al*. 2002; Leu *et al*. 2002). As described in section 1.1.4, there are various ECM proteins. By considering their functional associations with cancer, the role of Cyr61 in mediating HCC cell adhesion ability to 5 selected types of ECM proteins, including fibronectin, vitronectin, laminin, collagen I, and collagen IV were examined in this study. HepG2 and Hep3B cells transfected with either pDEST40-Cyr61/V5 or pcDNA3.1 control vectors were tested for their adhesion activities to the 5 various ECM proteins as described in section 2.9.1. It was first noted that the parental HepG2 cells without any treatment adhered strongly to vitronectin, laminin, collagen I and collagen IV, but barely to fibronectin (Figure 3.12A). This suggests a selective decreased adhesion to certain types of ECM proteins in HCC cells. While the pcDNA3.1 transfected HepG2 cells showed similar pattern of adhesion to ECM proteins as non-treated cells (data not shown), over-expression of Cyr61 extensively improved the adhesion of HepG2 cells to various ECM proteins, namely vitronectin to 144%, laminin to 132%, collagen I to 155%, collagen IV to 149% ($P < 0.05$), and most remarkably, fibronectin to about 260% as compared to the control ($P < 0.01$) (Figure 3.12B). The parental Hep3B cells adhered to the almost same extent to the fibronectin, laminin, collagen I and collagen IV, but weakly to vitronectin. The adhesion ability of Hep3B cells to vitronectin is only 26.3-44.6% of that to other 4 types of ECM proteins ($P < 0.01$) (Figure 3.12C). Over-expression of Cyr61 also significantly increased the adhesion of Hep3B cells to fibronectin to 132%, laminin to

144%, collagen I to 147%, collagen IV to 144% ($P < 0.05$), and vitronectin to 170% ($P < 0.01$) (Figure 3.12D). In conclusion, over-expression of Cyr61 promoted cell adhesion of HCC cells to a variety of ECM proteins.

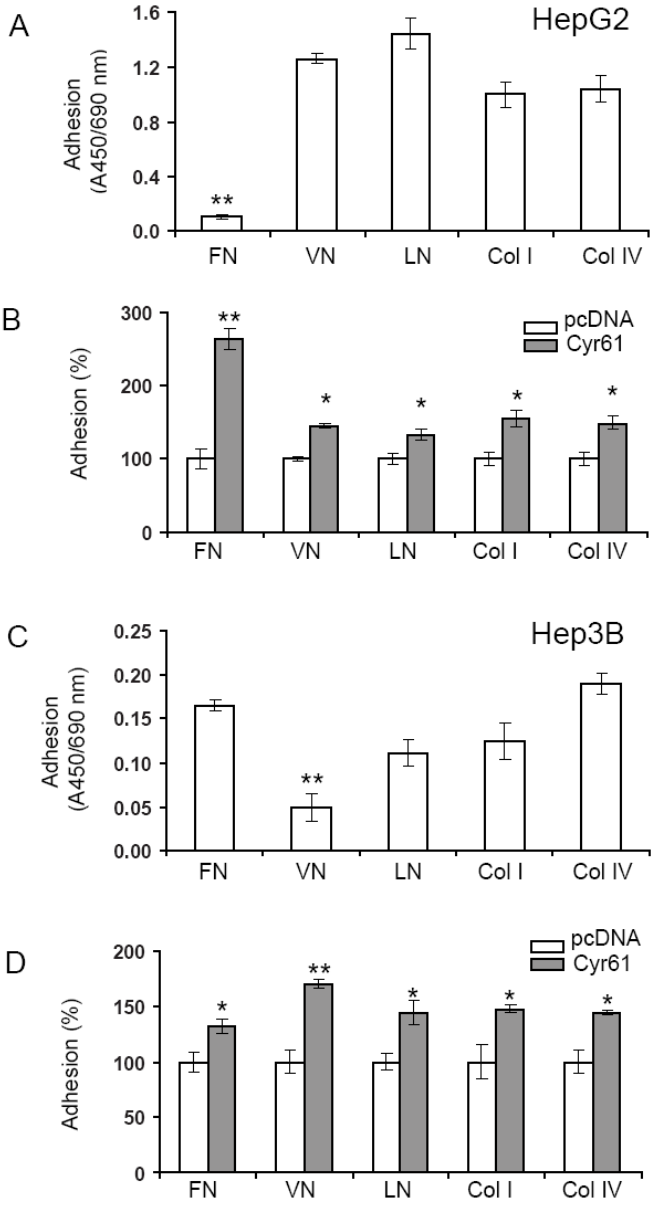

Figure 3.12 Cyr61 over-expression enhanced HCC cell adhesion to ECM proteins. Adhesiveness of non-treated HepG2 (A) and Hep3B (C) cells to ECM proteins, including fibronectin (FN), vitronectin (VN), laminin (LN), collagen I (Col I) and collagen IV (Col IV). Forty-eight hours after transient transfection with pDEST40-Cyr61/V5 (grey bars) or pcDNA3.1 (white bars), HepG2 (B) and Hep3B (D) cells were replated for cell adhesion assay. Adhesion efficiency to each ECM protein was presented as the percentage relative to that of the pcDNA3.1 control transfected cells, which was arbitrarily set at 100% (mean ± SD of triplicates). ** $P < 0.01$, * $P < 0.05$.

Effect of Cyr61 on HCC cell migration and invasion ability

Cell adhesion to ECM proteins is the initial step for cell migration and invasion. Dynamic regulations of adhesion assembly and disassembly are crucial determinants to control cell movement (Hood and Cheresh 2002; Ridley *et al*. 2003). Since Cyr61 was shown to be involved in the regulation of HCC cell adhesion, its potential role in cell migration and invasion during HCC progression was further explored. Microporous membrane inserts are widely used for cell migration and invasion assays. Currently, the most widely accepted assay is the Boyden chamber assay originally designed for the analysis of leukocyte chemotaxis (Chen 2005; Cheng *et al*. 2007). Firstly, the effect of transient over-expression of Cyr61 on cell migration and invasion ability in HepG2 or Hep3B cells was tested by using the modified Boyden chamber assay as described in section 2.9.2. The results reflected that the migratory activities of pDEST40-Cyr61/V5 transfected cells were inhibited 30.5% in HepG2 cells (Figure 3.13A) and up to 60.5% in Hep3B cells (Figure 3.13B) ($P < 0.01$) respectively as compared to pcDNA3.1 control. Furthermore, the invasive activities through ECM proteins were suppressed in both HepG2 (65.9% of control, $P < 0.05$) (Figure 3.13C) and Hep3B cells (44.8% of control, $P < 0.01$) (Figure 3.13D).

In addition, the HepG2 cell lines with stable Cyr61 over-expression (HepG2-Cyr61-1 and HepG2-Cyr61-2) and the control clone with Neo-resistant gene (HepG2-Neo) were also used for this study. The Boyden chamber assay showed that the migratory activities of the HepG2-Cyr61 stable cell lines were inhibited up to 58.6% (HepG2-Cyr61-1) and 55.0% (HepG2-Cyr61-2) respectively as compared to HepG2-Neo control ($P < 0.01$) (Figure 3.14A). Furthermore, the invasive activities through ECM proteins were suppressed in both HepG2-Cyr61 stable clones (40.7% and 28.0%

of control respectively, $P < 0.01$) (Figure 3.14B). These results support the conclusion that Cyr61 negatively regulated cell motility and invasiveness of human HCC cells.

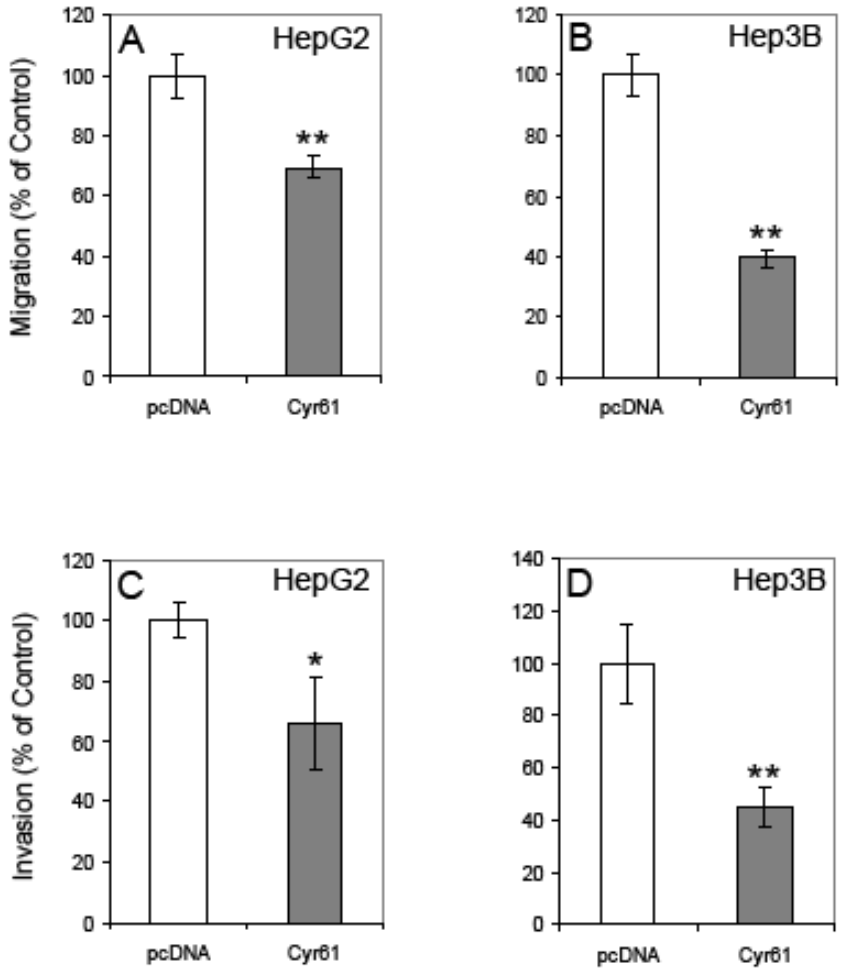

Figure 3.13 Cyr61 transient over-expression inhibited migration and invasion activities of HCC cells. After serum starvation for 24 hours, pcDNA3.1 (pcDNA, white bars) or pDEST40-Cyr61/V5 (Cyr61, grey bars) transfected HepG2 (1.0×10^5 cells / well) or Hep3B (5.0×10^4 cells /well) cells were replated for cell migration and invasion assays. Inhibitory effects on migration and invasion were presented as the percentage of fluorescent readings standardized to pcDNA3.1 control (mean ± SD of triplicates). *$P < 0.05$, ** $P < 0.01$. (A) Migration assay through 8μm microporous membranes in HepG2 cells. (B) Migration assay through 8μm microporous membranes in Hep3B cells. (C) Invasion assay through ECM proteins in HepG2 cells. (D) Invasion assay through ECM proteins in Hep3B cells.

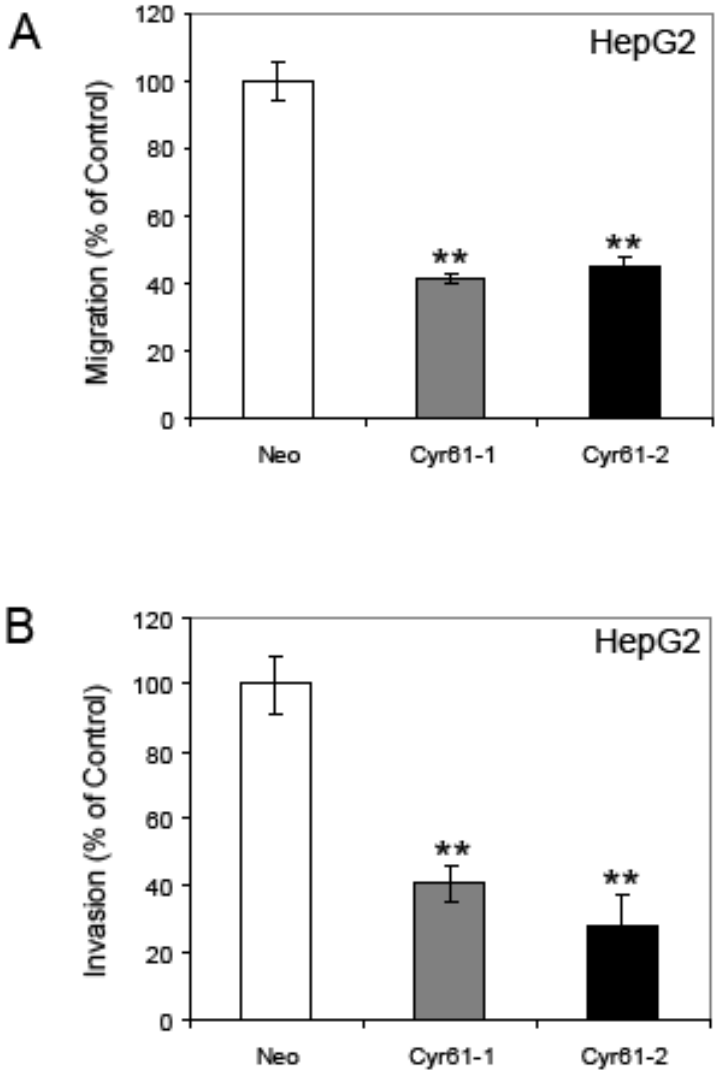

Figure 3.14 Cyr61 stable over-expression inhibited migration and invasion activities in HepG2 cells. After serum starvation for 24 hours, two stable clones HepG2-Cyr61-1 (Cyr61-1, grey bars), HepG2-Cyr61-2 (Cyr61-2, black bars), and the HepG2-Neo control cells (Neo, white bars) were plated (5.0×10^5 cells/well) for cell migration and invasion assays. Inhibitory effects on migration and invasion were presented as the percentage of fluorescent readings standardized to HepG2-Neo control (mean ± SD of triplicates). ** $P < 0.01$. (A) Migration assay through 8μm microporous membranes. (B) Invasion assay through ECM proteins.

3.1.5. Cellular localization study of Cyr61 in HCC

The protein cellular localization study may help to better understand the function and pathway of proteins in a particular cell type. In order to determine the intracellular distribution of Cyr61 protein in HCC cells, the Cyr61 fusion construct with green fluorescent protein (pDEST47-Cyr61/GFP) was transfected into HepG2, Hep3B and Huh-7 cells. 48 hours after transfection, the cells were fixed and analyzed under fluorescent confocal microscope. The fluorescent signals clearly showed that Cyr61/GFP fusion protein was present in perinuclear region and cytoplasmic granules, suggesting that Cyr61 was localized to the secretory pathway of cells (Figure 3.15A). Correspondingly, a substantial level of secreted Cyr61-V5 protein (~46kDa) was detected in the culture supernatant of pDEST40-Cyr61/V5 transfected HepG2, Hep3B and Huh-7 cells by Western blot, while culture medium from cells transfected with pcDNA3.1 empty vector showed no detectable Cyr61 secretion over a 48 hour's period (Figure 3.15B).

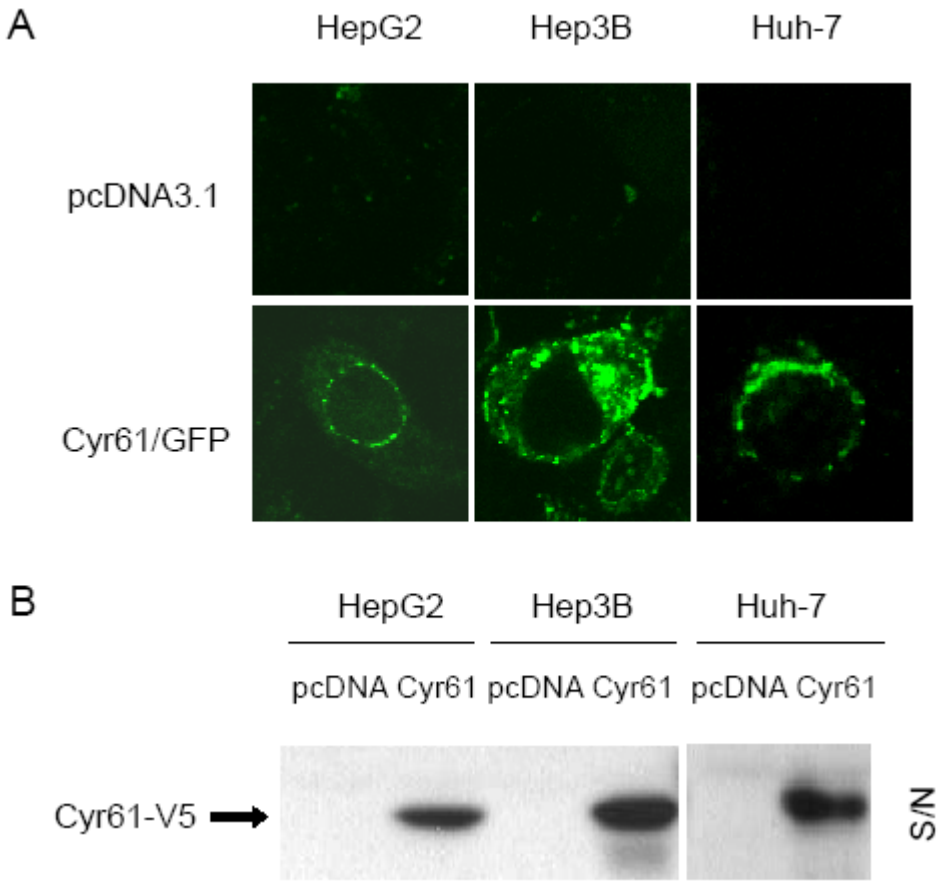

Figure 3.15 Subcellular localization of Cyr61 in HCC cells. (A) Intracellular distribution of Cyr61-GFP fusion protein observed under the fluorescent confocal microscope. HepG2, Hep3B and Huh-7 cells were transfected with pDEST47-Cyr61/GFP plasmid. 48 hours later, the fluorescent signals were observed and photographed (100 ×) under a confocal microscope. Cells transfected with pcDNA3.1 empty vector were used as background control. (B) Secreted Cyr61/V5 protein was detected in culture supernatant (S/N) by Western blot. Supernatant was collected from the culturing medium of HepG2, Hep3B or Huh-7 cells 48 hours after transfection with pDEST40-Cyr61/V5 or pcDNA3.1 plasmids, and separated on 10% SDS-PAGE gel followed by immunoblot analysis with anti-V5 antibody.

In summary, a comprehensive experimental *in vitro* system using human HCC cell lines was established in this study to explore the potential roles of Cyr61 in growth and metastasis of human HCC.

The cell proliferation study indicated that down-regulation of Cyr61 in HCC may represent a strategy developed by tumor cells to gain growth advantages. Over-expression of Cyr61 significantly suppressed the proliferation rate of HCC cells in monolayer. Cyr61 transfected cells formed fewer colonies in soft agar compared to mock transfected controls. It was also showed that the capability of anchorage-independent growth, which is an important indicator of malignant transformation, was inhibited by Cyr61 expression as well. Knockdown of endogenous Cyr61 by siRNA in HCC cell lines enhanced cell proliferation rate in monolayer instead, further confirmed that Cyr61 exerted an inhibitory effect in HCC cell growth.

Moreover, HCC may acquire high mobility and metastatic potential by suppressing Cyr61 expression as shown by the cell adhesion, migration and invasion study. Enhanced adhesion to ECM proteins was observed in Cyr61 over-expressing cells. Both transient and stable over-expression of Cyr61 in HCC cells efficiently inhibited cell migration and invasion abilities as compared to controls. All these results suggested that Cyr61 may be involved in the process of regulating HCC metastasis.

3.2. Part II: Lasp1 exerted enhancing roles in HCC growth and metastasis

3.2.1. Expression study of Lasp1 in HCC

Expression of Lasp1 in HCC clinical samples

Similarly as in Cyr61 expression study, in order to confirm our early observation from cDNA microarray analysis that Lasp1 was up-regulated in HCC tumors, mRNA expression of Lasp1 in clinical specimens was assessed by one-step quantitative real-time RT-PCR using Lasp1 specific primers (Lasp1-F, Lasp1-R, sequence listed in Table 2.1). The experiment has been repeated for three times and a representative result is shown in Figure 3.16A. Data were presented as the fold change of Lasp1 expression in each tumor tissue relative to its corresponding non-tumor sample after normalized to the housekeeping gene HPRT. In the same collection of eight pairs of randomly chosen samples from 37 HCC patients, Lasp1 expression was up-regulated in all tumor tissues compared to the corresponding non-tumor liver specimens. Moreover, the fold change of Lasp1 expression for each pair of samples was highly correlated to the value obtained in our cDNA microarray study ($r = 0.992$, $P < 0.01$, Figure 3.16B), further confirming the up-regulated expression of Lasp1 observed in HCC tumors (Neo *et al.*, 2004).

Expression of Lasp1 in normal tissues

Next, the expression level of Lasp1 in normal human tissues was checked by semi-quantitative RT-PCR. The cDNA synthesized from the total RNA of 15 types of normal human tissues was here used for detecting Lasp1 mRNA expression with Lasp1 specific primer set (Lasp1-F, Lasp1-R) with GAPDH as the housekeeping gene. Lasp1 was shown to be ubiquitously expressed in most human normal tissues, including fetal liver tissues, whereas its expression was barely detectable in adult liver

tissues and in skeletal muscle (Figure 3.17). The high level of Lasp1 mRNA expression in normal human fetal liver tissues suggests that Lasp1 may have important roles in newly regenerating hepatocytes.

Expression of Lasp1 in HCC cell lines

The expression profile of Lasp1 was further analyzed in 14 HCC cell lines. The cell lysates from the 14 HCC cell lines were separated by 10% SDS-PAGE followed by Western blot using a rabbit-anti-Lasp1 specific antibody with α-tubulin as a protein loading control. As indicated in Figure 3.18, except in PLC/PRF/5 and Huh-6, Lasp1 had high level of expression in HCC cell lines, further confirming the conclusion that Lasp1 was up-regulated in human hepatocellular carcinoma.

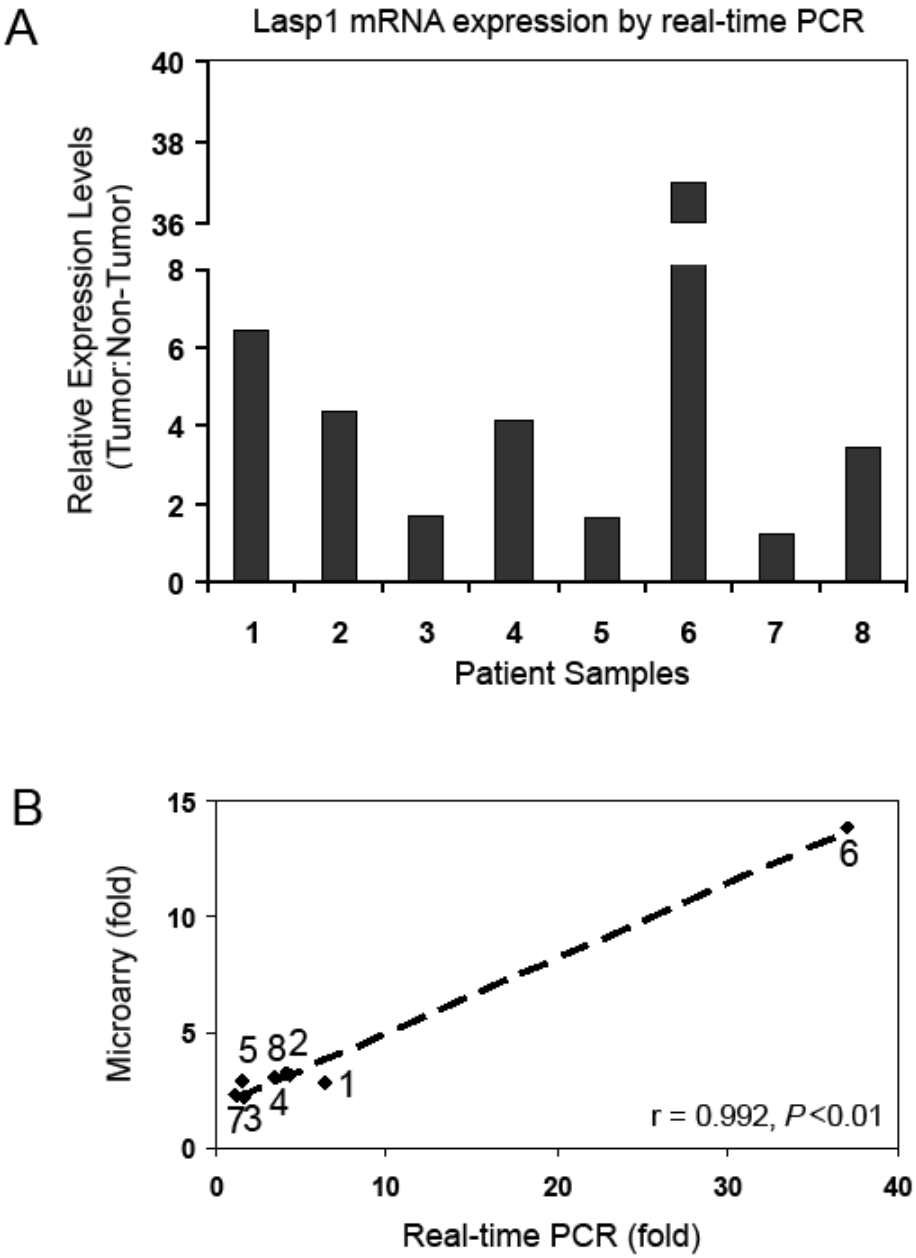

Figure 3.16 Lasp1 mRNA expression in HCC clinical samples. (A) Lasp1 mRNA expression was up-regulated in eight randomly chosen HCC tumors detected by one-step quantitative real-time PCR. Data were presented as the fold change of the gene expression in each tumor tissue against its corresponding adjacent non-tumor tissue sample after normalized to a housekeeping gene HPRT. (B) Correlation of the fold changes in each paired tumor and non-tumor samples between the results of real-time quantitative PCR and the original cDNA microarray. r: correlation coefficient.

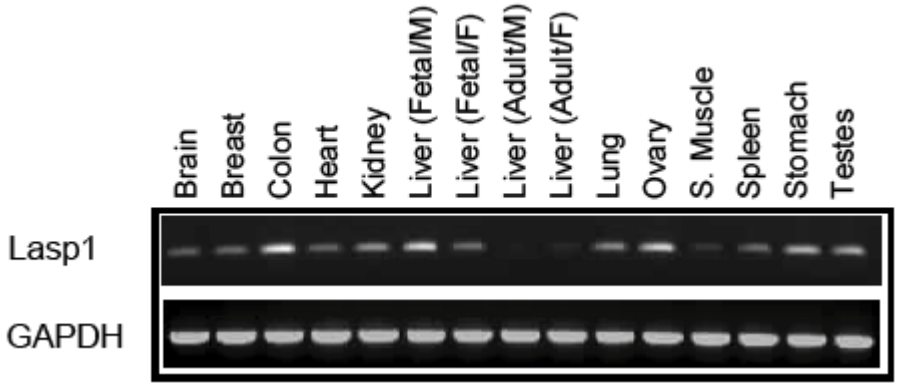

Figure 3.17 Lasp1 mRNA expression in human normal tissues. Lasp1 mRNA expression in 15 normal human tissues was measured by semi-quantitative RT-PCR analysis. GAPDH was used as an internal control for the quality and quantity of RNA samples.

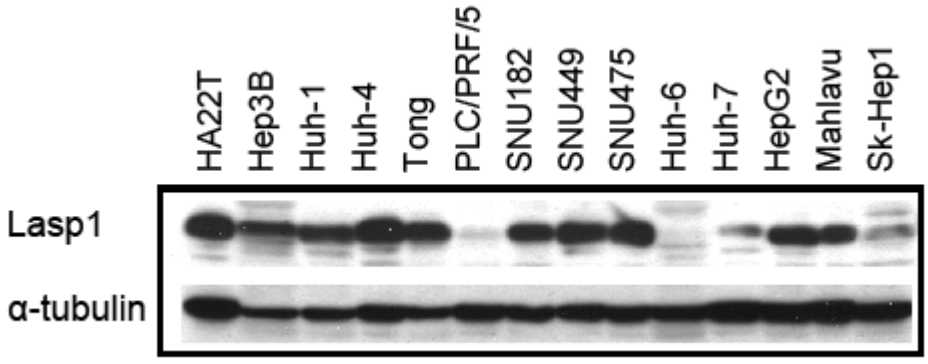

Figure 3.18 Lasp1 protein expression in HCC cell lines. 20μg of cell lysate from 14 HCC cell lines was separated on 10% SDS-PAGE gel and analyzed by Western blot with specific antibody against Lasp1. α-tubulin blotting was used as a control for protein loading and transfer.

3.2.2. Gateway cloning of Lasp1 expression constructs

To examine the potential roles of Lasp1 in human HCC growth and metastasis, the Lasp1 expression vectors pDEST40-Lasp1/V5 and pDEST47-Lasp1/GFP were constructed by using Gateway cloning system. The constructed Lasp1 Gateway plasmids were illustrated in Figure 3.19A. As Lasp1 mRNA has the highest expression level in normal human colon tissue among 15 different tissue samples tested (Figure 3.17), the full ORF of Lasp1 (783bp) was first amplified from the normal colon tissue cDNA by two rounds of PCR using gene-specific primers (GW-Lasp1-F, GW-Lasp1-R) and a set of adaptor-primers (*att*B1, *att*B2) (sequence listed in Table 2.3) (Figure 3.19B). BP recombination reaction was then performed by using the purified *att*B-flanking Lasp1 PCR product and the *att*P-containing pDONR^{TM}221 vector (Figure 2.1) to create the Lasp1-221 entry clone (also names as Lasp1-DONOR221). Further LR recombination reactions between the entry clone and the destination vectors produced the Lasp1 expression constructs pDEST40-Lasp1/V5 (also named as Lasp1-DEST40 or Lasp1-40) and pDEST47-Lasp1/GFP (also named as Lasp1-DEST47 or Lasp1-47). Enzymatic digestion (Figure 3.19C) and sequencing validated the right sequence of desired donor and expression vectors, with reference to the Lasp1 ORF sequence (NM_006148).

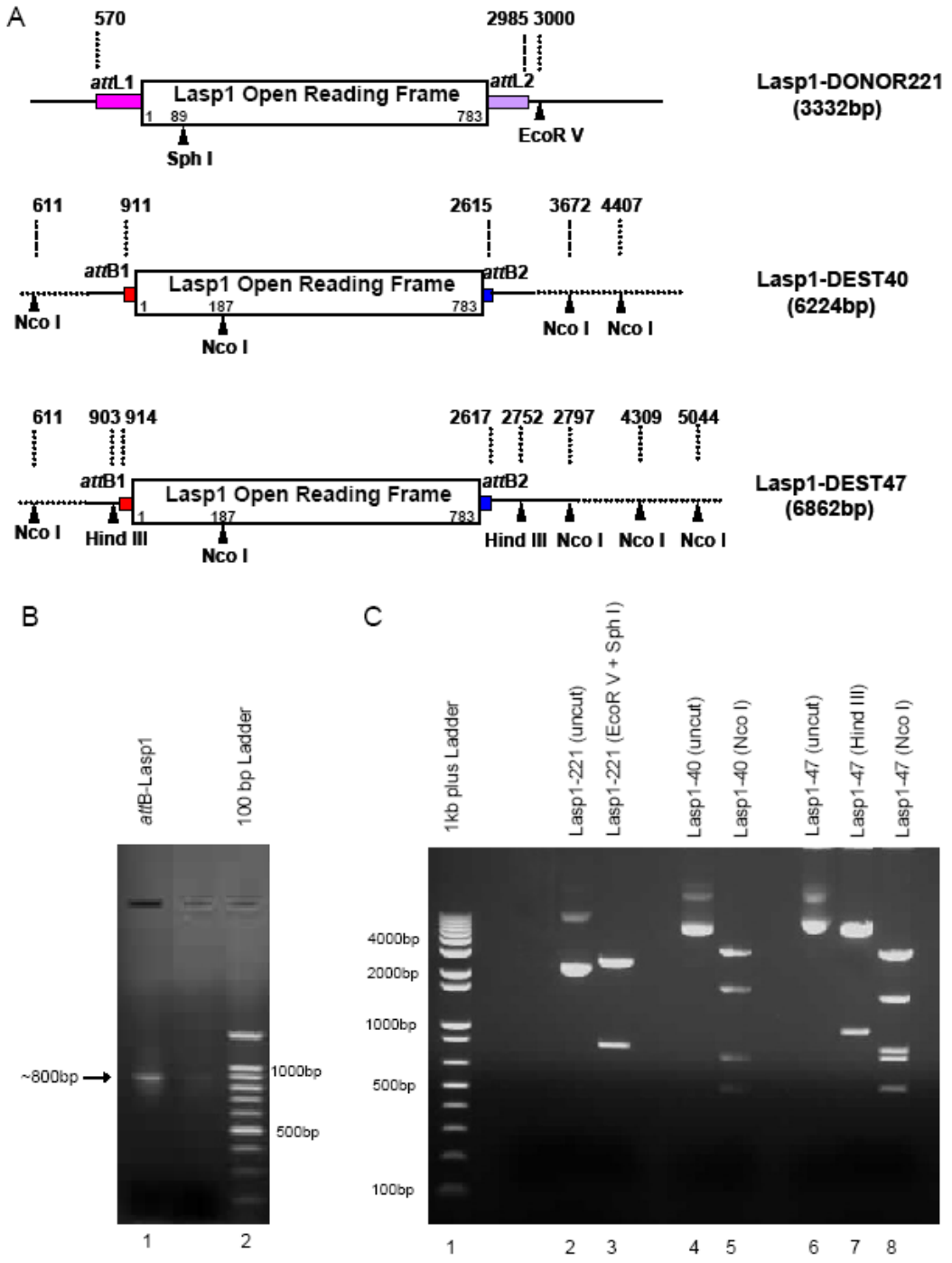

Figure 3.19 Gateway cloning for Lasp1 ORF. (A) Illustrations of the constructed plasmids. *att*L1 (pink), *att*L2 (purple), *att*B1 (red), *att*B2 (blue) sites and the restriction enzyme sites (▲) are indicated. (B) PCR amplification of Lasp1 ORF carrying part of *att*B recombination sites. Lane1: *att*B-Lasp1 PCR product of about 800bp; Lane2: 100bp Ladder. (C) Enzyme digestion of the constructed donor and expression vectors. Lane1: 1kb plus ladder; Lane2: Lasp1-DONOR221 uncut; Lane3: Lasp1-DONOR221 EcoR V + Sph I digested, 2 fragments (815bp, 2517bp); Lane4: Lasp1-DEST40 uncut; Lane5: Lasp1-DEST40 Nco I digested, 4 fragments (487bp, 735bp, 1655bp, 3347bp); Lane6: Lasp1-DEST47 uncut; Lane7: Lasp1-DEST47 Hind III digested, 2 fragments (931bp, 5931bp); Lane8: Lasp1-DEST47 Nco I digested, 5 fragments (490bp, 735bp, 778bp, 1512bp, 3347bp).

In order to understand the potential biological roles of Lasp1 in human HCC, commercially available Lasp1 specific siRNA oligos were used to knockdown the high endogenous expression of Lasp1 in HCC cell lines followed by examination of the role of Lasp1 in HCC cell proliferation, anchorage-independent growth, cell migration and cell invasion ability.

In addition, the constructed recombinant expression vectors pDEST40-Lasp1/V5 and pDEST47-Lasp1/GFP were also utilized to transfect selected HCC cell lines to over-express Lasp1 level in these cells. Two HepG2 stable cell lines with Lasp1 over-expression (defined as HepG2-Lasp1-1 and HepG2-Lasp1-2) were established for this study as well. The same control clone (HepG2-Neo) used in section 3.1 were included as the control cell line in all experiments in this part of study when using HepG2-Lasp1 stable transfectants. Next, a series of functional assays, including WST-1 cell proliferation assay, soft agar assay, cell migration and invasion assay, and cellular localization study by confocal microscopy, were performed based on Lasp1 transient or stable over-expression.

3.2.3. Function study of Lasp1 on HCC cell growth

Effect of Lasp1 siRNA knockdown in monolayer

To characterize the potential roles of Lasp1 in HCC cell growth, Lasp1 specific siRNA were transfected into HepG2, Hep3B and Huh-7 cell lines, all of which had high level of Lasp1 expression (Figure 3.18). 48 hours after transfection, total RNA and cell lysates were separately collected and the knockdown effect was confirmed by both two-step real-time quantitative RT-PCR and Western blot. As shown in Figure 3.20A, both Lasp1 siRNA oligos significantly down-regulated Lasp1 mRNA. Correspondingly, the Lasp1 protein level was significantly reduced based on

the endogenous high amount of Lasp1 protein in the parental HCC cells, as indicated by showing the Lasp1 protein in Negative Control siRNA transfected cells (Figure 3.20B). Lasp1#2 had a more significant effect in decreasing both Lasp1 mRNA and protein expression in all three HCC cells. Especially in HepG2 cells, Lasp1#1 only slightly reduced Lasp1 protein level, whereas Lasp1#2 effectively down-regulated the Lasp1 protein.

Twenty-four hours after transfection, the cells were replated proportionally into 96-well plates (2-5 × 10^4 per well) in triplicates. The effect on cell growth in monolayer was measured by WST-1 cell proliferation assay daily. Figure 3.21 showed that the Lasp1 siRNA transfected cells had a reduced proliferation rate compared to Negative Control siRNA transfected cells, and the inhibitory effect corresponded well to the knockdown effect of Lasp1 protein level. At Day 4 post transfection, the cell number of Lasp1#2 transfected HepG2 cells was only 65.8% (98.8 × 10^3 per well) of that of Negative Control siRNA transfected HepG2 cells (145.8 × 10^3 per well), which was significant ($P < 0.01$). While in Hep3B and Huh-7 cell lines, both Lasp1#1 and Lasp1#2 siRNA transfected cells showed suppressed cell proliferation rate compared to Negative Control siRNA transfected cells as both oligos significantly down-regulated Lasp1 protein level (Figure 3.20B). In Hep3B, at Day 5, the cell number of Lasp1#1 and Lasp1#2 transfected cells was only 67.4% (76.4 × 10^3 per well) and 33.4% (35.1 × 10^3 per well) respectively of control (115.9 × 10^3 per well) ($P < 0.01$). At Day 4 post transfection, the cell number of Lasp1#1 and Lasp1#2 transfected Huh-7 cells was about 72.7% (157.5 × 10^3 per well) ($P < 0.05$) and 36.0% (76.8 × 10^3 per well) ($P < 0.01$) of Negative Control siRNA transfected Huh-7 cells (217.5 × 10^3 per well). These results reflected that the endogenous Lasp1 exerted an enhancing effect on HCC cell growth in monolayer.

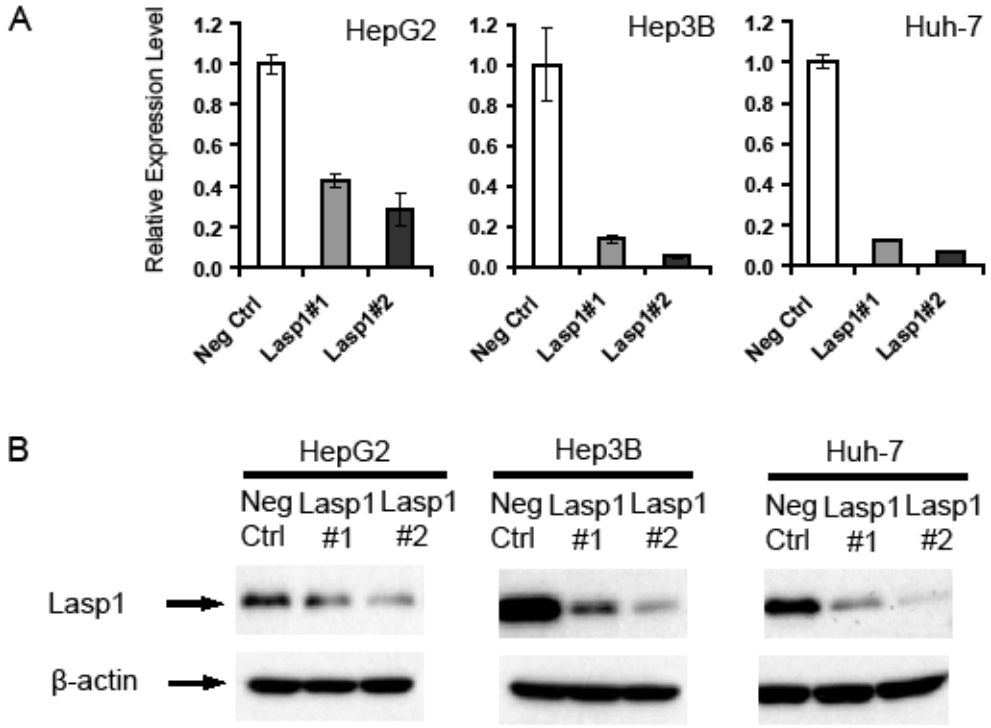

Figure 3.20 Lasp1 siRNA oligos efficiently down-regulated the mRNA and protein expression in HCC cells. Both Lasp1 mRNA and protein level was down-regulated by Lasp1 siRNA oligos (Lasp1#1, Lasp1#2) compared to Negative Control siRNA (Neg Ctrl) transfected HepG2, Hep3B and Huh-7 cells. 48 hours after transfection, the total RNA and cell lysates were separately collected. (A) Total RNA was subjected to real-time quantitative RT-PCR analysis. In each cell line, after normalized to a housekeeping gene HPRT, the Lasp1 mRNA expression in Negative Control siRNA (Neg Ctrl) transfected cells was arbitrarily set as 1.0. The mean ± SD of triplicates are shown. (B) Protein lysates were separated on 10% SDS-PAGE followed by Western blot using a rabbit anti-Lasp1 specific antibody with β-actin included as a control for protein loading and transfer.

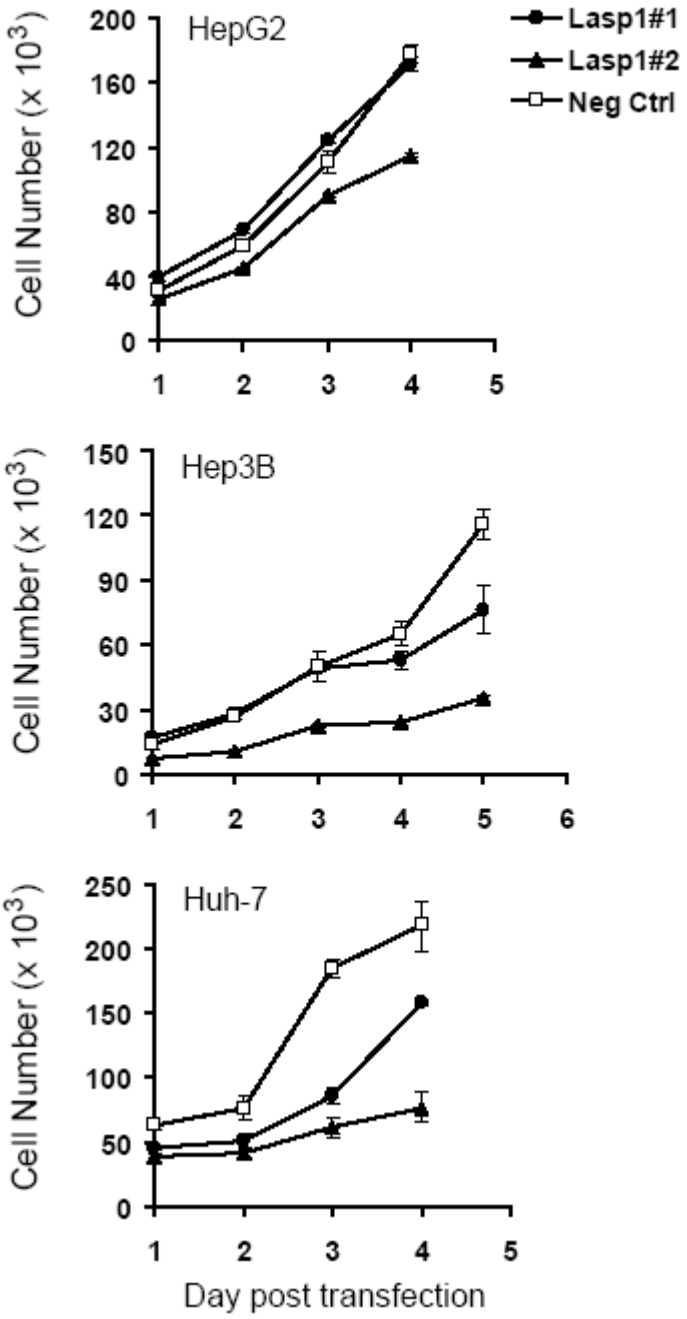

Figure 3.21 Lasp1 siRNA knockdown inhibited HCC cell proliferation in monolayer. Negative Control siRNA (open square), Lasp1#1 (filled circle) or Lasp1#2 (filled triangle) transfected HepG2, Hep3B or Huh-7 cells were replated into 96-well plates in triplicates 24 hours after transfection and the growth rates at indicated time points were measured by WST-1 reagent. The mean ± SD of triplicates are shown for each point. Both siRNA oligos transfected Hep3B or Huh-7 cells (Lasp1#1, Lasp1#2) showed a reduced cell proliferation rate than Negative Control siRNA transfected cells. However in HepG2, only Lasp1#2 transfected cells showed obvious inhibition in cell proliferation rate.

Effect of Lasp1 transient over-expression in monolayer

To further examine the potential biological effects of Lasp1 in growth of HCC, The recombinant plasmid pDEST40-Lasp1/V5 was introduced into HCC cell lines. As a cell line with extremely low endogenous Lasp1 protein level compared to other HCC cell lines, PLC/PRF/5 was included in this study besides HepG2 and Hep3B cells. Over-expression of Lasp1-V5 fusion protein in these cell lines was confirmed by Western blot by using specific mouse anti-V5 antibody with α-tubulin blotting as a control for protein loading and transfer (Figure 3.22).

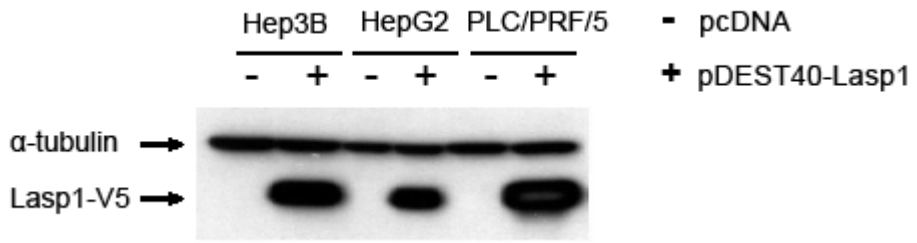

Figure 3.22 Lasp1-V5 fusion protein expression in transient Lasp1 over-expressed HCC cells. 48 hours after transfection of pDEST40-Lasp1/V5 (+: pDEST40-Lasp1) or pcDNA3.1 (–: pcDNA) into Hep3B, HepG2 or PLC/PRF/5 cells, the cell lysates were collected and the proteins were separated on 10% SDS-PAGE followed by Western blot using a specific anti-V5 antibody. The V5-tagged over-expressed protein was clearly shown as indicated by the arrow. α-tubulin blotting was used as a protein loading control.

After 24 hours of transfection, the cells were trypsinized, counted and replated proportionally (1-3 × 10^4 per well) into 96-well plates in triplicates. Then the effect of Lasp1 over-expression on cell growth in monolayer was measured by WST-1 assay daily. As obviously shown in Figure 3.23, all three HCC cell lines transfected with pDEST40-Lasp1/V5 showed increased cell growth rates over a 4 to 5-day culturing period as compared to control cells transfected with pcDNA3.1 empty vector. At Day 4 post transfection, the cell number of Lasp1 over-expressed HepG2 and PLC/PRF/5 cells reached 132.7% (131.1 × 10^3 per well) and 133.1% (32.4 × 10^3 per well) respectively of their corresponding control cells ($P < 0.05$). While in Hep3B cells, the difference is more significant by exhibiting a 1.3 fold increase (230%) in cell number in Lasp1 over-expressed cells (280.2 × 10^3 per well) compared to the pcDNA3.1 control transfected cells (117.2 × 10^3 per well) ($P < 0.01$).

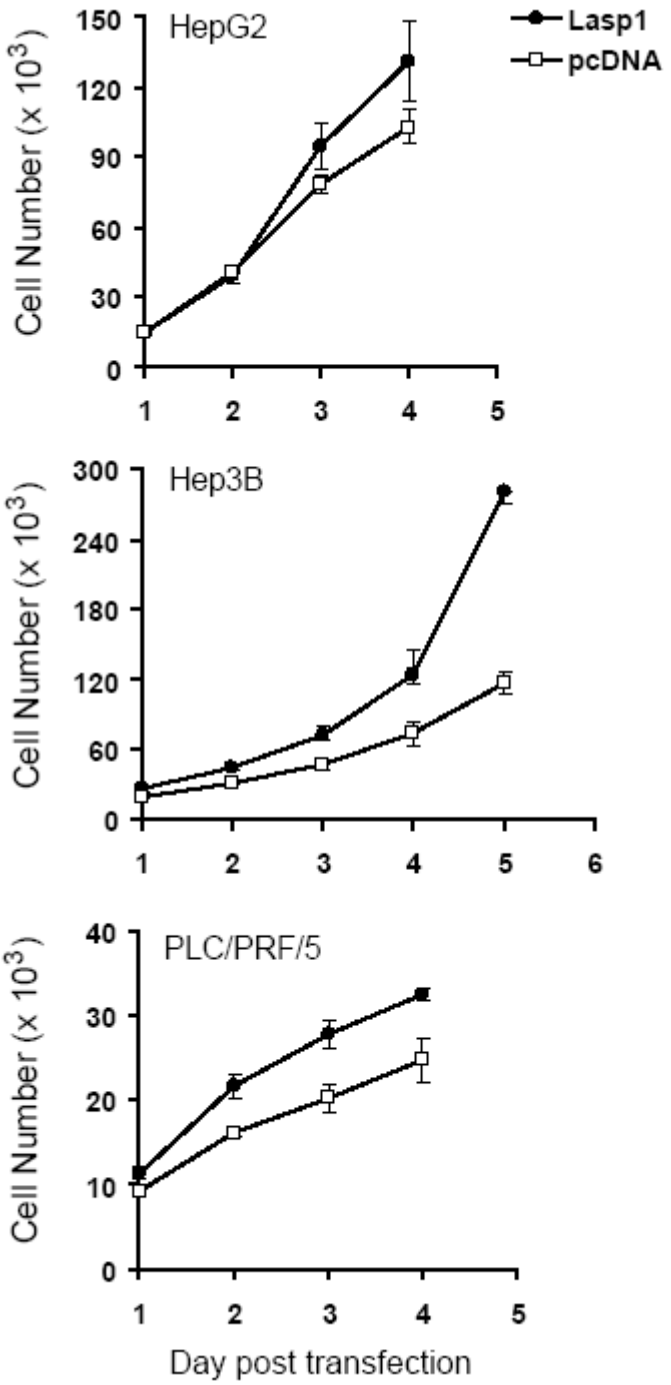

Figure 3.23 Lasp1 transient over-expression enhanced HCC cell proliferation in monolayer. pcDNA3.1 (pcDNA, open square) or pDEST40-Lasp1/V5 (Lasp1, filled circle) transfected HepG2, Hep3B or PLC/PRF/5 cells were replated into 96-well plates in triplicates 24 hours after transfection and the growth rates at indicated time points were measured by WST-1 reagent. The mean ± SD of triplicates are shown for each point. In all three cell lines, pDEST40-Lasp1/V5 transfected cells showed an enhanced cell proliferation rate compared to pcDNA3.1 transfected cells.

Effect of Lasp1 stable over-expression in monolayer

Two HepG2 stable cell lines with Lasp1 over-expression (HepG2-Lasp1-1 and HepG2-Lasp1-2) were established for this study as well. The stable over-expression of Lasp1 was confirmed by Western blot. As shown in Figure 3.24, over-expression of lasp1-V5 fusion protein was maintained in both HepG2-Lasp1-1 and HepG2-Lasp1-2 stable cell lines up to 9 passages. While in HepG2-Neo control cells (same control used in HepG2-Cyr61 stable cell lines), Lasp1 protein level was relatively lower than HepG2-Lasp1-1 and HepG2-Lasp1-2 if compared at the same passage number, as shown by blotting with rabbit anti-Lasp1 specific antibody.

At the passage of three to four, two HepG2-Lasp1 stable cell lines and HepG2-Neo control cells cultured in tissue culture flask were trypsinized, counted, seeded at the same concentration ($\sim 2 \times 10^4$/well) into 96-well plates in triplicates. WST-1 cell proliferation assay were performed daily to examine the growth rate of each cell line. The results of WST-1 assay at each time point were presented as the percentage relative to the cell number seeded at Day 0 for each line, which was set at 100% as Day 0 control. Figure 3.25 demonstrated that Lasp1 stable expression also promoted HepG2 cell growth in monolayer. At Day 4 post seeding, the cell number of HepG2-Lasp1 stable cell lines reached 186.8% (HepG2-Lasp1-1, 1469.2% of Day 0 control) and 239.6% (HepG2-Lasp1-2, 1925.9% of Day 0 control) relative to that of the HepG2-Neo control (1043.8% of Day 0 control), respectively ($P < 0.01$). These results further demonstrated that Lasp1 played a promoting role in HCC cell growth in monolayer.

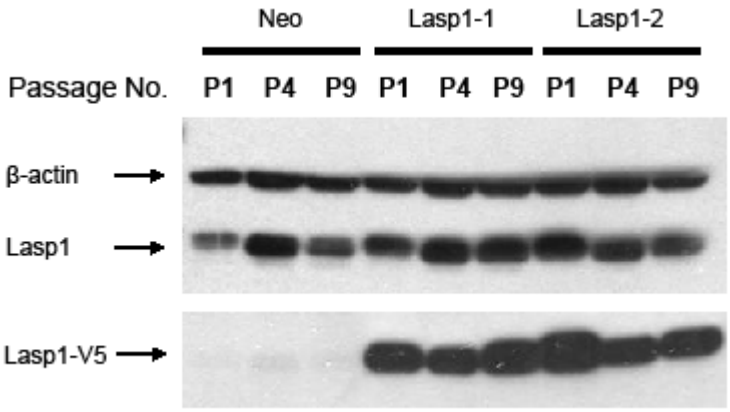

Figure 3.24 Lasp1-V5 fusion protein expression in HepG2-Lasp1 stable cell lines. HepG2 stable transfectants were selected in DMEM/10% FBS supplemented with 800μg/ml G418. Cell lysates from different passage were collected and the Lasp1 over-expression of two stable HepG2-Lasp1 clones (Lasp1-1, Lasp1-2) was confirmed by Western blot with both specific anti-V5 and anti-Lasp1 antibody. β-actin blotting was used as a protein loading control.

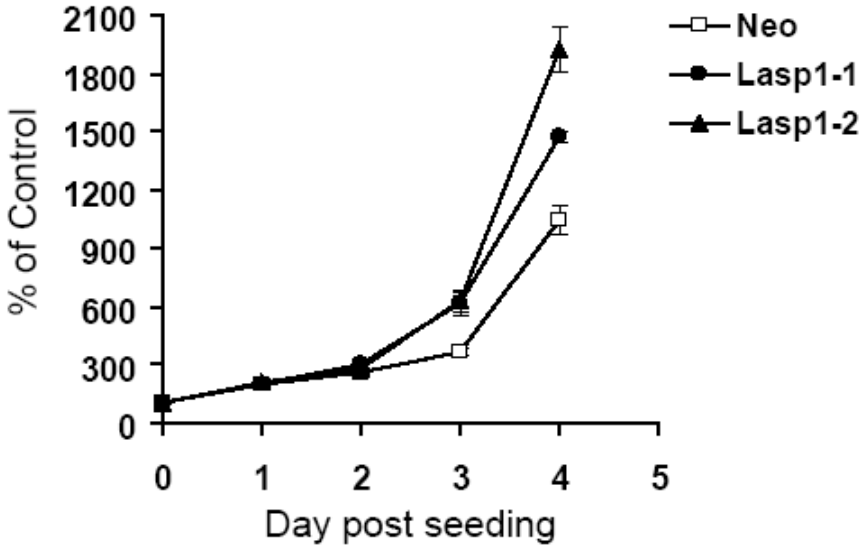

Figure 3.25 Lasp1 stable over-expression enhanced cell proliferation in HepG2 cells. Two HepG2-Lasp1 stable transfectants (HepG2-Lasp1-1, HepG2-Lasp1-2) and the HepG2-Neo control cell line were seeded in 96-well plate in triplicates. The cell growth rates were monitored daily by WST-1 assay. At each time point, the data were presented as the percentage relative to the cell number seeded at Day 0 for each line, which was arbitrarily set at 100% as Day 0 control. The mean ± SD of triplicates are shown for each point. Both HepG2-Lasp1-1 (filled circle) and HepG2-Lasp1-2 (filled triangle) stable cell lines showed increased cell proliferation rate compared to HepG2-Neo (open square) control cells over a 4-day continuous culture.

Effect of Lasp1 siRNA knockdown in soft agar assay

In order to explore the roles of Lasp1 on HCC cell growth under more stringent conditions, the anchorage-independent assay was performed to test the colony formation ability in soft agar culture. HepG2 or Huh-7 cells transfected with either Lasp1 siRNA (Lasp1#1, Lasp1#2) or Negative Control siRNA (Neg Ctrl) were trypsinized 24 hours after transfection, 5×10^3 and/or 1×10^4 cells re-suspended in 0.25ml of 0.35% agar dissolved in DMEM/10%FBS were plated in 24-well plate in triplicates overlying a 0.7% agar bottom layer and cultured at 37°C for additional three weeks. The colonies were stained, photographed and the number of colonies > 100μm in diameter was counted. In sharp contrast to the controls transfected with Negative Control siRNA, HepG2 cells transfected with Lasp1#2 siRNA formed much fewer colonies in semi-soft agar. The colony number formed by the panel of cells of 10000 cells/well at the starting point (Figure 3.26A, upper panel) was counted. Lasp1#2 siRNA transfected cells only formed 16.3% of colonies compared to that of control ($P < 0.01$) (Figure 3.26B). While in Huh-7 cells, since both siRNA oligos significantly down-regulated Lasp1 protein level (Figure 3.20), substantial differences were observed between cells transfected with Lasp1#1 or Lasp1#2 siRNA oligo and that transfected with Negative Control siRNA. The colony formation efficiency was only 14.8% (Lasp1#1) and 12.3% (Lasp1#2) respectively of that of control as reflected by colony count ($P < 0.01$) (Figure 3.26C, 3.26D). These results indicated that knockdown of Lasp1 expression by siRNA significantly inhibited the anchorage-independent growth of HCC cells.

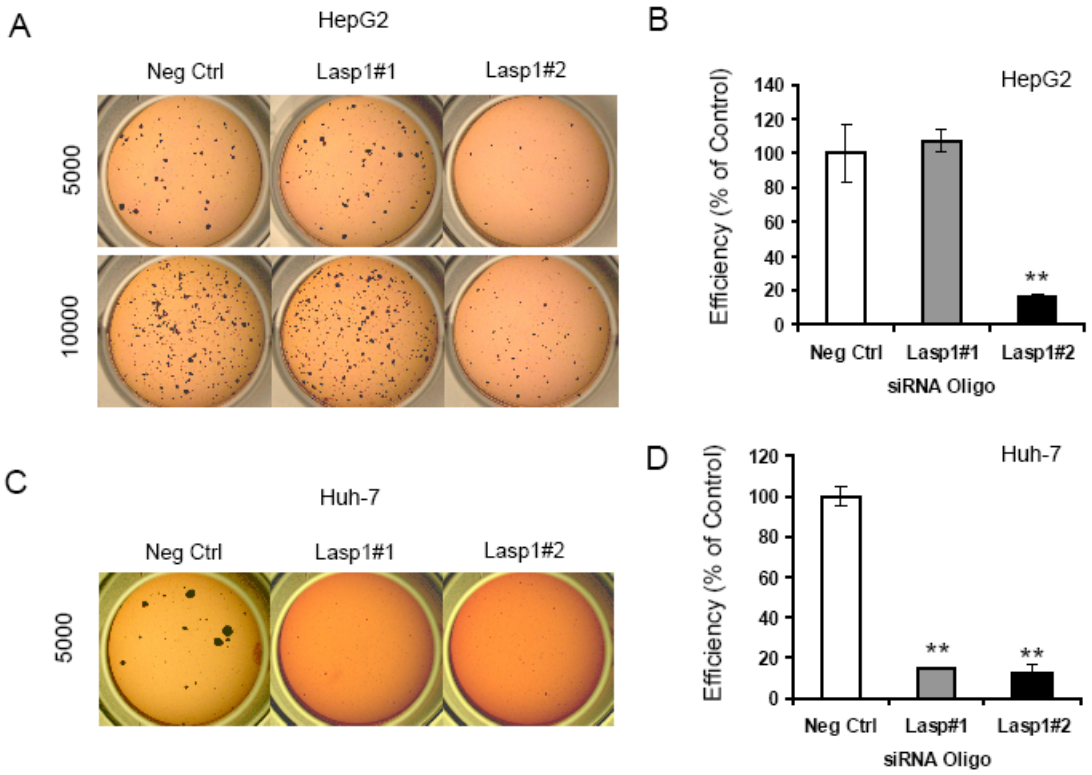

Figure 3.26 Lasp1 siRNA knockdown inhibited anchorage-independent growth of HCC cells in soft agar. HepG2 or Huh-7 cells transfected with Lasp1 siRNA (Lasp1#1, Lasp1#2) or Negative Control siRNA (Neg Ctrl) were replated for soft agar assay. After three weeks of incubation, the cells were stained and the colonies were photographed and counted. The colony forming efficiency was calculated as the percentage of the colony number formed by Lasp1 siRNA oligos transfected cells (Lasp1#1, grey bar; Lasp1#2, black bar) relative to that formed by Negative Control siRNA transfected cells (white bar), which was arbitrarily set at 100%. The mean ± SD of triplicates are shown as well. (A) Representative images showed that HepG2 cells transfected with Lasp1 siRNA (Lasp1#2) formed much smaller and fewer colonies in soft agar than those transfected with Negative Control siRNA (Neg Ctrl). The starting cell number was 5000 or 10000 per well, which were shown in the upper and lower panel respectively. (B) Colony count (10000 cells per well at starting point) for HepG2 cells. $^{**}P < 0.01$. (C) Representative images showed Huh-7 cells transfected with Lasp1 siRNA oligos (Lasp1#1, Lasp1#2) formed much smaller and fewer colonies in soft agar than those transfected with control siRNA (Neg Ctrl). The starting cell number was 5000 per well. (D) Colony count for Huh-7 cells. $^{**}P < 0.01$.

Effect of Lasp1 transient over-expression in soft agar assay

Similarly, an anchorage-independent assay was performed to examine the function of over-expression of Lasp1 in colony formation ability in soft agar culture by using HepG2 and PLC/PRF/5 cells. 24 hours after transfection with pDEST40-Lasp1/V5 or pcDNA3.1, 1×10^4 cells re-suspended in 0.25ml of 0.35% agar dissolved in DMEM/10%FBS were plated in 24-well plate in triplicates overlying a 0.7% agar bottom layer and cultured at 37°C for additional three weeks. In sharp contrast to the controls transfected with pcDNA3.1, both HepG2 and PLC/PRF/5 cells transfected with pDEST40-Lasp1/V5 formed much more micro-colonies in semi-soft agar (Figure 3.27A, Figure 3.27C), which is about 273.0% (Figure 3.27B) and 178.0% (Figure 3.27D) respectively of control ($P < 0.05$). These results reflected that Lasp1 over-expression significantly enhanced the anchorage-independent growth of HepG2 and PLC/PRF/5 cells, suggesting that Lasp1 can promote both HCC cell proliferation rate and cloning efficiency.

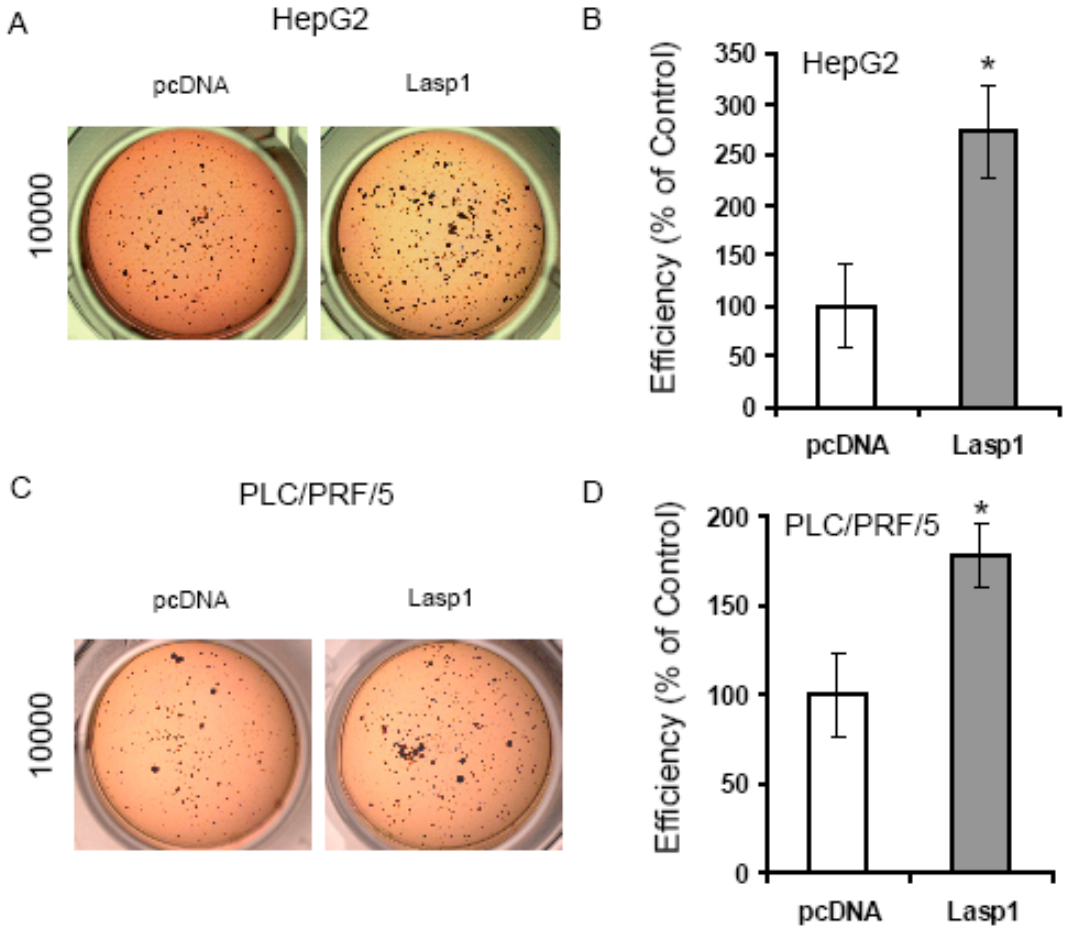

Figure 3.27 Lasp1 over-expression enhanced anchorage-independent growth of HCC cells in soft agar. HepG2 or PLC/PRF/5 cells transfected with pDEST40-Lasp1/V5 or pcDNA3.1 control were trypsinized 24 hours after transfection and replated for soft agar assay. After three weeks of incubation, the cells were stained and the colonies were photographed and counted. The colony forming efficiency was calculated as the percentage of the colony number formed by pDEST40-Lasp1/V5 transfected cells (grey bar) relative to that formed by pcDNA3.1 transfected cells (white bar), which was arbitrarily set at 100%. The mean ± SD of triplicates are shown as well. (A) Representative images showed that HepG2 cells transfected with pDEST40-Lasp1/V5 (Lasp1) formed more and larger colonies in soft agar than those transfected with pcDNA3.1 control (pcDNA). The starting cell number was 10000 per well. (B) Colony count for HepG2 cells. $*P < 0.05$. (C) Representative images showed that PLC/PRF/5 cells transfected with pDEST40-Lasp1/V5 (Lasp1) formed more and larger colonies in soft agar than those transfected with pcDNA3.1 control (pcDNA). The starting cell number was 10000 per well. (D) Colony count for PLC/PRF/5. $*P < 0.05$.

3.2.4. Function study of Lasp1 on HCC cell adhesion, migration and invasion

Effect of Lasp1 on cell adhesion to ECM proteins

Lasp1 was reported to be necessary for cell migration, but not adhesion and spreading on the ECM using Cos-7 cells as a model (Lin *et al*. 2004). However, by considering that the cell adhesion to ECM proteins is the initial and critical step for cell migration and invasion, the role of Lasp1 on HCC cell adhesion was still tested in this study. HepG2 and Hep3B cells transfected with either Lasp1#2 siRNA oligo or pDEST40-Lasp1/V5 were examined for their adhesion activities to the set of 5 different ECM proteins (fibronectin, vitronectin, laminin, collagen I and collagen IV). No significant difference in cell adhesion ability to the 5 types of ECM proteins was observed in cells either with reduced Lasp1 expression by siRNA knockdown (Figure 3.28, $P > 0.05$) or with over-expressed Lasp1 by transfection of pDEST40-Lasp1/V5 (Figure 3.29, $P > 0.05$) compared to their corresponding control cells. These results indicate that, consistent with previous report, Lasp1 does not play important roles in regulating HepG2 or Hep3B cell adhesion ability to ECM proteins.

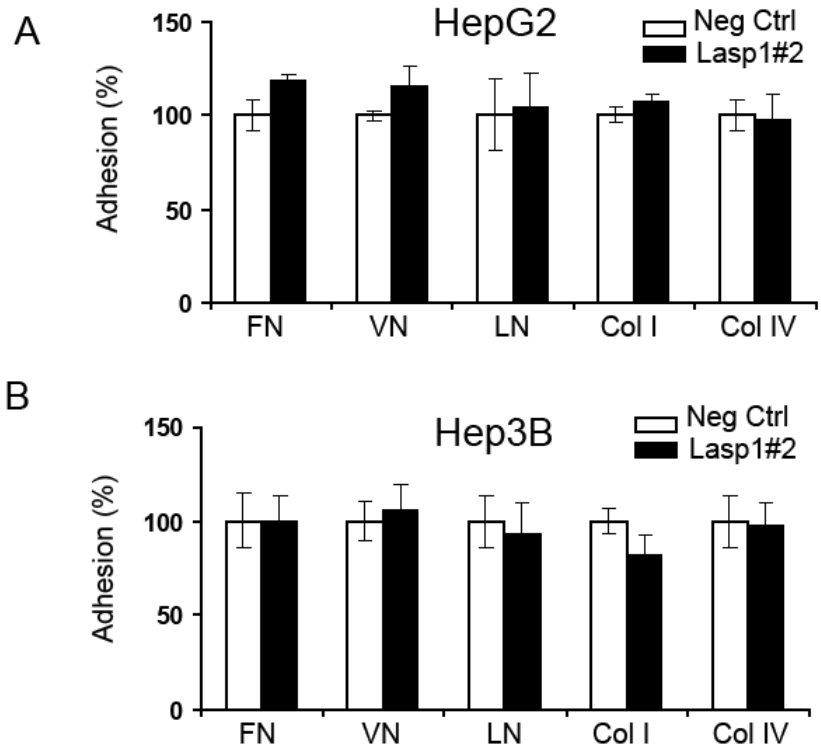

Figure 3.28 Lasp1 siRNA knockdown did not alter HCC cell adhesion ability to ECM proteins. 48 hours after transient transfection with Lasp1#2 siRNA (Lasp1#2, black bars) or Negative Control siRNA (Neg Ctrl, white bars), HepG2 (A) and Hep3B (B) cells were replated for cell adhesion assay. Adhesion efficiency to each ECM protein was presented as the percentage relative to that of the Negative Control siRNA transfected cells, which was arbitrarily set at 100% (mean ± SD of triplicates). FN: fibronectin, VN: vitronectin, LN: laminin, Col I: collagen I, Col IV: collagen IV.

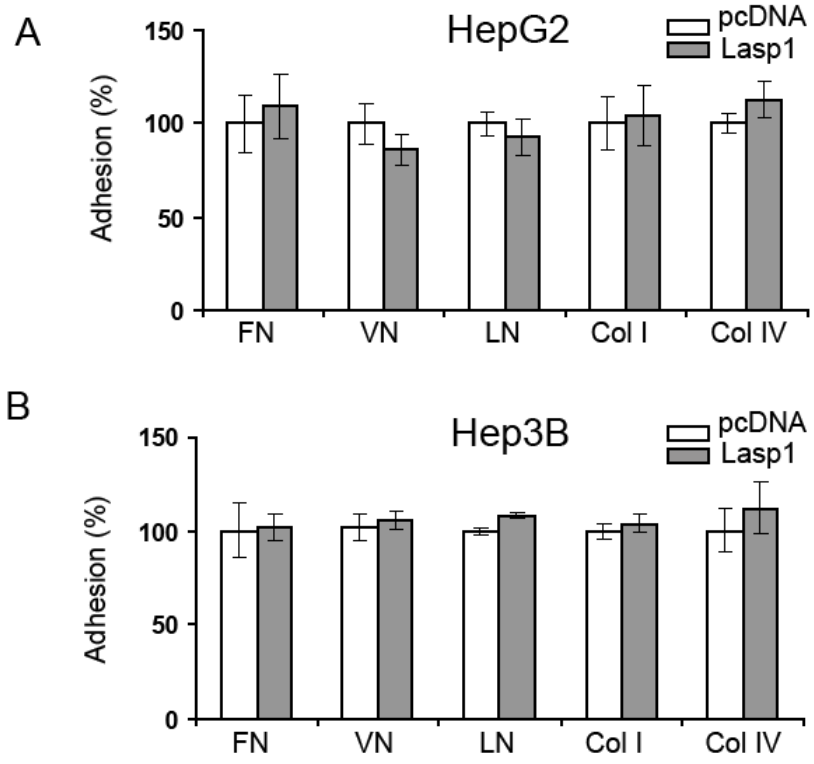

Figure 3.29 Lasp1 over-expression did not alter HCC cell adhesion ability to ECM proteins. 48 hours after transient transfection with pDEST40-Lasp1/V5 (grey bars) or pcDNA3.1 (white bars), HepG2 (A) or Hep3B (B) cells were replated for cell adhesion assay. Adhesion efficiency to each ECM protein was presented as the percentage relative to that of the pcDNA3.1 control transfected cells, which was arbitrarily set at 100% (mean ± SD of triplicates). FN: fibronectin, VN: vitronectin, LN: laminin, Col I: collagen I, Col IV: collagen IV.

Effect of Lasp1 on HCC cell migration and invasion ability

As Lasp1 was reported to be involved in breast cancer metastasis, the function of Lasp1 in regulating cell migration and invasion ability in HCC cell lines was further explored as an indicator of its potential role in HCC metastasis. Firstly, the migration and invasion ability of Lasp1 siRNA transfected HepG2, Hep3B and Huh-7 cells was tested. The results from the modified Boyden chamber assay showed that the migratory activities of Lasp1#2 transfected HepG2, Hep3B cells or Huh-7 were inhibited by 74.2% (Figure 3.30A), 74.3% (Figure 3.30B) ($P < 0.01$) and 86.9% (Figure 3.30C) ($P < 0.05$) respectively, as compared to corresponding Negative Control siRNA transfected cells. Furthermore, the invasive activities through ECM proteins were also suppressed in HepG2 (46.1% of control, $P < 0.01$) (Figure 3.30D), Hep3B (53.3% of control, $P < 0.05$) (Figure 3.30E) and Huh-7 cells (35.0% of control, $P < 0.01$) (Figure 3.30F). These results indicate that depletion of Lasp1 by siRNA in HCC cells suppresses the cell migratory and invasive ability, suggesting that HCC cells may acquire higher metastasis potential by over-expressing Lasp1.

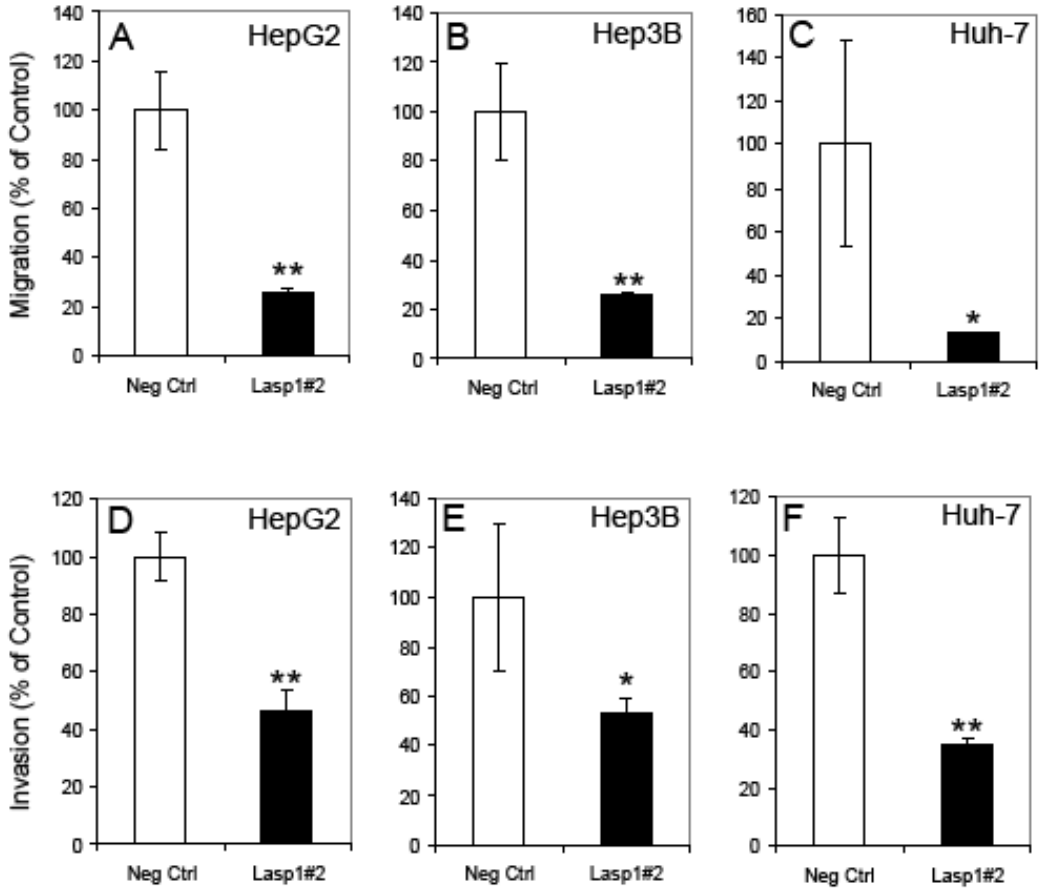

Figure 3.30 Lasp1 siRNA knockdown inhibited migration and invasion activities of HCC cells. After serum starvation for 24 hours, Negative Control siRNA (white bars) or Lasp1#2 siRNA (black bars) transfected HepG2 (1.0×10^5 cells / well), Hep3B cells (5.0×10^4 cells /well) or Huh-7 cells (5.0×10^4 cells /well) were replated for cell migration and invasion assays. Inhibitory effects on migration and invasion were presented as the percentage of fluorescent readings standardized to Negative Control siRNA transfected cells (mean ± SD of triplicates). *$P < 0.05$, ** $P < 0.01$. (A) Migration assay through 8μm microporous membranes in HepG2 cells. (B) Migration assay through 8μm microporous membranes in Hep3B cells. (C) Migration assay through 8μm microporous membranes in Huh-7 cells. (D) Invasion assay through ECM proteins in HepG2 cells. (E) Invasion assay through ECM proteins in Hep3B cells. (F) Invasion assay through ECM proteins in Huh-7 cells.

The migration and invasion ability of Lasp1 transient over-expression in both HepG2 and Hep3B cells were examined as well. We first noticed that several previous studies showed that further over-expression of Lasp1 in cancer cell lines which already up-regulated Lasp1 expression level also inhibited cell migration and invasion activities (Lin *et al*. 2004; Grunewald *et al*. 2006). Consistent with these previous reports, HepG2 cells transfected with pDEST40-Lasp1/V5 showed 41.2% ($P < 0.01$) inhibition in cell migration and 33.5% ($P < 0.05$) inhibition in cell invasion activity compared to pcDNA3.1 transfected cells (Figure 3.31A and 3.31D). The experiments were repeated using Hep3B and Huh-7 cells with similar results achieved (Figure 3.31B, 3.31C, 3.31E and 3.31F).

In addition, the HepG2 cell lines with Lasp1 stable over-expression (HepG2-Lasp1-1 and HepG2-Lasp1-2) and the control clone with Neo-resistant gene (HepG2-Neo) were used for this study. The results showed that the migratory activities of both Lasp1 stable cell lines were inhibited up to 36.3% (HepG2-Lasp1-1) and 45.8% (HepG2-Lasp1-2) respectively as compared to HepG2-Neo control ($P < 0.01$) (Figure 3.32A). The invasive activities through ECM proteins were also significantly suppressed in both HepG2-Lasp1 stable clones (40.8% and 28.3% of control respectively, $P < 0.01$) (Figure 3.32B).

These results support the conclusion that Lasp1 plays important roles in regulating cell migration and invasion ability of human HCC cell lines.

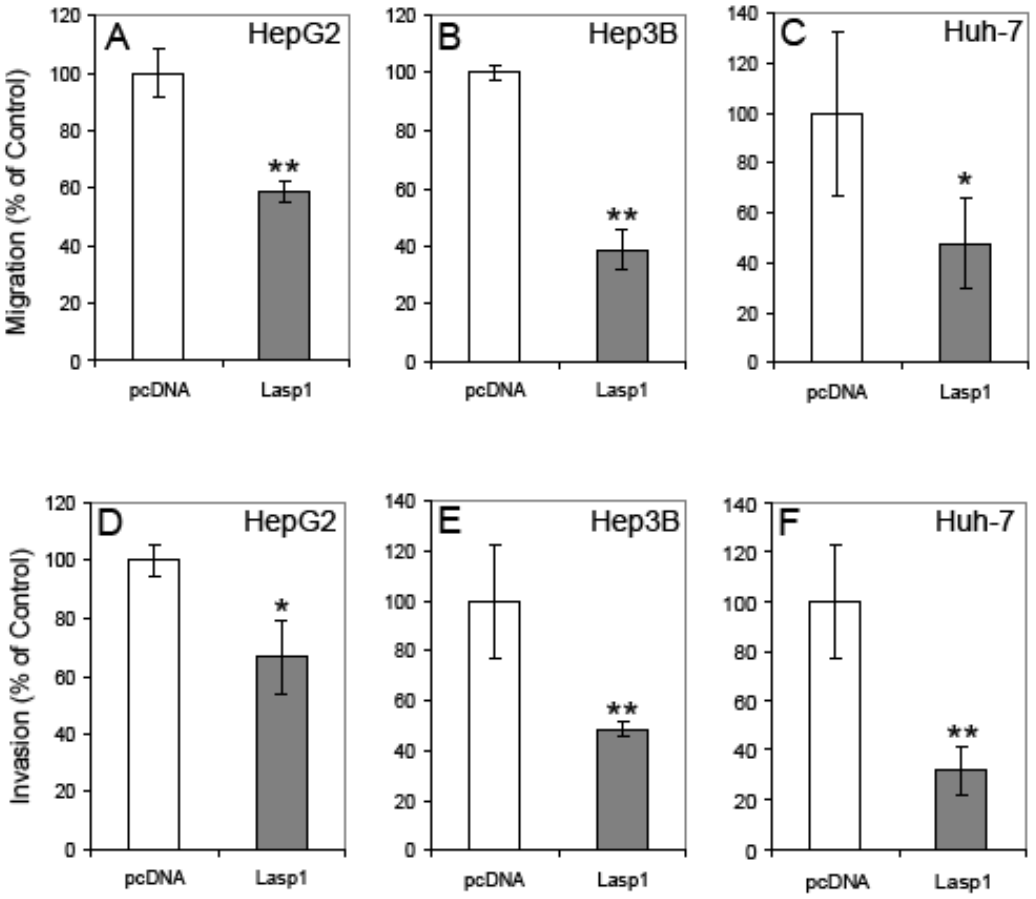

Figure 3.31 Lasp1 transient over-expression inhibited migration and invasion activities of HCC cells. After serum starvation for 24 hours, pcDNA3.1 (white bars) or Lasp1-DEST40/V5 (grey bars) transfected HepG2 (1.0×10^5 cells / well), Hep3B (5.0×10^4 cells /well) or Huh-7 (5.0×10^4 cells /well) cells were replated for cell migration and invasion assays. Inhibitory effects on migration and invasion were presented as the percentage of fluorescent readings standardized to pcDNA3.1 control (mean ± SD of triplicates). *$P < 0.05$, ** $P < 0.01$. (A) Migration assay through 8μm microporous membranes in HepG2 cells. (B) Migration assay through 8μm microporous membranes in Hep3B cells. (C) Migration assay through 8μm microporous membranes in Huh-7 cells. (D) Invasion assay through ECM proteins in HepG2 cells. (E) Invasion assay through ECM proteins in Hep3B cells. (F) Invasion assay through ECM proteins in Huh-7 cells.

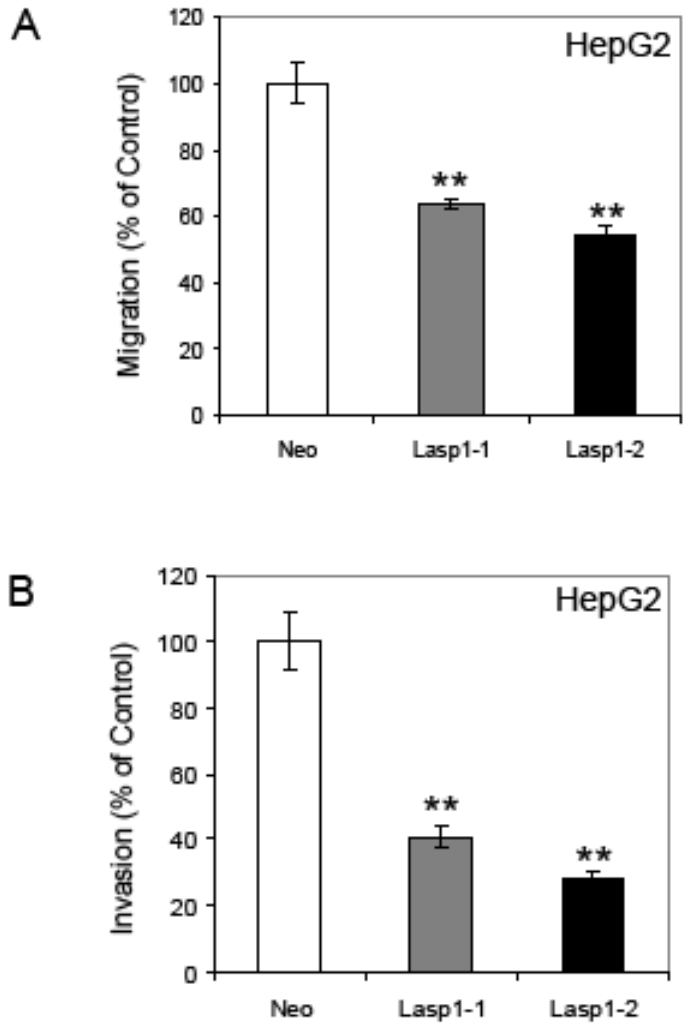

Figure 3.32 Lasp1 stable over-expression inhibited migration and invasion activities in HepG2 cells. After serum starvation for 24 hours, two stable clones HepG2-Lasp1-1 (grey bars), HepG2-Lasp1-2 (black bars), and a HepG2-Neo control (white bars) were plated (5.0×10^5 cells/well) for cell migration and invasion assays. Inhibitory effects on migration and invasion were presented as the percentage of fluorescent readings standardized to HepG2-Neo control (mean ± SD of triplicates). ** $P < 0.01$. (A) Migration assay through 8μm microporous membranes. (B) Invasion assay through ECM proteins.

3.2.5. Cellular localization study of Lasp1 in HCC

Two recent reports uncovered that depletion of Lasp1 by specific siRNA led to change of zyxin localization in both breast cancer and ovarian cancer cells, which may explain the phenomenon that Lasp1 siRNA knockdown inhibited the cell migration and invasion ability in these cancer cell lines (Grunewald *et al*. 2006; Grunewald *et al*. 2007). As both previous reports and the current study showed that further over-expression of Lasp1 in those cancer cell lines which had already up-regulated Lasp1 level also significantly suppressed the cell migration and invasion activities, it would be interesting to explore the mechanism underneath. Thus, in this study, the confocal microscopy analyses were performed to determine whether over-expression of Lasp1 can influence the localization of zyxin as well as some other focal adhesion proteins.

Hep3B and Huh-7 cells were chosen for this study due to their ability to form monolayer when cultured *in vitro*, which is suitable for immunofluorescence study. The Gateway expression vector pDEST47-Lasp1/GFP was introduced into Hep3B or Huh-7 cells plated in 6-well plate by transient transfection. 24 hours later, cells were replated onto the 35mm glass bottom microwell dishes for overnight incubation. The cells were then fixed and stained with specific mouse monoclonal antibodies to zyxin, VASP, and paxillin followed by staining with goat-anti-mouse secondary antibody conjugated with Alexa Fluor-647. F-actin was stained by Alexa Fluor-635 conjugated Phalloidin.

Similar to the depletion of Lasp1 by specific siRNA in breast cancer or ovarian cancer cells, Lasp1 over-expression in both Hep3B (Figure 3.33A) and Huh-7 (Figure 3.33B) cells which had high endogenous Lasp1 expression (Figure 3.18), also changed the localization of zyxin. In Lasp1 over-expressed Hep3B cells, zyxin

showed diffused distribution in both cytoplasm and nucleus co-localized with Lasp1-GFP (yellow color, white arrow), whereas in cells without Lasp1-GFP expression, zyxin was mainly localized to the site of the focal adhesion. Similarly in Huh-7 cells, zyxin lost its localization at focal contact or along the F-actin fibers, but co-localized with over-expressed Lasp1-GFP as indicated in the merged picture. More interestingly, the morphology of the Lasp1-GFP expressing cells was quite different from Lasp1-GFP non-expressing cells. Those cells with very high level of Lasp1-GFP expression were often observed in oval shape without obvious polarity. However, the Lasp1-GFP non-expressing Hep3B or Huh-7 cells tend to spread out with clear lamellipodia structures and/or with extended shape showing obvious F-actin fibers, as observed in Huh-7 cells (enlarged images for the areas defined by white boxes) (Figure 3.33B, bottom panel).

Besides zyxin, localization of VASP and paxillin was also tested in this study. As shown in Figure 3.34, the confocal microscopy study revealed that Lasp1 also altered the localization of VASP, which was reported to be a binding partner of Lasp1 and play an important role in actin dynamics as a scaffolding protein in F-actin polymerization (Krause *et al*. 2003). It was clearly shown that VASP was fully co-localized with Lasp1-GFP (yellow). In Lasp1 over-expressed cells (white arrow), VASP was diffused in the whole cell instead of being localized exclusively at the cell peripheral as observed in cells without Lasp1-GFP expression.

Paxillin, a focal-adhesion LIM protein which binds to various cytoskeletal and signaling proteins and can mediate integrin signaling (Schaller 2001), was also shown to be co-localized with Lasp1 as indicated in yellow in the merged pictures. Further over-expression of Lasp1 in Hep3B and Huh-7 cells significantly changed its

localization from focal adhesion site at the cell peripheral to the whole cell body (white arrow) (Figure 3.35).

The protein lysates were extracted from Lasp1 over-expressed cells and subjected to Western blot using the same antibodies applied in confocal staining in order to show the antibody specificity and to exclude the possibility that Lasp1 over-expression affect their expression. As shown in Figure 3.36, the protein level of zyxin, VASP or paxillin as compared to pcDNA3.1 control transfected cells in all three cell lines did not have obvious change upon Lasp1 over-expression. Another noteworthy finding was that the expression of zyxin in HepG2 cells was almost undetectable as compared to that in Hep3B or Huh-7 cells. Lasp1 blotting showed over-expression of Lasp1, with β-actin blotting used as a protein loading control.

Zyxin, VASP and paxillin were reported to be involved in focal adhesion signaling and/or F-actin dynamics (Turner 2000b; Welch and Mullins 2002). Also, Lasp1 was shown to be an actin binding protein and function as a scaffold protein in F-actin polymerization and cell migration. Thus, it would be interesting to test whether the F-actin polymerization is also affected by Lasp1 further over-expression in HCC cell lines. F-actin was stained by Alexa Fluor-635 conjugated Phalloidin. The results showed that much fewer F-actin stress fibers were detected in Lasp1 over-expressed Hep3B or Huh-7 cells, while those cells without expressing Lasp1-GFP had normal F-actin fibers (Figure 3.37).

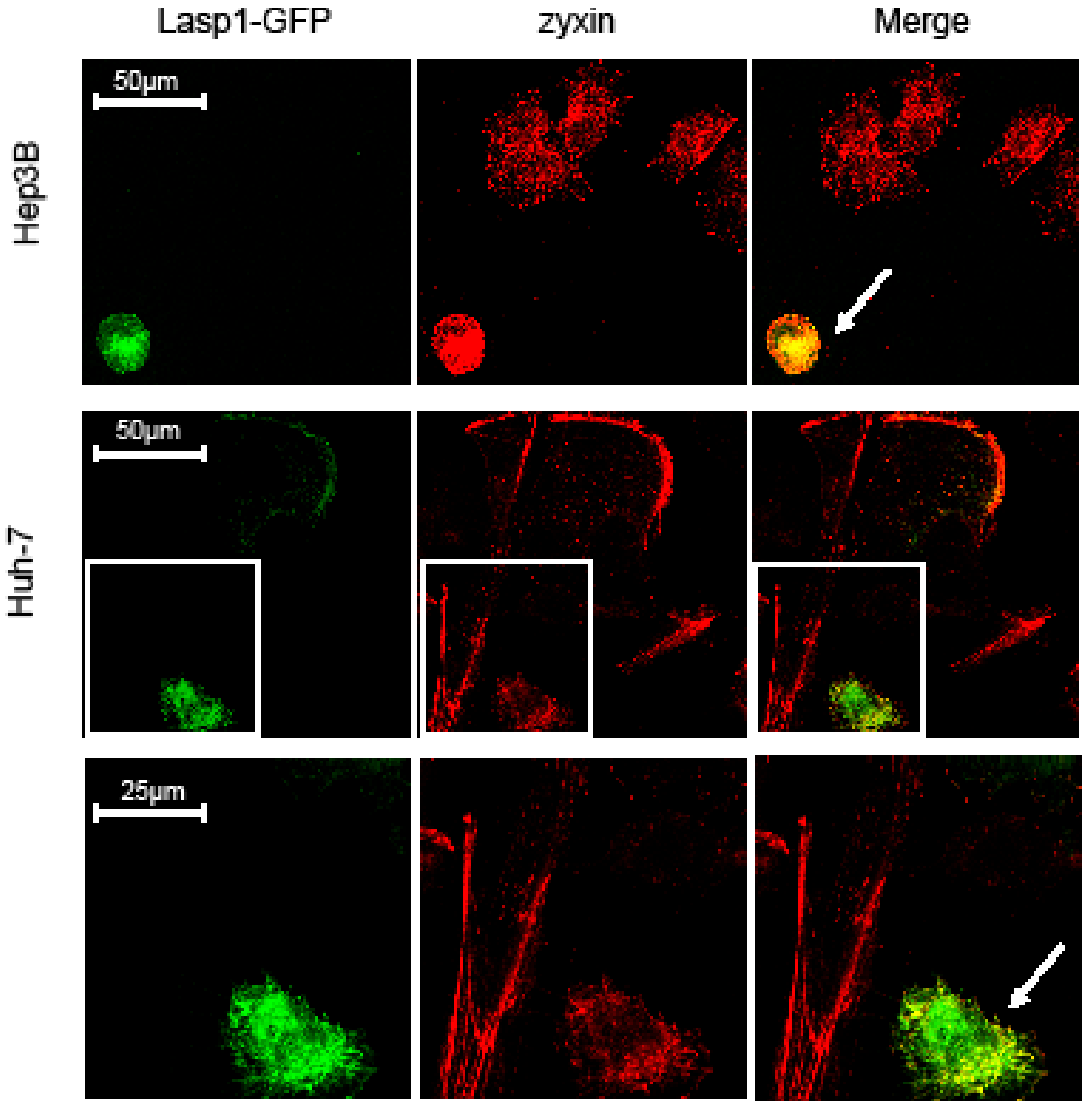

Figure 3.33 Lasp1 over-expression changed the localization of zyxin. pDEST47-Lasp1/GFP was transfected into Hep3B (A) or Huh-7 (B) cells plated in 6-well plate. 24 hours after transfection, cells were replated onto glass bottom microwell dishes for overnight incubation. Zyxin was stained with specific mouse monoclonal anti-zyxin antibody followed by goat-anti-mouse AF647. The images were captured under confocal microscope for Lasp1-GFP (green, 488nm), zyxin (red, 633nm). The areas defined by white boxes were shown as enlarged images at the bottom panel. Co-localization of Lasp1 and zyxin was shown in the merged pictures as yellow indicated by the white arrow.

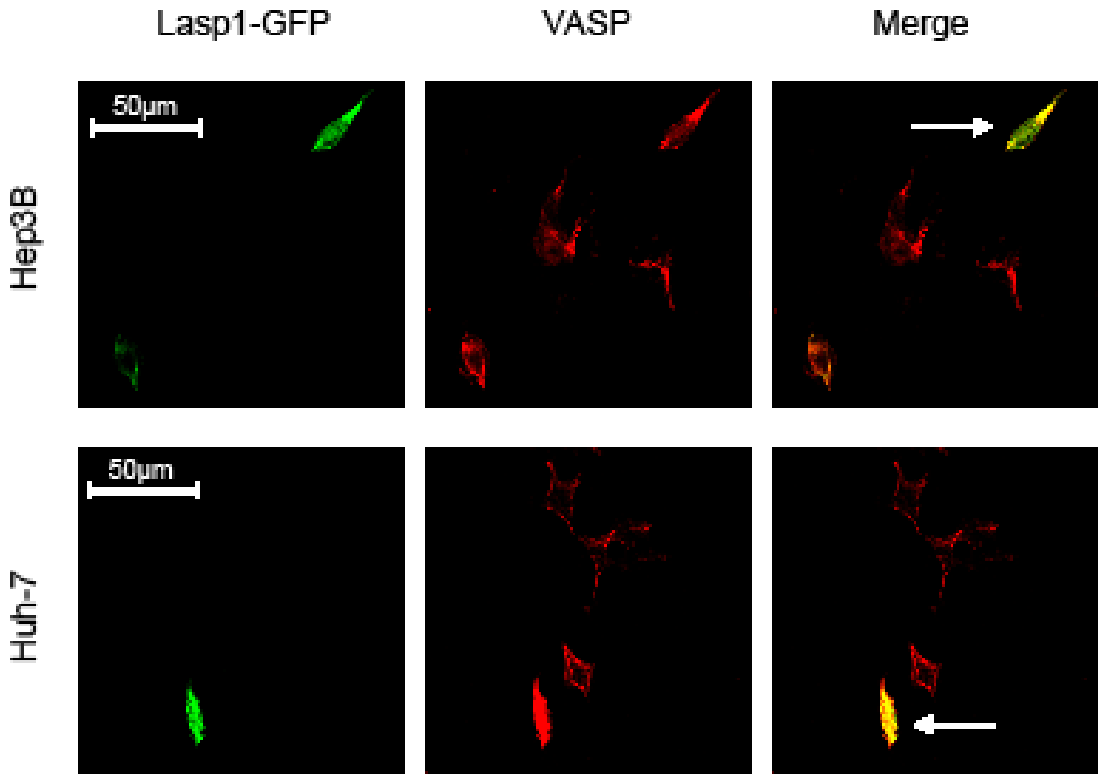

Figure 3.34 Lasp1 over-expression changed the localization of VASP. pDEST47-Lasp1/GFP was transfected into Hep3B or Huh-7 cells plated in 6-well plate. 24 hours after transfection, cells were replated onto glass bottom microwell dishes for overnight incubation. VASP was stained with specific mouse monoclonal anti-VASP antibody followed by goat-anti-mouse AF647. The images were captured under confocal microscope for Lasp1-GFP (green, 488nm), VASP (red, 633nm). Co-localization of Lasp1 and VASP was shown in the merged pictures as yellow indicated by the white arrow. Hep3B: upper panel; Huh-7: lower panel.

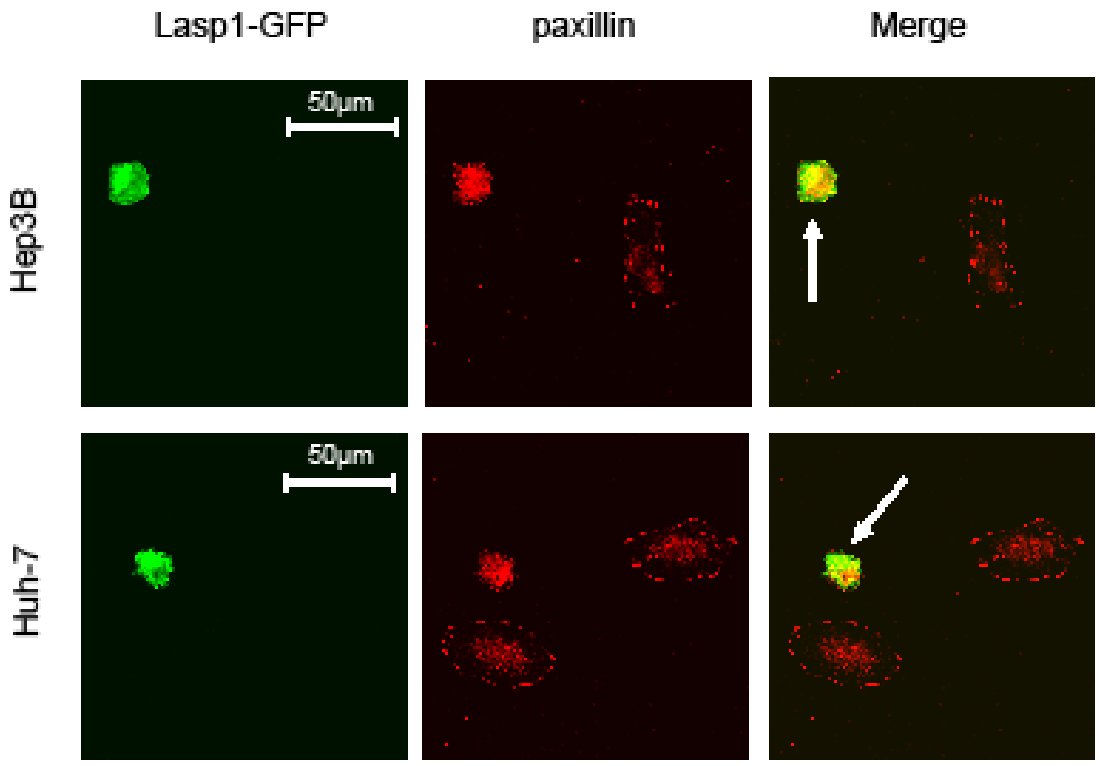

Figure 3.35 Lasp1 over-expression changed the localization of paxillin. pDEST47-Lasp1/GFP was transfected into Hep3B or Huh-7 cells plated in 6-well plate. 24 hours after transfection, cells were replated onto glass bottom microwell dishes for overnight incubation. Paxillin were stained with specific mouse monoclonal anti-paxillin antibody followed by goat-anti-mouse AF647. The images were captured under confocal microscope for Lasp1-GFP (green, 488nm), paxillin (red, 633nm). Co-localization of Lasp1 and paxillin was shown in the merged pictures as yellow indicated by the white arrow. Hep3B: upper panel; Huh-7: lower panel.

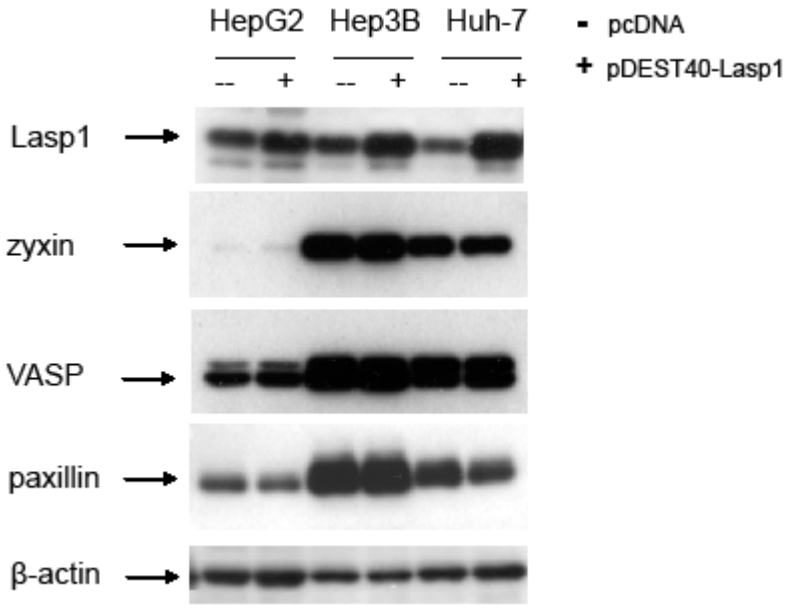

Figure 3.36 Lasp1 over-expression did not alter the protein level of zyxin, VASP or paxillin. 48 hours after transfection of pDEST40-Lasp1/V5 (+: pDEST40-Lasp1) or pcDNA3.1 (–: pcDNA) into HepG2, Hep3B or Huh-7 cells, the cell lysates were collected and the proteins were separated by 10% SDS-PAGE followed by Western blot using a series of antibodies, including Rabbit-anti-Lasp1, Mouse-anti-zyxin, Mouse-anti-VASP and Mouse-anti-paxillin. β-actin blotting was used as a protein loading control.

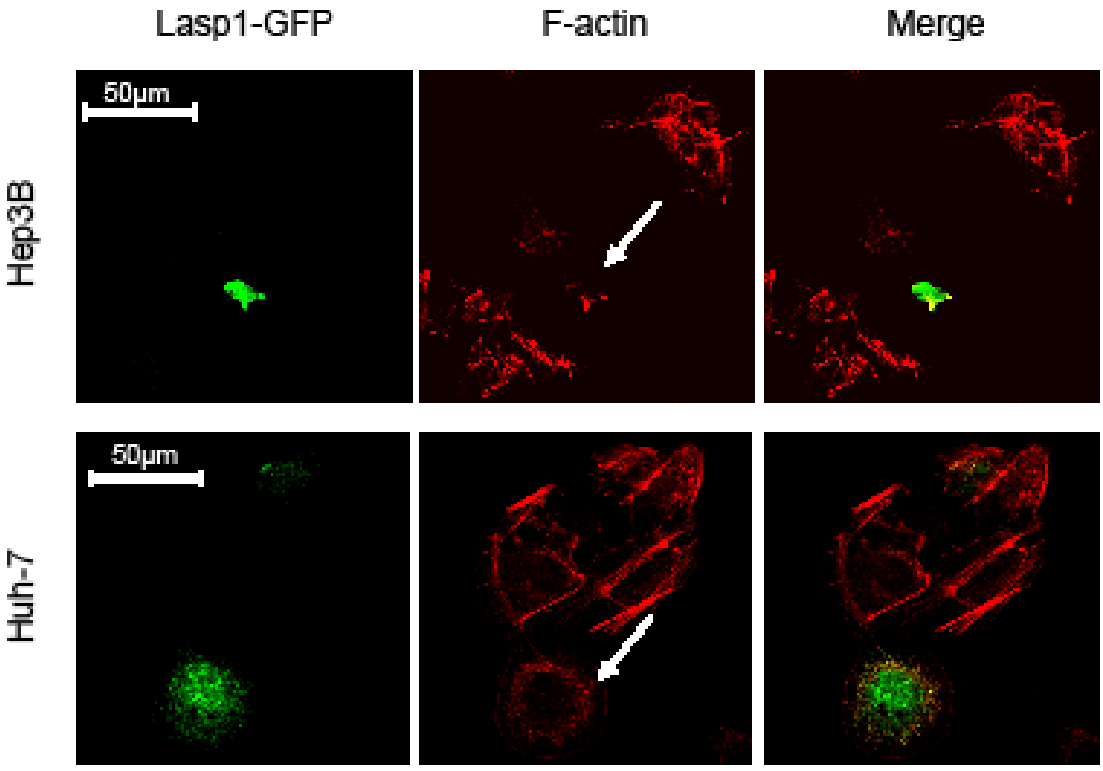

Figure 3.37 Lasp1 over-expression inhibited the formation of F-actin bundles. pDEST47-Lasp1/GFP was transfected into Hep3B or Huh-7 cells plated in 6-well plate. 24 hours after transfection, cells were replated onto glass bottom microwell dishes for overnight incubation. F-actin was stained with Phalloidin-AF635. The images were captured under confocal microscope for Lasp1-GFP (green, 488nm), F-actin (red, 633nm). Lasp1-GFP expressing cells were indicated by white arrow. Hep3B: upper panel; Huh-7: lower panel.

In summary, a similar *in vitro* experimental system used in Cyr61 functional characterizations was applied in this part of study to explore the possible roles of Lasp1 in HCC growth and metastasis.

The cell proliferation study indicated that up-regulation of Lasp1 in HCC also represented a strategy of tumor cells to gain growth advantage. Knockdown of Lasp1 significantly inhibited the proliferation rate of HCC cells in monolayer. The capability of anchorage-independent growth, which is an important indicator of malignant transformation, was also suppressed by depleting Lasp1. Whereas, further over-expression of Lasp1 in HCC cell lines promoted cell growth both in monolayer and in soft agar, confirmed that Lasp1 exerted an enhancing effect in HCC cell growth.

In addition, both siRNA knockdown and further over-expression of Lasp1 in HCC cell lines suppressed the cell migratory and invasive activities, suggesting that Lasp1 functions within a certain optimal concentration in cancer cells in regulating cell migration and invasion ability. The confocal microscopy study implied the possible mechanism for Lasp1 in regulating HCC cell migration and invasion ability. As a scaffolding protein, Lasp1 may determine the localization of a series of focal adhesion proteins, such as zyxin, VASP and paxillin, which in turn affect the F-actin polymerization at the focal adhesion sites.

3.3. Part III: p53 is a central master protein in the pathway involving Cyr61 and Lasp1 in HCC

3.3.1. Cyr61 is an upstream regulator of p53 in HCC

Role of Cyr61 in HCC cell cycle regulation

Cell cycle analysis was carried out in an attempt to understand the mechanisms involved in the suppression of HCC cell growth by Cyr61. As described in section 2.10.1 and 2.11, HepG2-Cyr61 stable transfectants (HepG2-Cyr61-1 and HepG2-Cyr61-2) and HepG2-Neo control cell lines were either untreated or treated with 5- Fluorouracil (5-FU, 50μg/ml) or UV irradiation (20J/m^2) for flow cytometry analysis. It was first noted that both stable cell lines without any treatment had higher percentage of cells (16.5% and 18.6% respectively) arrested in the G2/M phase compared to the Neo control (13.1%) (Figure 3.38, 1st row). Furthermore, a more prominent G2/M arrest was maintained in the two HepG2-Cyr61 stable cells lines (13.7% and 12.7% respectively) compared to HepG2-Neo control (5.5%) after being subjected to 5-FU treatment (Figure 3.38, 2nd row). Similar observation was obtained from the cells undergone UV irradiation, which caused a dramatic reduction of cells at G2/M phase as observed in HepG2-Neo control cells (5.7%) compared to HepG2-Cyr61 stable cells (15.8% and 13.1% respectively) (Figure 3.38, 3rd row). However, no significant difference of sub-G1 percentage was observed.

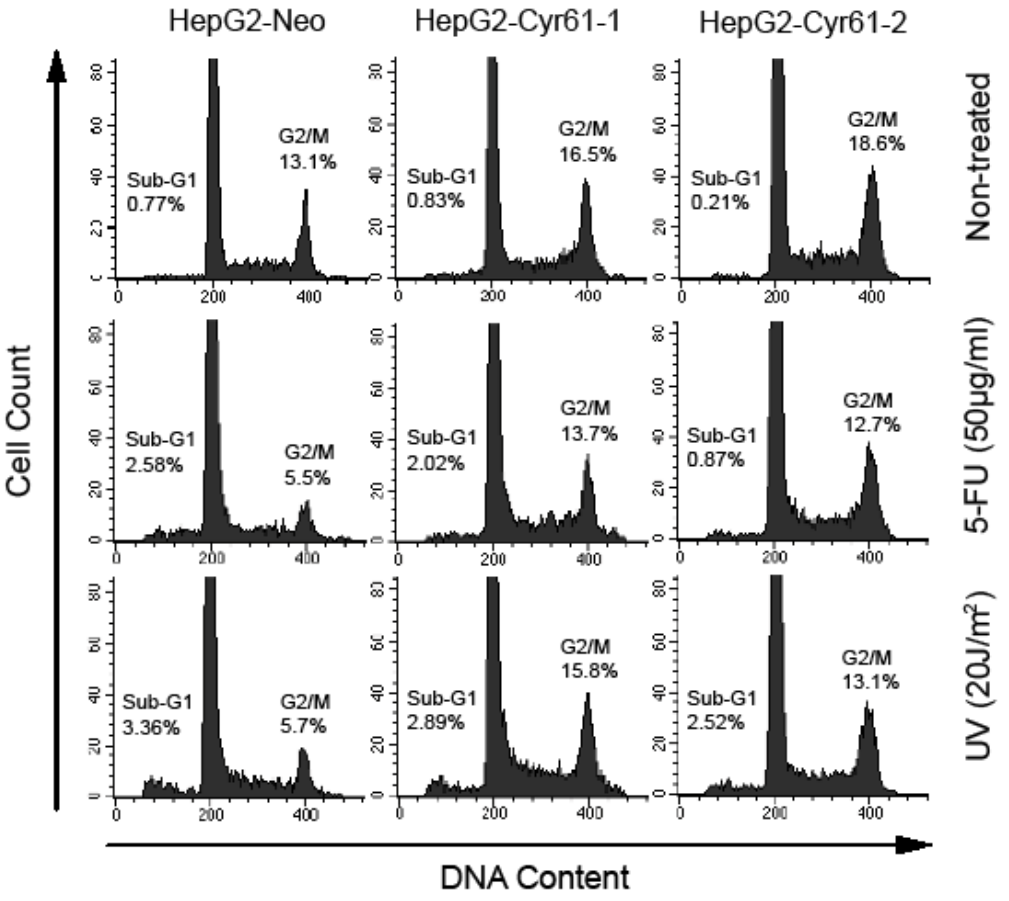

Figure 3.38 Cyr61 over-expression induced G2/M arrest of HepG2 cells. HepG2-Cyr61 stable cells (HepG2-Cyr61-1, HepG2-Cyr61-2) and HepG2-Neo cells under different treatments were separately collected, fixed in 70% ethanol, treated with RNase A (100μg/ml) and stained with propidium iodide (50μg/ml) for flow cytometry analysis. The percentage of cells in G2/M and Sub-G1 phase is indicated. Cell cycle analysis of non-treated HepG2-Cyr61 stable cell lines and HepG2-Neo cells is shown on the top panel, and the analyses of 5-FU (50μg/ml) or UV (20J/m^2) treated cells are shown on the middle and bottom panel, respectively.

Cyr61 up-regulates p53 expression in p53 wild-type HCC cells

At the same passage (4^{th} passage), cellular proteins extracted from HepG2-Cyr61-1, HepG2-Cyr61-2 and HepG2-Neo cells were separated by SDS-PAGE followed by Western blot using a series of antibodies specific to Cyr61, p53 and p21, the latter two of which were known to be important cell cycle regulators involved in G1, S and G2/M arrests. The protein levels of p53 and its downstream target gene p21 were shown to be significantly up-regulated in HepG2-Cyr61 stable cells (Figure 3.39, left panel). Similar findings were observed in HepG2 cells transiently transfected with pDEST40-Cyr61/V5 plasmid, which showed up-regulating levels of p53 and p21 proteins in HepG2 cells with increasing expression of Cyr61/V5 (Figure 3.39, upper right panel). In addition, the mRNA levels of two G2/M arrest marker gene, 14-3-3σ and GADD45 (Hermeking *et al*. 1997; Wang *et al*. 1999), were tested by semi-quantitative RT-PCR with GAPDH as a housekeeping control. The results demonstrated up-regulation of the mRNA of both 14-3-3σ and GADD45 upon transient transfection of increasing doses of pDEST40-Cyr61/V5 in HepG2 cells (Figure 3.39, lower right panel). All the above findings suggested that over-expression of Cyr61 in HepG2 cells induced G2/M arrest, at least in part, by up-regulating the cell cycle regulator p53.

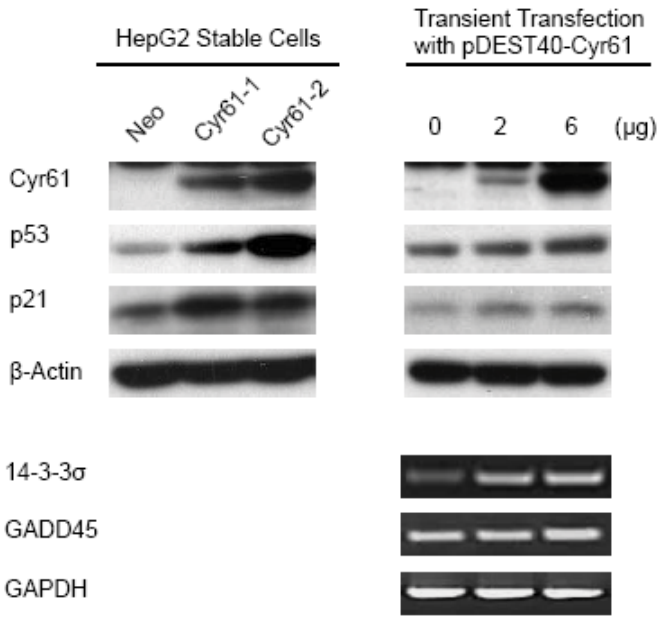

Figure 3.39 Cyr61 over-expression led to up-regulation of p53 and its downstream targets. Western blot and RT-PCR indicated up-regulation of protein and mRNA level of p53 and several well-defined p53 downstream targets in Cyr61-expressing cells. The left panel shows the results of cell lysates collected from HepG2 stable cell lines (Cyr61-1, Cyr61-2, and Neo control), while the data from HepG2 cells transiently transfected with increasing dose of pDEST40-Cyr61/V5 are shown on the upper right panel. Semi-quantitative RT-PCR showed the mRNA up-regulation of two G2/M arrest marker gene 14-3-3σ and GADD45 in Cyr61 transient over-expressed HepG2 cells, which is presented on the lower right panel.

Cyr61 is a genotoxic stress responsive gene

To further explore the potential roles of Cyr61 in cell cycle progression, we investigated the endogenous expression of Cyr61 upon genotoxic stress induction, which are known to trigger cellular processes of growth arrest or apoptosis, with p53 being the major cellular sensor and signal of DNA damage (Amundson *et al*. 1998). As illustrated in section 2.10.2, both p53 wild-type (p53+/+) HepG2 cell line and p53 null (p53-/-) Hep3B cells line were used in the experiments. As expected, p53 and p21 proteins significantly accumulated in p53+/+ HepG2 cells over the 48-hour period after 5-FU treatment or UV irradiation (Figure 3.40A, upper panel), whereas both proteins remained undetectable in p53-/- Hep3B cells (Figure 3.40B, upper panel). Remarkably, the endogenous expression of Cyr61, which was barely detectable in non-treated HepG2 and Hep3B cells by Western blot, was dramatically increased in response to the genotoxic stress in both HCC cells regardless of p53 status (Figure 3.40A and 3.40B, upper panel). Concomitantly, mRNA expression of Cyr61 was also up-regulated in both HepG2 and Hep3B cells upon genotoxic treatment as measured by RT-PCR (Figure 3.40A and 3.40B, lower panel). The mRNA expression of Cyr61 in HepG2 cells quickly peaked at 4h after treatments, compared to a gradually increased mRNA expression throughout the 48h period occurred in Hep3B cells, though the protein expression of Cyr61 reached a maximal level around 24-48h similarly in both HCC cell lines.

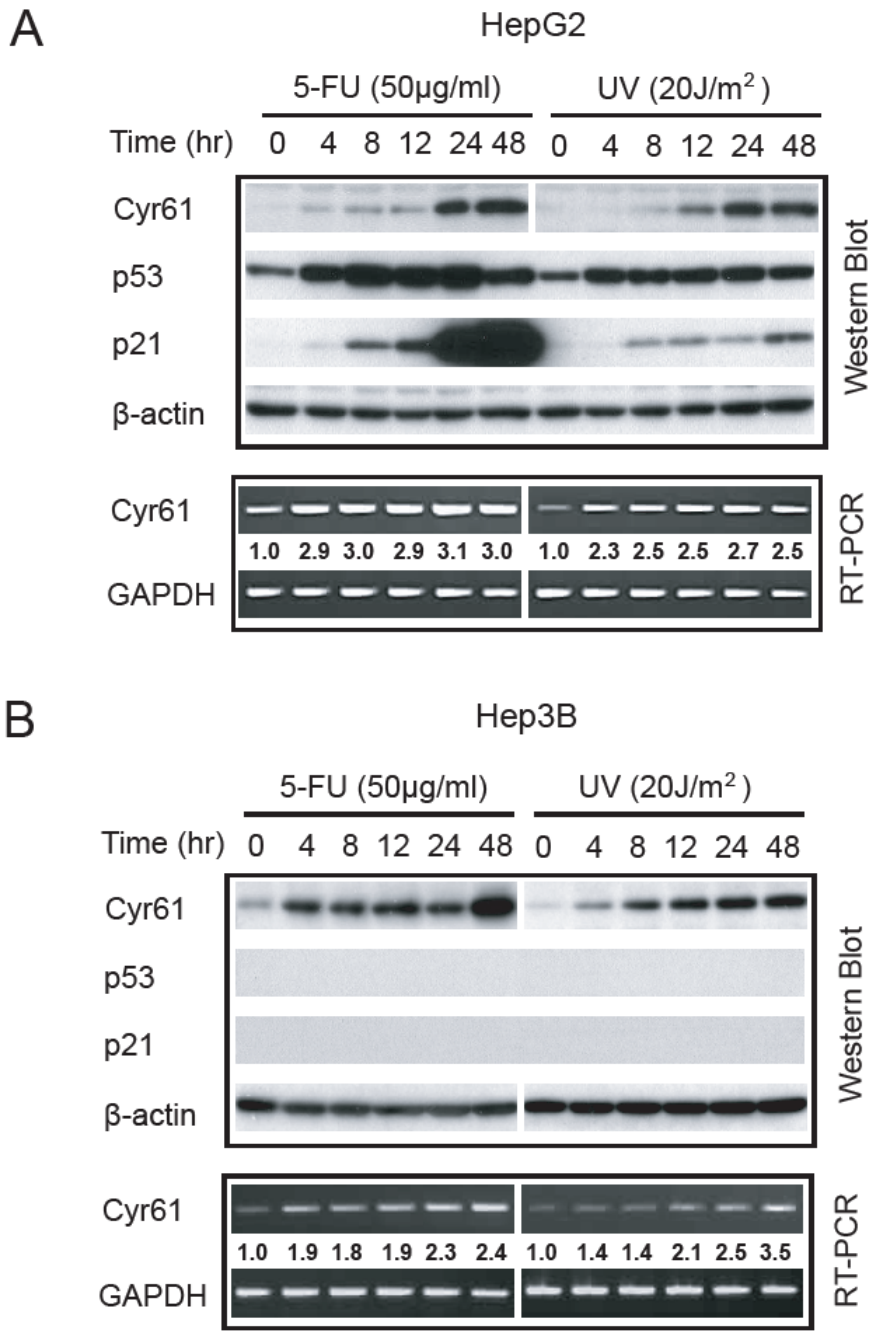

Figure 3.40 Expression of endogenous Cyr61 was up-regulated in response to genotoxic stress regardless of p53 status in HCC cell lines. HepG2 (A) and Hep3B (B) cells treated with 5-FU (50μg/ml) or UV irradiation (20J/m^2) were harvested at indicated time points for lysate extraction and RNA isolation. Cell lysates were analyzed by Western blot for the expression of Cyr61, p53 and p21 using specific antibodies (upper panel). The transcription level of Cyr61 was measured by semi-quantitative RT-PCR (lower panel). Band intensities were measured by densitometry, and expression levels of Cyr61 for each point relative to the 0h point in each group are indicated beneath each band. GAPDH was used to indicate the integrity and comparable quantity of RNA samples in RT-PCR.

To further confirm the conclusion that Cyr61 is a genotoxic stress inducible gene involved in DNA damage response, HCT116 and its derived isogenic p53-/- cells were also used for this study as another paired cell lines in parallel to HepG2 and Hep3B cells. Cell lysates collected at different time points after 5-FU (50µg/ml) treatments were subjected to Western blot using Cyr61 specific antibody. The same results as in HepG2 and Hep3B cells were observed, i.e. Cyr61 protein level were dramatically up-regulated upon 5-FU treatment in both HCT116 and HCT116 (p53-/-) cells (Figure 3.41).

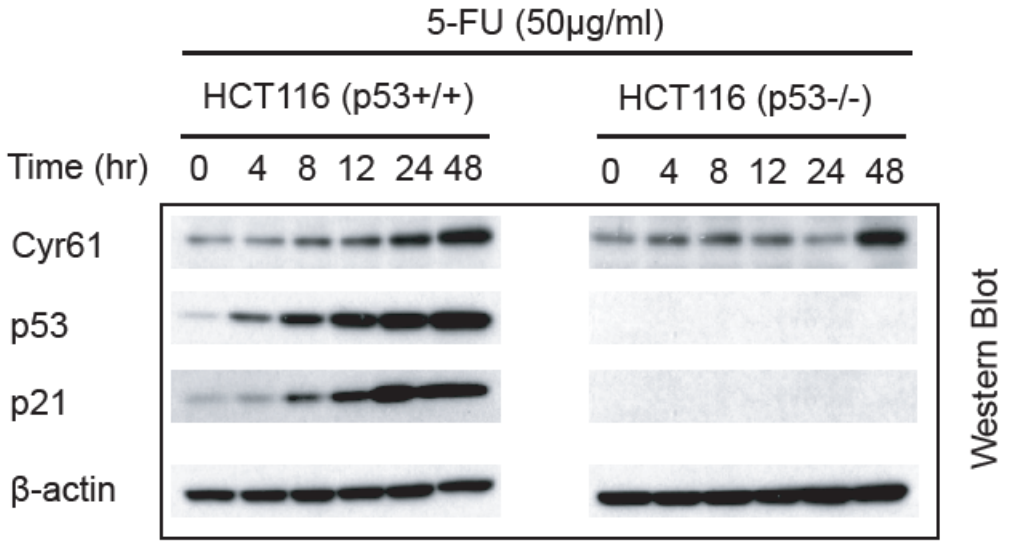

Figure 3.41 Expression of endogenous Cyr61 was up-regulated in response to genotoxic stress regardless of p53 status in colon cancer cell lines. HCT116 (p53+/+) and HCT116 (p53-/-) cells treated with 5-FU (50µg/ml) were harvested at indicated time points for lysate extraction. Cell lysates were analyzed by Western blot for the expression of Cyr61, p53 and p21 using specific antibodies. β-actin blotting was used as a control for equal protein loading.

3.3.2. Lasp1 is a downstream target of p53

Chromatin immunoprecipitation (ChIP) is a powerful technique for analyzing transcription factor binding site (TFBS) in living cells. This technology was most commonly employed to map TFBS in high-throughput manner, such as ChIP-on-CHIP. Recently, a paired-end ditag method, which extracts 36bp signatures with 18bp from the 5' end and another 18bp from the 3' end of each cDNA clone, was established to concatenate the PETs for efficient sequencing and map the PET sequences to the genome to demarcate gene-transcription boundaries (Ng *et al*. 2005). In a more recent study, Lasp1 was found to be a potential p53 target gene identified by coupled ChIP with the paired-end ditag technologies (ChIP-PET) (Wei *et al*. 2006).

In the current study, having shown the biological functions of Lasp1 in HCC growth and metastasis, we further demonstrated the role of p53 in transcriptionally regulating Lasp1 using p53 wild-type HepG2 and p53 null Hep3B cells as a model cell system. Moreover, in order to exclude any possibility of factors other than p53, the colon cancer cell line HCT116 and its derived isogenic p53-/- cell line were also included as a parallel cell system, which were obtained from Dr. Bert Vogelstein as a gift.

ChIP-PET and ChIP validation

As shown in Figure 3.42A, three PETs positioning at Chr17: 34278957-34279301, 34279232-34279970, and 34279673-34280068 were identified from the previous ChIP-PET study (Wei *et al*. 2006). These PETs were mapped to -937~-593bp, -662~+76bp, and -221~+174bp relative to the transcription start site of Lasp1 transcript with two overlap regions (-662~-593bp, -221~+76bp), which presumably contained TFBS.

As the original ChIP data were only obtained from HCT116 cells, both HCT116 and HepG2 cells carrying wild-type p53 gene were used in a ChIP assay in order to further validate the ChIP-PET results. As described in section 2.12, six hours after 5-FU treatment, cells were cross-linked with formaldehyde and the chromatin extracts containing DNA fragments of average size of 500bp were immuno-precipitated using anti-p53 antibody. ChIP-qPCR was then performed using p53-antibody enriched chromatin DNA. Primers were designed to match different regions spanning the Lasp1 promoter and part of the transcript, and more specifically to target the ChIP-PET overlap region. The ChIP-qPCR primer sequences were listed in Table 2.11, and their positions relative to the Lasp1 transcription start site (Lasp1 TSS) and to the identified PETs (Wei *et al.*, 2006) were illustrated in Figure 3.42A as well. Relative occupancy values (fold enrichments) were calculated by determining the immuno-precipitation efficiency and normalized to the level observed at a control region, which was set at 1.0 as indicated by dashed line in Figure 3.42B. The ChIP-qPCR results revealed two enrichment regions covered by primer set 3 and 4 (P3 and P4), 5 and 6 (P5 and P6) respectively, which spanned -598~-333bp and -92~+96bp relative to the Lasp1 transcription start site (TSS). Although the second enrichment region spanned by primer set P5 and P6 had a lower enrichment fold than the first region, it corresponded well to the second overlap region identified by the previous p53 ChIP-PET study (Wei *et al*. 2006). Thus it is highly possible that the p53 binding site(s) locate in one or both regions.

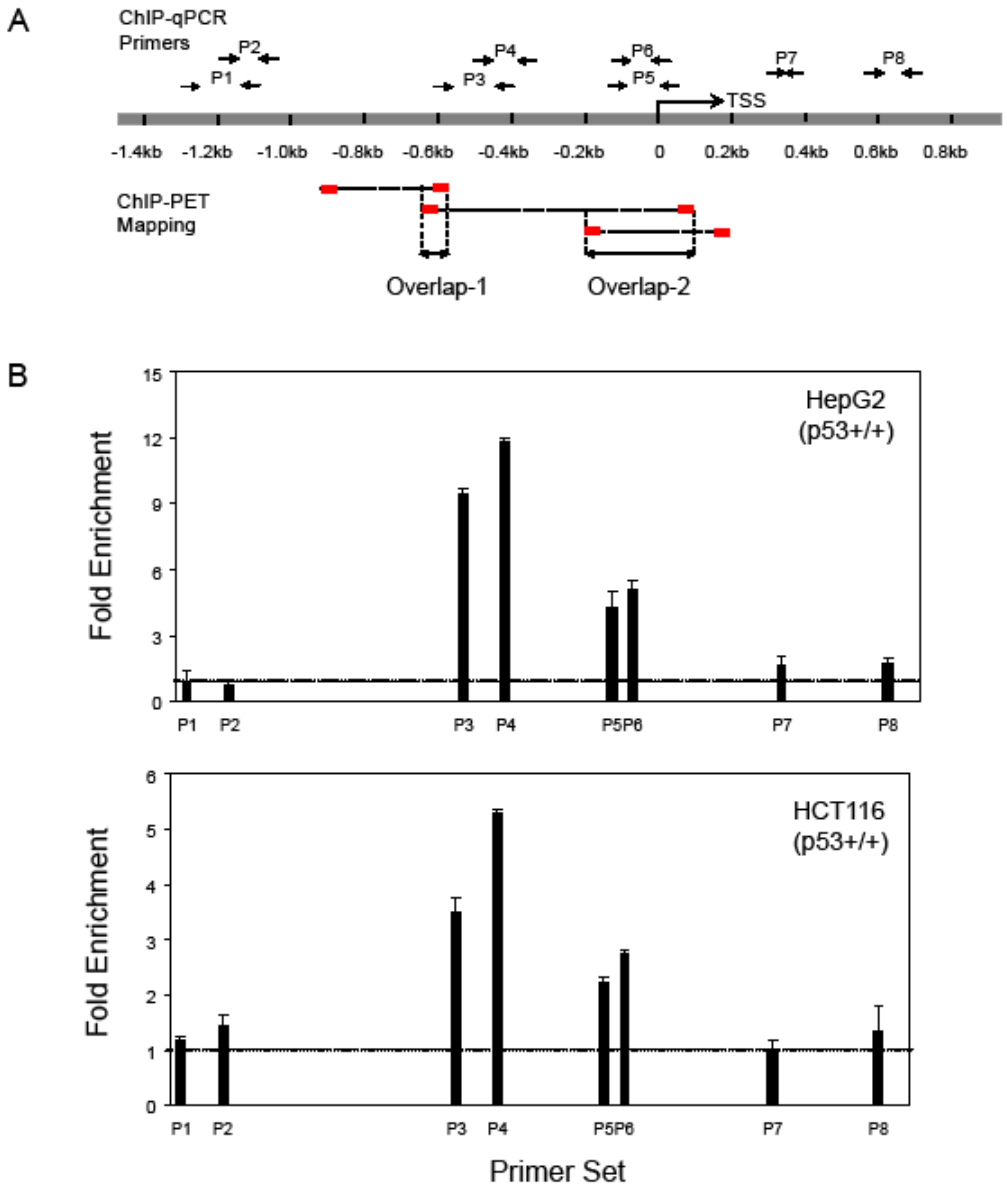

Figure 3.42 ChIP-PET and ChIP validation. (A) Illustrations of 3 ChIP-PETs located on the Lasp1 promoter region. The PET sequences shown as red rectangles are mapped to genome to demarcate the boundaries of DNA fragments. The amplified regions of the primer sets (P1~P8) used in ChIP-qPCR are also mapped to the Lasp1 5'flanking region and part of the Lasp1 transcript. Lasp1 transcription start site (Lasp1 TSS) is indicated by the black arrow. (B) Results of ChIP-qPCR. HepG2 and HCT116 (p53+/+) cells were treated by 5-FU for 6 hours. ChIP was performed with antibody against p53. The p53 binding was tested by using Lasp1 promoter specific primer sets P1~P8. Relative occupancy values (fold enrichments) were calculated by determining the immuno-precipitation efficiency and normalized to the level observed at the control region, which was arbitrarily set at 1.0 as indicated by dashed line.

p53 transcriptionally suppresses Lasp1 expression

Although Chromatin-IP can enrich for TFBS-containing DNA fragments, a significant amount of background DNA will still be present in the immuno-precipitated DNA. With a limited survey of the cloned ChIP DNA fragment pool, it is difficult to distinguish between genuine binding sites and noise. Thus, the molecular validation is very critical in defining *bona fide* p53 target genes.

To test whether p53 can functionally suppress Lasp1 gene expression, we first over-expressed p53 gene in p53 null Hep3B cells. The cells were plated in 6-well plates for overnight incubation followed by pCMV-p53 (wild-type p53) or pCMV-p53-R175H (DNA binding domain mutated p53) transfection. Total RNA and lysate were collected at different time points (0h, 6h, 10h, 24h, 48h, 72h) for real-time quantitative RT-PCR analysis for mRNA expression and Western blot for protein expression, respectively. The results of Figure 3.43A showed that the Lasp1 mRNA was down-regulated by wild-type p53 but not by mutant p53 in a time-dependent manner. The significant change started as early as 6 hours after transfection. As a positive control, p21 mRNA was rapidly up-regulated by wild-type p53 but not by p53-R175H. The decrease of Lasp1 protein expression was only obviously observed in wild-type p53 over-expressed cells after 48 hours of transfection, reaching less than half of the original amount at 72 hours (Figure 3.43B, upper panel). After transfection with increasing doses of wild-type p53 expression vectors, the down-regulation of Lasp1 protein expression was confirmed by Western blot as expected (Figure 3.43C). The same set of experiments was performed using HCT116 (p53-/-) cell lines. Similar results were obtained as in Hep3B cells, i.e. over-expression of wild-type p53 but not mutant p53 down-regulated both Lasp1 mRNA (Figure 3.44A) and protein levels in HCT116 (p53-/-) cells (Figure 3.44B).

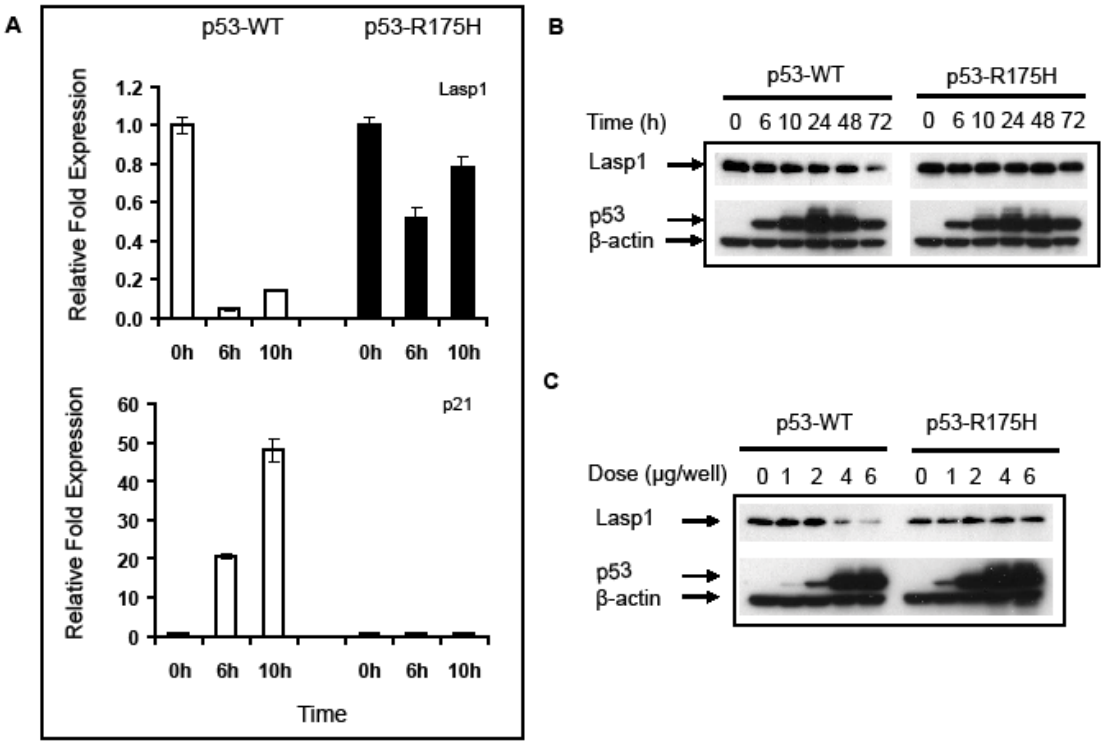

Figure 3.43 p53 but not p53 mutant over-expression down-regulated Lasp1 expression in Hep3B cells. Hep3B cells transfected with pCMV-p53 or pCMV-p53-R175H (4μg/well for 6-well plates) were harvested at indicated time points for total RNA isolation followed by cDNA synthesis or lysate extraction. (A) The transcription level of Lasp1 was measured by real-time quantitative RT-PCR using Lasp1 specific primers. After normalized to a housekeeping gene HPRT, Lasp1 expression level was presented as the percentage relative to the level at 0h time point, which was arbitrarily set at 1.0. The mean ± SD of triplicates are shown for each point. p21 was included as a positive control to indicate the functionality of over-expressed p53. (B) Cell lysates were analyzed by Western blot for the expression of Lasp1 and p53 using specific antibodies. β-actin was used as a control for equal protein loading. (C) Hep3B cells transfected with increasing doses of pCMV-p53 or pCMV-p53-R175H (0, 1, 2, 4, 6μg/well for 6-well plates) were harvested at indicated time points for lysate collection. Western blot using Lasp1 and p53 antibodies showed that p53 over-expression also down-regulated Lasp1 expression in a dose-dependent manner.

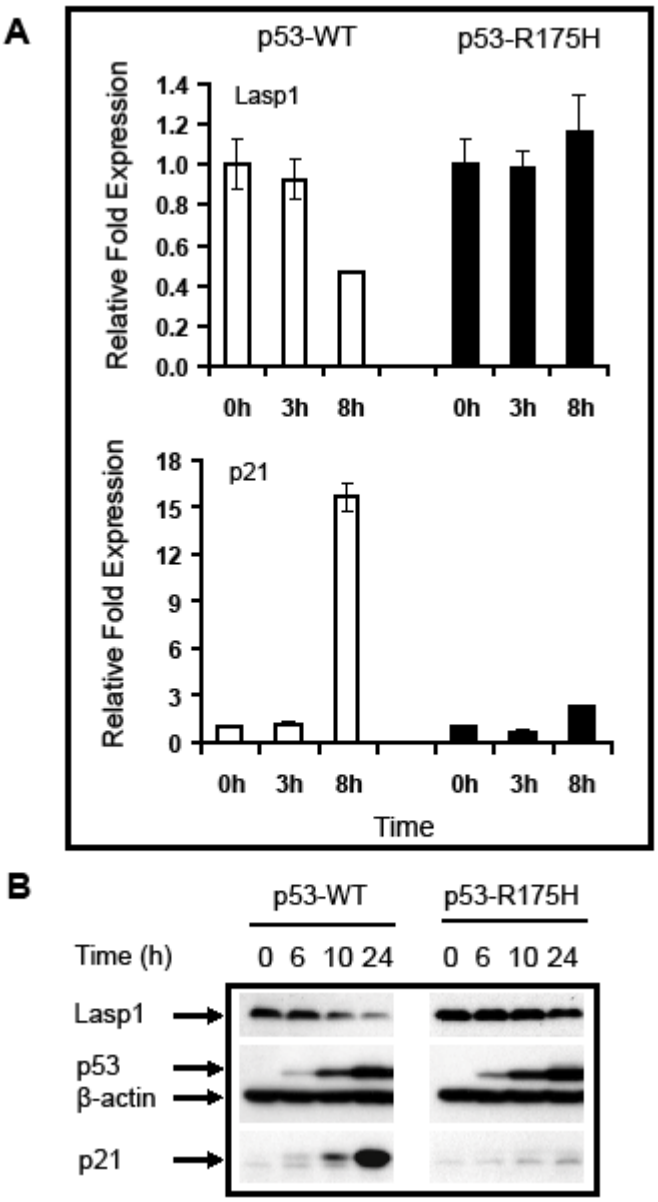

Figure 3.44 p53 but not p53 mutant over-expression down-regulated Lasp1 expression in HCT116 (p53-/-) cells. HCT116 (p53-/-) cells transfected with pCMV-p53 or pCMV-p53-R175H (4μg/well for 6-well plates) were harvested at indicated time points for total RNA isolation followed by cDNA synthesis or lysate extraction. (A) The transcription level of Lasp1 was measured by real-time quantitative RT-PCR using Lasp1 specific primers. After normalized to a housekeeping gene HPRT, Lasp1 expression level was presented as the percentage relative to the level at 0h time point, which was arbitrarily set at 1.0. The mean ± SD of triplicates are shown for each point. p21 was included as a positive control to indicate the functionality of over-expressed p53. (B) Cell lysates were analyzed by Western blot for the expression of Lasp1, p53 and p21 using specific antibodies. β-actin was used as a control for equal protein loading.

Treatment of cells with chemotherapeutic drug 5-FU has been shown to induce rapid accumulation of p53 (Fritsche *et al*. 1993; Muller *et al*. 1998). At different time points up to 48 hours, the total RNA and protein lysate from HepG2 (p53 wild-type) and Hep3B (p53 null) cells treated with 5-FU (50μg/ml) were separately collected. In HepG2 cells, a sharp increase was observed in the protein expression of p53 and its defined target p21 after 5-FU treatment over the basal expression level, while in p53 null Hep3B cells, the p53 and p21 protein level remained undetectable (Figure 3.45B). Then the expression of both Lasp1 mRNA and protein level was examined by real-time quantitative RT-PCR and Western blot, respectively. It was clearly shown that both Lasp1 mRNA and protein levels were decreased upon 5-FU treatment in p53 wild-type HepG2 cells but not in p53 null Hep3B cells (Figure 3.45A and 3.45B). Since the p53 status is not the only difference between HepG2 and Hep3B cells, the same set of experiments was performed in HCT116 and its derived isogenic p53-/- cell lines. The similar results were achieved as in HepG2 and Hep3B cells (Figure 3.46).

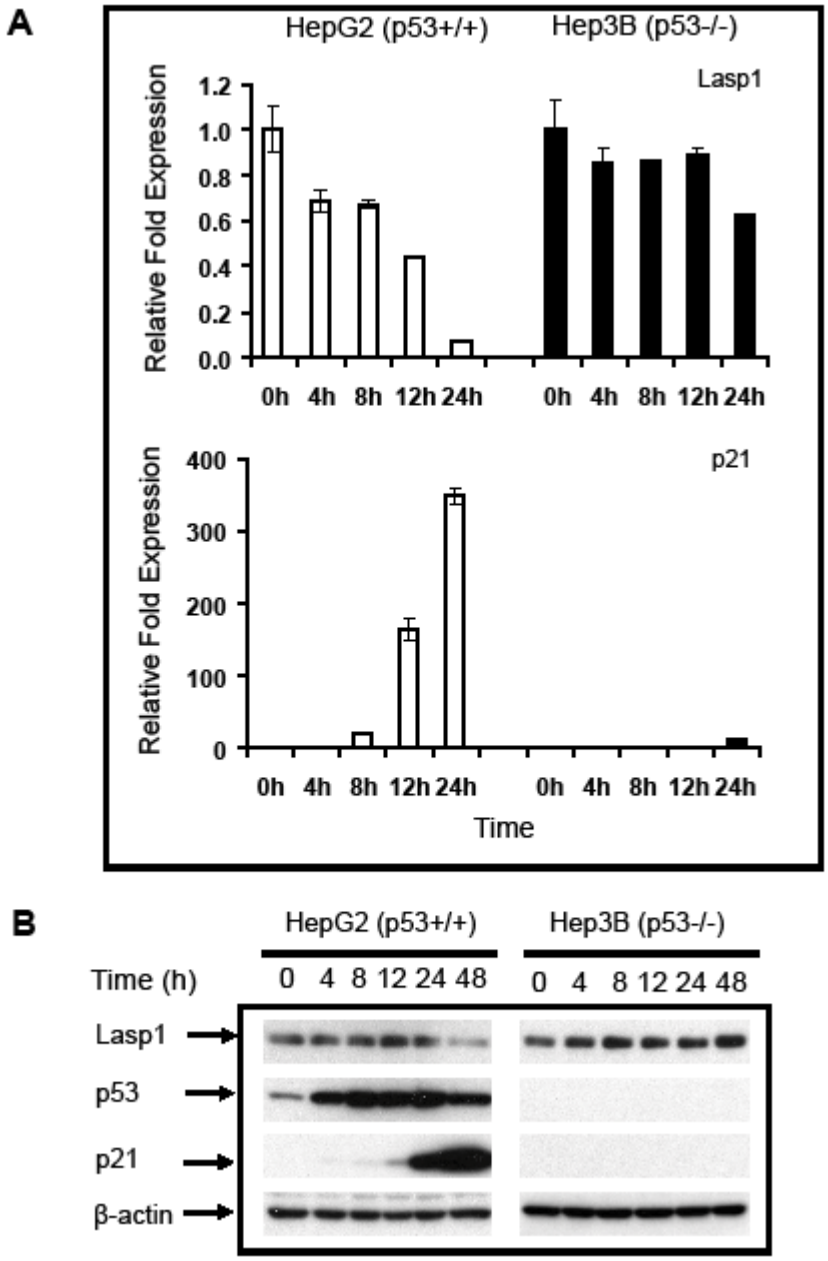

Figure 3.45 Endogenous p53 induced upon 5-FU treatment down-regulated Lasp1 expression in HepG2 but not in Hep3B cells. HepG2 and Hep3B cells treated with 5-FU (50μg/ml) were harvested at indicated time points for lysate extraction and RNA isolation. (A) The transcription level of Lasp1 was measured by real-time quantitative RT-PCR using Lasp1 specific primers. After normalized to a housekeeping gene HPRT, Lasp1 expression level was presented as the percentage relative to the level at 0h time point, which was arbitrarily set at 1.0. The mean ± SD of triplicates are shown for each point. p21 was included as a positive control to indicate the functionality of p53. (B) Cell lysates were analyzed by Western blot for the expression of Lasp1, p53, and p21 using specific antibodies. β-actin was used as a control for equal protein loading.

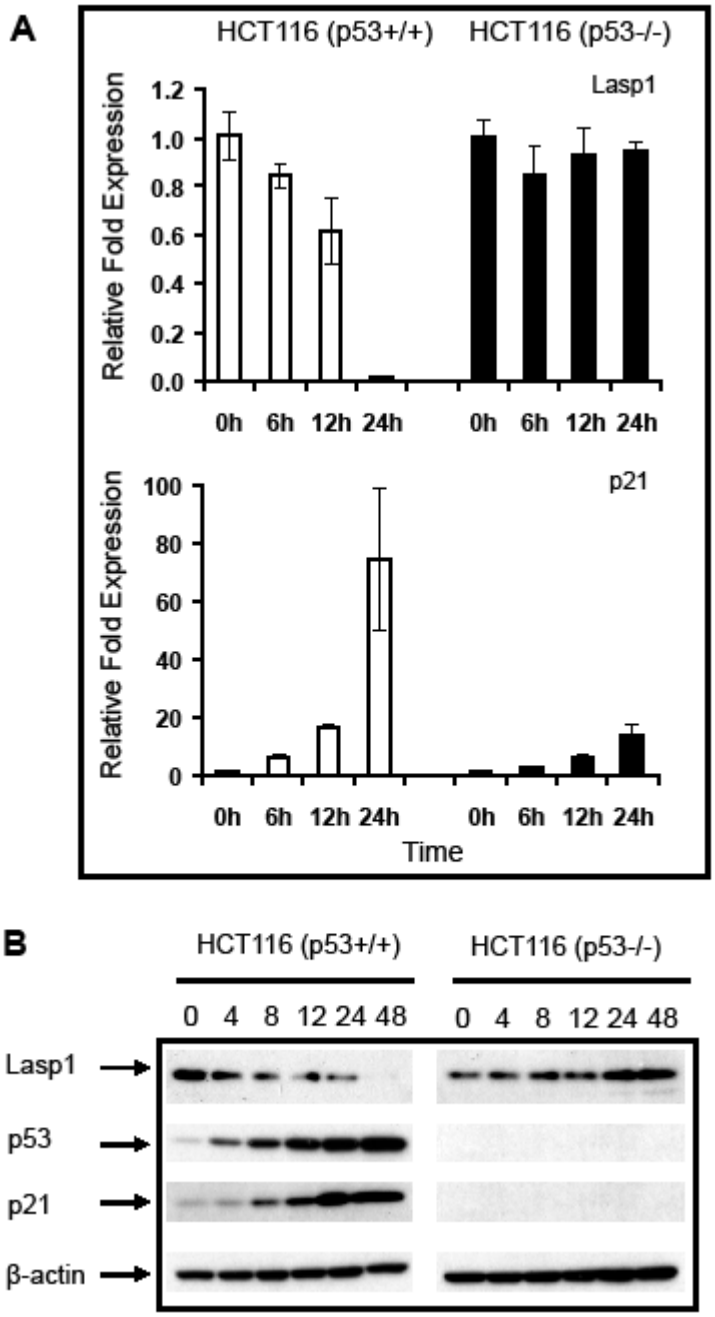

Figure 3.46 Endogenous p53 induced upon 5-FU treatment down-regulated Lasp1 expression in HCT116 (p53+/+) but not in HCT116 (p53-/-) cells. HCT116 (p53+/+) and its isogenic p53-null HCT116 (p53-/-) cells treated with 5-FU (50μg/ml) were harvested at indicated time points for lysate extraction and RNA isolation. (A) The transcription level of Lasp1 was measured by real-time quantitative RT-PCR using Lasp1 specific primers. After normalized to a housekeeping gene HPRT, Lasp1 expression level was presented as the percentage relative to the level at 0h time point, which was arbitrarily set at 1.0. The mean ± SD of triplicates are shown for each point. p21 was included as a positive control to indicate the functionality of p53. (B) Cell lysates were analyzed by Western blot for the expression of Lasp1, p53, and p21 using specific antibodies. β-actin was used as a control for equal protein loading.

To further confirm the role of p53 in transcriptionally regulating Lasp1, we transfected p53 specific siRNA into p53 wild-type HepG2 and HCT116 cells to knockdown the endogenous p53 expression and examined the change of Lasp1 mRNA. 24 hours after siRNA transfection, total RNA was extracted and the synthesized cDNA was subjected to real-time quantitative RT-PCR. In both HepG2 (Figure 3.47A) and HCT116 cells (Figure 3.47B) transfected with p53 siRNA, the p53 mRNA was down-regulated by its specific siRNA to only 39% (HepG2) and 32% (HCT116) compared to the control. Moreover, mRNA expression of its well-known downstream target p21 was also suppressed to 55% (HepG2) and 37% (HCT116) relative to that in the control siRNA (siControl) transfected cells. Real-time quantitative PCR using Lasp1 specific primer set clearly showed that, compared to siControl transfected cells, the Lasp1 mRNA expression was up-regulated to 228% in HepG2 (Figure 3.47A) and 154% in HCT116 cells (Figure 3.47B) respectively. In conclusion, all above experiments demonstrate that Lasp1 expression is negatively regulated by p53 at the transcriptional level.

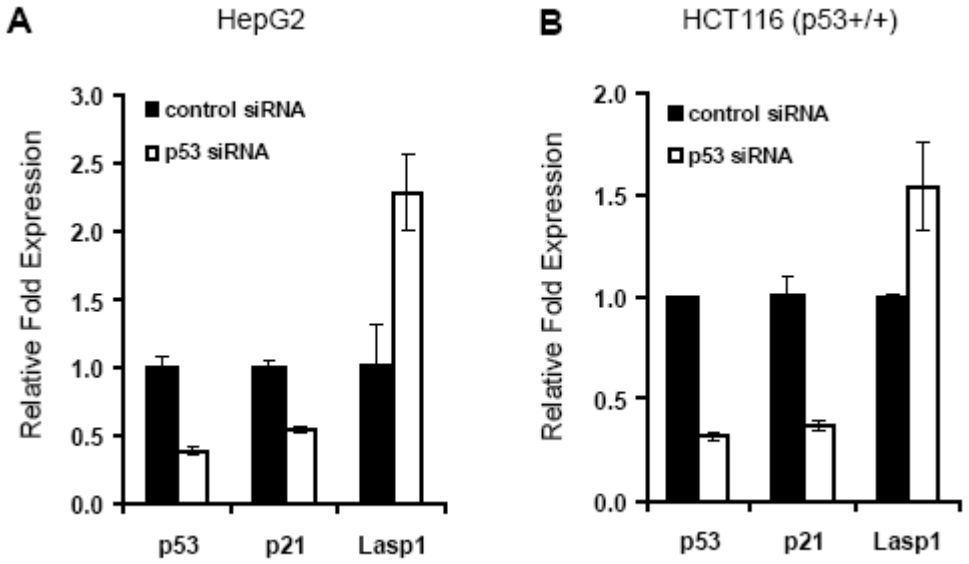

Figure 3.47 Knockdown of endogenous p53 by p53 specific siRNA up-regulated Lasp1 mRNA in HepG2 and HCT116 (p53+/+) cells. HepG2 (A) or HCT116 (p53+/+) (B) cells transfected with p53 specific siRNA (white bar) or control siRNA (siControl) (black bar) (40nM) were harvested at 24 hours post transfection for RNA isolation. Following cDNA synthesis, the mRNA expression level of p53, p21 and Lasp1 was analyzed by real-time quantitative RT-PCR. After normalized to a housekeeping gene HPRT, gene expression level for all three genes was presented as the percentage relative to the level of the siControl transfected cells, which was arbitrarily set at 1.0. The mean ± SD of triplicates are shown. p21 was included as a positive control to indicate the functionality of endogenous p53.

pGL3-cloning of Lasp1 promoter region

To determine an inhibitory effect of p53 on Lasp1 gene transcription, a ~1.95kb genomic fragment of Lasp1 gene covering -1872bp to +74bp relative to the transcription start site was cloned into pGL3-Basic luciferase reporter vector (Figure 2.5). The ATG translation start codon was excluded from the fragment to ensure the correct translation of luciferase reporter gene. The detailed protocol was described in section 2.4.3, and the constructed vectors were illustrated in Figure 3.48A. Briefly, the insert DNA was isolated by a PCR reaction using HepG2 human genomic DNA as a template (Figure 3.48B). The PCR product was first cloned into pCR-BluntII-TOPO vector (Figure 2.4) (defined as TOPO-Lasp1-PR) and then sub-cloned into the pGL3-Basic vector (defined as pGL3-Lasp1-PR). Enzymatic digestion (Figure 3.48C) and sequencing confirmed the right sequence of desired constructs.

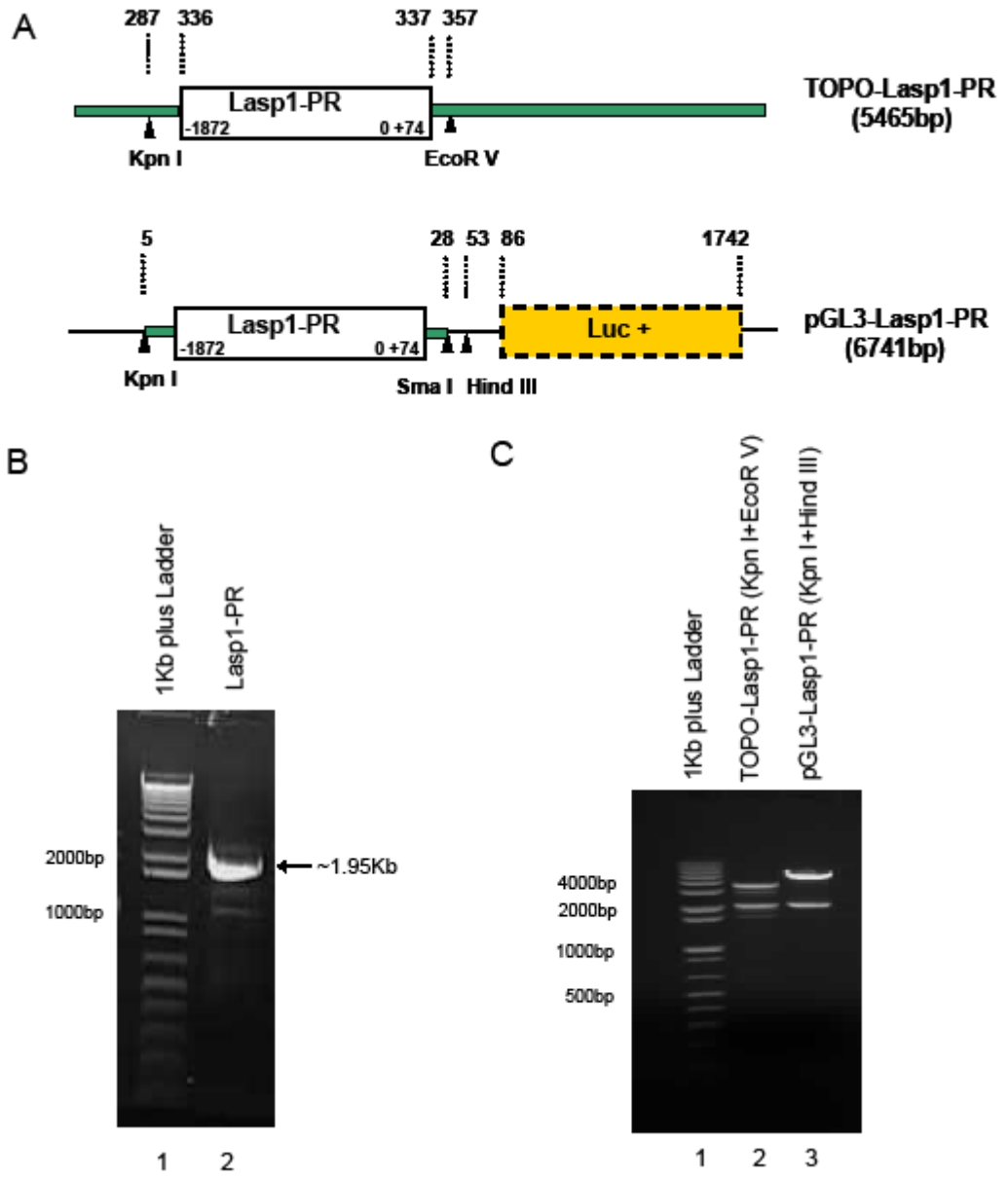

Figure 3.48 pGL3-cloning for Lasp1 promoter region. (A) Illustrations of the constructed plasmids. TOPO-Blunt II flanking region (green boxes), luciferase gene product (luc+, orange box) and the restriction enzyme sites (▲) are indicated. (B) PCR amplification of Lasp1 promoter region using HepG2 genomic DNA as a template. Lane1: 1kb plus DNA Ladder; Lane2: Lasp1-PR PCR product of about 1.95kb. (C) Enzyme digestion of the constructed vectors. Lane1: 1kb plus DNA ladder; Lane2: TOPO-Lasp1-PR Kpn I + EcoR V digested, 2 fragments (1977bp, 3488bp); Lane3: pGL3-Lasp1-PR Kpn I + Hind III digested, 2 fragments (2002bp, 4770bp).

p53 down-regulates Lasp1 promoter activity

Genetic reporter systems are widely used to study eukaryotic gene expression and cellular physiology. The Dual-Luciferase® Reporter Assay System (Promega) provides an efficient means of performing dual-reporter assays, in which the impact from different transfection efficiency is removed by sequentially measuring the activities of Firefly and Renilla luciferases from a single sample. Hence in this study, in order to examine the effect of p53 on Lasp1 promoter activity, pGL3-Lasp1-PR in the presence of different doses of pCMV-p53 or pCMV-p53-R175H was transfected into HCT116 (p53-/-) or Hep3B cells in a 96-well plate format. 36 hours after transfection, the Lasp1 promoter activities in transfected cells were determined by the Dual-Luciferase® Reporter Assay System. The results in Figure 3.49 showed that p53 but not p53-R175H mutant inhibited the pGL3-Lasp1-PR promoter activity in a dose-dependent manner in both p53-/- HCT116 (Figure 3.49A) and Hep3B cells (Figure 3.49C). The pGL3-vector carrying the promoter region of PTPRM2, which was a defined p53 target gene, was included as a parallel positive control (Figure 3.49B and 3.49D).

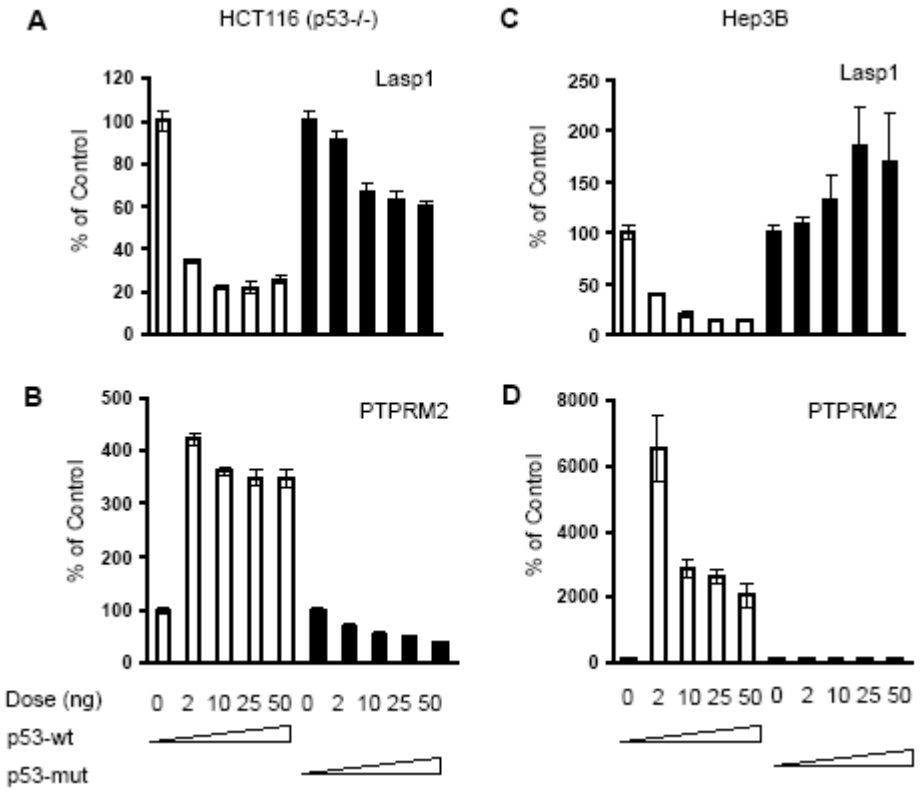

Figure 3.49 p53 down-regulated Lasp1 promoter activity. The pGL3-Lasp1-PR vector was co-transfected with an increasing doses of pCMV-p53 or pCMV-p53-R175H (0, 2, 10, 25, 50ng) into HCT116 (p53-/-) or Hep3B cells. pGL3-PTPRM2-PR was used as positive control. 36 hours after transfection, the Lasp1 promoter activities in transfected cells were determined by luciferase assay. After the reporter Firefly luciferase activity was normalized to Renilla luciferase activity (F/R ratio), the data were presented as the percentage relative to basal promoter activity co-transfected with pcDNA3.1 control only (0ng), which was arbitrarily set at 100%. The mean ± SD of triplicate wells are shown for each point. (A) Lasp1 promoter activity in HCT116 (p53-/-) cells. (B) PTPRM2 promoter activity in HCT116 (p53-/-) cells. (C) Lasp1 promoter activity in Hep3B cells. (D) PTPRM2 promoter activity in Hep3B cells.

pGL3-cloning of Lasp1 promoter region deletion constructs

In order to locate the potential p53 binding motif in Lasp1 promoter, I manually searched the promoter sequences from -937bp to +174bp, which covers 3 PETs identified from the previous p53 ChIP-PET study. Two putative p53 binding sites corresponding to the well-defined consensus sequence (PuPuPu**C**(A/T)(A/T)**G** PyPyPy † PuPuPu**C**(A/T)(A/T)**G**PyPyPy, Pu: purine, Py: pyrimidine, †: spacer of 0-13 nucleotides) (el-Deiry *et al*. 1992) were found located at each of the two enrichment regions defined by ChIP-qPCR, which are 5'-agt**C**AA**G**gtc-gcaagtc-ctc**C**TA**G**gtt-3' (-400bp~-374bp) and 5'-agg**C**CA**G**ttc-ccca-gct**C**CA**G**ccg-3' (-59bp~-36bp) (Figure 3.50).

To predict the genuine p53 binding sites, a series of pGL3- constructs with truncated Lasp1 promoter region were generated as shown in Figure 3.51A. PCR amplification using pGL3-Lasp1-PR as template was performed to generate DNA fragment of Lasp1 promoter region with different sizes carrying Kpn I and Hind III restriction sites (Figure 3.51B). These PCR products were cloned into pCR®4-TOPO® vector to generate a series of intermediate constructs (TOPO-Lasp1-PR-DelA, B, C, D, E, F, G, H, I, J, K). Then, those pCR4-TOPO deletion constructs were digested by Kpn I and Hind III and sub-cloned into pGL3-Basic vector to achieve 11 deletion constructs (pGL3-Lasp1-PR-DelA, B, C, D, E, F, G, H, I, J, K). Enzyme digestion (Figure 3.51C) and sequencing confirmed the desired pGL3- deletion constructs.

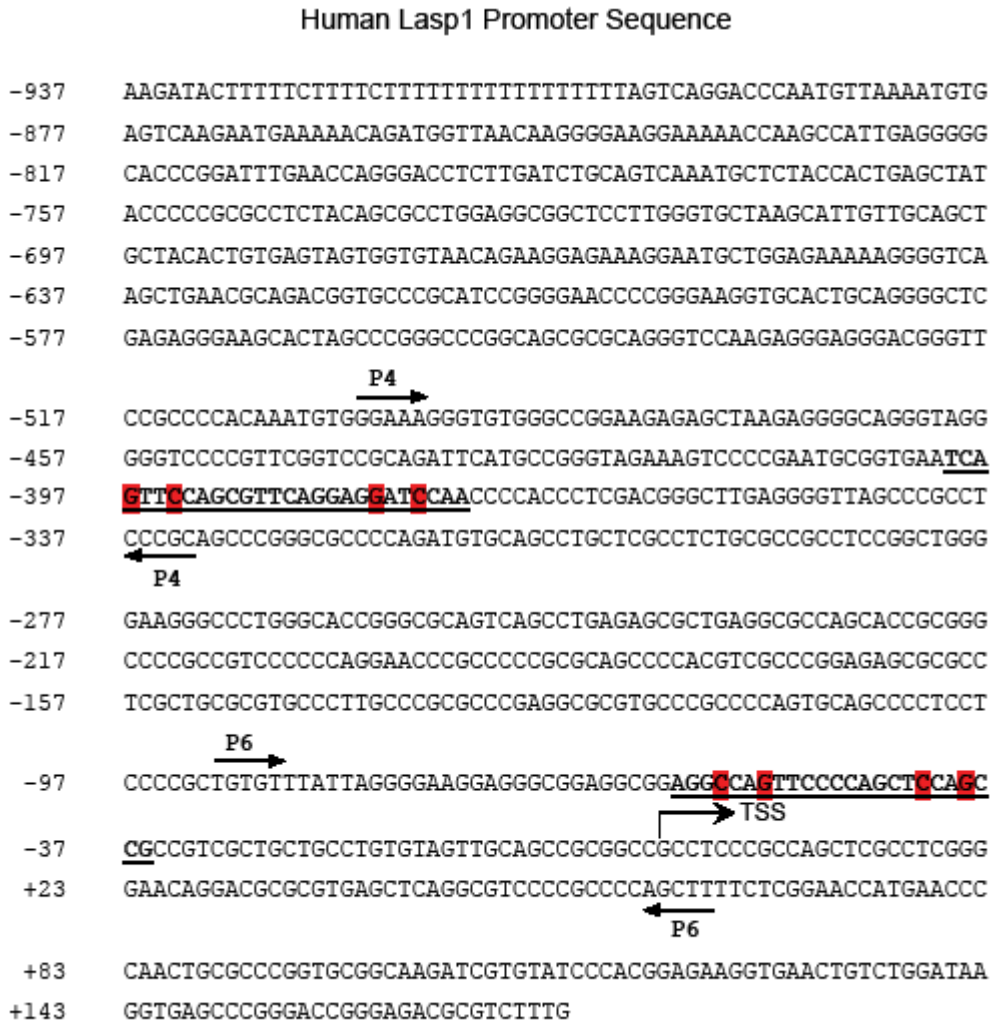

Figure 3.50 Prediction of potential p53 binding site(s) in Lasp1 promoter. The sequences (-937bp~+174bp) which covered 3 PETs identified from the previous p53 ChIP-PET study were manually searched. Two putative p53 binding sequences were in bold and underlined with the strictly conserved C/G highlighted in red. TSS: transcription start site.

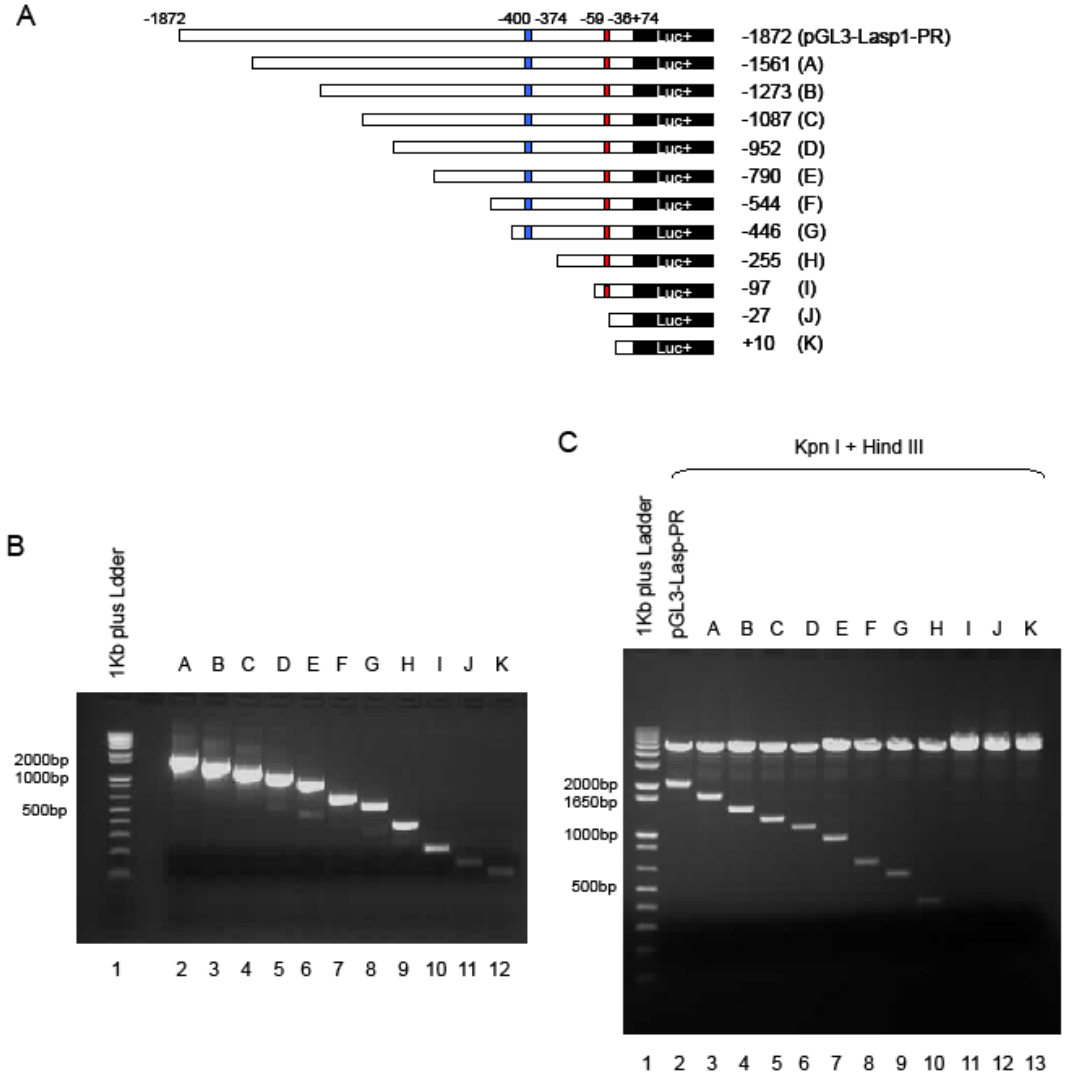

Figure 3.51 pGL3-cloning for Lasp1-PR deletion constructs. (A) Illustrations of 11 deletion constructs. The length and position of the inserts of the original pGL3-Lasp1-PR and deletion constructs (A~K) were shown. The two putative p53 binding motifs were illustrated as blue and red boxes, respectively. (B) PCR amplification of Lasp1-PR deletion constructs. Lane1: 1kb plus DNA Ladder; Lane2-12: PCR product of Lasp1-PR-DelA~K. (C) Enzyme digestion of the constructed vectors. Lane1: 1kb plus DNA Ladder; Lane2: pGL3-Lasp1-PR Kpn I + Hind III digested, 2 fragments (2002bp, 4770bp); Lane3-13: pGL3-Lasp1-PR-DelA~K Kpn I + Hind III digested, 2 fragments for each.

The basal promoter activity of all deletion constructs was analyzed by luciferase assay in order to locate the region of important transcription regulators in Lasp1 promoter by using p53-/- HCT116 and Hep3B cells. As shown in Figure 3.52, a significant drop in basal promoter activity was observed in both cells transfected with Lasp1-PR-DelI (-97bp) compared to that transfected with Lasp1-PR-DelH (-255bp), indicating that the most important transcription regulatory sequences are located in the small region of -255bp~-97bp relative to Lasp1 transcription start site.

Next, the luciferase assay for predicting p53-responsive region was performed. All deletion constructs, the original full length construct (pGL3-Lasp1-PR) and the pGL3-Basic vector were co-transfected with pCMV-p53 or pcDNA3.1 empty vector (10ng/well) into HCT116 (p53-/-) or Hep3B cells for luciferase assay. The responsiveness to p53 for each deletion construct was presented as the F/R ratio in pCMV-p53 co-transfected cells standardized to the F/R ratio observed in control vector pcDNA3.1 co-transfected cells, which was arbitrarily set at 100%. The results of the response of different constructs to p53 co-transfection shown in Figure 3.53 identified -97bp~-27bp as the p53-responsive region, where there was a clear restoration of the suppression effect by p53 ($P < 0.05$), indicating that the second putative site (-59bp~-36bp) found by manual search (Figure 3.50), which localizes in the small p53-responsive region, is the genuine p53 binding site.

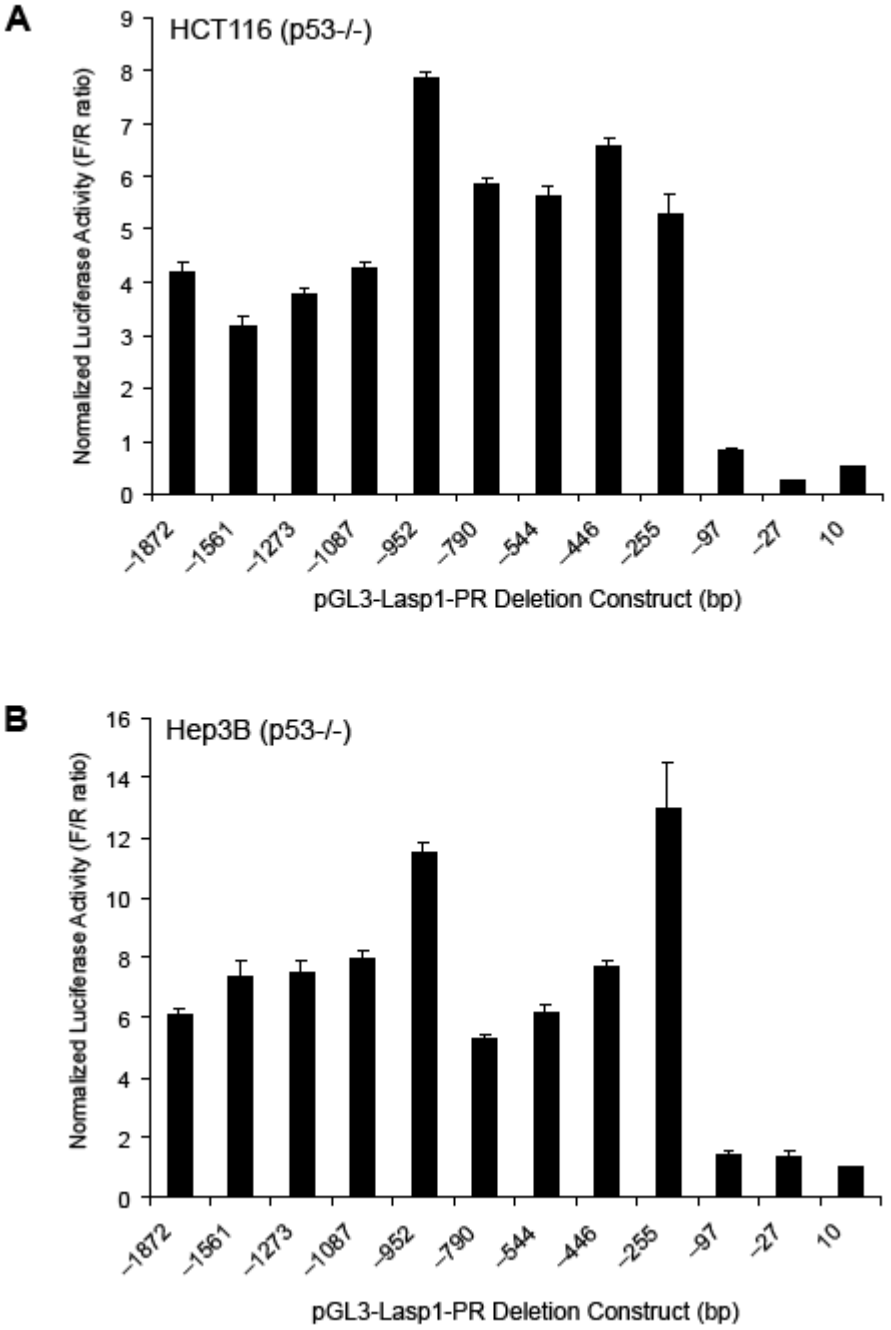

Figure 3.52 Truncation analyses of Lasp1 basal promoter activity. Comparison of the Lasp1 promoter activities driven by different lengths of 5'-flanking sequences. HCT116 (p53-/-) (A) or Hep3B (B) cells were transfected with pGL3-Lasp1-PR (-1872bp) or different pGL3-Lasp1-PR deletion constructs pGL3-Lasp1-PR-DelA ~ K, which corresponds to -1561 ~ +10bp relative to the Lasp1 transcription start sites. Cell lysates were harvested 36h after transfection and the Firefly luciferase activity and the Renilla luciferase activity were measured using the Dual-luciferase assay kit.

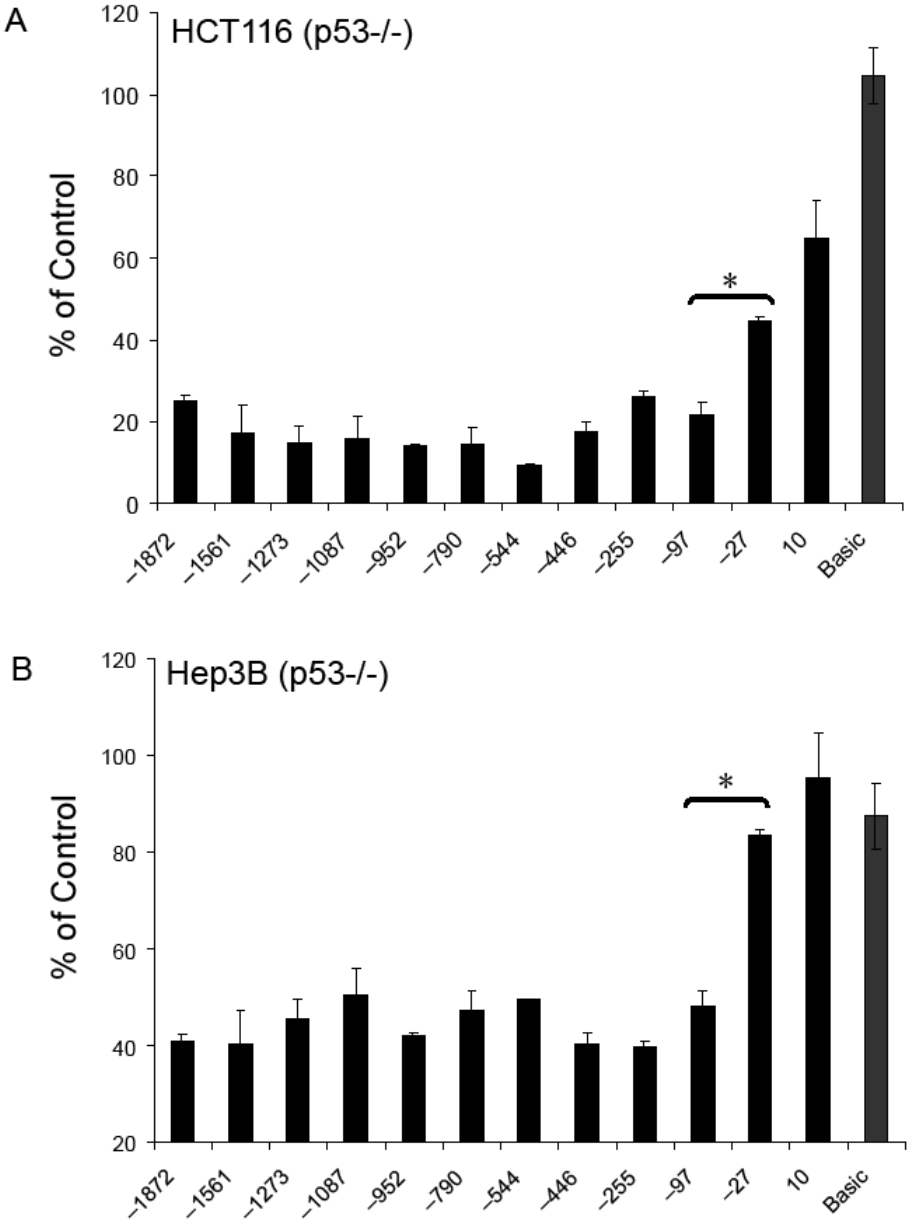

Figure 3.53 Localization of the p53-responsive region in Lasp1 promoter. HCT116 (p53-/-) (A) or Hep3B (p53-/-) (B) cells were transfected with different Lasp1 promoter constructs with pCMV-p53 or pcDNA3.1 empty vector. At 36 hours post transfection, cells were harvested and the luciferase activities were determined by the Dual-luciferase reporter system. The normalized luciferase activity of each construct in the pCMV-p53 transfected cells was compared to that of the pcDNA3.1 vector, which was expressed as 100%. The different responses to p53 between pGL3-Lasp1-PR-DelI (-97bp) and pGL3-Lasp1-PR-DelJ (-27bp) were considered as statistically significant (*$P < 0.05$). The pGL3-Basic vector was included to filter out nonspecific effects of p53 on luciferase activity.

In summary, a variety of experimental strategies were manipulated in this part of study to explore the potential pathways in linking Cyr61 and Lasp1 in HCC, which was illustrated in Figure 3.54. The transcription factor p53 was given a prior consideration as it is a well-known central master protein involved in progression of almost all cancers.

Cyr61 was shown to inhibit HCC cell growth, at least in part, by up-regulating p53 in p53 wild-type HepG2 cells. HepG2-Cyr61 stable transfectants showed G2/M arrest when compared to HepG2-Neo control cells. Furthermore, both transient and stable over-expression of Cyr61 in HepG2 cells up-regulated p53 protein level. In addition, Cyr61 was shown as a genotoxic stress responsive gene, the expression of which was rapidly induced at both mRNA and protein level, regardless of p53 status. All these evidences suggested that Cyr61 may behave as an upstream molecule of p53 in HCC and function in inhibiting HCC growth and metastasis, at least in part, through p53-dependent pathways.

On the other hand, Lasp1 was identified as a potential p53 downstream target through a ChIP-PET analysis (Wei *et al.*, 2006). In this current study, both biochemical and biological validations for the roles of p53 in transcriptionally suppressing Lasp1 gene expression were performed. ChIP-qPCR showed that p53 could bind Lasp1 promoter region *in vivo*. The transcription factor p53 was also shown to be able to negatively regulate Lasp1 expression through a series of experimental investigations, such as over-expression of p53 in p53 null cell lines, rapid accumulation of endogenous p53 upon 5-FU treatment or knockdown of p53 by p53 specific siRNA in p53 wild-type cell lines. Moreover, the role of p53 in repressing Lasp1 promoter activity was confirmed by Dual-luciferase reporter assay. All these evidences demonstrated Lasp1 as a *bona fide* p53 target, which could be transcriptionally suppressed by p53.

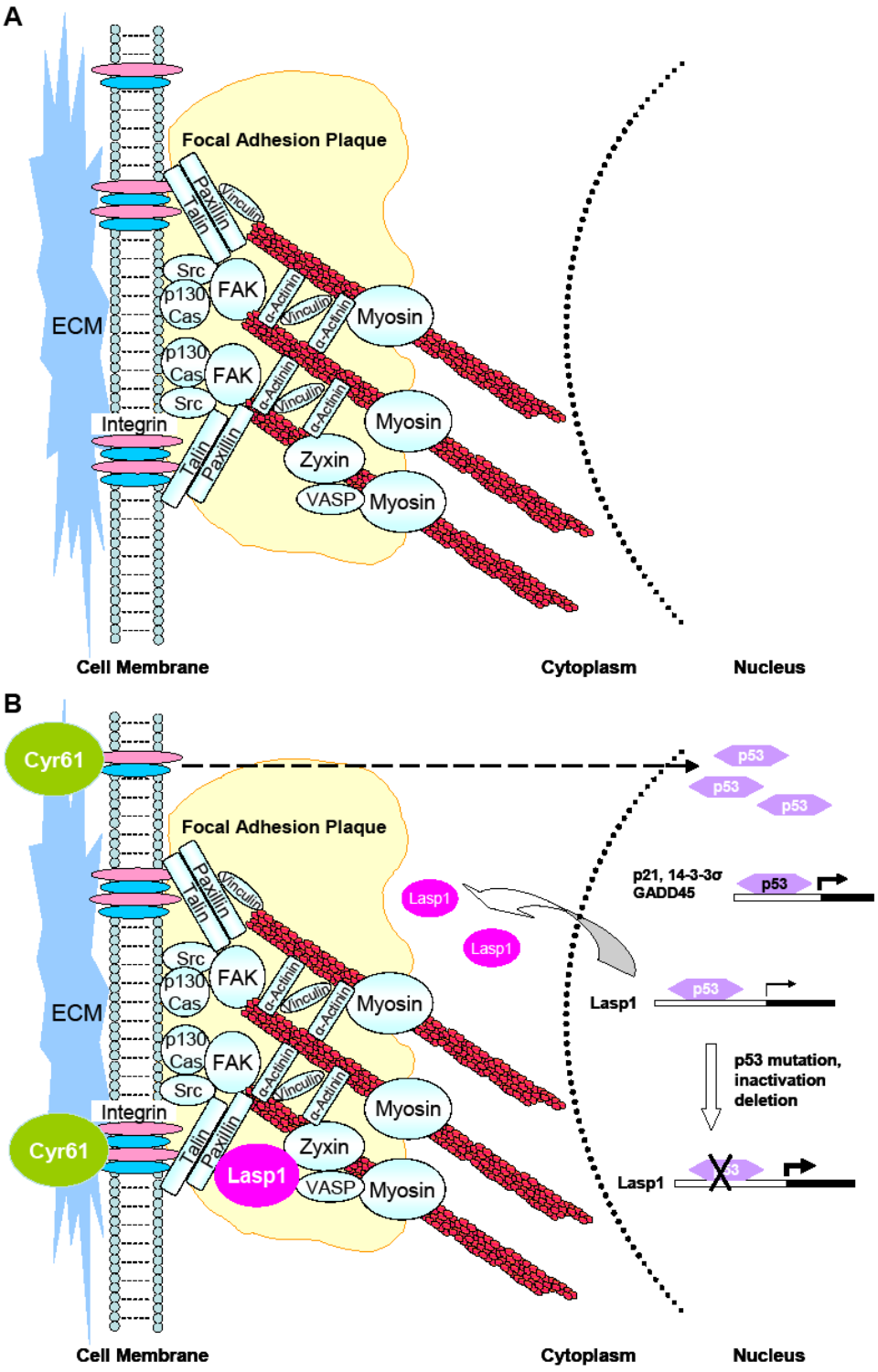

Figure 3.54 Model of pathways involving Cyr61 and Lasp1 in HCC. (A) Structure of focal adhesion plaques. Main focal adhesion proteins and F-actin stress fibers (red bundles) are shown. (B) Comprehensive Cyr61-Lasp1 pathway in p53 wild-type HCC cell lines with added information generated by this study. Cyr61 (green) interacts with integrins at ECM (extracellular matrix). Lasp1 (pink) co-localize with zyxin, VASP and paxillin at focal adhesion plaque. Cyr61 up-regulates the tumor suppressor p53 (purple hexagon), which transcriptionally repress Lasp1 expression. When p53 is mutated, deleted or inactivated, Lasp1 expression is up-regulated upon release of the suppressing effect by p53.

CHAPTER 4

DISCUSSION

As the fifth most common cancer worldwide and the third leading cause of cancer-related death, hepatocellular carcinoma remains as a big challenge to human beings due to lack of early diagnostic markers and effective therapeutic strategies. High frequency of recurrence for those resectable tumors due to metastasis also contributes to its high fatal rate (Llovet *et al*. 2003), which poses a major question in understanding the mechanisms of hepatocarcinogenesis, especially that of HCC metastasis.

Gene expression profiling study using HCC clinical tumor samples is a logical approach to describe the multiple genetic aberrations and heterogeneous dysregulation of oncogenic pathways in HCC development. From our previously published microarray data, two metastasis-associated genes, Cyr61 and Lasp1 were identified as significant differentially expressed genes in matched HCC tumor and adjacent non-tumor samples (Neo *et al*. 2004). In follow-up studies, we report here that Cyr61 and Lasp1 may play important roles in growth and metastasis of human hepatocellular carcinoma. As a secreted extracellular matrix associated protein, Cyr61 was down-regulated in both HCC clinical tumors and HCC cell lines. Over-expression of Cyr61 suppressed HCC cell proliferation through p53 dependent as well as alternative pathways. Moreover, Cyr61 exerted inhibitory effects in regulating HCC cell migration and invasion by interfering with ECM-integrin signaling pathways. In contrast, the focal adhesion scaffolding protein Lasp1 was found to be up-regulated in HCC. Knockdown of Lasp1 by siRNA significantly inhibited HCC cell growth. Alterations in Lasp1 expression in HCC cells inhibited cell migration and invasion ability, possibly through influencing F-actin dynamics. More interestingly, Lasp1 is transcriptionally suppressed by p53. The current study, therefore, adds information to the existing knowledge on the molecular pathogenesis of HCC and provides support for an as yet poorly understood role of p53 in relation to the cytoskeleton in cancer.

4.1. Cyr61 inhibits the growth and metastasis of HCC

4.1.1. Cyr61 is down-regulated in HCC

As the first identified member of the novel CCN family of growth regulators, Cyr61 has been shown not only to influence a myriad of cellular functions that contribute to many physiological conditions, but also to be actively involved in the pathogenesis of various diseases, especially in the development of tumors from diverse origins (Brigstock 2003; Planque and Perbal 2003; Perbal 2004). Down-regulation of Cyr61 had been observed in prostate cancer (Pilarsky *et al*. 1998), leiomyoma (Sampath *et al*. 2001), non-small cell lung carcinoma (Tong *et al*. 2001), and papillary thyroid carcinoma (Wasenius *et al*. 2003). In the previous cDNA microarray analysis, we revealed that the expression of Cyr61 was down-regulated in HCC tumor tissues compared to matched non-tumor samples (Neo *et al*. 2004). In this current study, down-regulation of Cyr61 was consistently shown to occur in both HCC tumor tissues by real-time quantitative PCR (Figure 3.1) and HCC cell lines by Western blot (Figure 3.3). This was in agreement with at least three previous studies (Xu *et al*. 2001; Chen *et al*. 2002a; Wang *et al*. 2005), but contradicted others which failed to find any difference of Cyr61 expression in HCC (Hirasaki *et al*. 2001) or observed up-regulated Cyr61 in HCC compared to non-tumor tissues (Zeng *et al*. 2004). Wang *et al* (2005) had pointed out that the usage of a non-quantitative gel-based RT-PCR technique may contribute to the negative findings observed by Hirasaki *et al* (2001). Similarly, the Cyr61 expression level was also measured by gel-based RT-PCR by Zeng *et al* (2004), and the data were presented as an average relative yield (mean ± SD) of total 31 HCC tumor tissues against that of 31 non-tumor tissues, but the detailed information of difference between each paired sample was not provided.

It was reported that increased d(CA) microsatellite repeat instability in the Cyr61 promoter may account in part for the down-regulation of Cyr61 in HCC (Wang *et al*. 2005). The author also discussed other possible mechanisms, e.g. differential promoter methylation as the CG-rich Cyr61 promoter contains at least 49 CGs within a region of approximately 1kb. However, the exact mechanism of Cyr61 down-regulation has not been fully characterized so far, which may deserve further analysis. It was also noticed that the level of Cyr61 mRNA expression in normal human fetal liver tissues, which had been known to resemble hepatic neoplasm in many aspects, was extremely low as compared to adult normal liver samples (Figure 3.2). This finding suggests that Cyr61 expression may be under certain extent of suppression in newly regenerating hepatocytes.

4.1.2. Cyr61 may inhibit HCC cell growth, at least in part, through up-regulating p53 and inducing G2/M arrest.

Abnormal expression of Cyr61 has been reported in various cancers. Moreover, the multiple roles of Cyr61 in the progression of a number of tumors have been broadly explored. However, although several previous studies reported the expression of Cyr61 in HCC, the potential roles of Cyr61 in the development of HCC have not been fully understood as yet. In this study, we further investigated the biological functions of Cyr61 in HCC cells and for the first time demonstrated that Cyr61 may function as a tumor suppressor in hepatocellular carcinoma.

Our functional study indicates that down-regulation of Cyr61 in HCC may represent a mechanism by which tumor cells can gain growth advantages. Over-expression of Cyr61 in HCC cells significantly suppressed the cell proliferation rate both in monolayer and the anchorage independent colony formation of HepG2 cells in

soft agar, which is an important indicator of malignant transformation. The anchorage-independent growth ability was also tested using Hep3B cells. However, it is hard to score any difference as they cannot form sufficiently large colonies even after culturing for 3 weeks (data not shown).

As the progression of cell growth is tightly controlled through cell cycle at a series of checkpoints, we performed cell cycle analysis using HepG2-Cyr61 stable cell lines in this study, which usually generate more consistent results by removing the variability of different transient transfection efficiency. The results suggest that Cyr61 may act as a tumor suppressor gene in HCC by inhibiting tumor cell growth through G2/M arrest induction. Interestingly, it had also been reported that Cyr61 suppressed the growth of non-small cell lung cancer cells by inducing G1 arrest, and it inhibited the growth of endometrial cancer cells by promoting apoptosis (Tong *et al*. 2001; Chien *et al*. 2004). Taken together, these observations imply that Cyr61 may function as a tumor suppressor through various mechanisms depending on the tissue of origin and cellular context, most likely by binding to diverse integrin receptors that are differentially expressed on various tumor cells.

In addition, consistent with two early reports on lung cancer study (Tong *et al*. 2001; Tong *et al*. 2004), the p53 and p21 proteins were found being up-regulated in both stably and transiently transfected HepG2 cells with over-expressed Cyr61 in this study. The mRNA level of two G2/M marker gene, 14-3-3σ and GADD45, which are well-characterized p53 downstream targets (Hermeking *et al*. 1997; Wang *et al*. 1999), were also found up-regulated upon Cyr61 over-expression (Figure 3.39). As Tong *et al* suggested that Cyr61 is a tumor suppressor in non-small-cell lung cancer and may suppress the growth of these cells via the β-catenin-c-*myc*-p53 pathway (Tong *et al*. 2004), we propose that the induction of G2/M arrest by Cyr61 in HCC cells might be, at

least in part, mediated through activating p53 and subsequently up-regulating its downstream target genes implicated in G2/M arrest.

However, p53 dependent pathway is by no means the only mechanism which Cyr61 can act upon to interfere with HCC cellular proliferation, since its growth inhibitory effects were similarly observed in both p53 null Hep3B cells and p53 mutated Huh-7 cells (Figure 3.6). This was indirectly supported by a novel finding in this study that endogenous expression of Cyr61 was induced in both p53+/+ HepG2 and p53-/- Hep3B cells in response to genotoxic stress at both transcriptional and protein levels (Figure 3.40). To the best of our knowledge, this is the first description of Cyr61 as a gene involved in DNA damage response upon genotoxic stress, though it is already known as an immediate-early gene induced by a variety of growth factors and other stimuli (O'Brien *et al*. 1990). The question of whether the induction of Cyr61 upon genotoxic stress directly contributes to the activation of p53 in p53+/+ HepG2 (Figure 3.40) or HCT116 cells (Figure 3.41) is at the moment unclear as there are several independent pathways known to activate p53 (Appella and Anderson 2001). We plan to explore the relationship between Cyr61 and these pathways in our future work. Although the molecular mechanism underlying the growth inhibitory effects of Cyr61 in HCC cells is not fully understood yet, the immediate induction of Cyr61 in response to genotoxic stress suggests an influential role of this gene in regulating cellular growth and survival, which may be critical to hepatocarcinogenesis. As a potential tumor suppressor in HCC, Cyr61 may suppress the growth of HCC cells via both p53-dependent and alternative pathways.

Cyr61 is a secreted protein associated with the ECM and cell surfaces to exert diverse biological functions. We have consistently found that Cyr61 is localized at the secretory pathway in HCC cells as illustrated by the cellular localization study of the

GFP fusion proteins under confocal microscope, and the secreted Cyr61 was detected in the culture supernatants of transfected HCC cells (Figure 3.15). These results indicate that Cyr61 is secreted out of the cells where it functions as an extracellular signaling molecule in HCC development.

4.1.3. Cyr61 regulates HCC cell adhesion and mobility through interfering with ECM-Integrin signaling pathways.

In our study, both transient and stable over-expression of Cyr61 in HCC cells efficiently inhibited cell migration and invasion abilities as compared to controls. Enhanced adhesion to ECM proteins observed in Cyr61 over-expressed HCC cells probably in part contributed to their reduced migratory and invasive activities. Adhesion to extracellular matrix molecules through integrin receptors is a fundamental requirement for cell movement. Interestingly, the maximal rate of cell migration occurs at intermediate levels of adhesiveness, which allow traction at the cell front while detaching at the rear, resulting in net forward movement (Ridley *et al*. 2003). Therefore, at high levels of adhesiveness, as occurred in HepG2 and Hep3B cells transfected with Cyr61, cells cannot break contact properly and become less mobile.

Cyr61 may regulate cell adhesion and mobility through interfering with ECM-integrin signaling pathways, which are actively engaged in diverse cellular functions including cell movement (Hood and Cheresh 2002; Carragher and Frame 2004). Cyr61 is a known ligand for several integrins, such as αIIbβ3, αvβ5, αvβ3 and α6β1 (Jedsadayanmata *et al*. 1999; Grzeszkiewicz *et al*. 2001; Grzeszkiewicz *et al*. 2002; Schober *et al*. 2002; Menendez *et al*. 2005), some of which were found up-regulated in hepatocarcinoma cells and involved in hepatocarcinogenesis (Carloni *et al*. 2001; Nejjari *et al*. 2002). It was discovered in the current study that the cell adhesion abilities

to fibronectin and vitronectin respectively in HepG2 and Hep3B cells were most significantly enhanced upon Cyr61 over-expression (Figure 3.12). As both αvβ3 and αIIbβ3 were known as receptors for fibronectin and vitronectin (Stamatoglou and Hughes 1994), and CCN2 was reported to bind directly to fibronectin through the C-terminal heparin binding cystine knot domain (Chen *et al*. 2004; Hoshijima *et al*. 2006; Leask and Abraham 2006), it is highly possible that, analogous to CCN2, Cyr61 can also function as a scaffolding protein to link fibronectin/vitronectin and integrin and strengthen their associations.

Cyr61 may also manipulate ECM-integrin interactions by directly up-regulating the expression of some integrin receptors, including β1, α3, α5 and αvβ3 (Chen *et al*. 2001b; Xie *et al*. 2004; Menendez *et al*. 2005). The fact that the adhesiveness to fibronectin was extremely weak in HepG2 cells may be explained by the finding that the expression of the fibronectin-binding integrin α5β1 in transformed cell lines was often markedly reduced during tumorigenesis. Re-expression of integrin α5β1 in cell lines showed decreased proliferation and loss of the transformed phenotype (Varner *et al*. 1995; Hood and Cheresh 2002). Thus, the cell surface integrin α5β1 may be up-regulated upon over-expression of Cyr61 and lead to prominent enhancement in HCC cell adhesion ability to fibronectin. Similarly in Hep3B cells, the increased adhesion ability to vitronectin upon Cyr61 over-expression may be explained partly by the up-regulation of the major vitronectin receptor–integrin αvβ3, as observed in U343 glioma cells (Xie *et al*. 2004).

Besides its receptor, fibronectin has also been found down-regulated in a variety of tumors and oncogene-transformed cells, and its over-expression resulted in reversion of transformed cells to an untransformed normal morphology (Oliver *et al*., 1983; Akamatsu *et al*., 1996; Brenner *et al*., 2000). Fibronectin is not a passive adhesion

molecule but an active participant in the cell adhesive process that triggers signal transductions, for example, engagement of integrins by fibronectin activated Rho-ROCK signaling and led to focal adhesions and stress fiber formation, which subsequently suppressed cell migration/invasion (Akiyama 1996; Clark *et al*. 1998; Spence *et al*. 2006). It is likely that over-expression of Cyr61 may exert inhibitory signals for HCC cell migration by initially enhancing the ECM-integrin interactions. More comprehensive studies on the interactions between Cyr61, integrins and multiple ECM proteins in HCC cells and downstream signal pathways involved in the processes are under further investigations.

4.1.4. Cyr61 may have disparate roles in HCC itself depending on the differentiation status.

Increasing evidences confirmed that CCN proteins can indeed act either as oncogenes or tumor suppressors, depending upon the type of cancers considered. Divergent pro-proliferative and anti-proliferative effects of Cyr61 were suggested to involve a balance between β-catenin induced stimulation of p53 via c-*myc* and integrin linked kinase (ILK) inhibition of p53 (Brigstock *et al*. 2005). An interesting observation from this study was that, based on Cyr61 protein expression analysis, the current panel of 14 HCC cell lines can be partitioned into 2 distinct groups of expressors and non-expressors (Figure 3.3). It was noticed that the three cell lines (HA22T, Mahlavu and SK-Hep1) which had high expression of Cyr61 are all poorly-differentiated HCC cell lines, whereas almost all Cyr61 negative cell lines are well-differentiated (Lin *et al*. 1998; Seki *et al*. 1999; Hu *et al*. 2003b; Yang *et al*. 2005) . In addition, several studies in the global gene expression profiles of HCC by microarray indicated that HCC can be divided into divergent subtypes (Lee and Thorgeirsson 2002; Lee *et al*. 2006). Hence,

this intriguing finding from our study suggests that Cyr61 may have distinct expression level and elicit disparate biological roles in HCC itself depending on the cellular origin and the differentiation stage. Hence, whether Cyr61 has different functions in a more aggressive HCC cell line such as Sk-Hep1 deserves our further investigations.

In addition, Cyr61 is a well-known angiogenic factor (Lau and Lam 1999). Angiogenesis is an essential step, not only in the growth of primary tumors but also in the formation of metastases (Fidler and Ellis 1994). Angiogenesis facilitates metastasis formation by providing a mechanism to increase the possibility of tumor cells entering the blood circulation and provide nutrients and oxygen for growth at the metastatic site. The establishment of metastatic lesions depends on the activation of multiple angiogenic pathways at both primary and metastatic sites (Takeda *et al*. 2002). HCC is a typical hypervascular tumor, with largely different angiogenesis capacities between different subtypes of HCC (Sakamoto *et al*. 1993; Sun and Tang 2004). As emphasized above, Cyr61 only exists in low-differentiated, highly aggressive HCC cell lines but not in high-differentiated, less aggressive HCC cell lines, indicating that the angiogenic factor Cyr61 may have important role in HCC metastasis at a later stage of liver cancer progression by restoring its expression.

A recent interesting report showed that human Cyr61 is a transcriptional target of TGF-β signaling in cancer cells (Bartholin *et al*. 2007). Therefore, the potential disparate roles of Cyr61 in HCC may also be substantiated by the well-known dual nature of TGF-β as tumor suppressor versus tumor promoter (Bachman and Park 2005). Specifically in hepatocytes, TGF-β was suggested to have a dual role as it induces proliferation arrest but provides a crucial function in promoting late malignant events in collaboration with activated Ha-Ras (Gotzmann *et al*. 2002), which may possibly be

explained by the proposed tumor promoting role of the TGF-β downstream effector Cyr61 in a more malignant HCC.

4.2. Lasp1 promotes the growth and metastasis of HCC

4.2.1. Lasp1 is up-regulated in HCC

As a gene initially identified from a cDNA library of human metastatic lymph node during breast cancer progression, Lasp1 (LIM and SH3 protein) was found to be over-expressed in both breast cancer and ovarian cancer tissues (Tomasetto *et al*. 1995; Grunewald *et al*. 2006; Grunewald *et al*. 2007). However, unlike Cyr61, which were shown to be involved in a wide range of tumors, not much information is known regarding the associations of Lasp1 with cancer. Our study revealed for the first time that Lasp1 was up-regulated in hepatocellular carcinoma. Real-time quantitative PCR confirmed the over-expression of Lasp1 in HCC tumor tissues used in previous cDNA microarray study (Figure 3.16) and the Western blot analysis indicated that Lasp1 had high expression levels in most HCC cell lines tested (Figure 3.18).

4.2.2. Possible mechanisms for Lasp1 up-regulation in HCC

Although the mechanism of up-regulation of Lasp1 in HCC is unclear, the known information on the genetic or epigenetic regulation of Lasp1 provides us with clues in understanding this aspect.

Lasp1 gene was mapped to chromosome 17q12-21, a region including several well-characterized genes involved in breast cancer progression and prognosis, for example, the proto-oncogene c-erbB-2 (Fukushige *et al*. 1986). Interestingly, this region was also reported to be amplified sporadically in HCC tumor and several HCC cell lines, such as Sk-Hep1 and Li7 (Marchio *et al*. 1997; Zondervan *et al*. 2000; Chen *et al*.

2002b; Yasui *et al*. 2002; Okamoto *et al*. 2003). Thus, one possible reason for Lasp1 over-expression in HCC may reside in gene amplification by chromosome gain. However, this may not be the primary consideration as the amplification of c-erbB-2 was reported as an uncommon event in HCC (Prange and Schirmacher 2001; Xian *et al*. 2005).

Lasp1 is a known transcriptional target of the morphogen Sonic Hedgehog (Ingram *et al*. 2002) and IGF-1R pathway (Loughran *et al*. 2005). There is evidence showing the frequent activation of Hedgehog pathway in HCC (Huang *et al*. 2006) and the role of deregulated IGF-1R signaling in hepatocarcinogenesis (Scharf *et al*. 2001; Alexia *et al*. 2004), suggesting that the Sonic Hedgehog pathway and/or IGF-1 signaling may be altered to some degree in HCC leading to the up-regulation of Lasp1. Thus, it would be also interesting for us to investigate whether these deregulated signaling pathways act through Lasp1 to promote hepatocarcinogenesis.

Moreover, the transcriptional repression of Lasp1 by the tumor suppressor p53 demonstrated in this current study may contribute to the explanation of the observed increase of Lasp1 mRNA in HCC as well. As introduced in Chapter 1 that the sequential loss of p53 function through mutation and/or deletion and/or inhibition by virus in hepato-carcinogenesis was frequently detected (Feitelson *et al*. 2002; Thorgeirsson and Grisham 2002; Hussain *et al*. 2007), Lasp1 mRNA may be up-regulated upon release of the suppressing effect by p53 in HCC.

4.2.3. Lasp1 may promote HCC cell growth through multiple pathways associated with cytoskeleton

In the current study, after showing the over-expression of Lasp1 in both HCC clinical tumors and HCC cell lines, we further investigated the functional roles of Lasp1 in growth and metastasis of human HCC. This is the first evidence that besides breast cancer and ovarian cancer, Lasp1 may also be associated with other cancer types, such as liver cancer. A series of functional assays were performed to explore the potential roles of Lasp1 in HCC cell growth. Depletion of Lasp1 by specific siRNA inhibited cell proliferation in monolayer and anchorage-independent growth in soft agar. Whereas, over-expression of Lasp1 in both high and low Lasp1 expressing HCC cell lines significantly enhanced cell proliferation rate. These results suggest that Lasp1 may trigger cellular signaling pathways leading to cell survival, cell proliferation or inhibiting apoptosis.

Although Lasp1 was defined as a focal adhesion adaptor protein, the specific mechanisms are poorly understood (Chew *et al*. 1998; Keicher *et al*. 2004). Lasp1 could interact with several focal adhesion molecules, including the F-actin binding protein zyxin, LPP, VASP and F-actin itself. Several previous studies have reported the potential pathways in which Lasp1 may participate and regulate cancer cell growth and survival. For instance, Lin *et al*. (2004) reported that Lasp1 directly contributed to H_2O_2- and cisplatin-induced apoptosis in a phosphorylation-dependent manner. It was postulated that those apoptotic agents may prevent Lasp1 localization to focal adhesions through phosphorylation of Lasp1 on Tyr-171 by Abl only in apoptotic cells and thus disrupt survival signals from these structures (Lin *et al*. 2004). It was also reported that Lasp1 silencing in breast cancer and ovarian cancer cells led to reduced cell cycle progression and an induced G2/M phase accumulation. This was accompanied by

change of cellular localization of zyxin in these cancer cell lines plus up-regulation or down-regulation of several proteins, such as pyruvate kinase, enolase-1, glucose dehydrogenase, 14-3-3 and heat-shock protein HSP27 in ovarian cancer cells (Grunewald *et al*. 2006; Grunewald *et al*. 2007). It was proposed by Grunewald *et al* (2007) that part of zyxin enters the nucleus, binds to the tumor suppressor h-warts, leads to G2/M cell cycle arrest and inhibits cell proliferation as observed after Lasp1 silencing. Pyruvate kinase, enolase-1 and glucose dehydrogenase are part of the glycolytic metabolism and their regulation correlates well with the cell cycle arrest in G2/M. In addition, over-expression of 14-3-3, which are well-known inhibitors of G2/M progression (Pietromonaco *et al*. 1996; Hermeking *et al*. 1997; Peng *et al*. 1997; Alvarez *et al*. 2002), might also lead to cell cycle arrest in cell culture models (Tzivion *et al*. 2006) and therefore contribute to the observed G2/M arrest in ovarian cancer cells lacking Lasp1.

By considering findings from our current study, it is likely that in HCC cell lines such as HepG2 and Hep3B, Lasp1 siRNA knockdown triggers a similar inhibitory pathway as in ovarian cancer cells. However, in Lasp1 over-expressed HCC cells, where zyxin also shows diffused distribution in the cells (Figure 3.33), the cell proliferation rate is promoted rather than suppressed, which implies that Lasp1 may have important function in regulating HCC cell growth through interfering with multiple cellular pathways triggered by its various binding partners. Our confocal microscopy analysis suggests that Lasp1 may also bind to the integrin associating protein – paxillin, leading to further interactions between Lasp1 and the multiple integrin signaling pathways. In addition to regulating cell adhesion to the ECM, integrins also relay molecular cues regarding the cellular environment that influence cell shape, survival, proliferation, gene transcription and migration. Upon binding to its

ligands, integrins cluster and activate tyrosine protein kinases, such as focal adhesion kinase (FAK), where paxillin supports a platform for it. Activated FAK can trigger signaling pathways, such as Ras-Raf-MEK-MAPK pathway and PI3K-Akt pathway, leading to altered cell proliferation rate and survival (Mitra and Schlaepfer 2006). Thus, Lasp1 may also regulate HCC cell growth through its potential binding partner, paxillin. To demonstrate this hypothesis, the potential direct association between Lasp1 and paxillin, as well as the related downstream pathways deserve our further characterizations.

In conclusion, though the mechanism underlying the Lasp1 regulation on HCC cell growth is largely unexplored, the results from this current study suggest that, similar to the down-regulation of Cyr61 in HCC, up-regulation of Lasp1 also represents a strategy of tumor cells to gain growth advantages. More experimental evidences, such as cell cycle analysis, may facilitate our understanding in the proposed mechanisms discussed above, by which Lasp1 may participate in influencing HCC cell growth.

4.2.4. Lasp1 regulates HCC cell mobility through influencing F-actin dynamics at focal adhesion sites.

Cell migration and the controlled assembly and disassembly of focal adhesions are highly integrated multi-step processes and central features in the molecular pathology of cancer (Ridley *et al*. 2003). Focal adhesion plaque contains diverse molecules such as adapter proteins, protein kinases and proteins that propagate signals arising from the activation of integrins following their engagement with ECM proteins as well as regulate the rate and organization of actin polymerization and focal adhesion turnover in protrusion (Turner 2000b; Grunewald *et al*. 2006). Unlike the secreted extracellular matrix protein Cyr61, which inhibits HCC cell migration and invasion

partly through enhancing the cell adhesion activity to ECM proteins, Lasp1 does not play a role in affecting cell adhesion but exert important functions in influencing F-actin dynamics as a focal adhesion adaptor protein.

In our study, silencing of Lasp1 by siRNA in HCC cell lines inhibited cell migration and invasion ability. Depletion of Lasp1 by siRNA in breast and ovarian cancer cells was reported to change zyxin localization, which was suspected to be the mechanism of Lasp1 siRNA treatment in suppressing the cell migration and invasion ability (Grunewald *et al*. 2006; Grunewald *et al*. 2007). Interestingly, both our analysis and several previous studies showed that further over-expression of Lasp1 in cancer cell lines also inhibited cell migration and invasion activities (Lin *et al*. 2004; Grunewald *et al*. 2006; Grunewald *et al*. 2007). It was discussed by Grunewald *et al* (2006) that the amplification of Lasp1 in cancer cells already overexpressing this scaffolding protein led to disrupted pathways and changes in the cytoskeleton structure that influence cell migration. Nonetheless, how exactly Lasp1 over-expression in cancer cells influences the cytoskeleton dynamics still remains obscure. In the current study, we showed that further over-expression of Lasp1 in HCC cell lines may disrupt the signal pathways leading to F-actin polymerization presumably through affecting the localization of several focal adhesion proteins, including zyxin, VASP and paxillin. All of these three Lasp1 associating proteins are known to influence actin filament dynamics as well as influence multiple signaling pathways (Beckerle 1997; Krause *et al*. 2003; Keicher *et al*. 2004; Spence *et al*. 2006).

As a member belonging to one subfamily of LIM proteins, zyxin is localized primarily at focal adhesion plaques and plays a central role in actin filament polymerization in mammalian cells (Beckerle 1997). Silencing of zyxin in HeLa cells resulted in significantly reduced actin stress fibers (Griffith *et al*. 2005). In genetically

zyxin-deficient fibroblasts, focal adhesions are depleted from Mena and VASP, and cells lacking zyxin display deficits in actin cytoskeleton remodelling (Hoffman *et al*. 2006). From our immuno-fluorescence experiments, we observed a diffused cellular localization of zyxin co-localized with over-expressed GFP-tagged Lasp1 without obvious protein loss as identified by Western blot analysis, indicating the important roles of Lasp1 in binding and recruiting zyxin to focal contacts. The decreased cell motility after Lasp1-GFP over-expression can thus be explained by the sequestration of zyxin by Lasp1, otherwise it acts as a scaffolding protein that facilitates the formation of molecular complexes to promote site-specific actin assembly required for cell movement.

Another interesting finding revealed that HepG2 cells had no detectable zyxin protein by Western blot analysis (Figure 3.36). As described in Chapter 1, zyxin mainly exists in mature focal contact (Mitra *et al*. 2005). However, the question of whether HepG2 cells do not require the formation of mature focal contact where zyxin may play a role when cultured *in vitro*, or there is an intrinsic mechanism to down-regulate zyxin expression in HepG2 cells and in turn inhibit the formation of more mature focal adhesion, is still unclear and needs further characterizations. Our observations showing that Lasp1 did play a role in regulating the migration and invasion ability of HepG2 cells, indicate that Lasp1-mediated localization of zyxin may not be a mere or indispensable function in which Lasp1 may participate.

As a member of a zyxin-related subfamily of LIM domain containing proteins, paxillin is also localized primarily at focal adhesion plaques. Despite being relatively small (599 amino acids), paxillin contains many protein-binding modules that allow it to become one of the prototypical adaptor proteins involved in integrin signaling by recruiting many signaling proteins to the plasma membrane (Turner 2000a). It provides

a platform for FAK, which is also known to activate Rho-family of GTPases (RhoA/Rac/Cdc42) directing local actin assembly into stress fibers, lamellipodia or filopodia and thus regulates cell migration (Mitra *et al*. 2005). Besides those protein kinases, paxillin has been demonstrated to interact with many proteins that are implicated in effecting changes in organization of the actin cytoskeleton, which are necessary for cell motility associated with embryonic development, wound repair and tumor metastasis, as reviewed by Turner (2000b). In this current study, Lasp1 was for the first time shown to be co-localized with paxillin and able to change its localization most probably due to a direct or indirect binding. As paxillin is a multi-functional adaptor protein which could integrate signaling of cell growth and mobility, this suggests potential novel cellular functions of Lasp1.

Ena/VASP proteins are a conserved family of actin regulatory proteins. One potential link between VASP proteins and actin dynamics involves their ability to bind to the actin monomer-binding protein profilin. Profilin promotes the formation of ATP-actin, and actin monomers bound to profilin can be added to the free barbed-ends, but not pointed-ends of the actin filaments. Ena/VASP proteins function to recruit profilin-actin complexes to sites of actin assembly, promote actin filament nucleation, bundling and elongation by antagonizing the activity of capping proteins (Kwiatkowski *et al*. 2003). Recruitment of Ena/VASP proteins to mitochondria or to the surface of Listeria that cannot activate Arp2/3 causes no detectable F-actin assembly (Bear *et al*. 2000; Skoble *et al*. 2000). All the above evidences may provide a sound explanation for the observation from our immunofluorescence study that the sequestration of zyxin, paxillin and VASP by over-expressed Lasp1-GFP is concomitant with less F-actin bundles formed in Hep3B and Huh-7 cells.

Upon over-expression of Lasp1, HCC cells shows decreased cell invasion ability, which is also substantiated by the morphology change from elongated shape with pseudopodia/lamellipodia (mesenchymal-like) to oval shape (epithelial-like). The formation and elongation of pseudopodia/lamellipodia structure are critical for cell migration and invasion process. Lasp1, as well as its co-localized binding partner Krp1, were reported to have a role in elongation of pseudopodia structures which are required for v-Fos-transformed rat fibroblast (FBR) cells to invade (Spence *et al*. 2006). Thus, the inhibited formation of F-actin stress fibers and changed cell morphology in Lasp1-GFP over-expressed HCC cell lines may partly represent a reversion of the pathway model similar to that of the transformation of 208F fibroblast cells to FBR cells by v-fos as proposed by Spence *et al* (2006). In this new model, further over-expression of Lasp1 in HCC cells somehow disrupted the interaction of Lasp1 with Krp1 and in turn inhibited the formation of focal adhesion and elongation of stress fibers that would otherwise support cell invasion.

The confocal microscopic analysis from both previous reports on Lasp1 depletion and our current study on Lasp1 over-expression suggests that Lasp1 function within a certain optimal concentration. There is possibly an intrinsic regulation system in maintaining Lasp1 expression to this optimal saturated level, upon which either increasing or decreasing it will reduce the cell mobility and inhibit cancer metastasis. Through this mechanism, tumors may acquire a maximal metastatic potential.

4.3. The tumor suppressor p53 may inhibit tumor metastasis via novel mechanism in negatively regulating metastasis-promoting genes

A legion of p53-responsive genes and genome-wide p53 binding sites has been identified by various means, including differential display, SAGE, microarray and the more recent ChIP-PET strategy. For example, in the recent genome-wide ChIP-PET study that we referred to (Wei *et al*. 2006), at least 542 binding loci of p53 with high confidence and 98 previously unidentified p53 target genes were discovered. However, whether all of these will prove to be *bona fide* target genes of p53 is unknown, and, to some extent, the criteria that we used to apply to verify the authenticity of a direct p53-target gene themselves are not sufficiently reliable. We now realize that identification of p53-binding sites within gene promoter sequences might not reflect p53 responsiveness, and the p53 responsiveness might be mediated by sequences other than the defined p53-binding sites. Therefore, it is valuable to identify and validate biologically important genes transcriptionally regulated by p53 through multiple methodologies, which can help us to understand p53 gene regulatory network. On the other hand, elucidating the roles of those characterized p53 target genes with previously unknown functions is also fascinating as it confers p53 with novel biological significance.

4.3.1. Role of p53 in transcriptionally suppressing gene expression

There is now compelling evidence that the transcriptional activity of tumor suppressor p53 is required for its growth suppressing and tumor suppressing activities. Most of these studies have focused on the trans-activation function of p53 because of the strong association between trans-activation and tumor suppression. However, p53 is known to be able to repress transcription from various viral and cellular promoters (Ginsberg *et al*. 1991; Kley *et al*. 1992; Seto *et al*. 1992; Jackson *et al*. 1993; Mack *et al*.

1993). Emerging evidences suggest that the transcriptional repression by p53 also plays important roles for its ability to promote apoptosis. Examples including Bcl-2, *survivin*, MAP4, PIK3CA, which are transcriptionally repressed by p53, were shown to inhibit p53-dependent apoptosis (Wang *et al*. 1993; Chiou *et al*. 1994; Murphy *et al*. 1996; Hoffman *et al*. 2002; Mirza *et al*. 2002; Singh *et al*. 2002). However, the underlying mechanisms and the functional consequence of this suppression are largely unexplored. Thus, by showing that p53 is able to transcriptionally suppress the expression of Lasp1, our study adds critical information to the existing pool of p53 negatively regulated genes as well as expands the roles of p53 via its transcriptional repression function.

4.3.2. Role of p53 in regulating cytoskeleton and tumor metastasis

Recently, increasing lines of evidences suggest that p53 also functions in regulating cell migration, invasion, and cancer metastasis through targeting genes functionally linked to cytoskeletons. As mentioned earlier, several tumor metastasis suppressor genes, such as Maspin, KAI1/CD82 have been demonstrated to be *bona fide* p53 targets which can be transcriptionally activated by p53 (Mashimo *et al*. 1998; Zou *et al*. 2000; Liu and Zhang 2006). These findings underscore the role of p53 in the negative regulation of cell invasion and metastasis. The emerging p53 function may provide a mechanistic explanation for the increased metastatic susceptibility of tumors harboring p53 mutations. From this point of view, our finding that p53 transcriptionally represses a novel metastasis-related protein Lasp1 has great significance as it not only strengthens the association of p53 with cytoskeleton but also propose a hypothesis to the mechanisms of the p53-mediated suppression of tumor metastasis, that is, p53 inhibits hepatocarcinogenesis and liver cancer metastasis by transcriptionally suppress the expression of metastasis promoting genes, such as Lasp1.

4.3.3. p53 may repress gene expression through direct binding to a p53 response element

Besides directly binding to specific DNA sequences, the transcription factor p53 is also shown to interact with co-activators or co-repressors under various conditions. A number of studies have investigated the mechanism of p53-mediated repression and found that although the wild-type p53 almost always up-regulates the expression of genes containing a p53-binding site, it tends to down-regulate expression of a myriad of genes without the classical p53 binding motif, such as c-fos, c-jun, Rb, Bcl-2 and hsc70 (Donehower and Bradley 1993; Jackson *et al*. 1993; Zambetti and Levine 1993; Miyashita *et al*. 1994), where p53 exerts its function by engaging in complexes with other proteins (Espinosa and Emerson 2001) or by acting as a transcriptional co-activator or co-repressor (Levine 1997). For instance, p53 represses the AFP gene by inhibiting the promoter binding of hepatic nuclear factor 3 (HNF-3), a transcription factor that activates AFP transcription (Lee *et al*. 2006).

Alternatively, a model in which the existence of a p53-binding motif in the promoter of some genes is indispensable for the p53-mediated transcriptional repression of these particular genes was also established, as exemplified by one study indicating that a p53 binding site at the *survivin* promoter is required for its transcriptional repression by p53 (Hoffman *et al*. 2002). At the end of this study, the p53 response element in Lasp1 promoter was confirmed by luciferase assay using truncated constructs (Figure 3.53), indicating that p53 inhibits Lasp1 transcription by a direct binding to this binding site though it violate the rule of the strict p53 concensus binding sequence defined by el-Deiry *et al* (1992). However, it complies well with the experimentally verified model of p53 binding motif (Figure 4.1) as suggested by a recent comprehensive study of p53 response element sequence (Ma *et al*. 2007). Further

confirmation experiments, such as luciferase assay using construct with internal deletion of the predicted binding site only and gel shift assay, are required to be performed in the future.

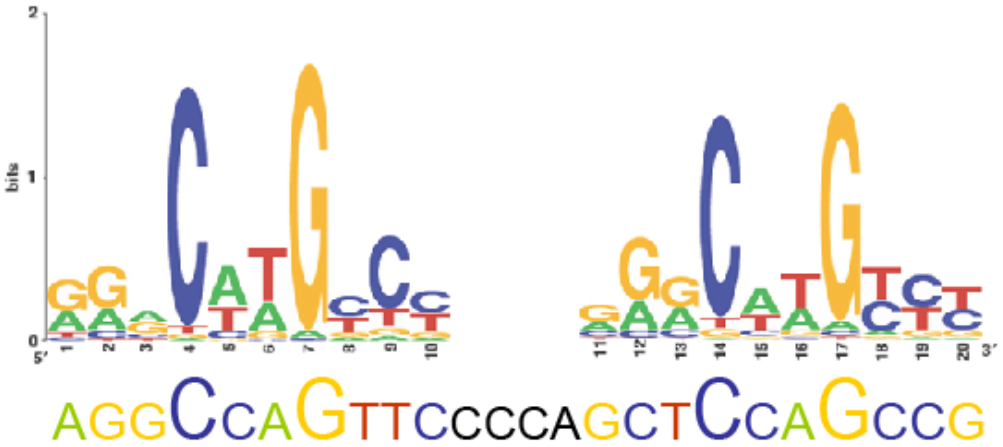

Figure 4.1 Comparison of the identified p53 response element in Lasp1 promoter with a pooled representation of p53 binding consensus sequences. The p53 logo compiled from 100 experimentally verified p53 response elements defined by Ma et al. (2007) is shown in the top panel, while the identified p53 response element in Lasp1 promoter (-59bp to -36bp) is shown in the bottom panel. A (Green), T (Red), G (Yellow), C (Blue), 4-nulceotide spacer (Black).

4.4. Build a comprehensive signaling pathway in HCC involving Cyr61 and Lasp1

Focal adhesion plaques form a structural link between the ECM and the actin cytoskeleton, and are also the important sites of signal transduction. The trans-membrane molecules of the integrin superfamily are the primary proteins at focal adhesion plaques and function to integrate the extracellular matrix into the actin filaments. This connection also requires many actin-attachment proteins and other cytoplasmic adhesion proteins. Thus, proteins at focal contacts form multiple interactions and signal transduction pathways, which not only influence cell adhesion, spreading, and migration, but also convey signals into the nucleus to regulate gene transcription, cell proliferation, differentiation and apoptosis (Wang and Gilmore 2003).

Both Cyr61 and Lasp1 studied in this work are proteins located at the focal adhesion pathway and play active roles in the formation of focal adhesion and trigger pathways into the cell interior, integrating multiple functions in cell proliferation, adhesion, migration and invasion in HCC cell lines. From this view of whole cell signaling transduction networks, the pathways in which Cyr61 or Lasp1 are involved in HCC cells in one way or another connected together or have crosstalk with each other. A diagram illustrating an overview for the regulation and consequences of these cellular pathways involving Cyr61 and Lasp1 in HCC cells is presented in Figure 4.2.

In this figure of overview, the tumor suppressor p53 is a central master protein in linking Cyr61 and Lasp1 in HCC cells. Cyr61 could up-regulate p53 expression in p53 positive HepG2 cells and cause G2/M arrest most probably due to the effect of p53. Coincidently, Lasp1 was identified as a novel p53 target gene which could be transcriptionally suppressed by p53. Hence, in HCC cells carrying wild-type p53, given that other unclear contributing molecules are functional, Cyr61 should be able to down-

regulate Lasp1 through up-regulating p53 level. The pathway could be sketched as Cyr61→p53┤Lasp1. It is known that only Huh-1, Huh-6, HepG2 and Sk-Hep1 cells harbor wild-type p53 among 14 HCC cell lines used in this current study (Cagatay and Ozturk 2002). However, as the mutant p53 known to be carried by the rest cell lines except Hep3B (p53 null) may still be partially functional, whether the observed inverse correlation of the Cyr61 and Lasp1 expression in most HCC cell lines relates to the p53 status needs our further characterizations. Taken together, this finding strengthens the point that Cyr61 may function as a tumor suppressor in liver cancer metastasis by inhibiting cell migration and invasion ability partly through down-regulating the expression level of Lasp1, which has high potential in causing metastasis of HCC.

Both Cyr61 and Lasp1 are functionally linked to integrins in HCC. Cyr61 is a well-known ligand to several types of integrins. Inhibition of cell migration and invasion by over-expression of Cyr61 in HCC cells may be due to the enhanced cell adhesion to ECM mediated by Cyr61-integrin interactions, which in turn trigger multiple pathways in regulating actin cytoskeleton dynamics leading to modified cell migration and invasion activities. Lasp1, on the other hand, functions as an F-actin binding adaptor protein. It may also associate with integrin through its various direct or indirect binding partners. Thus we may conclude that Lasp1 is perhaps located at one or more of Cyr61-integrin triggered focal adhesion associated pathways or pathways which crosstalk or converge with Cyr61 downstream signaling.

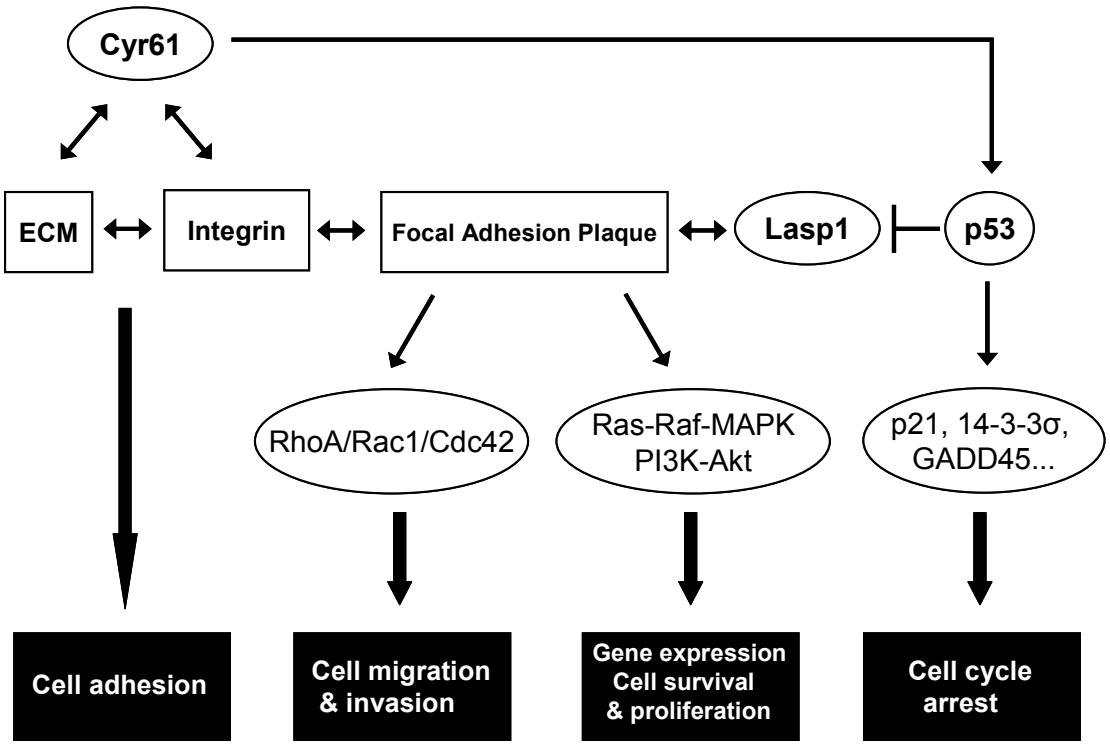

Figure 4.2 Cyr61 and Lasp1 integrate signals to influence various cellular functions in HCC cells. Cyr61 up-regulates p53, which induces cell cycle arrest through activating the expression of its well-characterized downstream target genes (p21, 14-3-3σ, GADD45…) as well as regulates cell migration and invasion via repressing the expression of the newly-identified target gene Lasp1. Cyr61 interacts with extracellular matrix (ECM) and various integrins, strengthening the cell adhesion ability to ECM and in turn regulating cell migration and invasion ability. On the other hand, Lasp1 indirectly associate with integrin through its multiple binding partners localized at focal adhesion plaque. These interactions regulate focal adhesion mediated pathways, e.g. the RhoA/Rac1/Cdc42 pathway to influence cell migration/invasion, the Ras-Raf-MAPK or PI3K-Akt pathway to influence gene expression, cell survival and cell proliferation.

4.5. Significance of the study in HCC

4.5.1. Cyr61 may be used as a diagnostic and prognostic marker for HCC

As the mortality rate of HCC ranks high among all malignancies due to high rate of recurrence or metastasis even after curative resection, the early diagnosis of HCC is of the utmost importance. Since its discovery, the serum AFP remains as the most widely used tumor marker in detecting patients with hepatocellular carcinoma, and has been proven to have capability of prefiguring the prognosis. Nonetheless, some reports have indicated that it has a limited utility in both efficiently and specifically diagnosing HCC for its high false-positive and false-negative rates, for example, markedly increased AFP levels are also detected in patients with acute exacerbation of viral hepatitis but without HCC (Soresi *et al*. 2003; Bae *et al*. 2005). Therefore, there is urgent need to identify new early markers for HCC as a valuable supplement or even substitute for the serum AFP.

As we discussed earlier, the current panel of 14 HCC cell lines can be partitioned into 2 distinct groups of expressors and non-expressors. Interestingly, there is a remarkable inverse correlation with α-fetoprotein (AFP) expression patterns reported by Lee and Thorgeirsson (2002) i.e. Cyr61 negative cell lines (e.g. HepG2, Hep3B, Huh-7) correspond to the high AFP group defined by Lee and Thorgeirsson, while the Cyr61 expressing lines (e.g. SNU449, Sk-Hep1) are within the second subgroup cluster which are AFP negative. Furthermore, in both normal fetal liver and adult liver tissues (Figure 3.2), Cyr61 expression also had an inverse relationship with that of AFP, which is well-known as being primarily produced by the fetal liver and detected in the serum of about 50-70% of HCC patients (Lee and Thorgeirsson 2002). These intriguing findings suggest that Cyr61 may have distinct expression level in HCC

depending on differentiation stage and may be used as a novel potential diagnostic marker for AFP negative liver tumors.

In a recent study, a strong correlation of the expression of Cyr61 with the clinical features of lung cancer has been disclosed. More interestingly, levels of Cyr61 are tightly related to pivotal clinical and prognostic features of non-small-cell lung cancer (NSCLC), as the patients with high-expression of Cyr61 showed a significantly extended mean survival time in comparison with other patients with low level of Cyr61 (Chen *et al*. 2007). This finding also substantiates the earlier conclusion drawn by the same research group that Cyr61 is a tumor suppressor in NSCLC (Tong *et al*. 2001). As our current study applied in HCC shows similar results of down-regulated Cyr61 expression and pathway involving up-regulation of p53 as in NSCLC, it is conceivable that Cyr61 may be used as a novel biomarker for the clinical features and prognosis of HCC patients as well.

4.5.2. Lasp1 may be used as a metastasis and prognostic marker for HCC

The ability to predict HCC patients at higher risk of recurrence or tumor metastasis with a poor prognosis would help to guide surgical and chemotherapeutic treatment according to individual risks. Attempts have been made to define a multitude of metastasis and prognostic markers for HCC patients with potential clinical significance, such as PTEN, p16, p27, MMP-2, serum VEGF, and osteopontin (Honda *et al*. 1998; Ito *et al*. 1999; Sugo *et al*. 1999; Niu *et al*. 2000; Hu *et al*. 2003a; Matsuda *et al*. 2003; Pan *et al*. 2003; Cui *et al*. 2004). Nevertheless, the conclusions from these independent studies are often conflicting due to differing methodologies applied in these studies (Mann *et al*. 2007). Even though many prognostic markers for HCC have been put forward, the well-characterized candidates for HCC prognosis and the

underlying mechanisms still remain rather limited. Thus, it is of great importance and necessity to validate these potential markers in large cohorts of patients, as well as to identify novel metastatic and prognostic markers for HCC.

A large number of studies have examined the prognostic role of p53 in HCC. Among them, several analyses showed that p53 mutation is associated with shorter interval of recurrence or decreased overall survival (Hayashi *et al*. 1995; Honda *et al*. 1998; Sugo *et al*. 1999; Park *et al*. 2001). In our study, Lasp1 is shown to have an important role in inhibiting the migration and invasion ability of HCC cells. In addition, by considering its previously characterized role in metastatic breast cancer and ovarian cancer, as well as the novel findings from the current study that Lasp1 is a p53 target which could be suppressed by p53, it is reasonable to propose that Lasp1 may be a novel metastatic and prognostic marker for HCC or even possibly for other tumors as it is localized at the crossroads of p53 regulated pathway network and the focal adhesion signaling in controlling cell motility.

4.5.3. Cyr61 and Lasp1 may be used as potential therapeutic targets for HCC

Curative treatments for HCC such as resection, liver transplantation and percutaneous ablations induce clinical remissions in a high proportion of patients and are expected to improve the overall survival. However, these treatments can only be applied to a small portion of HCC patients excluding cases such as cirrhotic tumors or big multi-nodules. Besides curative therapy, palliative treatments like embolisation or chemoembolisation, arterial or systemic chemotherapy, radiation, and immunotherapy, in some cases, can obtain good response and even improve survival of patients (Llovet *et al*. 2003). Despite the many treatment options, the prognosis of HCC remains dismal. A majority (70-85%) of patients with advanced or unresectable disease is excluded

from curative treatments. Even for those patients who undergo resection, the recurrence rates can be as high as 50% at 2 years (Yamamoto *et al*. 1996; Poon *et al*. 1999). Hence, prevention of metastatic recurrence after HCC resection is one of the major goals for the further improvement of prognosis of HCC patients.

Identification of key molecular targets and pathways involved in hepatocarcinogenesis has significant therapeutic implications. In this current study, both Cyr61 and Lasp1 were demonstrated to play important roles in regulating the growth and metastasis of HCC based on *in vitro* assays, though the roles of Cyr61 and Lasp1 in HCC will need to be strengthened by conducting *in vivo* study in the future. Cyr61 acts as a potential tumor suppressor in HCC in inhibiting cell proliferation, migration and invasion. Cyr61 is a protein secreted to ECM where it interacts with its binding partners and triggers multiple signaling pathways to regulate cell growth and motility. Neutralizing antibodies and purified recombinant proteins are often applied in biomedical research to abrogate or restore the functions of some membrane and extracellular proteins, as exemplified by an early study on Cyr61 in which recombinant Cyr61 protein produced in the baculovirus expression system was proven to be able to regulate cell proliferation, migration, and adhesion in NIH 3T3 cells and HUVECs (Kireeva *et al*. 1996). The identification of the roles of Cyr61 in HCC from this current study and the functionality of recombinant Cyr61 proteins provide a theoretical basis for its potential application as a therapeutic target. On the other hand, Lasp1 seems to play an important role in controlling the metastatic potential of HCC as well. As suggested by our study, it is critical for the HCC cells to maintain an optimal cellular level of Lasp1 to acquire their maximal potential of movement. Therefore, Lasp1 may also be an interesting therapeutic target for controlling HCC metastasis. In general, the

emergence of these well-characterized molecular targets provides the rationale and opportunity for novel therapeutic strategies which will be applied in HCC.

4.6. Conclusions

Hepatocellular carcinoma (HCC) is one of the most deadly cancers with poor prognosis associated with tumor invasion and metastasis. In this current study, we report that two metastasis related genes – Cyr61 and Lasp1, may play important roles in growth and metastasis of human HCC. This is the first time that abnormal expression of Lasp1 in HCC is demonstrated and its role in growth and metastasis is revealed. In addition, by demonstrating Lasp1 as a *bona fide* p53 target, this study provides new insights into the role that p53 may play in tumor metastasis. The above characterization of the roles of Cyr61 and Lasp1 in HCC will shed more light on the complex mechanisms underlying the tumorigenesis of HCC as well as suggest two interesting genes which are potential therapeutic targets and/or diagnostic markers to control the progression and the metastatic potential of human HCC.

CHAPTER 5

REFERENCES

(1997) Hepatitis C: global prevalence. Wkly Epidemiol Rec 72:341-344

Aguilar F, Hussain SP, Cerutti P (1993) Aflatoxin B1 induces the transversion of G-->T in codon 249 of the p53 tumor suppressor gene in human hepatocytes. Proc Natl Acad Sci U S A 90:8586-8590

Akiyama SK (1996) Integrins in cell adhesion and signaling. Hum Cell 9:181-186

Alexia C, Fallot G, Lasfer M, Schweizer-Groyer G, Groyer A (2004) An evaluation of the role of insulin-like growth factors (IGF) and of type-I IGF receptor signalling in hepatocarcinogenesis and in the resistance of hepatocarcinoma cells against drug-induced apoptosis. Biochem Pharmacol 68:1003-1015

Alvarez D, Novac O, Callejo M, Ruiz MT, Price GB, Zannis-Hadjopoulos M (2002) 14-3-3sigma is a cruciform DNA binding protein and associates in vivo with origins of DNA replication. J Cell Biochem 87:194-207

Amundson SA, Myers TG, Fornace AJ, Jr. (1998) Roles for p53 in growth arrest and apoptosis: putting on the brakes after genotoxic stress. Oncogene 17:3287-3299

Anthony P. (2002) in Pathology of the Liver, edited by MacSween R, Burt A, Portmann B, Ishak K, Scheuer P, Anthony P. (Churchill Livingstone, London, New York, Sydney, Toronto), 711 – 775.

Appella E, Anderson CW (2001) Post-translational modifications and activation of p53 by genotoxic stresses. Eur J Biochem 268:2764-2772

Arber S, Caroni P (1996) Specificity of single LIM motifs in targeting and LIM/LIM interactions in situ. Genes Dev 10:289-300

Aron M, Nair M, Hemal AK (2004) Renal metastasis from primary hepatocellular carcinoma. A case report and review of the literature. Urol Int 73:89-91

Attallah AM, Tabll AA, Salem SF, El-Sadany M, Ibrahim TA, Osman S, El-Dosoky IM (1999) DNA ploidy of liver biopsies from patients with liver cirrhosis and hepatocellular carcinoma: a flow cytometric analysis. Cancer Lett 142:65-69

Babic AM, Kireeva ML, Kolesnikova TV, Lau LF (1998) CYR61, a product of a growth factor-inducible immediate early gene, promotes angiogenesis and tumor growth. Proc Natl Acad Sci U S A 95:6355-6360

Bachman KE, Park BH (2005) Duel nature of TGF-beta signaling: tumor suppressor vs. tumor promoter. Curr Opin Oncol 17:49-54

Bae JS, Park SJ, Park KB, Paik SY, Ryu JK, Choi CK, Hwang TJ (2005) Acute exacerbation of hepatitis in liver cirrhosis with very high levels of alpha-fetoprotein but no occurrence of hepatocellular carcinoma. Korean J Intern Med 20:80-85

Baker SJ, Fearon ER, Nigro JM, Hamilton SR, Preisinger AC, Jessup JM, vanTuinen P, Ledbetter DH, Barker DF, Nakamura Y, White R, Vogelstein B (1989) Chromosome 17 deletions and p53 gene mutations in colorectal carcinomas. Science 244:217-221

Baker SJ, Markowitz S, Fearon ER, Willson JK, Vogelstein B (1990) Suppression of human colorectal carcinoma cell growth by wild-type p53. Science 249:912-915

Bartholin L, Wessner LL, Chirgwin JM, Guise TA (2007) The human Cyr61 gene is a transcriptional target of transforming growth factor beta in cancer cells. Cancer Lett 246:230-236

Bear JE, Loureiro JJ, Libova I, Fassler R, Wehland J, Gertler FB (2000) Negative regulation of fibroblast motility by Ena/VASP proteins. Cell 101:717-728

Beckerle MC (1997) Zyxin: zinc fingers at sites of cell adhesion. Bioessays 19:949-957

Benn J, Schneider RJ (1994) Hepatitis B virus HBx protein activates Ras-GTP complex formation and establishes a Ras, Raf, MAP kinase signaling cascade. Proc Natl Acad Sci U S A 91:10350-10354

Biden K, Young J, Buttenshaw R, Searle J, Cooksley G, Xu DB, Leggett B (1997) Frequency of mutation and deletion of the tumor suppressor gene CDKN2A (MTS1/p16) in hepatocellular carcinoma from an Australian population. Hepatology 25:593-597

Bishop AL, Hall A (2000) Rho GTPases and their effector proteins. Biochem J 348:241–255

Bissell MJ, Radisky D (2001) Putting tumours in context. Nat Rev Cancer 1:46-54

Boige V, Laurent-Puig P, Fouchet P, Flejou JF, Monges G, Bedossa P, Bioulac-Sage P, Capron F, Schmitz A, Olschwang S, Thomas G (1997) Concerted nonsyntenic allelic losses in hyperploid hepatocellular carcinoma as determined by a high-resolution allelotype. Cancer Res 57:1986-1990

Bork P (1993) The modular architecture of a new family of growth regulators related to connective tissue growth factor. FEBS Lett 327:125-130

Bosch FX, Ribes J, Borras J (1999) Epidemiology of primary liver cancer. Semin Liver Dis 19:271-285

Bouvet M, Ellis LM, Nishizaki M, Fujiwara T, Liu W, Bucana CD, Fang B, Lee JJ, Roth JA (1998) Adenovirus-mediated wild-type p53 gene transfer down-regulates vascular endothelial growth factor expression and inhibits angiogenesis in human colon cancer. Cancer Res 58:2288-2292

Bowen DG, Walker CM (2005) Adaptive immune responses in acute and chronic hepatitis C virus infection. Nature 436:946-952

Bressac B, Kew M, Wands J, Ozturk M (1991) Selective G to T mutations of p53 gene in hepatocellular carcinoma from southern Africa. Nature 350:429-431

Brigstock DR, Steffen CL, Kim GY, Vegunta RK, Diehl JR, Harding PA (1997) Purification and characterization of novel heparin-binding growth factors in uterine secretory fluids. Identification as heparin-regulated Mr 10,000 forms of connective tissue growth factor. J Biol Chem 272:20275-20282

Brigstock DR (1999) The connective tissue growth factor/cysteine-rich 61/nephroblastoma overexpressed (CCN) family. Endocr Rev 20:189-206

Brigstock DR (2003) The CCN family: a new stimulus package. J Endocrinol 178:169-175

Brigstock D, Lau L, Perbal B (2005) Report and abstracts of the 3rd International Workshop on the CCN Family of Genes. St Malo, France, 20-23 October 2004. J Clin Pathol 58:463-478

Burridge K, Fath K (1989) Focal contacts: transmembrane links between the extracellular matrix and the cytoskeleton. Bioessays 10:104-108

Butt E, Gambaryan S, Gottfert N, Galler A, Marcus K, Meyer HE (2003) Actin binding of human LIM and SH3 protein is regulated by cGMP- and cAMP-dependent protein kinase phosphorylation on serine 146. J Biol Chem 278:15601-15607

Cagatay T, Ozturk M (2002) p53 mutation as a source of aberrant β-catenin accumulation in cancer cells.

Calderwood DA, Ginsberg MH (2003) Talin forges the links between integrins and actin. Nat Cell Biol 5:694-697

Calvisi DF, Factor VM, Loi R, Thorgeirsson SS (2001) Activation of beta-catenin during hepatocarcinogenesis in transgenic mouse models: relationship to phenotype and tumor grade. Cancer Res 61:2085-2091

Campbell JS, Hughes SD, Gilbertson DG, Palmer TE, Holdren MS, Haran AC, Odell MM, Bauer RL, Ren HP, Haugen HS, Yeh MM, Fausto N (2005) Platelet-derived growth factor C induces liver fibrosis, steatosis, and hepatocellular carcinoma. Proc Natl Acad Sci U S A 102:3389-3394

Caput D (1997) [P73: a kin to the p52 tumor suppressor gene]. Bull Cancer 84:1081-1082

Carloni V, Mazzocca A, Pantaleo P, Cordella C, Laffi G, Gentilini P (2001) The integrin, alpha6beta1, is necessary for the matrix-dependent activation of FAK and MAP kinase and the migration of human hepatocarcinoma cells. Hepatology 34:42-49

Carragher NO, Frame MC (2004) Focal adhesion and actin dynamics: a place where kinases and proteases meet to promote invasion. Trends Cell Biol 14:241-249

Cattaruzza M, Lattrich C, Hecker M (2004) Focal adhesion protein zyxin is a mechanosensitive modulator of gene expression in vascular smooth muscle cells. Hypertension 43:726-730

Chang DF, Belaguli NS, Iyer D, Roberts WB, Wu SP, Dong XR, Marx JG, Moore MS, Beckerle MC, Majesky MW, Schwartz RJ (2003) Cysteine-rich LIM-only proteins CRP1 and CRP2 are potent smooth muscle differentiation cofactors. Dev Cell 4:107-118

Chen CC, Chen N, Lau LF (2001a) The angiogenic factors Cyr61 and connective tissue growth factor induce adhesive signaling in primary human skin fibroblasts. J Biol Chem 276:10443-10452

Chen CC, Mo FE, Lau LF (2001b) The angiogenic factor Cyr61 activates a genetic program for wound healing in human skin fibroblasts. J Biol Chem 276:47329-47337

Chen HC (2005) Boyden chamber assay. Methods Mol Biol 294:15-22

Chen J, Lin J, Levine AJ (1995) Regulation of transcription functions of the p53 tumor suppressor by the mdm-2 oncogene. Mol Med 1:142-152

Chen N, Chen CC, Lau LF (2000) Adhesion of human skin fibroblasts to Cyr61 is mediated through integrin alpha 6beta 1 and cell surface heparan sulfate proteoglycans. J Biol Chem 275:24953-24961

Chen PP, Li WJ, Wang Y, Zhao S, Li DY, Feng LY, Shi XL, Koeffler HP, Tong XJ, Xie D (2007) Expression of Cyr61, CTGF, and WISP-1 correlates with clinical features of lung cancer. PLoS ONE 2:e534

Chen X, Cheung ST, So S, Fan ST, Barry C, Higgins J, Lai KM, Ji J, Dudoit S, Ng IO, Van De Rijn M, Botstein D, Brown PO (2002a) Gene expression patterns in human liver cancers. Mol Biol Cell 13:1929-1939

Chen Y, Abraham DJ, Shi-Wen X, Pearson JD, Black CM, Lyons KM, Leask A (2004) CCN2 (connective tissue growth factor) promotes fibroblast adhesion to fibronectin. Mol Biol Cell 15:5635-5646

Chen YJ, Chen PJ, Lee MC, Yeh SH, Hsu MT, Lin CH (2002b) Chromosomal analysis of hepatic adenoma and focal nodular hyperplasia by comparative genomic hybridization. Genes Chromosomes Cancer 35:138-143

Cheng GZ, Chan J, Wang Q, Zhang W, Sun CD, Wang LH (2007) Twist transcriptionally up-regulates AKT2 in breast cancer cells leading to increased migration, invasion, and resistance to paclitaxel. Cancer Res 67:1979-1987

Chew CS, Parente JA, Jr., Zhou C, Baranco E, Chen X (1998) Lasp-1 is a regulated phosphoprotein within the cAMP signaling pathway in the gastric parietal cell. Am J Physiol 275:C56-67

Chew CS, Chen X, Parente JA, Jr., Tarrer S, Okamoto C, Qin HY (2002) Lasp-1 binds to non-muscle F-actin in vitro and is localized within multiple sites of dynamic actin assembly in vivo. J Cell Sci 115:4787-4799

Chien W, Kumagai T, Miller CW, Desmond JC, Frank JM, Said JW, Koeffler HP (2004) Cyr61 suppresses growth of human endometrial cancer cells. J Biol Chem 279:53087-53096

Chiou SK, Rao L, White E (1994) Bcl-2 blocks p53-dependent apoptosis. Mol Cell Biol 14:2556-2563

Claassen G, Ke N, Yu D, Chatterton JE, Hu X, Albers A, Nguy V, Chionis J, Truong T, Meyhack B, Wong-Staal F, Li QX (2004) Comprehensive assessment of cell growth properties using an integrated and nonsubjective approach. Preclinica 2: 435-439

Clark EA, King WG, Brugge JS, Symons M, Hynes RO (1998) Integrin-mediated signals regulated by members of the rho family of GTPases. J Cell Biol 142:573-586

Cui J, Dong BW, Liang P, Yu XL, Yu DJ (2004) Effect of c-myc, Ki-67, MMP-2 and VEGF expression on prognosis of hepatocellular carcinoma patients undergoing tumor resection. World J Gastroenterol 10:1533-1536

d'Arville CN, Nouri-Aria KT, Johnson P, Williams R (1991) Regulation of insulin-like growth factor II gene expression by hepatitis B virus in hepatocellular carcinoma. Hepatology 13:310-315

Dameron KM, Volpert OV, Tainsky MA, Bouck N (1994) Control of angiogenesis in fibroblasts by p53 regulation of thrombospondin-1. Science 265:1582-1584

De Souza AT, Hankins GR, Washington MK, Fine RL, Orton TC, Jirtle RL (1995) Frequent loss of heterozygosity on 6q at the mannose 6-phosphate/insulin-like growth factor II receptor locus in human hepatocellular tumors. Oncogene 10:1725-1729

Donehower LA, Bradley A (1993) The tumor suppressor p53. Biochim Biophys Acta 1155:181-205

Dong JT, Lamb PW, Rinker-Schaeffer CW, Vukanovic J, Ichikawa T, Isaacs JT, Barrett JC (1995) KAI1, a metastasis suppressor gene for prostate cancer on human chromosome 11p11.2. Science 268:884-886

Effert PJ, Neubauer A, Walther PJ, Liu ET (1992) Alterations of the P53 gene are associated with the progression of a human prostate carcinoma. J Urol 147:789-793

Egeblad M, Werb Z (2002) New functions for the matrix metalloproteinases in cancer progression. Nat Rev Cancer 2:161-174

Ehler E, Horowits R, Zuppinger C, Price RL, Perriard E, Leu M, Caroni P, Sussman M, Eppenberger HM, Perriard JC (2001) Alterations at the intercalated disk associated with the absence of muscle LIM protein. J Cell Biol 153:763-772

el-Deiry WS, Kern SE, Pietenpol JA, Kinzler KW, Vogelstein B (1992) Definition of a consensus binding site for p53. Nat Genet 1:45-49

El-Serag HB, Mason AC (1999) Rising incidence of hepatocellular carcinoma in the United States. N Engl J Med 340:745-750

Eliyahu D, Raz A, Gruss P, Givol D, Oren M (1984) Participation of p53 cellular tumour antigen in transformation of normal embryonic cells. Nature 312:646-649

Espinosa JM, Emerson BM (2001) Transcriptional regulation by p53 through intrinsic DNA/chromatin binding and site-directed cofactor recruitment. Mol Cell 8:57-69

Farazi PA, DePinho RA (2006) Hepatocellular carcinoma pathogenesis: from genes to environment. Nat Rev Cancer 6:674-687

Feitelson MA, Zhu M, Duan LX, London WT (1993) Hepatitis B x antigen and p53 are associated in vitro and in liver tissues from patients with primary hepatocellular carcinoma. Oncogene 8:1109-1117

Feitelson MA (1999) Hepatitis B virus in hepatocarcinogenesis. J Cell Physiol 181:188-202

Feitelson MA, Sun B, Satiroglu Tufan NL, Liu J, Pan J, Lian Z (2002) Genetic mechanisms of hepatocarcinogenesis. Oncogene 21:2593-2604

Feuerstein R, Wang X, Song D, Cooke NE, Liebhaber SA (1994) The LIM/double zinc-finger motif functions as a protein dimerization domain. Proc Natl Acad Sci U S A 91:10655-10659

Fidler IJ, Ellis LM (1994) The implications of angiogenesis for the biology and therapy of cancer metastasis. Cell 79:185-188

Fields AC, Cotsonis G, Sexton D, Santoianni R, Cohen C (2004) Survivin expression in hepatocellular carcinoma: correlation with proliferation, prognostic parameters, and outcome. Mod Pathol 17:1378-1385

Finlay CA, Hinds PW, Levine AJ (1989) The p53 proto-oncogene can act as a suppressor of transformation. Cell 57:1083-1093

Fontana T, Siciliano M, Franceschelli A, Annicchiarico BE, Rossi P, Bigotti G, Bombardieri G (2004) An atypical bone metastasis of hepatocellular carcinoma: case report and review of the literature. Clin Ter 155:447-451

Forns X, Bukh J, Purcell RH (2002) The challenge of developing a vaccine against hepatitis C virus. J Hepatol 37:684-695

Frazier KS, Grotendorst GR (1997) Expression of connective tissue growth factor mRNA in the fibrous stroma of mammary tumors. Int J Biochem Cell Biol 29:153-161

Fritsche M, Haessler C, Brandner G (1993) Induction of nuclear accumulation of the tumor-suppressor protein p53 by DNA-damaging agents. Oncogene 8:307-318

Fukushige S, Matsubara K, Yoshida M, Sasaki M, Suzuki T, Semba K, Toyoshima K, Yamamoto T (1986) Localization of a novel v-erbB-related gene, c-erbB-2, on human chromosome 17 and its amplification in a gastric cancer cell line. Mol Cell Biol 6:955-958

Ginsberg D, Mechta F, Yaniv M, Oren M (1991) Wild-type p53 can down-modulate the activity of various promoters. Proc Natl Acad Sci U S A 88:9979-9983

Glukhova L, Angevin E, Lavialle C, Cadot B, Terrier-Lacombe MJ, Perbal B, Bernheim A, Goguel AF (2001) Patterns of specific genomic alterations associated with poor prognosis in high-grade renal cell carcinomas. Cancer Genet Cytogenet 130:105-110

Gotzmann J, Huber H, Thallinger C, Wolschek M, Jansen B, Schulte-Hermann R, Beug H, Mikulits W (2002) Hepatocytes convert to a fibroblastoid phenotype through the cooperation of TGF-beta1 and Ha-Ras: steps towards invasiveness. J Cell Sci 115:1189-1202

Gozuacik D, Murakami Y, Saigo K, Chami M, Mugnier C, Lagorce D, Okanoue T, Urashima T, Brechot C, Paterlini-Brechot P (2001) Identification of human cancer-related genes by naturally occurring Hepatitis B Virus DNA tagging. Oncogene 20:6233-6240

Greenblatt MS, Bennett WP, Hollstein M, Harris CC (1994) Mutations in the p53 tumor suppressor gene: clues to cancer etiology and molecular pathogenesis. Cancer Res 54:4855-4878

Griffith E, Coutts AS, Black DM (2005) RNAi knockdown of the focal adhesion protein TES reveals its role in actin stress fibre organisation. Cell Motil Cytoskeleton 60:140-152

Grunewald TG, Kammerer U, Schulze E, Schindler D, Honig A, Zimmer M, Butt E (2006) Silencing of LASP-1 influences zyxin localization, inhibits proliferation and reduces migration in breast cancer cells. Exp Cell Res 312:974-982

Grunewald TG, Kammerer U, Winkler C, Schindler D, Sickmann A, Honig A, Butt E (2007) Overexpression of LASP-1 mediates migration and proliferation of human ovarian cancer cells and influences zyxin localisation. Br J Cancer 96:296-305

Grzeszkiewicz TM, Kirschling DJ, Chen N, Lau LF (2001) CYR61 stimulates human skin fibroblast migration through Integrin alpha vbeta 5 and enhances mitogenesis through integrin alpha vbeta 3, independent of its carboxyl-terminal domain. J Biol Chem 276:21943-21950

Grzeszkiewicz TM, Lindner V, Chen N, Lam SC, Lau LF (2002) The angiogenic factor cysteine-rich 61 (CYR61, CCN1) supports vascular smooth muscle cell adhesion and stimulates chemotaxis through integrin alpha(6)beta(1) and cell surface heparan sulfate proteoglycans. Endocrinology 143:1441-1450

Hanada K, Saito A, Nozawa H, Haruyama K, Hayashi N, Yamada M, Katagiri S, Katsuragawa H, Otsubo T, Takasaki K (2004) Histopathologically-diagnosed splenic metastasis in a hepatocellular carcinoma case with adrenal metastasis. Intern Med 43:484-489

Harlow E, Williamson NM, Ralston R, Helfman DM, Adams TE (1985) Molecular cloning and in vitro expression of a cDNA clone for human cellular tumor antigen p53. Mol Cell Biol 5:1601-1610

Hayashi H, Sugio K, Matsumata T, Adachi E, Takenaka K, Sugimachi K (1995) The clinical significance of p53 gene mutation in hepatocellular carcinomas from Japan. Hepatology 22:1702-1707

Heidenberg HB, Bauer JJ, McLeod DG, Moul JW, Srivastava S (1996) The role of the p53 tumor suppressor gene in prostate cancer: a possible biomarker? Urology 48:971-979

Hellawell GO, Turner GD, Davies DR, Poulsom R, Brewster SF, Macaulay VM (2002) Expression of the type 1 insulin-like growth factor receptor is up-regulated in primary prostate cancer and commonly persists in metastatic disease. Cancer Res 62:2942-2950

Hermeking H, Lengauer C, Polyak K, He TC, Zhang L, Thiagalingam S, Kinzler KW, Vogelstein B (1997) 14-3-3 sigma is a p53-regulated inhibitor of G2/M progression. Mol Cell 1:3-11

Hirasaki S, Koide N, Ujike K, Shinji T, Tsuji T (2001) Expression of Nov, CYR61 and CTGF genes in human hepatocellular carcinoma. Hepatol Res 19:294-305

Irwin MS, Kaelin WG (2001) p53 family update: p73 and p63 develop their own identities. Cell Growth Differ 12:337-349

Ho WC, Fitzgerald MX, Marmorstein R (2006) Structure of the p53 core domain dimer bound to DNA. J Biol Chem 281:20494-20502

Hobert O, Westphal H (2000) Functions of LIM-homeobox genes. Trends Genet 16:75-83

Hoffman LM, Jensen CC, Kloeker S, Wang CL, Yoshigi M, Beckerle MC (2006) Genetic ablation of zyxin causes Mena/VASP mislocalization, increased motility, and deficits in actin remodeling. J Cell Biol 172:771-782

Hoffman WH, Biade S, Zilfou JT, Chen J, Murphy M (2002) Transcriptional repression of the anti-apoptotic survivin gene by wild type p53. J Biol Chem 277:3247-3257

Hojo T, Akiyama Y, Nagasaki K, Maruyama K, Kikuchi K, Ikeda T, Kitajima M, Yamaguchi K (2001) Association of maspin expression with the malignancy grade and tumor vascularization in breast cancer tissues. Cancer Lett 171:103-110

Holloway SE, Beck AW, Girard L, Jaber MR, Barnett CC, Jr., Brekken RA, Fleming JB (2005) Increased expression of Cyr61 (CCN1) identified in peritoneal metastases from human pancreatic cancer. J Am Coll Surg 200:371-377

Hollstein M, Sidransky D, Vogelstein B, Harris CC (1991) p53 mutations in human cancers. Science 253:49-53

Holt GD, Pangburn MK, Ginsburg V (1990) Properdin binds to sulfatide [Gal(3-SO4)beta 1-1 Cer] and has a sequence homology with other proteins that bind sulfated glycoconjugates. J Biol Chem 265:2852-2855

Honda K, Sbisa E, Tullo A, Papeo PA, Saccone C, Poole S, Pignatelli M, Mitry RR, Ding S, Isla A, Davies A, Habib NA (1998) p53 mutation is a poor prognostic indicator for survival in patients with hepatocellular carcinoma undergoing surgical tumour ablation. Br J Cancer 77:776-782

Hood JD, Cheresh DA (2002) Role of integrins in cell invasion and migration. Nat Rev Cancer 2:91-100

Hoshijima M, Hattori T, Inoue M, Araki D, Hanagata H, Miyauchi A, Takigawa M (2006) CT domain of CCN2/CTGF directly interacts with fibronectin and enhances cell adhesion of chondrocytes through integrin alpha5beta1. FEBS Lett 580:1376-1382

Hu TH, Huang CC, Lin PR, Chang HW, Ger LP, Lin YW, Changchien CS, Lee CM, Tai MH (2003a) Expression and prognostic role of tumor suppressor gene PTEN/MMAC1/TEP1 in hepatocellular carcinoma. Cancer 97:1929-1940

Hu TH, Huang CC, Liu LF, Lin PR, Liu SY, Chang HW, Changchien CS, Lee CM, Chuang JH, Tai MH (2003b) Expression of hepatoma-derived growth factor in hepatocellular carcinoma. Cancer 98:1444-1456

Huang GW, Yang LY, Lu WQ (2005) Expression of hypoxia-inducible factor 1alpha and vascular endothelial growth factor in hepatocellular carcinoma: Impact on neovascularization and survival. World J Gastroenterol 11:1705-1708

Huang J, Shen W, Li B, Luo Y, Liao S, Zhang W, Cheng N (2000) [A study on the inactivation of p16 genes and the expression of P16 protein in primary hepatocellular carcinomas]. Hua Xi Yi Ke Da Xue Xue Bao 31:306-309

Huang S, He J, Zhang X, Bian Y, Yang L, Xie G, Zhang K, Tang W, Stelter AA, Wang Q, Zhang H, Xie J (2006) Activation of the hedgehog pathway in human hepatocellular carcinomas. Carcinogenesis 27:1334-1340

Huang SF, Hsu HC, Fletcher JA (1999) Investigation of chromosomal aberrations in hepatocellular carcinoma by fluorescence in situ hybridization. Cancer Genet Cytogenet 111:21-27

Hunter K (2006) Host genetics influence tumour metastasis. Nat Rev Cancer 6:141-146

Huo TI, Wang XW, Forgues M, Wu CG, Spillare EA, Giannini C, Brechot C, Harris CC (2001) Hepatitis B virus X mutants derived from human hepatocellular carcinoma retain the ability to abrogate p53-induced apoptosis. Oncogene 20:3620-3628

Hussain SP, Harris CC (1998) Molecular epidemiology of human cancer: contribution of mutation spectra studies of tumor suppressor genes. Cancer Res 58:4023-4037

Hussain SP, Harris CC (2006) p53 biological network: at the crossroads of the cellular-stress response pathway and molecular carcinogenesis. J Nippon Med Sch 73:54-64

Hussain SP, Schwank J, Staib F, Wang XW, Harris CC (2007) TP53 mutations and hepatocellular carcinoma: insights into the etiology and pathogenesis of liver cancer. Oncogene 26:2166-2176

Igarashi A, Hayashi N, Nashiro K, Takehara K (1998) Differential expression of connective tissue growth factor gene in cutaneous fibrohistiocytic and vascular tumors. J Cutan Pathol 25:143-148

Ingram WJ, Wicking CA, Grimmond SM, Forrest AR, Wainwright BJ (2002) Novel genes regulated by Sonic Hedgehog in pluripotent mesenchymal cells. Oncogene 21:8196-8205

Iso Y, Sawada T, Okada T, Kubota K (2005) Loss of E-cadherin mRNA and gain of osteopontin mRNA are useful markers for detecting early recurrence of HCV-related hepatocellular carcinoma. J Surg Oncol 92:304-311

Ito Y, Matsuura N, Sakon M, Miyoshi E, Noda K, Takeda T, Umeshita K, Nagano H, Nakamori S, Dono K, Tsujimoto M, Nakahara M, Nakao K, Taniguchi N, Monden M (1999) Expression and prognostic roles of the G1-S modulators in hepatocellular carcinoma: p27 independently predicts the recurrence. Hepatology 30:90-99

Ito Y, Takeda T, Sakon M, Tsujimoto M, Higashiyama S, Noda K, Miyoshi E, Monden M, Matsuura N (2001) Expression and clinical significance of erb-B receptor family in hepatocellular carcinoma. Br J Cancer 84:1377-1383

Jackson P, Bos E, Braithwaite AW (1993) Wild-type mouse p53 down-regulates transcription from different virus enhancer/promoters. Oncogene 8:589-597

Jay P, Berge-Lefranc JL, Marsollier C, Mejean C, Taviaux S, Berta P (1997) The human growth factor-inducible immediate early gene, CYR61, maps to chromosome 1p. Oncogene 14:1753-1757

Jedsadayanmata A, Chen CC, Kireeva ML, Lau LF, Lam SC (1999) Activation-dependent adhesion of human platelets to Cyr61 and Fisp12/mouse connective tissue growth factor is mediated through integrin alpha(IIb)beta(3). J Biol Chem 274:24321-24327

Jin JP, Wang K (1991) Cloning, expression, and protein interaction of human nebulin fragments composed of varying numbers of sequence modules. J Biol Chem 266:21215-21223

Jost CA, Marin MC, Kaelin WG, Jr. (1997) p73 is a simian [correction of human] p53-related protein that can induce apoptosis. Nature 389:191-194

Kadrmas JL, Beckerle MC (2004) The LIM domain: from the cytoskeleton to the nucleus. Nat Rev Mol Cell Biol 5:920-931

Kawate S, Fukusato T, Ohwada S, Watanuki A, Morishita Y (1999) Amplification of c-myc in hepatocellular carcinoma: correlation with clinicopathologic features, proliferative activity and p53 overexpression. Oncology 57:157-163

Keicher C, Gambaryan S, Schulze E, Marcus K, Meyer HE, Butt E (2004) Phosphorylation of mouse LASP-1 on threonine 156 by cAMP- and cGMP-dependent protein kinase. Biochem Biophys Res Commun 324:308-316

Kew MC (2002) Epidemiology of hepatocellular carcinoma. Toxicology 181-182:35-38

Kew MC (2003) Synergistic interaction between aflatoxin B1 and hepatitis B virus in hepatocarcinogenesis. Liver Int 23:405-409

Kim SO, Park JG, Lee YI (1996) Increased expression of the insulin-like growth factor I (IGF-I) receptor gene in hepatocellular carcinoma cell lines: implications of IGF-I receptor gene activation by hepatitis B virus X gene product. Cancer Res 56:3831-3836

Kimura H, Kagawa K, Deguchi T, Nakajima T, Kakusui M, Ohkawara T, Katagishi T, Okanoue T, Kashima K, Ashihara T (1996) Cytogenetic analyses of hepatocellular carcinoma by in situ hybridization with a chromosome-specific DNA probe. Cancer 77:271-277

Kireeva ML, Mo FE, Yang GP, Lau LF (1996) Cyr61, a product of a growth factor-inducible immediate-early gene, promotes cell proliferation, migration, and adhesion. Mol Cell Biol 16:1326-1334

Kirk GD, Camus-Randon AM, Mendy M, Goedert JJ, Merle P, Trepo C, Brechot C, Hainaut P, Montesano R (2000) Ser-249 p53 mutations in plasma DNA of patients with hepatocellular carcinoma from The Gambia. J Natl Cancer Inst 92:148-153

Kirk GD, Lesi OA, Mendy M, Szymanska K, Whittle H, Goedert JJ, Hainaut P, Montesano R (2005) 249(ser) TP53 mutation in plasma DNA, hepatitis B viral infection, and risk of hepatocellular carcinoma. Oncogene 24:5858-5867

Kishimoto Y, Shiota G, Wada K, Kitano M, Nakamoto K, Kamisaki Y, Suou T, Itoh T, Kawasaki H (1996) Frequent loss in chromosome 8p loci in liver cirrhosis accompanying hepatocellular carcinoma. J Cancer Res Clin Oncol 122:585-589

Kley N, Chung RY, Fay S, Loeffler JP, Seizinger BR (1992) Repression of the basal c-fos promoter by wild-type p53. Nucleic Acids Res 20:4083-4087

Knuutila S, Aalto Y, Autio K, Bjorkqvist AM, El-Rifai W, Hemmer S, Huhta T, Kettunen E, Kiuru-Kuhlefelt S, Larramendy ML, Lushnikova T, Monni O, Pere H, Tapper J, Tarkkanen M, Varis A, Wasenius VM, Wolf M, Zhu Y (1999) DNA copy number losses in human neoplasms. Am J Pathol 155:683-694

Kolesnikova TV, Lau LF (1998) Human CYR61-mediated enhancement of bFGF-induced DNA synthesis in human umbilical vein endothelial cells. Oncogene 16:747-754

Konishi M, Kikuchi-Yanoshita R, Tanaka K, Sato C, Tsuruta K, Maeda Y, Koike M, Tanaka S, Nakamura Y, Hattori N, *et al*. (1993) Genetic changes and histopathological grades in human hepatocellular carcinomas. Jpn J Cancer Res 84:893-899

Krause M, Dent EW, Bear JE, Loureiro JJ, Gertler FB (2003) Ena/VASP proteins: regulators of the actin cytoskeleton and cell migration. Annu Rev Cell Dev Biol 19:541-564

Kress M, May E, Cassingena R, May P (1979) Simian virus 40-transformed cells express new species of proteins precipitable by anti-simian virus 40 tumor serum. J Virol 31:472-483

Kuroki T, Fujiwara Y, Tsuchiya E, Nakamori S, Imaoka S, Kanematsu T, Nakamura Y (1995) Accumulation of genetic changes during development and progression of hepatocellular carcinoma: loss of heterozygosity of chromosome arm 1p occurs at an early stage of hepatocarcinogenesis. Genes Chromosomes Cancer 13:163-167

Kusano N, Shiraishi K, Kubo K, Oga A, Okita K, Sasaki K (1999) Genetic aberrations detected by comparative genomic hybridization in hepatocellular carcinomas: their relationship to clinicopathological features. Hepatology 29:1858-1862

Kwiatkowski AV, Gertler FB, Loureiro JJ (2003) Function and regulation of Ena/VASP proteins. Trends Cell Biol 13:386-392

Lalikos JF, Sotereanos GC, Nawrocki JS, Tzakis AG (1992) Isolated mandibular metastasis of hepatocellular carcinoma. J Oral Maxillofac Surg 50:754-759

Lane DP, Crawford LV (1979) T antigen is bound to a host protein in SV40-transformed cells. Nature 278:261-263

Lau LF, Nathans D (1985) Identification of a set of genes expressed during the G0/G1 transition of cultured mouse cells. Embo J 4:3145-3151

Lau LF, Lam SC (1999) The CCN family of angiogenic regulators: the integrin connection. Exp Cell Res 248:44-57

Laurent-Puig P, Legoix P, Bluteau O, Belghiti J, Franco D, Binot F, Monges G, Thomas G, Bioulac-Sage P, Zucman-Rossi J (2001) Genetic alterations associated with hepatocellular carcinomas define distinct pathways of hepatocarcinogenesis. Gastroenterology 120:1763-1773

Leask A, Abraham DJ (2006) All in the CCN family: essential matricellular signaling modulators emerge from the bunker. J Cell Sci 119:4803-4810

Lee JS, Thorgeirsson SS (2002) Functional and genomic implications of global gene expression profiles in cell lines from human hepatocellular cancer. Hepatology 35:1134-1143

Lee JS, Heo J, Libbrecht L, Chu IS, Kaposi-Novak P, Calvisi DF, Mikaelyan A, Roberts LR, Demetris AJ, Sun Z, Nevens F, Roskams T, Thorgeirsson SS

(2006) A novel prognostic subtype of human hepatocellular carcinoma derived from hepatic progenitor cells. Nat Med 12:410-416

Lee SG, Rho HM (2000) Transcriptional repression of the human p53 gene by hepatitis B viral X protein. Oncogene 19:468-471

Leu SJ, Lam SC, Lau LF (2002) Pro-angiogenic activities of CYR61 (CCN1) mediated through integrins alphavbeta3 and alpha6beta1 in human umbilical vein endothelial cells. J Biol Chem 277:46248-46255

Levine AJ (1997) p53, the cellular gatekeeper for growth and division. Cell 88:323-331

Li B, Zhuang L, Trueb B (2004) Zyxin interacts with the SH3 domains of the cytoskeletal proteins LIM-nebulette and Lasp-1. J Biol Chem 279:20401-20410

Lin CH, Hsieh SY, Sheen IS, Lee WC, Chen TC, Shyu WC, Liaw YF (2001) Genome-wide hypomethylation in hepatocellular carcinogenesis. Cancer Res 61:4238-4243

Lin LI, Ke YF, Ko YC, Lin JK (1998) Curcumin inhibits SK-Hep-1 hepatocellular carcinoma cell invasion in vitro and suppresses matrix metalloproteinase-9 secretion. Oncology 55:349-353

Lin MT, Zuon CY, Chang CC, Chen ST, Chen CP, Lin BR, Wang MY, Jeng YM, Chang KJ, Lee PH, Chen WJ, Kuo ML (2005) Cyr61 induces gastric cancer cell motility/invasion via activation of the integrin/nuclear factor-kappaB/cyclooxygenase-2 signaling pathway. Clin Cancer Res 11:5809-5820

Lin YH, Park ZY, Lin D, Brahmbhatt AA, Rio MC, Yates JR, 3rd, Klemke RL (2004) Regulation of cell migration and survival by focal adhesion targeting of Lasp-1. J Cell Biol 165:421-432

Linzer DI, Levine AJ (1979) Characterization of a 54K dalton cellular SV40 tumor antigen present in SV40-transformed cells and uninfected embryonal carcinoma cells. Cell 17:43-52

Liu WM, Zhang XA (2006) KAI1/CD82, a tumor metastasis suppressor. Cancer Lett 240:183-194

Llovet JM, Burroughs A, Bruix J (2003) Hepatocellular carcinoma. Lancet 362:1907-1917

Lopez T, Hanahan D (2002) Elevated levels of IGF-1 receptor convey invasive and metastatic capability in a mouse model of pancreatic islet tumorigenesis. Cancer Cell 1:339-353

Loughran G, Huigsloot M, Kiely PA, Smith LM, Floyd S, Ayllon V, O'Connor R (2005) Gene expression profiles in cells transformed by overexpression of the IGF-I receptor. Oncogene 24:6185-6193

Lucito R, Schneider RJ (1992) Hepatitis B virus X protein activates transcription factor NF-kappa B without a requirement for protein kinase C. J Virol 66:983-991

Luo G, Zhang JQ, Nguyen TP, Herrera AH, Paterson B, Horowits R (1997) Complete cDNA sequence and tissue localization of N-RAP, a novel nebulin-related protein of striated muscle. Cell Motil Cytoskeleton 38:75-90

Luo G, Herrera AH, Horowits R (1999) Molecular interactions of N-RAP, a nebulin-related protein of striated muscle myotendon junctions and intercalated disks. Biochemistry 38:6135-6143

Ma B, Pan Y, Zheng J, Levine AJ, Nussinov R (2007) Sequence analysis of p53 response-elements suggests multiple binding modes of the p53 tetramer to DNA targets. Nucleic Acids Res 35:2986-3001

Maass N, Hojo T, Ueding M, Luttges J, Kloppel G, Jonat W, Nagasaki K (2001) Expression of the tumor suppressor gene Maspin in human pancreatic cancers. Clin Cancer Res 7:812-817

Mack DH, Vartikar J, Pipas JM, Laimins LA (1993) Specific repression of TATA-mediated but not initiator-mediated transcription by wild-type p53. Nature 363:281-283

Mackay J, Steel CM, Elder PA, Forrest AP, Evans HJ (1988) Allele loss on short arm of chromosome 17 in breast cancers. Lancet 2:1384-1385

Maillard M, Cadot B, Ball RY, Sethia K, Edwards DR, Perbal B, Tatoud R (2001) Differential expression of the ccn3 (nov) proto-oncogene in human prostate cell lines and tissues. Mol Pathol 54:275-280

Manara MC, Perbal B, Benini S, Strammiello R, Cerisano V, Perdichizzi S, Serra M, Astolfi A, Bertoni F, Alami J, Yeger H, Picci P, Scotlandi K (2002) The expression of ccn3(nov) gene in musculoskeletal tumors. Am J Pathol 160:849-859

Mann CD, Neal CP, Garcea G, Manson MM, Dennison AR, Berry DP (2007) Prognostic molecular markers in hepatocellular carcinoma: a systematic review. Eur J Cancer 43:979-992

Marchio A, Meddeb M, Pineau P, Danglot G, Tiollais P, Bernheim A, Dejean A (1997) Recurrent chromosomal abnormalities in hepatocellular carcinoma detected by comparative genomic hybridization. Genes Chromosomes Cancer 18:59-65

Marrogi AJ, Khan MA, van Gijssel HE, Welsh JA, Rahim H, Demetris AJ, Kowdley KV, Hussain SP, Nair J, Bartsch H, Okby N, Poirier MC, Ishak KG, Harris CC (2001) Oxidative stress and p53 mutations in the carcinogenesis of iron overload-associated hepatocellular carcinoma. J Natl Cancer Inst 93:1652-1655

Masci G, Magagnoli M, Grimaldi A, Covini G, Carnaghi C, Rimassa L, Santoro A (2004) Metastasis of hepatocellular carcinoma to the heart: a case report and review of the literature. Tumori 90:345-347

Mashimo T, Watabe M, Hirota S, Hosobe S, Miura K, Tegtmeyer PJ, Rinker-Shaeffer CW, Watabe K (1998) The expression of the KAI1 gene, a tumor metastasis suppressor, is directly activated by p53. Proc Natl Acad Sci U S A 95:11307-11311

Matsuda Y, Ichida T, Genda T, Yamagiwa S, Aoyagi Y, Asakura H (2003) Loss of p16 contributes to p27 sequestration by cyclin D(1)-cyclin-dependent kinase 4 complexes and poor prognosis in hepatocellular carcinoma. Clin Cancer Res 9:3389-3396

McLure KG, Lee PW (1998) How p53 binds DNA as a tetramer. Embo J 17:3342-3350

Mehlen P, Puisieux A (2006) Metastasis: a question of life or death. Nat Rev Cancer 6:449-458

Melino G, De Laurenzi V, Vousden KH (2002) p73: Friend or foe in tumorigenesis. Nat Rev Cancer 2:605-615

Menendez JA, Vellon L, Mehmi I, Teng PK, Griggs DW, Lupu R (2005) A novel CYR61-triggered 'CYR61-alphavbeta3 integrin loop' regulates breast cancer cell survival and chemosensitivity through activation of ERK1/ERK2 MAPK signaling pathway. Oncogene 24:761-779

Mercer WE, Shields MT, Amin M, Sauve GJ, Appella E, Romano JW, Ullrich SJ (1990) Negative growth regulation in a glioblastoma tumor cell line that conditionally expresses human wild-type p53. Proc Natl Acad Sci U S A 87:6166-6170

Michelsen JW, Schmeichel KL, Beckerle MC, Winge DR (1993) The LIM motif defines a specific zinc-binding protein domain. Proc Natl Acad Sci U S A 90:4404-4408

Ming L, Thorgeirsson SS, Gail MH, Lu P, Harris CC, Wang N, Shao Y, Wu Z, Liu G, Wang X, Sun Z (2002) Dominant role of hepatitis B virus and cofactor role of aflatoxin in hepatocarcinogenesis in Qidong, China. Hepatology 36:1214-1220

Mirza A, McGuirk M, Hockenberry TN, Wu Q, Ashar H, Black S, Wen SF, Wang L, Kirschmeier P, Bishop WR, Nielsen LL, Pickett CB, Liu S (2002) Human survivin is negatively regulated by wild-type p53 and participates in p53-dependent apoptotic pathway. Oncogene 21:2613-2622

Mitra SK, Hanson DA, Schlaepfer DD (2005) Focal adhesion kinase: in command and control of cell motility. Nat Rev Mol Cell Biol 6:56-68

Mitra SK, Schlaepfer DD (2006) Integrin-regulated FAK-Src signaling in normal and cancer cells. Curr Opin Cell Biol 18: 516-523

Miyashita T, Harigai M, Hanada M, Reed JC (1994) Identification of a p53-dependent negative response element in the bcl-2 gene. Cancer Res 54:3131-3135

Moncman CL, Wang K (2000) Architecture of the thin filament-Z-line junction: lessons from nebulette and nebulin homologies. J Muscle Res Cell Motil 21:153-169

Mousa SA (2002) Vitronectin receptors in vascular disorders. Curr Opin Investig Drugs 3:1191-1195

Muller JM, Metzger E, Greschik H, Bosserhoff AK, Mercep L, Buettner R, Schule R (2002) The transcriptional coactivator FHL2 transmits Rho signals from the cell membrane into the nucleus. Embo J 21:736-748

Muller M, Wilder S, Bannasch D, Israeli D, Lehlbach K, Li-Weber M, Friedman SL, Galle PR, Stremmel W, Oren M, Krammer PH (1998) p53 activates the CD95 (APO-1/Fas) gene in response to DNA damage by anticancer drugs. J Exp Med 188:2033-2045

Murakami Y, Saigo K, Takashima H, Minami M, Okanoue T, Brechot C, Paterlini-Brechot P (2005) Large scaled analysis of hepatitis B virus (HBV) DNA integration in HBV related hepatocellular carcinomas. Gut 54:1162-1168

Murphy M, Hinman A, Levine AJ (1996) Wild-type p53 negatively regulates the expression of a microtubule-associated protein. Genes Dev 10:2971-2980

Nakamuta K, Oda H, Omagari K, Itsuno M, Murata I, Makiyama K, Hara K, Takeshima F, Tanioka H, Haraguchi M (1992) [A autopsied case of primary hepatocellular carcinoma with expansive metastasis to the spleen]. Nippon Shokakibyo Gakkai Zasshi 89:2808-2812

Nejjari M, Hafdi Z, Gouysse G, Fiorentino M, Beatrix O, Dumortier J, Pourreyron C, Barozzi C, D'Errico A, Grigioni WF, Scoazec JY (2002) Expression, regulation, and function of alpha V integrins in hepatocellular carcinoma: an in vivo and in vitro study. Hepatology 36:418-426

Neo SY, Leow CK, Vega VB, Long PM, Islam AF, Lai PB, Liu ET, Ren EC (2004) Identification of discriminators of hepatoma by gene expression profiling using a minimal dataset approach. Hepatology 39:944-953

Ng P, Wei CL, Sung WK, Chiu KP, Lipovich L, Ang CC, Gupta S, Shahab A, Ridwan A, Wong CH, Liu ET, Ruan Y (2005) Gene identification signature (GIS) analysis for transcriptome characterization and genome annotation. Nat Methods 2:105-111

Nguyen DX, Massague J (2007) Genetic determinants of cancer metastasis. Nat Rev Genet 8:341-352

Nijhara R, Jana SS, Goswami SK, Kumar V, Sarkar DP (2001) An internal segment (residues 58-119) of the hepatitis B virus X protein is sufficient to activate MAP kinase pathways in mouse liver. FEBS Lett 504:59-64

Niketeghad F, Decker HJ, Caselmann WH, Lund P, Geissler F, Dienes HP, Schirmacher P (2001) Frequent genomic imbalances suggest commonly altered tumour genes in human hepatocarcinogenesis. Br J Cancer 85:697-704

Nishimaki H, Kasai K, Kozaki K, Takeo T, Ikeda H, Saga S, Nitta M, Itoh G (2004) A role of activated Sonic hedgehog signaling for the cellular proliferation of oral squamous cell carcinoma cell line. Biochem Biophys Res Commun 314:313-320

Niu Q, Tang ZY, Ma ZC, Qin LX, Zhang LH (2000) Serum vascular endothelial growth factor is a potential biomarker of metastatic recurrence after curative resection of hepatocellular carcinoma. World J Gastroenterol 6:565-568

O'Brien TP, Yang GP, Sanders L, Lau LF (1990) Expression of cyr61, a growth factor-inducible immediate-early gene. Mol Cell Biol 10:3569-3577

O'Brien TP, Lau LF (1992) Expression of the growth factor-inducible immediate early gene cyr61 correlates with chondrogenesis during mouse embryonic development. Cell Growth Differ 3:645-654

Ogden SK, Lee KC, Barton MC (2000) Hepatitis B viral transactivator HBx alleviates p53-mediated repression of alpha-fetoprotein gene expression. J Biol Chem 275:27806-27814

Oida Y, Ishii M, Dowaki S, Tobita K, Ohtani Y, Imaizumi T, Abe Y, Yamazaki H, Nakamura M, Makuuchi H (2005) Hepatocellular carcinoma with metastasis to the pharynx: report of a case. Tokai J Exp Clin Med 30:31-34

Okabe H, Satoh S, Kato T, Kitahara O, Yanagawa R, Yamaoka Y, Tsunoda T, Furukawa Y, Nakamura Y (2001) Genome-wide analysis of gene expression in human hepatocellular carcinomas using cDNA microarray: identification of genes involved in viral carcinogenesis and tumor progression. Cancer Res 61:2129-2137

Okada T, Iizuka N, Yamada-Okabe H, Mori N, Tamesa T, Takemoto N, Tangoku A, Hamada K, Nakayama H, Miyamoto T, Uchimura S, Hamamoto Y, Oka M (2003) Gene expression profile linked to p53 status in hepatitis C virus-related hepatocellular carcinoma. FEBS Lett 555:583-590

Okamoto CT, Li R, Zhang Z, Jeng YY, Chew CS (2002) Regulation of protein and vesicle trafficking at the apical membrane of epithelial cells. J Control Release 78:35-41

Okamoto H, Yasui K, Zhao C, Arii S, Inazawa J (2003) PTK2 and EIF3S3 genes may be amplification targets at 8q23-q24 and are associated with large hepatocellular carcinomas. Hepatology 38:1242-1249

Oren M, Levine AJ (1983) Molecular cloning of a cDNA specific for the murine p53 cellular tumor antigen. Proc Natl Acad Sci U S A 80:56-59

Osna NA, Clemens DL, Donohue TM, Jr. (2005) Ethanol metabolism alters interferon gamma signaling in recombinant HepG2 cells. Hepatology 42:1109-1117

Palecek SP, Huttenlocher A, Horwitz AF, Lauffenburger DA (1998) Physical and biochemical regulation of integrin release during rear detachment of migrating cells. J Cell Sci 111 (Pt 7):929-940

Palecek SP, Horwitz AF, Lauffenburger DA (1999) Kinetic model for integrin-mediated adhesion release during cell migration. Ann Biomed Eng 27:219-235

Pan HW, Ou YH, Peng SY, Liu SH, Lai PL, Lee PH, Sheu JC, Chen CL, Hsu HC (2003) Overexpression of osteopontin is associated with intrahepatic metastasis, early recurrence, and poorer prognosis of surgically resected hepatocellular carcinoma. Cancer 98:119-127

Pan LH, Beppu T, Kurose A, Yamauchi K, Sugawara A, Suzuki M, Ogawa A, Sawai T (2002) Neoplastic cells and proliferating endothelial cells express connective tissue growth factor (CTGF) in glioblastoma. Neurol Res 24:677-683

Panaviene Z, Moncman CL (2007) Linker region of nebulin family members plays an important role in targeting these molecules to cellular structures. Cell Tissue Res 327:353-369

Park NH, Chung YH, Youn KH, Song BC, Yang SH, Kim JA, Lee HC, Yu E, Lee YS, Lee SG, Kim KW, Suh DJ (2001) Close correlation of p53 mutation to microvascular invasion in hepatocellular carcinoma. J Clin Gastroenterol 33:397-401

Parkin DM, Bray F, Ferlay J, Pisani P (2001) Estimating the world cancer burden: Globocan 2000. Int J Cancer 94:153-156

Partridge MA, Marcantonio EE (2006) Initiation of attachment and generation of mature focal adhesions by integrin-containing filopodia in cell spreading. Mol Biol Cell 17:4237-4248

Peng CY, Graves PR, Thoma RS, Wu Z, Shaw AS, Piwnica-Worms H (1997) Mitotic and G2 checkpoint control: regulation of 14-3-3 protein binding by phosphorylation of Cdc25C on serine-216. Science 277:1501-1505

Pennica D, Swanson TA, Welsh JW, Roy MA, Lawrence DA, Lee J, Brush J, Taneyhill LA, Deuel B, Lew M, Watanabe C, Cohen RL, Melhem MF, Finley GG, Quirke P, Goddard AD, Hillan KJ, Gurney AL, Botstein D, Levine AJ (1998) WISP genes are members of the connective tissue growth factor family that are up-regulated in wnt-1-transformed cells and aberrantly expressed in human colon tumors. Proc Natl Acad Sci U S A 95:14717-14722

Perbal B, Martinerie C, Sainson R, Werner M, He B, Roizman B (1999) The C-terminal domain of the regulatory protein NOVH is sufficient to promote interaction with fibulin 1C: a clue for a role of NOVH in cell-adhesion signaling. Proc Natl Acad Sci U S A 96:869-874

Perbal B (2001) NOV (nephroblastoma overexpressed) and the CCN family of genes: structural and functional issues. Mol Pathol 54:57-79

Perbal B, Brigstock DR, Lau LF (2003) Report on the second international workshop on the CCN family of genes. Mol Pathol 56:80-85

Perbal B (2004) CCN proteins: multifunctional signalling regulators. Lancet 363:62-64

Phillips GR, Anderson TR, Florens L, Gudas C, Magda G, Yates JR, 3rd, Colman DR (2004) Actin-binding proteins in a postsynaptic preparation: Lasp-1 is a component of central nervous system synapses and dendritic spines. J Neurosci Res 78:38-48

Pietromonaco SF, Seluja GA, Aitken A, Elias L (1996) Association of 14-3-3 proteins with centrosomes. Blood Cells Mol Dis 22:225-237

Pilarsky CP, Schmidt U, Eissrich C, Stade J, Froschermaier SE, Haase M, Faller G, Kirchner TW, Wirth MP (1998) Expression of the extracellular matrix signaling molecule Cyr61 is downregulated in prostate cancer. Prostate 36:85-91

Planque N, Perbal B (2003) A structural approach to the role of CCN (CYR61/CTGF/NOV) proteins in tumourigenesis. Cancer Cell Int 3:15

Polyak K, Xia Y, Zweier JL, Kinzler KW, Vogelstein B (1997) A model for p53-induced apoptosis. Nature 389:300-305

Pomies P, Macalma T, Beckerle MC (1999) Purification and characterization of an alpha-actinin-binding PDZ-LIM protein that is up-regulated during muscle differentiation. J Biol Chem 274:29242-29250

Poon RT, Fan ST, Lo CM, Liu CL, Wong J (1999) Intrahepatic recurrence after curative resection of hepatocellular carcinoma: long-term results of treatment and prognostic factors. Ann Surg 229:216-222

Prange W, Schirmacher P (2001) Absence of therapeutically relevant c-erbB-2 expression in human hepatocellular carcinomas. Oncol Rep 8:727-730

Raucher D, Sheetz MP (2000) Cell spreading and lamellipodial extension rate is regulated by membrane tension. J Cell Biol 148:127-136

Ridley AJ, Schwartz MA, Burridge K, Firtel RA, Ginsberg MH, Borisy G, Parsons JT, Horwitz AR (2003) Cell migration: integrating signals from front to back. Science 302:1704-1709

Riley J, Mandel HG, Sinha S, Judah DJ, Neal GE (1997) In vitro activation of the human Harvey-ras proto-oncogene by aflatoxin B1. Carcinogenesis 18:905-910

Saito Y, Kanai Y, Sakamoto M, Saito H, Ishii H, Hirohashi S (2001) Expression of mRNA for DNA methyltransferases and methyl-CpG-binding proteins and DNA methylation status on CpG islands and pericentromeric satellite regions during human hepatocarcinogenesis. Hepatology 33:561-568

Sakamoto K, Yamaguchi S, Ando R, Miyawaki A, Kabasawa Y, Takagi M, Li CL, Perbal B, Katsube K (2002) The nephroblastoma overexpressed gene (NOV/ccn3) protein associates with Notch1 extracellular domain and inhibits myoblast differentiation via Notch signaling pathway. J Biol Chem 277:29399-29405

Sakamoto M, Ino Y, Fujii T, Hirohashi S (1993) Phenotype changes in tumor vessels associated with the progression of hepatocellular carcinoma. Jpn J Clin Oncol 23:98-104

Sampath D, Zhu Y, Winneker RC, Zhang Z (2001) Aberrant expression of Cyr61, a member of the CCN (CTGF/Cyr61/Cef10/NOVH) family, and dysregulation by 17 beta-estradiol and basic fibroblast growth factor in human uterine leiomyomas. J Clin Endocrinol Metab 86:1707-1715

Sampath D, Winneker RC, Zhang Z (2002) The angiogenic factor Cyr61 is induced by the progestin R5020 and is necessary for mammary adenocarcinoma cell growth. Endocrine 18:147-159

Sastry SK, Burridge K (2000) Focal adhesions: a nexus for intracellular signaling and cytoskeletal dynamics. Exp Cell Res 261:25-36

Schaller MD (2001) Paxillin: a focal adhesion-associated adaptor protein. Oncogene 20:6459-6472

Scharf JG, Dombrowski F, Ramadori G (2001) The IGF axis and hepatocarcinogenesis. Mol Pathol 54:138-144

Schlunegger MP, Grutter MG (1993) Refined crystal structure of human transforming growth factor beta 2 at 1.95 A resolution. J Mol Biol 231:445-458

Schmeichel KL, Beckerle MC (1994) The LIM domain is a modular protein-binding interface. Cell 79:211-219

Schober JM, Chen N, Grzeszkiewicz TM, Jovanovic I, Emeson EE, Ugarova TP, Ye RD, Lau LF, Lam SC (2002) Identification of integrin alpha(M)beta(2) as an adhesion receptor on peripheral blood monocytes for Cyr61 (CCN1) and connective tissue growth factor (CCN2): immediate-early gene products expressed in atherosclerotic lesions. Blood 99:4457-4465

Schreiber V, Masson R, Linares JL, Mattei MG, Tomasetto C, Rio MC (1998a) Chromosomal assignment and expression pattern of the murine Lasp-1 gene. Gene 207:171-175

Schreiber V, Moog-Lutz C, Regnier CH, Chenard MP, Boeuf H, Vonesch JL, Tomasetto C, Rio MC (1998b) Lasp-1, a novel type of actin-binding protein accumulating in cell membrane extensions. Mol Med 4:675-687

Schvartz I, Seger D, Shaltiel S (1999) Vitronectin. Int J Biochem Cell Biol 31:539-544

Seki S, Kitada T, Kawada N, Sakaguchi H, Kadoya H, Nakatani K, Satake K, Kuroki T (1999) Establishment and characteristics of human hepatocellular carcinoma cells with metastasis to lymph nodes. Hepatogastroenterology 46:2812-2817

Seto E, Usheva A, Zambetti GP, Momand J, Horikoshi N, Weinmann R, Levine AJ, Shenk T (1992) Wild-type p53 binds to the TATA-binding protein and represses transcription. Proc Natl Acad Sci U S A 89:12028-12032

Sheetz MP, Felsenfeld D, Galbraith CG, Choquet D (1999) Cell migration as a five-step cycle. Biochem Soc Symp 65:233-243

Sheng S, Carey J, Seftor EA, Dias L, Hendrix MJ, Sager R (1996) Maspin acts at the cell membrane to inhibit invasion and motility of mammary and prostatic cancer cells. Proc Natl Acad Sci U S A 93:11669-11674

Shin SI, Freedman VH, Risser R, Pollack R (1975) Tumorigenicity of virus-transformed cells in nude mice is correlated specifically with anchorage independent growth in vitro. Proc Natl Acad Sci U S A 72:4435-4439

Shirota Y, Kaneko S, Honda M, Kawai HF, Kobayashi K (2001) Identification of differentially expressed genes in hepatocellular carcinoma with cDNA microarrays. Hepatology 33:832-840

Shu KX, Li B, Wu LX (2007) The p53 network: p53 and its downstream genes. Colloids Surf B Biointerfaces 55:10-18

Simmons DL, Levy DB, Yannoni Y, Erikson RL (1989) Identification of a phorbol ester-repressible v-src-inducible gene. Proc Natl Acad Sci U S A 86:1178-1182

Singh B, Reddy PG, Goberdhan A, Walsh C, Dao S, Ngai I, Chou TC, P OC, Levine AJ, Rao PH, Stoffel A (2002) p53 regulates cell survival by inhibiting PIK3CA in squamous cell carcinomas. Genes Dev 16:984-993

Skoble J, Portnoy DA, Welch MD (2000) Three regions within ActA promote Arp2/3 complex-mediated actin nucleation and Listeria monocytogenes motility. J Cell Biol 150:527-538

Soresi M, Magliarisi C, Campagna P, Leto G, Bonfissuto G, Riili A, Carroccio A, Sesti R, Tripi S, Montalto G (2003) Usefulness of alpha-fetoprotein in the diagnosis of hepatocellular carcinoma. Anticancer Res 23:1747-1753

Soussi T, Kato S, Levy PP, Ishioka C (2005) Reassessment of the TP53 mutation database in human disease by data mining with a library of TP53 missense mutations. Hum Mutat 25:6-17

Spence HJ, McGarry L, Chew CS, Carragher NO, Scott-Carragher LA, Yuan Z, Croft DR, Olson MF, Frame M, Ozanne BW (2006) AP-1 differentially expressed

proteins Krp1 and fibronectin cooperatively enhance Rho-ROCK-independent mesenchymal invasion by altering the function, localization, and activity of nondifferentially expressed proteins. Mol Cell Biol 26:1480-1495

Stamatoglou SC, Hughes RC (1994) Cell adhesion molecules in liver function and pattern formation. Faseb J 8:420-427

Sugo H, Takamori S, Kojima K, Beppu T, Futagawa S (1999) The significance of p53 mutations as an indicator of the biological behavior of recurrent hepatocellular carcinomas. Surg Today 29:849-855

Sun HC, Tang ZY (2004) Angiogenesis in hepatocellular carcinoma: the retrospectives and perspectives. J Cancer Res Clin Oncol 130:307-319

Tadokoro S, Shattil SJ, Eto K, Tai V, Liddington RC, de Pereda JM, Ginsberg MH, Calderwood DA (2003) Talin binding to integrin beta tails: a final common step in integrin activation. Science 302:103-106

Takafuta T, Saeki M, Fujimoto TT, Fujimura K, Shapiro SS (2003) A new member of the LIM protein family binds to filamin B and localizes at stress fibers. J Biol Chem 278:12175-12181

Takeda A, Stoeltzing O, Ahmad SA, Reinmuth N, Liu W, Parikh A, Fan F, Akagi M, Ellis LM (2002) Role of angiogenesis in the development and growth of liver metastasis. Ann Surg Oncol 9:610-616

Tanabe H, Kondo A, Kinuta Y, Matsuura N, Hasegawa K, Chin M, Saiki M (1994) Unusual presentation of brain metastasis from hepatocellular carcinoma--two case reports. Neurol Med Chir (Tokyo) 34:748-753

Tang ZY, Ye SL, Liu YK, Qin LX, Sun HC, Ye QH, Wang L, Zhou J, Qiu SJ, Li Y, Ji XN, Liu H, Xia JL, Wu ZQ, Fan J, Ma ZC, Zhou XD, Lin ZY, Liu KD (2004) A decade's studies on metastasis of hepatocellular carcinoma. J Cancer Res Clin Oncol 130:187-196

Tarn C, Lee S, Hu Y, Ashendel C, Andrisani OM (2001) Hepatitis B virus X protein differentially activates RAS-RAF-MAPK and JNK pathways in X-transforming versus non-transforming AML12 hepatocytes. J Biol Chem 276:34671-34680

Terasaki AG, Suzuki H, Nishioka T, Matsuzawa E, Katsuki M, Nakagawa H, Miyamoto S, Ohashi K (2004) A novel LIM and SH3 protein (lasp-2) highly expressing in chicken brain. Biochem Biophys Res Commun 313:48-54

Terman JR, Mao T, Pasterkamp RJ, Yu HH, Kolodkin AL (2002) MICALs, a family of conserved flavoprotein oxidoreductases, function in plexin-mediated axonal repulsion. Cell 109:887-900

Thomas MB, Zhu AX (2005) Hepatocellular carcinoma: the need for progress. J Clin Oncol 23:2892-2899

Thorgeirsson SS, Grisham JW (2002) Molecular pathogenesis of human hepatocellular carcinoma. Nat Genet 31:339-346

Tokino T, Tamura H, Hori N, Matsubara K (1991) Chromosome deletions associated with hepatitis B virus integration. Virology 185:879-882

Tokino T, Nakamura Y (2000) The role of p53-target genes in human cancer. Crit Rev Oncol Hematol 33:1-6

Tomasetto C, Moog-Lutz C, Regnier CH, Schreiber V, Basset P, Rio MC (1995) Lasp-1 (MLN 50) defines a new LIM protein subfamily characterized by the association of LIM and SH3 domains. FEBS Lett 373:245-249

Tong X, Xie D, O'Kelly J, Miller CW, Muller-Tidow C, Koeffler HP (2001) Cyr61, a member of CCN family, is a tumor suppressor in non-small cell lung cancer. J Biol Chem 276:47709-47714

Tong X, O'Kelly J, Xie D, Mori A, Lemp N, McKenna R, Miller CW, Koeffler HP (2004) Cyr61 suppresses the growth of non-small-cell lung cancer cells via the beta-catenin-c-myc-p53 pathway. Oncogene 23:4847-4855

Tsai MS, Hornby AE, Lakins J, Lupu R (2000) Expression and function of CYR61, an angiogenic factor, in breast cancer cell lines and tumor biopsies. Cancer Res 60:5603-5607

Tsai MS, Bogart DF, Castaneda JM, Li P, Lupu R (2002) Cyr61 promotes breast tumorigenesis and cancer progression. Oncogene 21:8178-8185

Tu Y, Wu S, Shi X, Chen K, Wu C (2003) Migfilin and Mig-2 link focal adhesions to filamin and the actin cytoskeleton and function in cell shape modulation. Cell 113:37-47

Tung-Ping Poon R, Fan ST, Wong J (2000) Risk factors, prevention, and management of postoperative recurrence after resection of hepatocellular carcinoma. Ann Surg 232:10-24

Turner CE (2000a) Paxillin and focal adhesion signalling. Nat Cell Biol 2:E231-236

Turner CE (2000b) Paxillin interactions. J Cell Sci 113 Pt 23:4139-4140

Tzivion G, Gupta VS, Kaplun L, Balan V (2006) 14-3-3 proteins as potential oncogenes. Semin Cancer Biol 16:203-213

Ueda H, Ullrich SJ, Gangemi JD, Kappel CA, Ngo L, Feitelson MA, Jay G (1995) Functional inactivation but not structural mutation of p53 causes liver cancer. Nat Genet 9:41-47

Ueki T, Fujimoto J, Suzuki T, Yamamoto H, Okamoto E (1997) Expression of hepatocyte growth factor and its receptor, the c-met proto-oncogene, in hepatocellular carcinoma. Hepatology 25:619-623

Ueno N, Kanamaru T, Kawaguchi K, Tanaka K, Inoue K, Idei Y, Yamamoto M (2001) A hepatocellular carcinoma with lymph node metastasis and invasion into the gallbladder: preoperative difficulty ruling out a gallbladder carcinoma. Oncol Rep 8:331-335

Varner JA, Emerson DA, Juliano RL (1995) Integrin alpha 5 beta 1 expression negatively regulates cell growth: reversal by attachment to fibronectin. Mol Biol Cell 6:725-740

Varner JA, Cheresh DA (1996) Integrins and cancer. Curr Opin Cell Biol 8:724-730

Velyvis A, Vaynberg J, Yang Y, Vinogradova O, Zhang Y, Wu C, Qin J (2003) Structural and functional insights into PINCH LIM4 domain-mediated integrin signaling. Nat Struct Biol 10:558-564

Veprintsev DB, Freund SM, Andreeva A, Rutledge SE, Tidow H, Canadillas JM, Blair CM, Fersht AR (2006) Core domain interactions in full-length p53 in solution. Proc Natl Acad Sci U S A 103:2115-2119

Vorwerk P, Wex H, Hohmann B, Mohnike K, Schmidt U, Mittler U (2002) Expression of components of the IGF signalling system in childhood acute lymphoblastic leukaemia. Mol Pathol 55:40-45

Vousden KH, Lu X (2002) Live or let die: the cell's response to p53. Nat Rev Cancer 2:594-604

Wada H, Nagano H, Yamamoto H, Yang Y, Kondo M, Ota H, Nakamura M, Yoshioka S, Kato H, Damdinsuren B, Tang D, Marubashi S, Miyamoto A, Takeda Y, Umeshita K, Nakamori S, Sakon M, Dono K, Wakasa K, Monden M (2006) Expression pattern of angiogenic factors and prognosis after hepatic resection in hepatocellular carcinoma: importance of angiopoietin-2 and hypoxia-induced factor-1 alpha. Liver Int 26:414-423

Wang B, Ren J, Ooi LL, Chong SS, Lee CG (2005) Dinucleotide repeats negatively modulate the promoter activity of Cyr61 and is unstable in hepatocellular carcinoma patients. Oncogene 24:3999-4008

Wang G, Zhao Y, Liu X, Wang L, Wu C, Zhang W, Liu W, Zhang P, Cong W, Zhu Y, Zhang L, Chen S, Wan D, Zhao X, Huang W, Gu J (2001) Allelic loss and gain, but not genomic instability, as the major somatic mutation in primary hepatocellular carcinoma. Genes Chromosomes Cancer 31:221-227

Wang J, Chenivesse X, Henglein B, Brechot C (1990) Hepatitis B virus integration in a cyclin A gene in a hepatocellular carcinoma. Nature 343:555-557

Wang SN, Chuang SC, Yeh YT, Yang SF, Chai CY, Chen WT, Kuo KK, Chen JS, Lee KT (2006) Potential prognostic value of leptin receptor in hepatocellular carcinoma. J Clin Pathol 59:1267-1271

Wang XW, Forrester K, Yeh H, Feitelson MA, Gu JR, Harris CC (1994) Hepatitis B virus X protein inhibits p53 sequence-specific DNA binding, transcriptional activity, and association with transcription factor ERCC3. Proc Natl Acad Sci U S A 91:2230-2234

Wang XW, Gibson MK, Vermeulen W, Yeh H, Forrester K, Sturzbecher HW, Hoeijmakers JH, Harris CC (1995) Abrogation of p53-induced apoptosis by the hepatitis B virus X gene. Cancer Res 55:6012-6016

Wang XW, Zhan Q, Coursen JD, Khan MA, Kontny HU, Yu L, Hollander MC, O'Connor PM, Fornace AJ, Jr., Harris CC (1999) GADD45 induction of a G2/M cell cycle checkpoint. Proc Natl Acad Sci U S A 96:3706-3711

Wang Y, Szekely L, Okan I, Klein G, Wiman KG (1993) Wild-type p53-triggered apoptosis is inhibited by bcl-2 in a v-myc-induced T-cell lymphoma line. Oncogene 8:3427-3431

Wang Y, Gilmore TD (2003) Zyxin and paxillin proteins: focal adhesion plaque LIM domain proteins go nuclear. Biochim Biophys Acta 1593:115-120

Wasenius VM, Hemmer S, Kettunen E, Knuutila S, Franssila K, Joensuu H (2003) Hepatocyte growth factor receptor, matrix metalloproteinase-11, tissue inhibitor of metalloproteinase-1, and fibronectin are up-regulated in papillary

thyroid carcinoma: a cDNA and tissue microarray study. Clin Cancer Res 9:68-75

Watanabe J, Kushihata F, Honda K, Sugita A, Tateishi N, Mominoki K, Matsuda S, Kobayashi N (2004) Prognostic significance of Bcl-xL in human hepatocellular carcinoma. Surgery 135:604-612

Wei CL, Wu Q, Vega VB, Chiu KP, Ng P, Zhang T, Shahab A, Yong HC, Fu Y, Weng Z, Liu J, Zhao XD, Chew JL, Lee YL, Kuznetsov VA, Sung WK, Miller LD, Lim B, Liu ET, Yu Q, Ng HH, Ruan Y (2006) A global map of p53 transcription-factor binding sites in the human genome. Cell 124:207-219

Weinmann AS, Bartley SM, Zhang T, Zhang MQ, Farnham PJ (2001) Use of chromatin immunoprecipitation to clone novel E2F target promoters. Mol Cell Biol 21:6820-6832

Welch MD, Mullins RD (2002) Cellular control of actin nucleation. Annu Rev Cell Dev Biol 18:247-288

Wells J, Farnham PJ (2002) Characterizing transcription factor binding sites using formaldehyde crosslinking and immunoprecipitation. Methods 26:48-56

Wenger C, Ellenrieder V, Alber B, Lacher U, Menke A, Hameister H, Wilda M, Iwamura T, Beger HG, Adler G, Gress TM (1999) Expression and differential regulation of connective tissue growth factor in pancreatic cancer cells. Oncogene 18:1073-1080

Wong M, Kireeva ML, Kolesnikova TV, Lau LF (1997) Cyr61, product of a growth factor-inducible immediate-early gene, regulates chondrogenesis in mouse limb bud mesenchymal cells. Dev Biol 192:492-508

Wong N, Lai P, Lee SW, Fan S, Pang E, Liew CT, Sheng Z, Lau JW, Johnson PJ (1999) Assessment of genetic changes in hepatocellular carcinoma by comparative genomic hybridization analysis: relationship to disease stage, tumor size, and cirrhosis. Am J Pathol 154:37-43

Xia H, Winokur ST, Kuo WL, Altherr MR, Bredt DS (1997) Actinin-associated LIM protein: identification of a domain interaction between PDZ and spectrin-like repeat motifs. J Cell Biol 139:507-515

Xian ZH, Zhang SH, Cong WM, Wu WQ, Wu MC (2005) Overexpression/amplification of HER-2/neu is uncommon in hepatocellular carcinoma. J Clin Pathol 58:500-503

Xie D, Miller CW, O'Kelly J, Nakachi K, Sakashita A, Said JW, Gornbein J, Koeffler HP (2001) Breast cancer. Cyr61 is overexpressed, estrogen-inducible, and associated with more advanced disease. J Biol Chem 276:14187-14194

Xie D, Yin D, Tong X, O'Kelly J, Mori A, Miller C, Black K, Gui D, Said JW, Koeffler HP (2004) Cyr61 is overexpressed in gliomas and involved in integrin-linked kinase-mediated Akt and beta-catenin-TCF/Lef signaling pathways. Cancer Res 64:1987-1996

Xu L, Hui L, Wang S, Gong J, Jin Y, Wang Y, Ji Y, Wu X, Han Z, Hu G (2001) Expression profiling suggested a regulatory role of liver-enriched transcription factors in human hepatocellular carcinoma. Cancer Res 61:3176-3181

Yamamoto H, Itoh F, Adachi Y, Sakamoto H, Adachi M, Hinoda Y, Imai K (1997) Relation of enhanced secretion of active matrix metalloproteinases with tumor spread in human hepatocellular carcinoma. Gastroenterology 112:1290-1296

Yamamoto J, Kosuge T, Takayama T, Shimada K, Yamasaki S, Ozaki H, Yamaguchi N, Makuuchi M (1996) Recurrence of hepatocellular carcinoma after surgery. Br J Surg 83:1219-1222

Yamanishi K, Kishimoto S, Hosokawa Y, Yamada K, Yasuno H (1989) Cutaneous metastasis from hepatocellular carcinoma resembling granuloma teleangiectaticum. J Dermatol 16:500-504

Yang A, Kaghad M, Wang Y, Gillett E, Fleming MD, Dotsch V, Andrews NC, Caput D, McKeon F (1998) p63, a p53 homolog at 3q27-29, encodes multiple products with transactivating, death-inducing, and dominant-negative activities. Mol Cell 2:305-316

Yang LY, Chen WL, Lin JW, Lee SF, Lee CC, Hung TI, Wei YH, Shih CM (2005) Differential expression of antioxidant enzymes in various hepatocellular carcinoma cell lines. J Cell Biochem 96:622-631

Yasui K, Arii S, Zhao C, Imoto I, Ueda M, Nagai H, Emi M, Inazawa J (2002) TFDP1, CUL4A, and CDC16 identified as targets for amplification at 13q34 in hepatocellular carcinomas. Hepatology 35:1476-1484

Yeh SH, Chen PJ, Shau WY, Chen YW, Lee PH, Chen JT, Chen DS (2001) Chromosomal allelic imbalance evolving from liver cirrhosis to hepatocellular carcinoma. Gastroenterology 121:699-709

Yu C, Le AT, Yeger H, Perbal B, Alman BA (2003) NOV (CCN3) regulation in the growth plate and CCN family member expression in cartilage neoplasia. J Pathol 201:609-615

Zambetti GP, Levine AJ (1993) A comparison of the biological activities of wild-type and mutant p53. Faseb J 7:855-865

Zeng ZJ, Yang LY, Ding X, Wang W (2004) Expressions of cysteine-rich61, connective tissue growth factor and Nov genes in hepatocellular carcinoma and their clinical significance. World J Gastroenterol 10:3414-3418

Zondervan PE, Wink J, Alers JC, JN IJ, Schalm SW, de Man RA, van Dekken H (2000) Molecular cytogenetic evaluation of virus-associated and non-viral hepatocellular carcinoma: analysis of 26 carcinomas and 12 concurrent dysplasias. J Pathol 192:207-215

Zou Z, Anisowicz A, Hendrix MJ, Thor A, Neveu M, Sheng S, Rafidi K, Seftor E, Sager R (1994) Maspin, a serpin with tumor-suppressing activity in human mammary epithelial cells. Science 263:526-529

Zou Z, Gao C, Nagaich AK, Connell T, Saito S, Moul JW, Seth P, Appella E, Srivastava S (2000) p53 regulates the expression of the tumor suppressor gene maspin. J Biol Chem 275:6051-6054

Appendix I: Buffers and Solutions

Buffers and Solutions for Cell Culture

FBS (Fetal Bovine Serum)

500ml of FBS (Invitrogen) was thawed at 37°C water bath and heat inactivated at 56°C for 30 minutes. Aliquot in 50ml falcon tubes and store at -20°C

DMEM Culture Medium (DMEM/10% FBS)

DMEM (Invitrogen)	450ml (90%)
FBS (heat inactivated)	50ml (10%)
Total Volume	500ml

Filter to sterilize and store at 4°C.

DMEM/G418 Culture Medium

DMEM Culture Medium	492ml
G418 (50mg/ml stock from Invitrogen)	8ml (800μg/ml working concentration)
Total Volume	500ml

Filter to sterilize and store at 4°C.

Serum-free Medium (DMEM/0.5% FBS)

DMEM (Invitrogen)	497.5ml (99.5%)
FBS	2.5ml (0.5%)
Total Volume	500ml

Filter to sterilize and store at 4°C

2 × DMEM Medium

Dissolve 1 bag (for 1L 1 × DMEM Medium) of DMEM powder (high glucose) (Gibco, Invitrogen) in <400mL Mini-Q H_2O, adjust pH (just measure), add 100mL FBS, top-up to 500mL. Filter to sterilize and store at 4°C

FM (Freezing Medium)

DMEM	45ml (45%)
FBS	45ml (45%)
DMSO	10ml (10%)
Total Volume	100ml

Filter to sterilize and store at 4°C.

PBS (phosphate buffered saline) (10 ×)

NaCl	80g
KCl	2g
KH_2PO_4	2.4g
Na_2HPO_4	14.4g

Dissolve in ~800ml Mini-Q H_2O and adjust pH to 7.4 with HCl, make up the final volume to 1L, autoclave and store at 4°C

PBS with Ca^{++}, Mg^{++}

Add 130mg $CaCl_2.2H_2O$ and 100mg $MgCl_2.6H_2O$ into per liter 1 × PBS and store at room temperature

5-Fluorouracil (5-FU)

Re-constitute 5-FU powder (Sigma) in DMSO to make a 50mg/ml stock and store at -20°C. Dilute in DMEM/10%FBS to a working concentration of 50μg/ml (or 375μM) before use

Buffers and Solutions for Cloning

Luria Bertani Broth (LB Broth)

	Powder (for 1L)	Final Concentration (w/v)
Tryptone	10g	1%
Yeast Extract	5g	0.5%
NaCl	10g	1%

Dissolve in Mini-Q H_2O and make up the final volume to 1L, autoclave and store at 4°C

Luria Bertani Agar (LB Agar)

	Powder (for 400ml)	Final Concentration (w/v)
Tryptone	4g	1%
Yeast Extract	2g	0.5%
NaCl	4g	1%
Agarose	6g	1.5%

Make up the final volume to 400ml (for about 20 plates) with Mini-Q H_2O. Autoclave the solution and cool down at room temperature to about 55°C, add appropriate antibiotics before pour plate.

Ampicillin

Stock concentration: 200mg/ml in Mini-Q H_2O, filter to sterilize. Working concentration: 100μg/ml

Kanamycin

Stock concentration: 50mg/ml in Mini-Q H_2O, filter to sterilize. Working concentration: 50μg/ml

Buffers and Solutions for Agarose Electrophoresis, SDS-PAGE and Western Blot

TBE Buffer (Tris-Borate-EDTA) (10×)

Tris base	108g
Boric acid	55g
EDTA	9.3g

Make up the final volume to 1000ml with Mini-Q H_2O, autoclave and store at room temperature

Agarose gel (1% or 1.5%)

Dissolve 1.0g (for 1% gel) or 1.5g (for 1.5% gel) DNase-free agarose (Bio-Rad) in 100ml 1 × TBE, boil, allow to cool and add 5μl of 10mg/ml ethidium bromide, pour into the casting frame, allow the gel to harden in about 20 minutes

NP-40 Cell Lysis Buffer

	Stock	Volume (for 100ml)
50mM Tris-HCl (pH7.8)	1M Tris-HCl (pH7.8)	5ml
150mM NaCl	5M NaCl	3ml
1% Nonidet P-40	Nonidet P-40 (100%)	1ml

Top-up with Mini-Q H_2O, store at 4ºC. Add complete mini (final concentration: 1 ×) and PMSF (final concentration: 1mM) freshly before use

PMSF Stock (200×)

PMSF was dissolved in isopropanol at a concentration of 200mM and stored at -20ºC

Complete Mini Stock (7×)

1 tablet (Roche) was dissolved in 1.5mL ddH_2O to make a 7 × stock and stored at -20ºC

2 × SDS-PAGE Sample Buffer

	Stock	Volume (for 100ml)
50mM Tris-HCl (pH6.8)	1M Tris-HCl (pH6.8)	12.5ml
20% Glycerol	100% Glycerol	20ml
4% β-mercaptoethanol	β-mercaptoethanol	4ml
0.4% Bromophenol Blue (w/v)	Bromophenol Blue (Powder)	0.4g
4% SDS (w/v)	SDS (Powder)	4g

Top-up with Mini-Q H_2O, aliquoted and stored at -20°C

10 × Tris-Glycine SDS-PAGE Running Buffer

	Powder (for 1L)	Final Concentration (w/v)
Tris base	30.2g	25mM (× 10)
Glycine	144g	192mM (× 10)

Top-up to 1000 ml with Mini-Q H_2O, store at -20°C, add 10% SDS to 1 × buffer to 0.1% final concentration

10 × Transfer Buffer

	Powder (for 1L)	Final Concentration (w/v)
Tris base	58.2g	48mM (× 10)
Glycine	29.3g	39mM (× 10)

Top up to 1000 ml with Mini-Q H_2O. To make 1 liter 1 × buffer, add 100 ml 10 × buffer, 3.75 ml 10% SDS and 200 ml methanol, top up to 1000 ml with Mini-Q H_2O

TBST Buffer

	Stock	Volume (for 1L)
20mM Tris-HCl (pH7.6)	1M Tris-HCl, pH7.6	20ml
150mM NaCl	5M NaCl	30ml
0.1% Tween-20	100% Tween-20	1ml

Top up to 1000 ml with Mini-Q H_2O

Blocking Buffer

5% non-fat milk in 1 × TBST buffer, store at 4°C

Buffers and Solutions for Flow Cytometry Analysis

RNase A stock

RNase A (Sigma) was dissolved in DNase/RNase free H_2O (Invitrogen) to make a 1mg/ml stock, aliquot and store at 4°C, 10 × dilution in DNase/RNase free H_2O to 100μg/ml working concentration before use

PI (propidium iodide) stock

PI (Sigma) was dissolved in DNase/RNase free H_2O (Invitrogen) to make a 2mg/ml stock, aliquot and store at 4°C in dark, 40 × dilution in DNase/RNase free H_2O to 50μg/ml working concentration before use

Buffers and Solutions for Soft Agar Assay

Soft Agar Stock

Prepare 2% stock agar solution in Mini-Q H_2O, autoclave, aliquot and store at room temperature

INT (*p*-iodonitrotetrazolium) Stock

INT (Sigma) was dissolved in DMSO to make a 10mg/ml stock, store at 4°C, dilute into 1mg/ml with PBS before use

Buffers and Solutions for Chromatin Immunoprecipitation (ChIP)

TBSE Buffer

	Stock	Volume (for 1L)
20mM Tris-HCl (pH7.5)	1M Tris-HCl (pH7.5)	20ml
150mM NaCl	5M NaCl	30ml
1mM EDTA	0.5M EDTA	2ml

Top up to 1000 ml with autoclaved Mini-Q H_2O, store at 4°C

FA Cell Lysis Buffer

	Stock	Volume (for 1L)
10mM Tris-HCl (pH8.0)	1M Tris-HCl (pH8.0)	10ml
0.25% Triton-X100	20% Triton-X100	12.5ml
10mM EDTA	0.5M EDTA	20ml
0.1M NaCl	5M NaCl	20ml

Top up to 1000 ml with autoclaved Mini-Q H_2O, store at 4°C

1%SDS FA Lysis Buffer

	Stock	Volume (for 1L)
50mM HEPES-KOH (pH7.5)	1M HEPES-KOH	50ml
150mM NaCl	5M NaCl	30ml
2mM EDTA	0.5M EDTA	4ml
1% Triton-X100	20% Triton-X100	50ml
0.1% NaDOC	10% NaDOC	10ml
1%SDS	10% SDS	100ml

Top up to 1000 ml with autoclaved Mini-Q H_2O, store at 4°C

0.1%SDS FA Lysis Buffer

	Stock	Volume (for 1L)
50mM HEPES-KOH (pH7.5)	1M HEPES-KOH	50ml
150mM NaCl	5M NaCl	30ml
2mM EDTA	0.5M EDTA	4ml
1% Triton-X100	20% Triton-X100	50ml
0.1% NaDOC	10% NaDOC	10ml
0.1%SDS	10% SDS	10ml

Top up to 1000 ml with autoclaved Mini-Q H_2O, store at 4°C

ChIP Elution Buffer

	Stock	Volume (for 50mL)
50mM Tris-HCl (pH7.5)	1M Tris-HCl (pH8.0)	2.5ml
10mM EDTA	0.5M EDTA	1ml
1%SDS	10% SDS	5ml
autoclaved MiniQ-H_2O		41.5ml

NP-40/LiCl Buffer

	Stock	Volume (for 1L)
10mM Tris-HCl (pH8.0)	1M Tris-HCl (pH8.0)	10 ml
0.25M LiCl	4M LiCl	62.5ml
1mM EDTA	0.5M EDTA	2ml
0.5%NP-40	10% NP-40	50ml
0.5% NaDOC	10% NaDOC	50ml
autoclaved MiniQ-H_2O		825.5ml

TE buffer

	Stock	Volume (for 50mL)
10mM Tris-HCl (pH8.0)	1M Tris-HCl (pH8.0)	0.5 ml
1mM EDTA	0.5M EDTA	100µl
autoclaved MiniQ-H_2O		49.4ml

Glycine Stock

2.5M Glycine dissolved in Mini-Q H_2O. Freeze at -20°C

Pronase

20mg/ml Pronase stock in TBSE. Freeze at -20°C

Buffers and Solutions for Immunofluoresence

PFA (paraformaldehyde, 4% in PBS) (freshly prepared)

Dissolve 0.4g paraformaldehyde in ~8ml PBS, warm at 56°C waterbath. Add 10N NaCl dropwise until solution clears. Make up to 10ml with PBS

Triton-X100 (0.1% in PBS)

Add 1ml Triton-X100 (Bio-Rad) to 99ml PBS to prepare 1% stock. 10 × dilution with PBS to make 0.1% Triton-X100 before use

BSA (bovine serum albumin, 5% in PBS) (freshly prepared)

Dissolve 0.5g BSA in 10ml PBS before use

Appendix II: Publications

International Journal Papers

Feng P, Wang B (co-first author), Ren EC. 2008. Cyr61/CCN1 is a tumor suppressor in human hepatocellular carcinoma and involved in DNA damage response. *Int J Biochem Cell Biol*. 40: 98-109. (doi: 10.1016/j.biocel.2007.06.020)

Wang B, Feng P, Xiao ZW, Ren EC. Identification of Lasp1 as a novel p53 target involved in modulating the cytoskeleton. (Manuscript in preparation)

Conference Papers

Feng P, Wang B, Neo SY, Ren EC. 2005. Down-regulation of dermatopontin (DPT) in hepatocellular carcinoma (HCC) might promote liver cancer development. Presented at the 7th World Congress on Gastrointestinal Cancer. (Poster). Barcelona, Spain, 15-18 June, 2005

Wang B, Feng P, Ren EC. 2006. Identification of the role of a novel cell cycle regulatory gene D123 in hepato-carcinogenesis. Presented at the 19th Meeting of the European Association for Cancer Research (EACR-19) (Poster). Budapest, Hungary, 1-4 July, 2006